The role of phosphatase activity and expression in glucocorticoid modulation of preosteoblasts

by
Micheline Sanderson

Dissertation presented in partial fulfilment for the degree of Doctor of Philosophy (Internal Medicine) at the University of Stellenbosch

Promoter: Dr. W.F. Ferris
Co-promoter: Prof. J.C. Moolman-Smook
Faculty of Health Sciences
Department of Medicine

December 2011

Declaration

By submitting this thesis/dissertation electronically, I declare that the entirety of the work contained therein is my own, original work, and that I have not previously in its entirety or in part submitted it for obtaining any qualification.

December 2011

Abstract

The increase in the prescription and use of glucocorticoids (GCs) to treat various diseases and resulting decrease in bone density and development of osteoporosis is of growing concern. Glucocorticoid-induced osteoporosis (GCIO) is a relatively under-researched disease with the mechanism by which GCs affect bone metabolism not yet fully delineated. This holds especially true for the early events in bone development. The negative effects of GCs are predominantly seen in osteoblasts, the cells responsible for bone formation, in that GCs diminish both the numbers and function of osteoblastic cells.

Osteoblast precursor cell proliferation is crucial to ensure the existence of a healthy pool of osteoblastic cells needed to form new bone after bone resorption by osteoclasts. Previously, it was shown that GCs reduce the proliferation of immortalised osteoblastic cell lines. In addition, early immortalised preosteoblasts were more sensitive to GCs than their mature counterparts. However, these cells have corrupted cell cycles; therefore, primitive primary mesenchymal stromal cells (MSCs) were used in this study to examine the effect of GCs on the mitogen-induced proliferation of early osteoblast precursor cells (naïve MSCs and preosteoblasts) using the synthetic GC, dexamethasone (Dex).

Mitogenic conditions established for naïve rat mesenchymal stromal cells (rMSCs) indicated that mild (5% FBS) stimulation is sufficient to induce proliferation, whereas a higher FBS concentration (20% FBS) was mitogenic in primary preosteoblasts. It was also found that pharmacological doses of Dex drastically decreased the mitogen-induced proliferation of both naïve rat MSCs (rMSCs) and preosteoblasts. Mitogen-activated protein kinase (MAPK) signalling pathways, such as ERK1/2, govern cell proliferation. GCs have been shown to decrease the activity of ERK1/2, which is associated with decreased proliferation in osteoblastic cells. In the present study, western blot analysis showed that Dex reduced the proliferation-associated shoulder of the ERK1/2 activity profile in both naïve rMSCs and preosteoblasts. Moreover, the ERK1/2 signalling pathway was shown to be essential for mitogen-stimulated growth of naïve rMSCs and preosteoblasts as the MEK1/2 inhibitor, U0126, inhibited mitogen-induced proliferation. Using western blot analysis, it was shown that, after mitogen administration, ERK1/2 activity exhibited a typical proliferation profile, which was blocked by U0126.

Protein tyrosine phosphatases (PTPs) dephosphorylate and inactivate ERK1/2. Utilising sodium vanadate, an inhibitor of PTPs, *in vitro* phosphatase assays revealed that PTP activity was the

predominant phosphatase activity present in naïve rMSCs and preosteoblast lysates after concomitant mitogen and Dex stimulation. The mRNA of the dual specificity phosphatase, MKP-1, was rapidly (within 30 minutes) upregulated after mitogen and Dex administration in both naïve rMSCs and preosteoblasts. However, the protein expression pattern of MKP-1 did not correspond to the mRNA induction, suggesting that the MKP-1 protein could be subjected to rapid degradation. These findings suggest that MKP-1 could possibly be involved in the GC regulation of mitogen-induced proliferation of early osteoblast precursor cells, but closer investigation is needed to fully elucidate this role. In addition, the involvement of other PTPs should not be excluded and warrants further investigation.

During the course of the present study, it was found that strong mitogenic stimulation with 20% FBS led to oncogene-induced senescence (OIS). Flow cytometry analysis revealed the presence of two populations in naïve rMSCs preparations and DNA content analysis was consistent with that of cells undergoing OIS. These results indicated that the more primitive osteoblast precursor cells (naïve rMSCs) are more responsive to mitogens than their mature counterparts (preosteoblasts). In addition, it was found that the magnitude of ERK1/2 activation was increased in naïve rMSC after strong mitogenic stimulation, indicating that naïve rMSCs are still highly sensitive to stimulation with strong mitogens.

In summary, these findings show that Dex decreased the proliferation of naïve rMSCs and preosteoblasts concomitantly with a decrease in ERK1/2 activity. In addition, Dex upregulated MKP-1 mRNA, but the same effect was not seen on the MKP-1 protein levels. Therefore, this suggests that PTP/s other than MKP-1 could be responsible for the inactivation of ERK1/2 by Dex, leading to decreased proliferation in naïve rMSCs and preosteoblasts. Further identification of PTPs that regulate osteoblast precursor cell numbers and function could lead to the elucidation of the mechanism through which GCs act to negatively influence bone density. This will improve our insights into the pathogenesis of GCIO and aid in the identification of therapeutic targets which can be exploited to develop new agents to treat osteoporosis.

Opsomming

Die toename in voorskrifte en gebruik van glukokortikoïede (GKs) om verskillende siektes te behandel en die gevolglike afname in been digtheid, is kommerwekkend. Glukokortikoïed geïnduseerde osteoporosis (GKIO) is ‘n relatief min genavorste siekte waarvan die meganisme waardeur GKs been-metabolisme affekteer nog nie ten volle ontrafel is nie. Dit is veral waar ten opsigte van die vroeë stadia in beenontwikkeling. Die negatiewe uitwerking van GK’s word oorwegend in osteoblaste, die selle wat verantwoordelik is vir beenformasie, waargeneem, waar GKs beide die getalle en funksie van osteoblaste verminder.

Osteoblast voorloper-sel proliferasie is belangrik vir die handhawing van ‘n gesonde poel osteoblastiese selle wat benodig word om nuwe been te vorm na beenresorpsie deur osteoklaste. Daar is gevind dat GKs proliferasie van verewigde preosteoblastiese sellyne verminder en dat jong verewigde preosteoblaste meer sensitief is vir GKs as hul meer volwasse ekwivalent. Die selle se selsiklusse is egter gekorrupteer en daarom was primitiewe primêre rot mesenkiem stromaselle (rMSCs) in hierde studie gebruik om die effek van GKs op mitogeen-geïnduseerde proliferasie van vroeë osteoblasvoorloperselle (naïwe MSC en preosteoblaste) deur die sintetiese GK, deksametasoon (Dex), te bestudeer.

Mitogeniese kondisies vir naïwe rMSCs het getoon dat matige (5% FBS) stimulasie voldoende is om proliferasie te induseer, terwyl ‘n hoë FBS konsentrasie (20% FBS) mitogenies was in primêre preosteoblaste. Daar is ook gevind dat farmokolgiese dosisse Dex die mitogeen-geïnduseerde proliferasie van beide naïwe rMSCs en preosteoblaste verminder. Die mitogeen-geïnduseerde protein kinase (MAPK) pad beheer selproliferasie. Die ekstrasellulêre gereguleerde kinase pad (ERK1/2) is voorheen as die hoofpad wat MBA 15.4 and MG 63 proliferasie beheer geïdentifiseer. Daar is gewys dat GKs die aktiwiteit van ERK1/2 verlaag en proliferasie van die selle verminder. In die huidige studie het western blot analise gewys dat Dex die proliferasie geassosieerde skoueraktiwiteit van die ERK1/2 aktiwiteitsprofiel in beide naïwe rMSCs en preosteoblaste verminder. Die noodsaaklike rol van ERK1/2 pad in mitogeen-gestimuleerde groei van die selle is bevestig deur die MEK1/2 inhibitor, U0126, wat die mitogeen-geïnduseerde proliferasie geïnhibeer het. Western blot analise het gewys dat die ERK1/2 aktiwiteit na mitogeen toediening ‘n tipiese proliferasie profile toon wat deur U0126 geblokkeer word.

Protein tirosien fosfatases (PTPs) defosforileer and inaktiveer ERK1/2. *In vitro* fosfatase bepalings met natrium vanadaat, ‘n inhibitor van PTPs, het bevestig dat PTP die predominante fosfatase akitiwiteit is in naïwe rMSCs en preosteoblaste lisate is na gelyktydige mitogeen en Dex stimulasie.

Die mRNA van die dubbele spesifisiteits fosfatase, MKP-1, is vinnig (binne 30 minute) opgereguleer is na mitogeen en Dex toediening in beide naïwe rMSCs en preosteoblaste. Die proteinekspressie van MKP-1 het egter nie met die mRNA ekspressie ooreengestem nie, wat suggereer dat die MKP-1protein blootgestel is aan vinnige degradasie. Hierdie bevindings stel voor dat MKP-1 moontlik ‘n rol speel in die GC-regulering van mitogeen-geïnduseerde proliferasie van vroeë osteoblast voorloperselle maar verdere ondersoek is nodig om die rol ten volle te verklaar. Die betrokkenheid van ander PTPs moet egter nie uitgesluit word nie en regverdig verdere studie.

Die huidige studie het bevind dat sterk mitogeniese-stimulasie met 20% FBS tot onkogene-geïnduseerde selgroeistilte (senescence) (OIS) lei. Vloeisitometriese analise het die teenwoordigheid van twee afsonderlike populasies getoon in die naïwe rMSCs preparate en die DNA inhoud was verenigbaar met die van selle wat OIS ondergaan. Die bevindinge stel voor dat die meer primatiewe osteoblast voorloperselle (naïwe rMSCs) is meer vatbaar vir mitogene-stimulasie as hul volwasse ekwivalente (preosteoblaste). Ook is gevind dat die mate van ERK1/2 aktivering hoër was in naïwe rMSCs, selfs na sterk mitogeniese stimulasie wat daarop dui dat naïwe rMSCs steeds hoogs sensitifief is vir stimulasie met sterk mitogene.

In opsomming, dui die bevindinge dat Dex die proliferasie van naïwe rMSCs en preosteoblaste onderdruk wat met ‘n verlaging van ERK1/2 aktiwiteit gepaard gaan. Verder, het Dex, MKP-1 mRNA opgereguleer maar die effek is nie op die proteinvlak waargeneem nie. Dit suggereer dat PTP/s anders as MKP-1 verantwoordelik kan wees vir die Dex inaktivering van ERK1/2 wat die proliferasie van naïwe rMSCs en preosteoblaste onderdruk.

Acknowledgements

First and foremost, I want to express my undying gratitude to my Heavenly Father for granting me the strength, courage and perseverance to complete this project and thesis.

Financial support for this project was provided by National Research Foundation, the Medical research Council of South Africa, the Faculty of Health and the Department of Medicine of the University of Stellenbosch.

I would like to thank my supervisor Dr. W. F. Ferris and co-supervisor, Professor J. C. Moolman-Smook and Professor F. S. Hough, for their assistance and guidance throughout this project.

Special thanks go to my parents, Frank and Lilian Sanderson and my partner, Peter November, for their sacrifices and never-ending love and encouragement. Gratitude also goes to my brother and sister-in-law, extended family and friends for their support.

I also want to thank my colleagues at the Endocrinology and Metabolism Unit at the University of Stellenbosch as well as the Diabetes Discovery Platform at the Medical Research Council for the assistance given and friendships formed.

Finally, I want to express my thankfulness to the Department of Biomedical Sciences, Division of Molecular Biology and Human Genetics as well as the Division of Medical Physiology at the University of Stellenbosch for the supply of animals and use of equipment. Gratitude also goes to Dr. J. Michie for assistance with the flow cytometry work, Dr. H. Sadie-van Gijsen for images provided and Prof. L. van der Merwe for help with the statistical analysis for part of this work.

Table of Contents

List of Abbreviations

A

A	Ampere
ACTH	Adrenocorticotropic hormone
ALP	Alkaline phosphatase
AP-1	Activator protein 1
ARBP	Acidic ribosomal phosphoprotein

B

BMD	Bone mineral density
BMP	Bone morphogenetic protein
BMU	Basic multicellular unit
BSA	Bovine serum albumin
BSP	Bone sialoprotein

C

C	Control
Ca^{2+}	Calcium
cAMP	Cyclic adenosine monophosphate
Cbfa1	Core-binding factor 1
Cdk	Cyclin dependent kinase
CFU-GM	Colony-forming unit- granulocyte-macrophage
CFU-M	Colony-forming unit- macrophage
Col I	Collagen I
Cpm	Counts per minute
CRH	Corticotrophic releasing hormone
Ci	Curie

D

d	Day
Dex	Dexamethasone
Dlx5	Distal-less homeobox 5
DMEM	Dulbecco's Modified Eagle's Medium
DUSP	Dual specificity phosphatase

E

ECL	Enhanced chemiluminescence
EtOH	Ethanol
ELAV	Embryonic lethal abnormal vision
E2F	Elongation 2 factor
ecNOS	Endothelial cell nitric oxide synthase
EGF	Epidermal growth factor
ERK1/2	Extracellular regulated kinase 1/2

F

FACS	Fluorescence-activated cell sorting
FBS	Fetal bovine serum
FGF	Fibroblast growth factor
FHL-2	Four and a half LIM domain protein-2
Fig	Figure
FSH	Follicle stimulating hormone

G

G	Gram
GCIO	Glucocorticoid-induced osteoporosis
GCs	Glucocorticoids
GFs	Growth factors
GH	Growth hormone
GPCR	G-protein coupled receptor
GR	Glucocorticoid receptor
GRE	Glucocorticoid response element

H

[^{3}H]dT	Tritium labelled deoxythymidine
11-β-HSD	11-β-Hydroxysteroid dehydrogenase
HBSS	Hank's balanced salt solution
HPA	Hypothalamic-pituitary-adrenal axis
hr	Hour
hrs	Hours

I

IFN-β	Interferon-β
IGF-I	Insulin-like growth factor-I
IGF-II	Insulin-like growth factor-II
IL-1	Interleukin-1
IL-6	Interleukin-6

L

L	Litre

M

M	Molar
MAP2K	Mitogen-activated protein kinase kinase
MAP3K	Mitogen-activated protein kinase kinase kinase
MAPK	Mitogen-activated protein kinase
M-CSF	Macrophage colony-stimulating factor
MEK	MAPK/ERK kinase
min	Minute
miRNA	MicroRNA
MKP-1	Mitogen-activated protein kinase phosphatase-1

MMP-13	Matrix metalloproteinase-13
MMPs	Matrix metalloproteinases
MR	Mineralocorticoid
MSCs	Mesenchymal stromal cells
Msx	Homologue of the *Drosophila* muscle segment box
MVs	Matrix vesicles

N

n.a.	Not applicable
NF90	Nuclear factor 90
NF-κβ	Nuclear factor-κβ
NGF	Nerve growth factor
nm	Nanometer
NO	Nitric oxide

O

OCN	Osteocalcin
OD	Optical density
OM	Osteogenic medium
OPG	Osteoprotegerin
OPN	Osteopontin

P

P2	Passage 2 cells
PAO	Phenylarsine oxide
PBS	Phosphate buffered saline
PDGF	Platelet-derived growth factor
PGE2	Prostaglandin E2
Pi	Inorganic phosphate
PI	Propidium iodide
PI3K	Phosphatidyl-inositol-3-kinase
PKC	Protein kinase C
PMA	Phorbol 12-myristate 13-acetate
Pnpp	p-Nitrophenyl phosphate
PTH	Parathyroid hormone
PTHrP	Parathyroid hormone-related protein
PTP	Protein tyrosine phosphatase

R

RANK	Receptor activator of nuclear factor-κβ
RANKL	Receptor activator of nuclear factor-κβ ligand
Rb	Retinoblastoma
rMSCs	Rat mesenchymal stromal cells
RNA	Ribonucleic acid
rpm	Revolution per minute
RT	Room temperature
RTK	Receptor tyrosine kinase
RT-qPCR	Real time quantative polymerase chain reaction

Runx2	Runt-related transcription factor 2

S

s	Second/s
SHP-1	Src homology region 2-domain-containing protein
shRNA	Short hairpin Ribonucleic acid
Sos	Son-of-sevenless

T

TCA	Trichloroacetic acid
Tfs	Transcription factors
TGFβ1	Transforming growth factor β1
TGFβ2	Transforming growth factor β2
TMP	Thrombin-mimicking peptide
TNF	Tumour necrosis factor
TRAP	Tartrate resistant acid phosphatase
TTP	Tristetraprolin

U

U	Units
U/mg	Units per milligram
U/ml	Units per millilitre

V

1α-25-$(OH_2)D_3$	1- alpha-25 dihydroxy-Vitamin D3
V	Volts
v/v	Volume per volume
VEGF	Vascular endothelial growth factor
VO_4	Sodium orthovanadate

W

w/v	Weight per volume

List of Figures

List of Tables

Chapter 1

Bone formation and bone homeostasis: regulation of osteoblast development and the effects of glucocorticoids on osteoblast proliferation

1.1 Chapter Outline

A brief background for the presented work and a literature review on various aspects of the regulation of bone metabolism is included in this chapter. An overview on bone homeostasis, which covers key sections on the composition structure and function of bone; the cellular compartments within bone and the maintenance of the skeleton through bone remodeling, is incorporated. Signalling networks regulating osteoblast development are outlined, with focus on the ERK1/2 signalling pathway; the role of the ERK1/2 signalling pathway in osteoblast development; as well as regulation of ERK1/2 activity by phosphorylation and dephosphorylation. This includes the phosphatase regulation of ERK1/2 activity by MKP-1 and the action of MKP-1 in osteoblasts. The aims and strategies employed in this study are discussed.

1.2 Background

Glucocorticoid-induced osteoporosis (GCIO) is fast becoming a major medication-related disease. This could be ascribed to increased prescription and use of glucocorticoids (GCs) to treat a wide range of pathophysiological conditions, such as pulmonary diseases (like asthma), renal diseases, rheumatologic disorders (such as rheumatoid arthritis and lupus), inflammatory bowel disease and transplant rejection (Cohen and Adachi, 2004; Dore, 2010). GCIO shares many similarities with involutional and postmenopausal (age- and hormone-related) osteoporosis (Tamura et al., 2004; Compston, 2010). However, GCIO also has distinct characteristics (Tamura et al., 2004; Compston, 2010). In contrast to age-related osteoporosis, GCIO occurs in two phases: a characteristic rapid increase in initial bone breakdown by osteoclasts followed by a prolonged decrease in osteoblast development and reduced new bone formation by osteoblasts (Canalis, 1996; Canalis and Giustina, 2001; Compston, 2010). Bone histomorphometric studies show the major cause of GC-induced bone loss is due to the suppression of bone formation (Chavassieux et al., 1993; Lo, V et al., 1995;

Dalle et al., 2001). Even though GCs influence other types of bone cells like osteoclasts, the detrimental consequences of these steroid hormones are primarily seen in osteoblasts, the bone forming cells (Canalis, 1996; Canalis et al., 2004; Kalak et al., 2009). The effect of GCs on osteoblast development and bone formation will be addressed in Section 1.5.

The decrease in bone formation leads to a decreased bone density, which could culminate an increase in fracture risk during the GC treatment period (Canalis, 1996; Canalis and Giustina, 2001; Compston, 2010). Therefore, continued long term and high dose GC treatment can cause bone loss, resulting in reduced bone density (van Staa et al., 2002; van Staa et al., 2003) and decreased bone strength, which may ultimately lead to bone fractures (Canalis et al., 2004). In patients that are chronically exposed to GCs, 30% to 50% exhibit reduced bone mineral density (BMD) and develop vertebral fractures (Lukert and Raisz, 1990; van Staa et al., 2000a; Kalak et al., 2009). The extent of bone loss in these patients is correlated with the dose and duration of GC treatment (van Staa et al., 2000b). Interestingly, it was shown that although fracture risk increased within only 3-6 months after commencement of GC therapy, it decreased with cessation of GC therapy (van Staa et al., 2002).

Much work has been done to fully understand the cellular and molecular aspects of bone development and metabolism. However, the mechanism through which GCs exert their negative effects on bone is not yet completely understood. Therefore, a better understanding of the mechanisms through which GCs affect bone formation and homeostasis at a cellular and molecular level is needed. Furthermore, the effect of GCs on osteoblast precursor cell and younger osteoblasts is under-researched. The aim of the work presented here is to elucidate the mechanism through which GCs affect the development and thus the function of osteoblast precursor cells.

1.3 Literature Review

1.3.1 Bone Homeostasis

1.3.1.1 The function, composition and structure of bone

Bone is a vital, highly specialised organ, composed of mineralised connective tissue which performs biological, chemical and mechanical functions. The main functions of bone are to provide protection of the vital organs and to serve as a structural support to which muscles and tendons are attached to facilitate movement (Loveridge, 1999; Harada and Rodan, 2003; Rubin and Rubin, 2009). About 99% and 85% of the human body's total calcium and phosphorus, respectively, as well as other minerals are retained within bone, therefore making it a substantial mineral reservoir (Loveridge, 1999; Marks and Odgren, 2002; Rubin and Rubin, 2009). In addition, the bone marrow compartment is enveloped by bone, which also plays a role in the regulation of haematopoiesis (Marks and Odgren, 2002; Harada and Rodan, 2003; Rubin and Rubin, 2009).

Moreover, bone is rigid and strong, whilst retaining a measure of elasticity. These features are necessary for bone to fulfil its protective as well as structural roles (Marks and Odgren, 2002). The elasticity, firmness and strength of bone are determined by the composition and structure (Marks and Odgren, 2002; Seeman and Delmas, 2006). Therefore, factors negatively affecting these bone characteristics could compromise the integrity of the skeleton. Bone density, often referred to as bone mineral density (BMD) and bone quality, together influence bone strength (Lees, 1981; Felsenberg and Boonen, 2005; Boivin et al., 2009; Bouxsein and Seeman, 2009). BMD is defined as the amount of mineral per square centimetre bone and can be measured using various quantitative techniques including dual energy X-ray absorptiometry (DXA) (Kanis, 1994a; Kanis et al., 1994b). However, BMD is a measurement of the mineral content and area of bone but not the quantity and quality (Oleksik et al., 2000). Bone quality includes characteristics of bone composition and structure that ultimately play a role in bone strength. These include bone turnover, microarchitecture, mineralisation and microdamage. Various techniques are used to measure these aspects such as histomorphometry (bone turnover and microarchitecture), spectroscopy (mineralisation) and histology (microdamage) (Compston, 2006). As stated previously, DXA is used to measure bone quantity. The risk of fractures is dependent on bone strength (Mazziotti et al., 2006; Sipos et al., 2009; Compston, 2010). Therefore, it is important that the quality of bone is preserved. The World Health Organisation (WHO) classification of osteoporosis, using DXA measurements, is a BMD of the spine or proximal femur of 2.5 standard deviations or more below

normal peak bone mass (the mean BMD of a young, 20 year old, healthy Caucasian woman, which could also be used for the diagnosis of osteoporosis in men) (Kanis, 1994b; World Health Organization, 2003; Mazziotti et al., 2006).

Bone can be divided into three basic compartments. Firstly, an organic matrix, comprised of collagenous and non-collagenous proteins, forms a major part of bone (Marks and Odgren, 2002). This organic phase comprise 30% of total bone volume (Mistry and Mikos, 2005; Bueno and Glowacki, 2011). Type I collagen is the predominant organic matrix protein, constituting approximately 90% to 95% of the organic matrix, whereas non-collagenous proteins such as osteopontin, osteocalcin and bone sialoprotein represent only 5% (Marks and Odgren, 2002; Crichton, 2008). The second part of bone is the inorganic or mineral phase, which is the major constituent at 70% of total bone volume and includes a 10% water component (Mistry and Mikos, 2005; Bueno and Glowacki, 2011). In addition, the mineral phase is composed of at least 43% of calcium and phosphate ions. These ions are found in the form of hydroxyapetite ($Ca_{10}(PO_4)_5(OH)_2$), which hardens the organic matrix upon deposition. Thirdly, bone also has a cellular compartment.

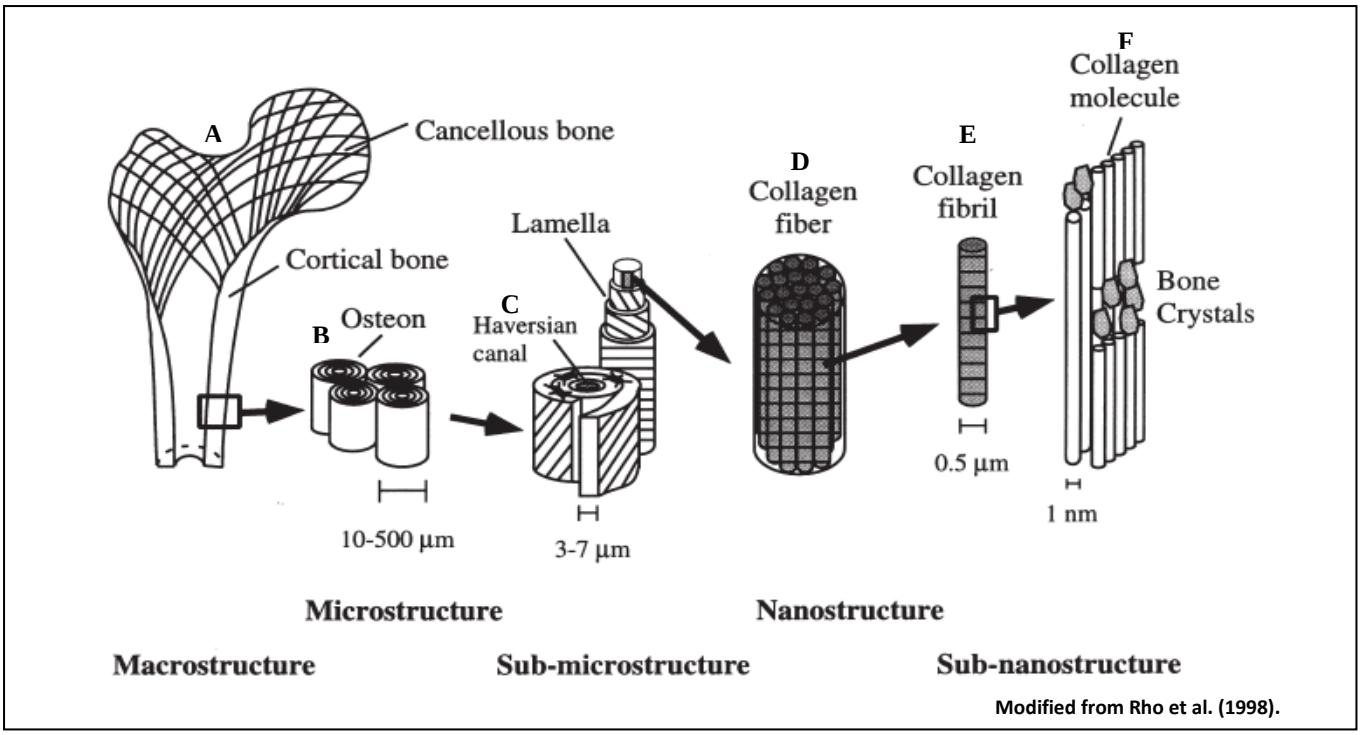

Figure 1.1: The hierarchy of bone structure.

The different levels of bone structure organisation are illustrated: (**A**) Macrostructure, (**B**) microstructure, (**C**) sub-microstructure, (**D**) nanostructure and (**E and F**) sub-nanostructure.

As stated earlier, bone surrounds the bone marrow which house cells from haematopoietic origin such as leukocytes, erythrocytes, thrombocytes and osteoclasts as well as stromal (stem) cells and

stromal-derived cells such fibroblasts, adipocytes and osteoblasts. In addition, bone is also richly supplied with blood vessels and nerve cells (Hurrell, 1937; Parfitt, 2000; Proff and Romer, 2009). The main types of cells found within bone itself are osteoblasts, osteoclasts, bone lining cells and osteocytes, which will be discussed further in section 1.3.1.2.

The basic architecture of bone is complex and highly structured, which is evident at the different levels of bone organisation (Fig. 1.1). Two types of bone can macroscopically be identified; cortical (compact) and cancellous (trabecular or spongy) bone (Fig. 1.1 A) (Rho et al., 1998; Rubin and Rubin, 2009). The differences between these two bone types can be seen in both structure and function. On lower levels of organisation (microstructure), cortical bone consists of densely packed collagen fibrils which form concentric lamellae (Fig. 1.1 F). Groups of 4 to 8 lamellae are then organised into osteons (Fig. 1.1 E-B) (Rho et al., 1998). This hierarchical structure contributes to the mechanical and protective function of cortical bone. In contrast, cancellous bone, which provides a more metabolic function, has less regular structural organisation and appear porous due to the marrow-filled cavities (Rho et al., 1998; Marks and Odgren, 2002). Flat bones such as calvaria in the skull, have a layered structure, much like a sandwich, where a thin layer of cancellous bone functions to reinforce a compact cortical envelope (Rho et al., 1998; Rubin and Rubin, 2009). Furthermore, long bones such as the femur form a compact tube of cortical bone which surrounds porous cancellous bone in the centre (Rho et al., 1998; Rubin and Rubin, 2009). Bone also contains a complex system of different canals (or canaliculi), for example the Haversian canals found in the centre of osteons (Fig. 1.1 C), which functions as reinforcement to provide ultimate strength (Rho et al., 1998; Rubin and Rubin, 2009). These features provide bone with maximal strength, whilst retaining minimal mass, to facilitate movement.

Bone strength is positively influenced by mechanical loading, although, numerous other factors negatively impact on bone strength (Robling et al., 2006; Rubin and Rubin, 2009). Such factors include aging, hormonal imbalances, certain metabolic diseases, as well as chronic and prolonged GC treatment, all of which decrease BMD (Canalis et al., 2004; Sipos et al., 2009; Compston, 2010). Reduced BMD could result in an increased propensity of bone fractures, which is characteristic of skeletal disorders like osteoporosis (Canalis et al., 2004; Sipos et al., 2009; Compston, 2010).

1.3.1.2 The cellular compartmentalisation of bone

Bone cells have different origins and, upon certain signals, progenitor cells undergo a process of progressive differentiation to give rise to mature, functioning cells. As stated previously, besides the haematopoietic and vasculature-related cells, the main types of cells found in bone are: (i) osteoclasts, the cells which break down the mineralised bone matrix, (ii) osteoblasts, the cells which are responsible for new bone formation, (iii) lining cells found on quiescent bone surfaces and (iv) osteocytes, which are old osteoblasts embedded in the mineralised bone matrix (Marks and Odgren, 2002; Rubin and Rubin, 2009). Despite having individual functions, these bone cells function in concert to regulate bone homeostasis. To maintain the equilibrium in bone, osteoclasts and osteoblasts function together in temporary cellular units known as the basic muticellular units (BMUs) (Parfitt, 1994). While the origin, development and function of the four major types of bone cells will be reviewed, the focus however, will be on osteoblast development and function.

1.3.1.2.1 The origin, development and function of osteoclasts

Osteoclasts are one of the major cell types found in bone. Mature osteoclasts are multinucleated, giant cells which, when activated, are able to breakdown (resorb) bone for calcium (Ca^{2+}) mobilisation. Activated osteoclasts are the principal cells in the body capable of bone resorption (Vaananen and Zhao, 2002; Roodman, 2006).

The earliest osteoclast precursor cells are the granulocyte-macrophage colony-forming units (CFU-GM) (Fig. 1.2) (Kurihara, 1990; Kurihara et al., 1991; Menaa et al., 2000). Research showed that osteoclasts can also develop from a more mature type of monocyte precursor cell, designated CFU-M (Fig. 1.2) (Kerby et al., 1992). Other cells found in the bone marrow, like T and B lymphocytes, marrow stromal cells and osteoblasts are involved in osteoclast differentiation and activation (Prockop, 1997; Phinney et al., 1999; Roodman, 2006). These cells secrete various cytokines and chemokines in the bone marrow milieu, such as IL-6 (Roodman, 1992) and IL-11 (Girasole et al., 1994), to stimulate, or IL-4 (Shioi et al., 1991; Lacey et al., 1995) and interferon γ (Lacey et al., 1995), to inhibit osteoclast formation and activity. Besides the ability to resorb bone, the mature osteoclast phenotype is characterised by the expression of osteoclast-related proteins such as tartrate-resistant acid phosphatase (TRAP) (Scheven et al., 1986; Lamp and Drexler, 2000; Kaunitz and Yamaguchi, 2008), Cathepsin K (Li et al., 1995; Zhao et al., 2009) and H-ATPase (Wang et al., 1992a; Yuan et al., 2010).

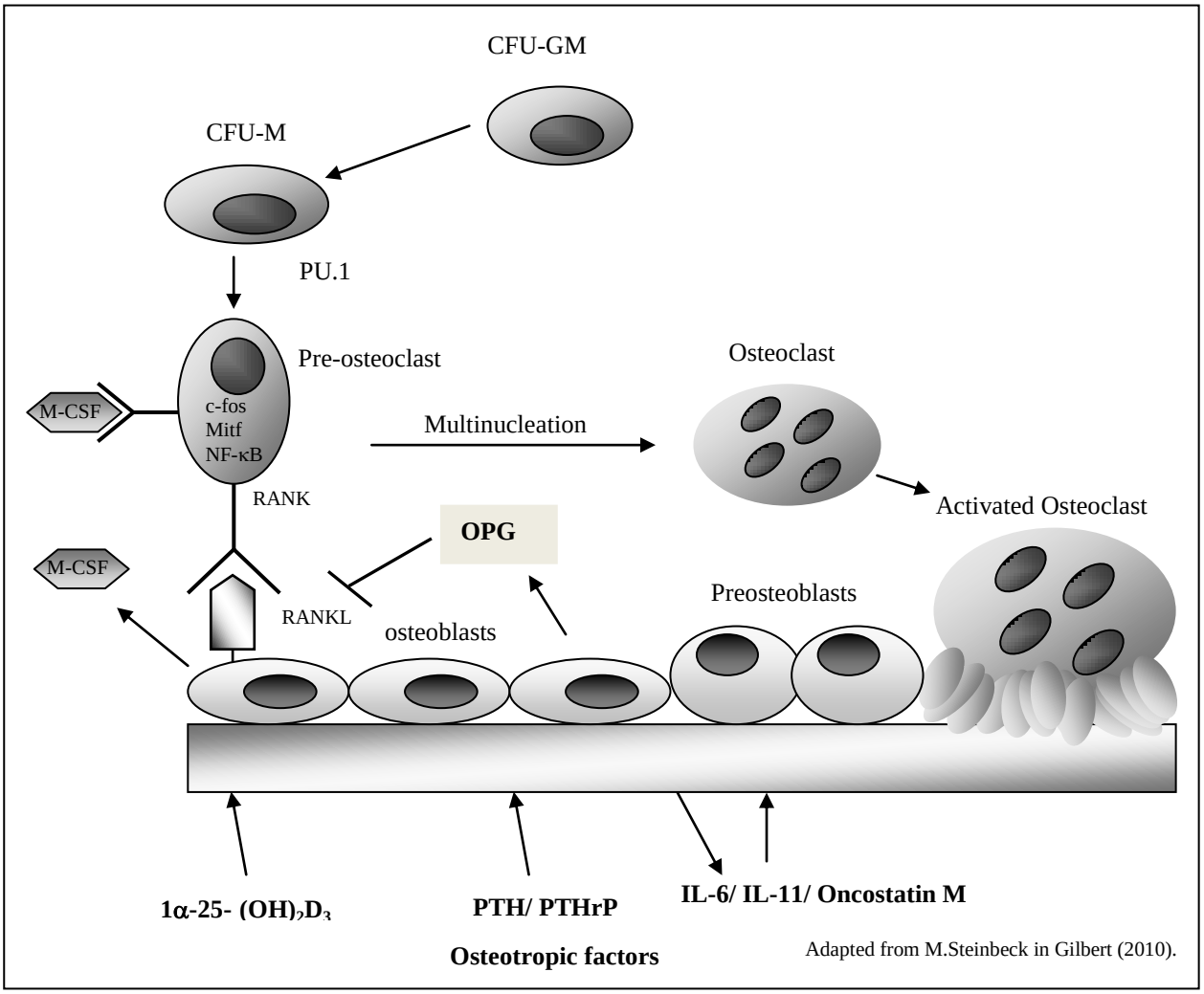

Figure 1.2: The stages of osteoclast development.

The various stages in osteoclast development as well as the respective growth factors and hormones involved are depicted. **Abbreviations**: **CFU-GM** colony forming unit-granulocyte-macrophage; **CFU-M** colony forming unit-macrophage; **IL-6** interleukin-6; **IL-11** interleukin-11; **M-CSF** macrophage colony stimulating factor; **NFκB** nuclear factor κ B; **OPG** osteoprotegerin; **PTH** parathyroid hormone; **PTHrP** parathyroid-related protein; **RANK** receptor activator of nuclear factor κ B; **RANKL** receptor activator of nuclear factor κ B ligand.; **1α-25- $(OH)_2D_3$** vitamin D3

During conditions of bone resorption, such as bone remodeling and microfracture repair, osteoclast precursor cells are recruited from the haematopoietic compartment (Schneider and Relfson, 1988; Udagawa et al., 1990; Kurihara, 1990; Menaa et al., 2000). Lineage restriction of these precursor cells towards the myeloid phenotype is determined by the transcription factor (TF), PU.1 (Fig. 1.2) (Teitelbaum et al., 1997; Henkel et al., 1996), which plays a key role in osteoclast formation and differentiation (Fig. 1.2) (Tondravi et al., 1997). Research has shown that PU.1 $^{(-/-)}$ mice are osteopetrotic (hard, dense bone) and devoid of osteoclasts and macrophages (Tondravi et al., 1997). This thus indicates that there is a restriction point in the differentiation of osteoclasts and

macrophages from a common precursor cell, and highlights the importance of PU.1 at this stage. Moreover, it was shown that PU.1 mRNA is detectable at all stages of osteoclast differentiation, progressively increasing as early osteoclasts reach maturity (Tondravi et al., 1997). Furthermore, PU.1 also regulates the expression of various osteoclast-specific proteins, by binding to specific promoters or enhancers of the encoding genes of these proteins (Matsumoto et al., 2004; Partington et al., 2004; Kwon et al., 2005). Such transcriptional targets of PU.1 include the Receptor Activator of Nuclear factor κB (RANK) (Kwon et al., 2005), Cathepsin K (Matsumoto et al., 2004) and TRAP (Partington et al., 2004).

Primitive osteoclast precursor cells proliferate and then differentiate into committed osteoclast precursors such as pre-osteoclasts, which have lost their proliferative capability (Roodman, 2006). The development of mononuclear cells into pre-osteoclasts is regulated by macrophage colony-stimulating factor or M-CSF (Fig. 1.2) (Lorenzo et al., 1987; Lee et al., 1994), which is secreted by stromal cells/osteoblasts to regulate osteoclast precursor proliferation, differentiation and survival (Tanaka et al., 1993; Felix et al., 1990; Woo et al., 2002). The binding of M-CSF to its receptor, c-fms, triggers the expression and activation of other TFs like c-fos and microphtalmia-associated transcription factor (Mitf). c-fos regulates the differentiation of committed precursors toward the osteoclast lineage rather than towards that of the macrophage (Grigoriadis et al., 1994; Wang et al., 1992b; Matsuo et al., 2000). Moreover, M-CSF/c-fms binding also regulates the expression of the receptor of another osteoblast-secreted factor necessary for osteoclast differentiation, namely receptor activator of nuclear factor κ B ligand or RANKL (Cappellen et al., 2002).

RANKL is a member of tumour necrosis factor (TNF) receptor family which is expressed on the membrane of osteoblastic cells and plays a major role in osteoclastogenesis (Fig. 1.2) (Anderson et al., 1997; Simonet et al., 1997; Tsuda et al., 1997; Wong et al., 1997; Lacey et al., 1998; Yasuda et al., 1998). Osteotrophic factors such as vitamin D3 (Kitazawa and Kitazawa, 2002; Kitazawa et al., 2003), parathyroid hormone (PTH) (Lee and Lorenzo, 1999; Fu et al., 2002), IL-1 (Wei et al., 2005) and IL-6 (Palmqvist et al., 2002) induce the expression of RANKL on the membrane of osteoblasts. It is known that cell-cell contact between osteoblast and osteoclast is required for osteoclastogenesis (Suda et al., 1999). This contact is achieved when RANKL binds to the cognate RANK receptor expressed on the membranes of pre-osteoclasts and osteoclasts (Fig. 1.2) (Nakagawa et al., 1998; Hsu et al., 1999). Binding of RANKL to RANK stimulates the differentiation and fusion of pre-osteoclasts into immature multinucleated osteoclasts (Li et al., 1999; Li et al., 2000). These immature osteoclasts are quiescent and must be activated to render them capable of bone resorption (Scheven et al., 1986; Takahashi et al., 1994; Burgess et al., 1999; Roodman, 2006). Factors like

RANKL (Fuller et al., 1998; Matsuzaki et al., 1998; Lacey et al., 1998; Burgess et al., 1999) and IL-1 (Suda et al., 1999; Fox et al., 2000) can activate these immature osteoclasts to form bone resorbing osteoclasts. Osteoprotegerin (OPG) is another member of the TNF receptor superfamily also secreted by stromal cells/osteoblasts (Simonet et al., 1997; Tan et al., 1997; Tsuda et al., 1997). Interestingly, the RANKL/RANK interaction can be blocked by OPG which acts as a soluble decoy receptor of RANKL (Simonet et al., 1997; Tsuda et al., 1997). The RANKL/OPG interaction leads to the inhibition of osteoclast formation and activation (Simonet et al., 1997; Tsuda et al., 1997).

Osteoclasts are activated upon attachment to the bone extracellular matrix via protein-protein interactions involving integrins and matrix proteins such as osteopontin and bone sialoproteins which are rich in arginine-glycine-aspartic acid (RGD) regions (Vaananen et al., 2000; Ross and Teitelbaum, 2005). This integrin-mediated activation of osteoclasts involves the cytoskeletal reorganisation and polarisation of the cell (Lakkakorpi and Vaananen, 1991; Vaananen et al., 2000). These changes result in the formation of unique bone resorption structures which give activated osteoclasts a distinct appearance: giant cells with podosomes which are swiftly constructed and deconstructed to facilitate osteoclast movement across the bone surface (Horne et al., 2005; Gil-Henn et al., 2007). Upon attachment to the bone matrix, the osteoclastic actin microfilaments reorganise into a ring-like structure to form the sealing zone, which surrounds the ruffled border to contain the acidic resorption area (Lakkakorpi and Vaananen, 1991; Vaananen et al., 2000). This isolates the area of resorption, thus stopping diffusion of factors released by resorption, as well as any aberrant digestion of bone. The ruffled border is formed when acidified vesicles, containing matrix metalloproteinases (MMPs) and Cathepsin K, move along microtubules and fuse with the cell membrane (Vaananen and Zhao, 2002; Clarke, 2008). By means of H^+ APTases and chloride channels, H^+ ions and proteases are secreted in the space between the osteoclast and the bone matrix (Baron, 1995; Vaananen and Zhao, 2002; Clarke, 2008). This leads to acidification only of the area under the ruffled border, resulting in the dissolution of mineral and digestion of the organic matrix to form resorption lacunae (Baron, 1995; Vaananen and Zhao, 2002; Clarke, 2008). Removal of the degraded bone material from the resorption site occurs through endocytosis into the osteoclasts, transportation through the cell (transcytosis) and secretion through the osteoclast membrane (either through exocytosis or via channels and pumps) (Salo et al., 1997; Nesbitt and Horton, 1997). The released mineral and organic factors can then be utilised elsewhere in the body, for example, Ca^{2+} signalling can influence the activities of other cell types such as osteoblasts.

1.3.1.2.2 The origin of osteoblasts

Mesenchymal stromal cells give rise to a number of cell types, amongst which are osteoblasts (Friedenstein, 1990; Prockop, 1997; Owen, 1998). The lineage restriction of mesenchymal and primitive osteoblast progenitor cells is controlled by transcription factors such as Msx2 (homologue of the *Drosophila* muscle segment homeobox gene) (Dodig et al., 1999; Liu et al., 1999; Satokata et al., 2000; Wilkie et al., 2000), Dlx5 (distal-less homeobox 5) (Ryoo et al., 1997; Newberry et al., 1998; Acampora et al., 1999), Runx 2 (Runt related protein x2) (Ducy et al., 1997; Komori et al., 1997; Otto et al., 1997; Mundlos et al., 1997) and Osx (Osterix) (Nakashima et al., 2002) (Fig.1.3).

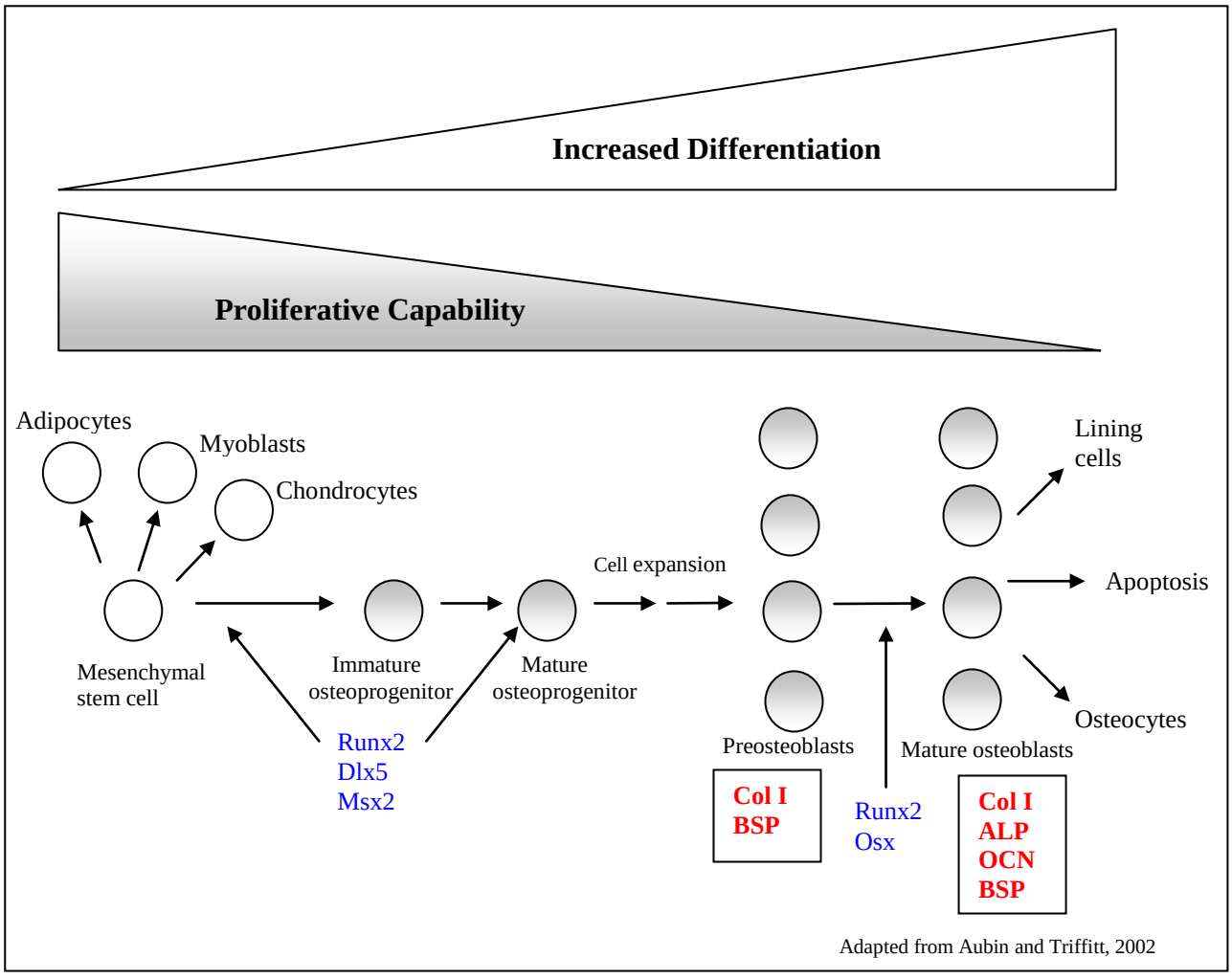

Figure 1.3: Schematic representation of the stepwise differentiation regime of osteoblasts from mesenchymal stromal cells to mature osteoblasts.

The hypothesised osteoblastic differentiation stages, with decreasing proliferative capabilities are depicted. The postulated positions of well-established transcription factors are indicated in blue, whilst characterised osteoblast-specific proteins are indicated in red. **Abbreviations**: **ALP** alkaline phosphatase; **BSP** bone sialoprotein; **Col I** collagen I; **Dlx5** distal-less homeobox 5; **OCN** osteocalcin

Osteoblast differentiation from mesenchymal progenitor cells occurs via a regimented and stepwise program (Fig. 1.3) (Aubin and Liu, 1996; Aubin and Triffitt, 2002; Franceschi, 1999). Attempts to elucidate the initial cellular and molecular events, mediating the transition of mesenchymal stromal cell into mature osteoblasts, have identified at least seven transition stages during osteoblastic differentiation (Aubin and Liu, 1996; Candeliere et al., 1999; Liu et al., 2003). However, this differentiation program, especially the early differentiation stages involving the more primitive osteoblast precursor cells, is not yet fully delineated.

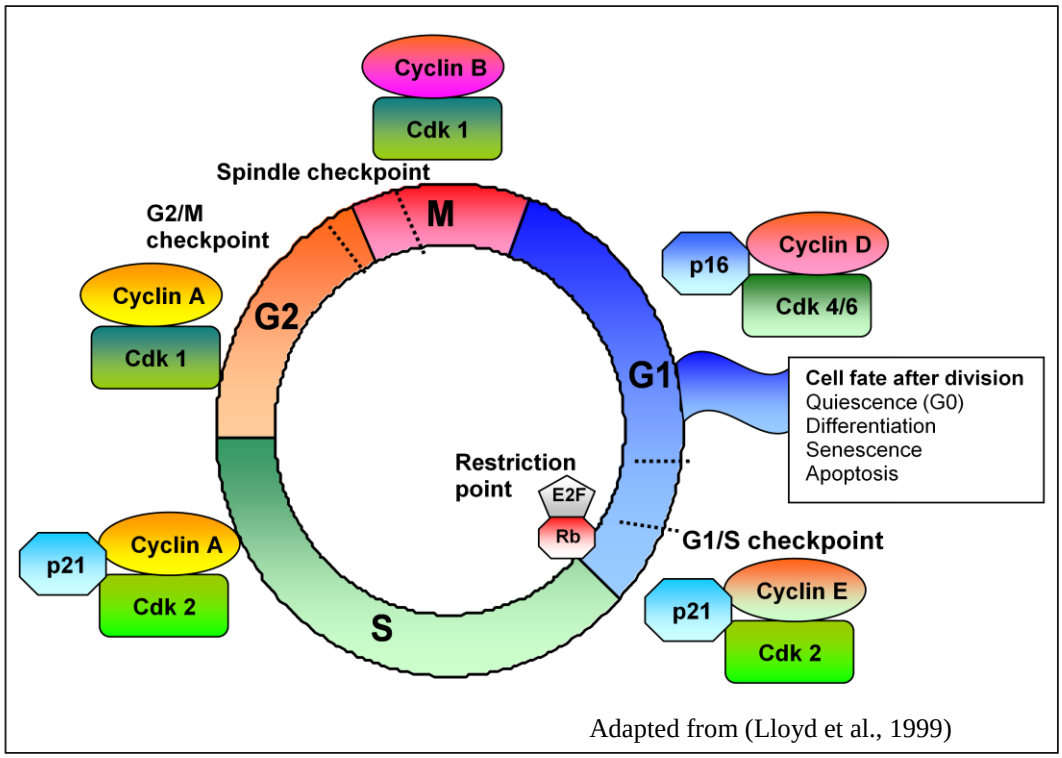

Figure 1.4: **Schematic diagram of the cell cycle, illustrating the cell cycle phases**.

The cell cycle phases are indicated as follows: G0 (specified in text box), G1 (blue); S phase (green); G2 (orange) and M phase (red). The dotted lines represent the cell cycle checkpoints as indicated. Respective cyclin homologues are indicated in varying shades of yellow to red, cyclin-dependent kinase homologues are indicated in shades of green whilst cyclin-dependent kinase inhibitors are indicated in varying shades of blue. **Abbreviations**: **Cdk** cyclin-dependent kinase; **E2F** elongation factor 2; **Rb** retinoblastoma protein

1.3.1.2.3 Osteoblast differentiation and function

As elucidated from *in vitro* studies of nodule formation, which only results from cells with a mature osteoblast phenotype, osteoblast differentiation can be divided into three phases: (i) the proliferation stage of osteoblast progenitor cells, such as MSCs and preosteoblasts; (ii) extracellular matrix deposition and maturation and (iii) mineralization (Stein et al., 1990; Lian and Stein, 1995; Aubin

and Triffitt, 2002). These differentiation stages are characterised by specific proteins and the appearance of these proteins define the osteoblastic phenotype, which are therefore used as osteoblastic markers.

1.3.1.2.3.1 Proliferation of osteoblast progenitor cells

Maintenance of Ca^{2+} balance and normal bone density requires that bone is constantly removed and replaced. Bone homeostasis is governed by the total number of cells and function of both osteoclasts and osteoblasts. Therefore, bone formation by osteoblasts is the result of the net amount of cells available, which is modulated by the rate of mitogenesis, differentiation, transdifferentiation of progenitor cells into other cell types, and cell death. Cellular expansion is essential to maintain functional osteoblast populations in order to replace bone that is resorbed by osteoclasts. As stated previously, this proliferative period of osteoblast precursor cells is an integral early part of the differentiation regime towards a mature osteoblast phenotype.

Various systemic hormones and growth factors regulate osteoblast biology. Systemic hormones, like parathyroid hormone (PTH) (Hock et al., 1989; Bringhurst and Strewler, 2002; Hock et al., 2002), growth hormone (GH) (Verhaeghe et al., 1996; Rosen and Rackoff, 2001; Rosen and Bilezikian, 2001), insulin (Hickman and McElduff, 1989; Thomas et al., 1996; Verhaeghe and Bouillon, 2002) and glucocorticoids (Pockwinse et al., 1995; Chang et al., 2006; Kalak et al., 2009), play an important role in regulating bone cell function by affecting osteoblasts directly. However, hormones can also affect osteoblast replication and function through altering the synthesis, activity or binding of growth factors (GFs) (Conover and Rosen, 2002; Canalis and Rydziel, 2002). Local growth factors, such as insulin-like GFs (IGF-I and IGF II) (Mohan et al., 1990; Durham et al., 1994; Conover and Rosen, 2002), platelet-derived growth factors (PDGF) (Betsholtz et al., 1986; Graves et al., 1989; Rydziel et al., 1992; Canalis and Rydziel, 2002), fibroblast growth factors (FGF) (basic and acidic) (Globus et al., 1989; Hurley et al., 1994; Mehrara et al., 1998; Rice et al., 2000) and bone morphogenetic proteins (BMPs) (Urist et al., 1982; Urist et al., 1984; Rosen and Wozney, 2002), are not only synthesised by osteoblasts, but by non-osteoblastic cells such as fibroblasts and are stored in the extracellular matrix (ECM) (Globus et al., 1989; Hurley et al., 1994; Rosen and Wozney, 2002). During bone remodeling, these local growth factors are liberated from the ECM (Hauschka et al., 1986; Mohan and Baylink, 1991; Mackie, 2003). The released GFs regulate bone formation by modulating osteoblast proliferation and differentiation in an autocrine and paracrine fashion (Mohan and Baylink, 1991; Lian and Stein, 1995; Mackie, 2003).

Importantly, the proliferative capability of osteoblastic cells diminishes concomitantly with an increase in differentiation (Fig.1.3) (Aubin and Liu, 1996; Franceschi, 1999). The decrease in the proliferation of mature osteoblasts occurs due to the down-regulation of the cell cycle, which normally accompanies the onset of differentiation (Stein and Lian, 1993; Lian and Stein, 1995). It was shown that the BMP-4 induction of MG63 osteoblasts differentiation occurred via the up-regulation of the cyclin-dependent kinase (cdk) inhibitors, $p21^{Cip1}$ and $p27^{Kip1}$, inhibiting cell cycle progression (Fig. 1.4) (Chang et al., 2009). In addition, $p27^{Kip1}$ was also found to be involved in the differentiation of ROS 17/2.8 (Fig. 1.4) (Drissi et al., 1999). Therefore, less differentiated osteoblast precursor cells, such as MSCs and preosteoblasts, proliferate, in contrast to their mature counterparts, which are post-mitotic (Fig. 1.3) (Strauss et al., 1990; Suva et al., 1993; Franceschi, 1999).

Furthermore, primary osteoblasts, isolated from rat calvaria, when grown *in vitro*, formed distinct multilayered foci referred to as nodules (Stein et al., 1990; Lian and Stein, 1993; Lian and Stein, 1995). It was observed that osteoblast cell proliferation first stopped within these individual nodules (Stein et al., 1990; Stein and Lian, 1993); this decline in proliferation is seen as an essential transition step in osteoblast differentiation (Stein and Lian, 1993; Lian and Stein, 1993).

1.3.1.2.3.2 Bone extracellular matrix formation and maturation

The deposition of the ECM by osteoblasts into the resorption pit formed by osteoclasts occurs before mineralisation. The ability to deposit the highly defined matrix, called osteoid, is a hallmark of differentiated osteoblasts. Shortly after the decrease in proliferation, proteins related to a more advance osteoblastic phenotype are expressed (Owen et al., 1990; Pockwinse et al., 1992; Stein and Lian, 1993). For instance, the enzyme activity and mRNA expression of alkaline phosphatase (ALP), which is essential for bone mineralisation, are dramatically increased (Stein et al., 1990; Stein and Lian, 1993). In addition, increased expression of histone H2B, a differentiation-specific histone, has also been observed (Collart et al., 1992; Lian and Stein, 1993; Lian and Stein, 1995). This second period in the osteoblastic differentiation pathway further involves an alteration in the constituents and organisation of the ECM (Stein and Lian, 1993; Lian and Stein, 1995). For example, Type I collagen (Col I) fibrils are converted into collagen fibres via hydroxylation of lysine and proline residues. These hydroxylysine residues are subsequently crosslinked via aldehyde formation, as catalysed by lysyl oxidases, and leads to the stabilisation of collagen fibrils (Siegel, 1974; Rossert and de Combrugghe, 2002). After fibre formation, collagen interacts with non-collagenous matrix proteins, such as fibronectin, and proteoglycans, such as decorin (Fisher and

Termine, 1985; Fisher et al., 1989; Hedbom and Heinegard, 1989). These proteins bind to collagen fibres and contribute to collagen fibre maturation (Hedbom and Heinegard, 1989). Moreover, these modifications render the ECM capable of mineralisation, a process where Col I fibres act as scaffolds for the calcification of osteoid by osteoblasts (Stein and Lian, 1993; Lian and Stein, 1995). When fetal rat calvaria cells were differentiated *in vitro* into mature osteoblasts, it was found that, as cells advance toward the mineralisation phase, all cells stained positive for ALP (Lian and Stein, 1995). ALP hydrolyses phosphomonoesters to release inorganic phosphate (P_i), hence providing Pi for the mineralisation of the ECM (Fernley, 1971; Harris, 1989; Orimo, 2010). In addition, the expression of the collagenase 3 gene (also known as MMP-13) is also increased in this post-proliferative stage and is maximally expressed in mature osteoblasts (Shalhoub et al., 1992). This is important as MMP-13 plays a role in ECM degradation and hence collagen turnover during ECM organisation and maturation by osteoblasts (Gerstenfeld et al., 1987; Stein and Lian, 1993).

1.3.1.2.3.3 Mineralisation of bone ECM

The onset of mineralization defines the third period of osteoblast development. Genes encoding other bone-related proteins, such as osteopontin (OPN), bone sialoprotein (BSP), and osteocalcin (OCN), are increased concomitantly with bone nodule mineralization (Stein and Lian, 1993; Lian and Stein, 1995). Interestingly, OPN is expressed at 25% of maximal levels during the proliferative stage and is maximally induced only during mineralization (Stein and Lian, 1993; Lian and Stein, 1995; Aubin, 1998; Aubin, 2001). The expression profile of BSP is biphasic, initially occurring transiently and then again upon osteoblast maturation (Aubin, 1998; Aubin, 2001). OCN is the matrix protein that is only expressed in the final stages of differentiation, simultaneously appearing with mineralization (Stein and Lian, 1993; Lian and Stein, 1995; Aubin, 1998; Aubin, 2001). Importantly, as ascertained by genetic and molecular studies, these bone-related proteins play an essential role in the development of a mature osteoblastic phenotype, which is the ability to deposit and mineralise osteoid (Narisawa et al., 1997; Fedde et al., 1999; Gordon et al., 2007). In turn, fully functioning osteoblasts are crucial for optimal bone remodeling and hence bone formation. In the case of ALP, a lack of alkaline phosphatase in man causes hypophosphatasia, a genetic disease which leads to disrupted bone mineralization and osteomalacia (bone softening) (Whyte, 1994; Whyte, 2008). In addition, homozygous deletion of ALP in mice (ALP $^{(-/-)}$) also results in severe hypophosphatasia, exhibiting hypomineralization, demonstrating a role for ALP in bone cell mineralisation and bone formation (Narisawa et al., 1997; Fedde et al., 1999). Moreover, overexpression of BSP, another protein essential for mineralization, in the immortalised MC 3T3E1

mouse preosteoblast cell line and in primary rat osteoblasts led to an increase in osteoblast-associated gene expression, calcium incorporation and nodule formation (Gordon et al., 2007). Conversely, inhibition of BSP expression using short hairpin RNA (shRNA) resulted in attenuation of osteoblast-linked gene expression and decreased nodule formation (Gordon et al., 2007). These results demonstrate that BSP is an essential ECM protein capable of promoting osteoblast differentiation and ECM mineralisation (Gordon et al., 2007).

The cellular endpoint of osteoblast function is the mineralization of the secreted osteoid. Although this process has been well-studied, the mechanism of mineralization is not yet completely understood. The most favoured proposed mechanism of bone mineralization involves deposition via small, lipid bilayer membrane-bound spheres called matrix vesicles (MVs) (Anderson, 2003; Golub, 2009; Orimo, 2010). MVs originate through polarised budding from the plasma membrane of chondrocytes, odontoblasts and osteoblasts and are deposited within the ECM (Glaser and Conrad, 1981; Hayashi and Nagasawa, 1990; Anderson, 1995; Xiao et al., 2007). It is noteworthy that the phospholipid content of MV membranes differs from that of the original plasma membrane (Glaser and Conrad, 1981; Hayashi and Nagasawa, 1990; Anderson, 1995; Xiao et al., 2007; Golub, 2009). The membrane of MVs contains several phospholipids, like phosphatidylserine (Peress et al., 1974; Wuthier, 1975), which effectively binds calcium (Ca^{2+}), various annexins (Balcerzak et al., 2003), Ca^{2+} ATPase (Takano et al., 1986; Anderson, 1995), carbonic anhydrase (Anderson, 1995) and alkaline phosphatase (Hoshi et al., 1997; Miao and Scutt, 2002; Balcerzak et al., 2003). These acidic proteins, phosphatases, ion transporters and channels function to regulate Ca^{2+} and Pi levels within the MVs as well as in the extracellular spaces (Anderson, 1995; Montessuit et al., 1991; Roberts et al., 2007). The ratio between Ca^{2+} and Pi above a certain threshold determines hydroxyapetite ($Ca_{10}(PO_4)_5(OH)_2$) crystal formation within the MVs (Orimo, 2010). Enlarged hydroxyapeptite crystals are released into the extracellular space by rupturing MV membranes (Balcerzak et al., 2003; Ozawa et al., 2008; Orimo, 2010). The concept of heterogenous nucleation, where critical nucleation sites other than calcium phosphate nuclei, such as MVs, aid hydroxyapeptite crystal formation, has been proposed as the most probable method of bone mineralization (Glimcher, 1981; Golub, 2009). This mechanism requires an organic or inorganic nucleation initiation site, which guides the subsequent formation of the inorganic hydroxyapetite matrix of bone (Glimcher, 1981; Golub, 2009). Although still a point of contention, it is proposed that MVs could most likely serve as such a primary nucleation site (Wuthier, 1989; Boyan et al., 1990; Anderson, 1995).

Mineralization of the ECM is a complex process and although much headway has been made in elucidating such mechanisms, much work still needs to be done to better our understanding of this biological process.

1.3.1.2.4 Bone lining cells and osteocytes

Once mature osteoblasts have completed their osteoid deposition cycle, they can undergo a number of cellular fates: some undergo programmed cell death (apoptosis), whilst others are either transformed into bone lining cells or osteocytes (Jilka et al., 1998; Manolagas, 2000).

Bone lining cells are flat, non-proliferative cells that cover the quiescent bone surfaces, that is, bone which is not undergoing formation, nor resorption (Jilka et al., 1998; Marks and Odgren, 2002). Not much is known concerning the functions of these cells. However, it has been proposed that bone lining cells are able to revert into an osteoblastic phenotype under certain conditions (Dobnig and Turner, 1995; Leaffer et al., 1995; Marks and Odgren, 2002). Therefore, bone lining cells could possibly serve as a precursor cell reservoir for osteoblasts. Another putative function for bone lining cells is the regulation of bone remodeling through BMU activation in response to stimuli from osteocytes and hormones (Rodan and Martin, 1981; Matsuo and Irie, 2008; Sims and Gooi, 2008).

Osteocytes are located regularly at sites within the hardened bone matrix or newly deposited osteoid in spaces, called lacunae, and canals, referred to as canaliculi (Marks and Odgren, 2002; Knothe Tate et al., 2004; Noble, 2008). Osteocytes are the most abundant cell type in bone (Marks and Odgren, 2002; Knothe Tate et al., 2004; Noble, 2008). Like bone lining cells, osteocytes are also post-mitotic cells and represent the terminal differentiation stage of osteoblasts (Marks and Odgren, 2002; Noble, 2008). Osteocytes have cytoplasmic/pseudopod-like processes that give them a dendritic appearance (Palumbo, 1986; Nijweide et al., 2002). The bodies of osteocytic cells are housed within the lacunae, whereas the dendrites are found in the canaliculi (Bonewald, 1999; Nijweide et al., 2002). The dendritic protrusions of osteocytes serve as channels for metabolic exchange (Baud, 1968; Plotkin et al., 2002; Knothe Tate, 2003). More importantly, they connect osteocytes to each other as well as to other bone cells, such as lining cells and osteoblasts (Palumbo et al., 1990; Marks and Odgren, 2002; Knothe Tate et al., 2004). Together with the gap junctions between adjacent osteocyte processes, these systems form intercellular communication networks between osteocytes (Doty, 1981; Knothe Tate, 2003; Knothe Tate et al., 2004). The connection of all these bone cells within the lacunocanalicular system in bone is referred to as a functional syncytium (Aarden et al., 1994; Nijweide et al., 2002; Knothe Tate, 2003). The lacunocanalicular

system, housing the syncytium of gap junctions, is filled with extracellular fluid and various proteoglycans (Knothe Tate, 2003). Therefore, the osteocyte syncytium consists of an intracellular system of lacuna connected to canaliculi as well as an extracellular network of fluid-saturated proteoglycans (Knothe Tate, 2003; Knothe Tate et al., 2004). These dendritic processes also appear to directly connect osteocytes with the bone marrow (Kamioka et al., 2001). Therefore, osteocytes could possibly function to recruit cells such as osteoclast precursors and MSCs from this compartment (Kamioka et al., 2001; Zhao et al., 2002; Heino et al., 2004).

The elucidation of osteocyte function is far from complete. To date, a number of osteocyte functions have been proposed, primarily involving the control of bone formation and resorption (Noble, 2008). It has been demonstrated that osteocytes regulate bone formation by producing factors that inhibit the activity of osteoblasts (Noble, 2008). For example, sclerostin is produced by osteocytes and is a negative modulator of osteoblast activity and hence bone formation (van Bezooijen et al., 2005). It has also been proposed that osteocytes might support osteoclast recruitment and function through a mechanism involving either (i) the loss of anti-resorptive signals or (ii) the acquisition of pro-resorptive signals, leading to heightened bone resorption (Noble, 2008). Such anti-resorptive factors secreted by osteocytes include oestrogen-stimulated TGF-β. Osteocytes may also increase the expression of endothelial cell nitric oxide synthase (ecNOS) and, consequently, the anti-resorptive factor, nitric oxide (NO) (Heino et al., 2002; Loveridge et al., 2002). In addition, it has also been shown that osteocytes produce factors such as RANKL and M-SCF that stimulate osteoclast generation from progenitors (Zhao et al., 2002). Therefore, by producing factors that promote osteoclast differentiation and activation, osteocytes could stimulate bone resorption. Moreover, osteocyte apoptosis has also been suggested as a mechanism to induce osteoclastic resorption (Noble, 2003; Noble, 2008). It has long been proposed that osteocytes function as sensors for mechanical strain or increased load as part of the adaptive response of bone to maintain bone health (Aarden et al., 1994; Burger and Klein-Nulend, 1999; Knothe Tate et al., 2004). The mechanisms through which osteocytes execute this function include the production or modification of factors such as prostaglandin E2 (PGE2), IGF-1 and Col I as well as mineral transport (Lean et al., 1995; Rawlinson et al., 1995; Sun et al., 1995; Ajubi et al., 1996). According to Noble (2008), despite osteocytes being the most copious cells in bone, they are the least researched. However, research is ongoing to determine the full scope of osteocytes as local regulators of bone turnover.

1.3.1.3 Bone Remodeling

Adult bone continuously undergoes remodeling in an asynchronous, cyclic manner throughout the skeleton, to maintain a healthy bone structure. Bone remodeling is activated in response to various signals. These include calcium imbalances, mechanical stress, fracture repair, bone cell turnover, hormones, cytokines and local growth factors (Parfitt, 1994; Datta et al., 2008). Aberrant bone remodeling can cause metabolic bone diseases, such as osteopetrosis and osteoporosis (Parfitt, 1994; Seeman and Delmas, 2006; Sims and Gooi, 2008). Normal bone remodeling requires that the delicate balance between bone resorption by osteoclasts and new bone synthesis by osteoblasts is sustained. Osteoclasts and osteoblasts form the executors of bone remodeling, known as the basic multicellular unit (BMU) (Frost, 1963; Parfitt, 1984; Parfitt, 1994; Buenzli et al., 2010). A fully functional BMU consists of a set of osteoclasts at the front, separated by a source of blood supply from a set of osteoblasts at the rear, a nerve supply and related extracellular matrix (Parfitt, 1994; Jilka, 2003). In addition, BMUs are temporary cellular formations which function as independent entities throughout bone remodeling events (Parfitt, 1994). As referred to in section 1.3.1.2.4, osteocytes and bone lining cells are also involved in the initiation of bone remodeling (Rodan and Martin, 1981; Zhao et al., 2002; Noble, 2003; Matsuo and Irie, 2008).

Bone remodeling is a complex cellular process. In short, once the bone remodeling program is initiated, the collagenous membrane of the inner lining of the cortex (called the endosteum) is digested by matrix metalloproteinases (MMPs) (Parfitt et al., 1996; Parfitt, 2002). This process is followed by mononuclear osteoclast recruitment from the bone marrow, their subsequent fusion to form multinuclear osteoclasts, and activation of differentiated osteoclasts (as described in section 1.3.1.2.1) (Engsig et al., 2000; Teitelbaum, 2000; Sims and Gooi, 2008). Activated osteoclasts then break down the underlying bone surfaces and remove the resultant minerals as outlined in section 1.3.1.2.1 (Baron, 1995; Vaananen and Zhao, 2002; Sims and Gooi, 2008). After the resorption by osteoclasts, the resorption pits are cleaned and bone formation starts in the “reversal phase”, which involves mononuclear cells, suggested to be either haematopoietic phagocytes or bone lining cells (Tran Van et al., 1982; Everts et al., 2002; Sims and Gooi, 2008). This reversal phase concludes the resorption process possibly by not only cleaning the resorption pit, but by the modification of the bone surface through developing a “reversal line” (Tran Van et al., 1982; Everts et al., 2002). Following the “reversal phase”, osteoblasts precursor cells are recruited to the resorption cavity from the bone marrow, possibly by factors released during resorption, and these cells are driven to expand and differentiate (as stated in sections 1.3.1.2.2 and 1.3.1.2.3). New osteoid, consisting, of collagenous and non-collagenous proteins, is then deposited by these osteoblasts in the resorption

cavity (see section 1.3.1.2.3.3) (Salo et al., 1997; Nesbitt and Horton, 1997). This extracellular matrix eventually becomes calcified to form bone (Balcerzak et al., 2003; Ozawa et al., 2008; Orimo, 2010).

The activity of osteoclasts and osteoblasts in the BMU is coupled (Frost, 1964; Parfitt, 1982; Sims and Gooi, 2008). This means that the amount of bone replaced by osteoblasts is the same as the amount of bone initially removed by osteoclasts (Frost, 1964; Parfitt, 1982; Sims and Gooi, 2008). The precise coupling mechanism between the activities of osteoclasts and osteoblasts is not yet fully understood. However, it is suggested to involve osteoclast-and osteoblast-derived factors as well as cell-cell contact between these cell types (Sims and Gooi, 2008). It was shown that ephrinB2, a ligand located on the membrane of osteoclasts, interacts with the corresponding receptor, EphB2, found on the surfaces of osteoblasts, to regulate osteoblast differentiation and bone formation (Zhao et al., 2006). Moreover, it was also illustrated that if the negative signal comes from the osteoblast, osteoclast differentiation is inhibited (Zhao et al., 2006).

The lifespan of osteoclasts and osteoblasts is approximately 2 weeks and 3 months, respectively (Manolagas, 2000). An active BMU, however, has an extended lifespan of between 6 and 9 months (Manolagas, 2000), as there is cell turnover within the unit. Consequently, the efficient functioning of the BMU is dependent on the continuous supply of precursor cells for both osteoclasts and osteoblast. Not only is this important for BMU origination (initiation of BMU formation), but also for advancement of the BMU on the bone surface. The net amount of functional osteoclasts and osteoblasts is thus determined by the constant replenishment of new cells as well as their average lifetime within the BMU. This highlights the need for continuous replacement of osteoclasts and osteoblasts in the BMU, throughout bone remodeling. Moreover, it has been demonstrated that osteoclasts and osteoblasts regulate their own development as well as that of each other, through intricately regulated intercellular communication networks. The primary focus of the work presented in this thesis is osteoblast development; hence, further discourse will concentrate on the signalling pathways regulating the development of osteoblasts.

1.4 Signalling pathways regulating osteoblast development

As stated before, bone homeostasis is controlled by the balance between osteoclastic bone resorption and osteoblastic bone formation. Osteoblast precursor cells undergo multiple stages of differentiation, coinciding with alterations in gene transcription and appearance of osteoblast-

related proteins, to ultimately become mature osteoblasts capable of forming bone. In addition, osteoblast precursor cells like stromal cells and preosteoblasts, receive certain stimuli to activate or inhibit the differentiation program towards a mature phenotype. Extracellular and intracellular signals are received by osteoblastic cells through appropriate receptors. These signals are then relayed, amplified and integrated via cascades of interacting proteins called signal transduction pathways to alter gene and protein expression and metabolism.

A number of protein signal transduction pathways involved in osteoblastic development have been characterised. For example, the wingless (wnt)/β-catenin pathway (or canonical wnt pathway) has been found to, through various mechanisms, be involved in aspects of osteoblast biology for instance it (i) regulates stromal cell renewal (Reya and Clevers, 2005), (ii) stimulates preosteoblasts proliferation (Bodine et al., 2004), (iii) induces osteoblastogenesis (Bodine et al., 2004; Bennett et al., 2005) and (iv) inhibits apoptosis of osteoblasts and osteocytes (Kato et al., 2002). Another signalling pathway recognized to modulate osteoblast differentiation is the transforming growth factor β (TGFβ)-BMP/SMAD pathway (Nohe et al., 2003; Nohe et al., 2004), through the regulation and interaction with osteoblast-related TFs such as Runx2 (Lee et al., 2000; Yang et al., 2003; Phimphilai et al., 2006) and Osx (Lee et al., 2003). Moreover, the wnt/β-catenin and the TGFβ-BMP/SMAD pathways can also regulate osteoblast development through cross-talk with each other (Nakashima et al., 2005; Guo and Wang, 2009) as well as other pathways such as the mitogen-activated protein kinase (MAPK) signal transduction pathways (Sowa et al., 2002; Hay et al., 2009; Kilian et al., 2010). Three MAPK signalling pathways, namely the c-Jun N-terminal kinase/stress-activated protein kinase (JNK/SAPK), p38 MAP kinase and the extracellular signal-regulated kinase (ERK1/2 ; also known as p44/p42 ERK) signalling cascades, have been extensively characterised in numerous cell types and cellular responses (Seger and Krebs, 1995; Robinson and Cobb, 1997; Krens et al., 2006; Keshet and Seger, 2010). MAPK signalling pathways have been shown to regulate many aspects of osteoblast development (Jaiswal et al., 2000; Suzuki et al., 2002; Engelbrecht et al., 2003; Mehrotra et al., 2004; Horsch et al., 2007; Ortuno et al., 2010).

Findings indicate that p38 MAPK is involved in the regulation of osteoblast differentiation (Suzuki et al., 1999; Suzuki et al., 2002; Ortuno et al., 2010) rather than proliferation (Suzuki et al., 2002). p38 MAPK was found to facilitate the BMP-2-induced differentiation of MC3T3-E1 preosteoblasts through the phosphorylation of the osteoblast-related TF, osterix (Osx) (Ortuno et al., 2010). Phosphorylation of Osx led to enhanced recruitment of transcriptional coactivators such as p300 to

the promoter region of the BSP gene (Ortuno et al., 2010). Also in MC3T3-E1 preosteoblasts, p38 MAPK was shown to regulate activity of the bone marker, ALP, after adrenalin and BMP-2 stimulation (Suzuki et al., 1999; Guicheux et al., 2003). In addition, results indicate that p38 MAPK is involved in the migration of MC3T3-E1 preosteoblasts, a response which is essential for bone remodeling and fracture repair (Mehrotra et al., 2004). Furthermore, p38 MAPK was found to regulate the Ca^{2+}-stress response elicited by the bone matrix protein, dentin matrix protein (DMP), to stimulate osteoblast-specific gene expression and differentiation (Eapen et al., 2010).

Although some findings show that JNK could be involved in the proliferation of osteoblastic cells (Mehrotra et al., 2004; Suzuki et al., 2002), other results indicate that JNK is involved in the regulation of late differentiation responses in osteoblasts (Guicheux et al., 2003; Matsuguchi et al., 2009). JNK was shown to play a role in the expression of late osteoblastic markers such as OCN and BSP in response to differentiation stimuli such as BMP-2, ascorbic acid /β-Glycerophosphate and fetal calf serum (Suzuki et al., 2002; Guicheux et al., 2003; Matsuguchi et al., 2009). Therefore, it appears that JNK regulates the later stages of osteogenesis. A role for JNK in the PDGF-induced migration of MC3T3-E1 has also demonstrated (Mehrotra et al., 2004).

The formation of microvasculature during bone remodeling is essential for processes such as osteoblast recruitment, growth factor synthesis and delivery as well as coupling of bone resorption and formation (Parfitt, 2000). JNK has been shown to regulate the FGF2-stimulated synthesis of vascular endothelial growth factor (VEGF), which promoted angiogenesis (Kato et al., 2010). Moreover, it was shown that JNK regulates the TGFβ-suppression of the ECM protein, nephronectin, which is an adhesion molecule involved in osteoblast differentiation (Miyazono et al., 2007). This is in accordance with the findings of Jaiswal et al. (2000), where JNK activation occurred 13 to 17 days into the differentiation program of hMSCs and was associated with ECM production and Ca^{2+} deposition.

Despite findings that these individual MAPKs have distinct roles (Suzuki et al., 2002; Guicheux et al., 2003), evidence indicates that p38, JNK and ERK1/2 MAPKs are also involved in crosstalk to regulate osteoblast differentiation (Sowa et al., 2002; Kato et al., 2010; Kilian et al., 2010). However, the precise role of ERK1/2 in osteoblast development is controversial (Schindeler and Little, 2006). Several studies show that ERK1/2 stimulates osteoblast differentiation (Lai et al., 2001; Xiao et al., 2002; Kaiser and Chandrasekhar, 2003; Miraoui et al., 2009; Peng et al., 2009), whereas others demonstrate that this pathway is inhibitory (Chaudhary and Avioli, 2000; Higuchi et al., 2002; Kono et al., 2007). Further discourse will concentrate on the ERK1/2 signalling pathway

and how ERK 1/2 is proposed to regulate osteoblast development. The regulation of ERK1/2 activity will be discussed, including the regulation of ERK1/2 dephosphorylation by phosphatases such as MAPK phosphatase-1 (MKP-1).

1.4.1 The ERK1/2 signalling pathway

Activation of the ERK1/2 signalling cascade occurs when ligands such GFs (EGF, IGF) (Marshall, 1995; Zhang et al., 1995; Vincent and Feldman, 2002; Qiao et al., 2004) or differentiating factors (for instance BMP-2 and integrin $\alpha 2\beta 1$) (Higuchi et al., 2002; Xiao et al., 2002; Barberis et al., 2000), bind to the corresponding receptors, resulting in receptor activation. ERK1/2 is activated in a signalling cascade by receptor tyrosine kinases (RTKs) (van der Geer et al., 1994; Weiss and Schlessinger, 1998) and by G-coupled protein receptors (GPCRs) (Gudermann et al., 1997; Gudermann et al., 2000; van et al., 1996) as depicted in Fig.1.5. Following RTK activation, adaptor proteins such Grb2 bind to the activated RTKs and interact with the guanine exchange factor, Sos, which is consequently recruited to the plasma membrane (Fig. 1.5) (Egan et al., 1993; Li et al., 1993; Buday and Downward, 1993; Langlois et al., 1998; Skolnik et al., 1993). Here the Grb2-Sos complex drives the exchange of GDP for GTP on the small GTP binding protein, Ras, thereby leading to Ras activation (Fig. 1.5) (Waters et al., 1995; Aronheim et al., 1994; Avruch et al., 1994). Activated Ras then binds to and consequently activates the mitogen-activated protein kinase kinase kinase (MAP3K), Raf, which then phosphorylates and thereby activates the mitogen-activated protein kinase kinase (MAP2K), MEK1/2, by phosphorylating the serine residue in the MEK activation loop (Fig. 1.5) (Kyriakis et al., 1992; Moodie et al., 1993; Vojtek et al., 1993; Avruch et al., 1994; Zheng and Guan, 1994). Upon activation, MEK phosphorylates the MAPK, ERK1/2, on adjacent threonine and tyrosine residues in the ERK1/2 activation loop, leading to ERK1/2 activation and nuclear translocation (Fig. 1.5) (Crews et al., 1991; Crews and Erikson, 1992; Crews et al., 1992). In turn, activated ERK1/2 can phosphorylate and regulate cytoplasmic-, membrane-associated-, and nuclear proteins such as p70RSK (p70 ribosomal S6 kinase), EGF receptor and numerous transcription factors, such as c-myc and Ets1 and Elk-1 (Murphy et al., 2002; Zhang and Liu, 2002; Murphy and Blenis, 2006). These ERK1/2 targets then regulate the downstream cellular and molecular events to culminate in the appropriate metabolic and physiological responses, such as proliferation, differentiation and survival.

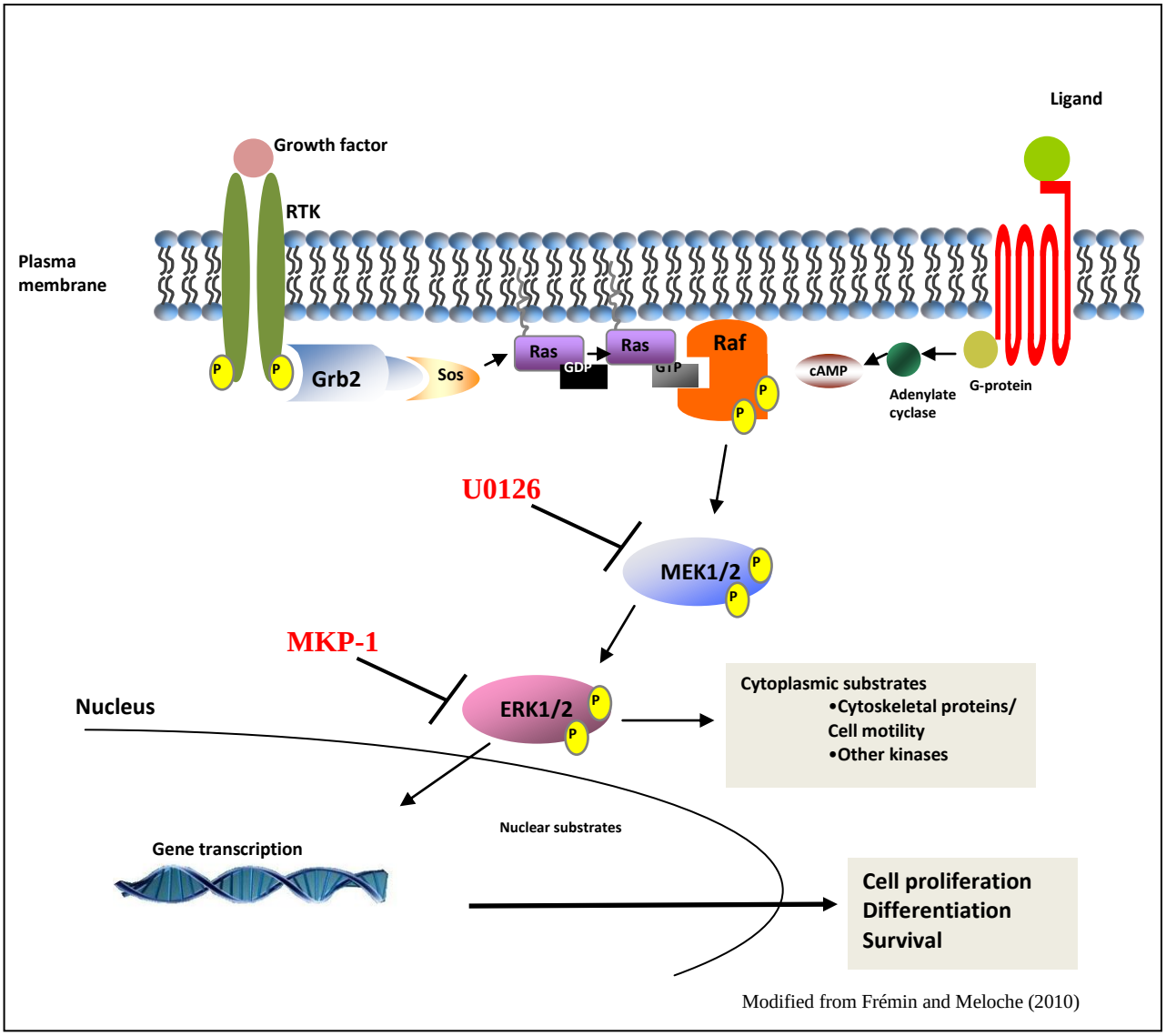

Figure 1.5: The ERK 1/2 signalling pathway.

Activation of the ERK1/2 pathway via RTKs and GPCRs is illustrated. For further details refer to text. **Abbreviations**: **cAMP** cyclic adenosine monophosphate; **ERK1/2** extracellular signal-regulated kinase; **GPCR** G-coupled protein receptors; **MKP-1** MAPK phosphatase; **RTK** receptor tyrosine kinase; **Sos** son-of-sevenless

1.4.2 Role of the ERK1/2 signalling pathway in osteoblast development

The ERK1/2 pathway is considered to be the major regulator of proliferative responses in many cell types in response to growth factors and mitogens (Zhang and Liu, 2002; Katz et al., 2007; Assoian and Schwartz, 2001). With regard to osteoblasts, studies using pharmacological inhibitors of the ERK1/2, JNK and p38 MAPK pathways demonstrated that ERK1/2 was the main pathway regulating proliferation in immortalised human (MG-63) and mouse preosteoblast (MBA-15.4 and MC3T3-E1) cell lines (Horsch et al., 2007; Mehrotra et al., 2004). However, the role of ERK1/2 in osteogenesis is contentious; as findings that ERK1/2 acts as an antagonist of osteogenesis have also been reported (Schindeler and Little, 2006). It has been shown that elevated ERK1/2 signalling, as

elicited by concomitant stimulation with GFs (EGF and FGF) and osteogenic factors (ascorbic acid, β-glycerophosphate and BMP-2), prevented the osteogenic differentiation of several osteoblastic cell lines including MC 3T3-E1, MG 63 and bone marrow cells (Higuchi et al., 2002; Xiao et al., 2002). Therefore, increased GF-induced ERK1/2 activity can be associated with decreased osteoblast differentiation. Furthermore, inhibition of the ERK1/2 pathway by using pharmacological inhibitors such as U0126 and PD98059 resulted in improved differentiation of osteoblasts in culture (Higuchi et al., 2002; Xiao et al., 2002).

However, there is growing support for the theory that ERK1/2 is an agonist of osteoblast differentiation (Lai et al., 2001; Xiao et al., 2002; Kaiser and Chandrasekhar, 2003; Miraoui et al., 2009; Peng et al., 2009). The treatment of human MSCs with osteogenic stimulants like ascorbic acid and β-Glycerophosphate resulted in osteogenic differentiation of these cells which coincided with the sustained activation of ERK1/2 (Jaiswal et al., 2000). In C2C12 mouse myoblasts and MC3T3-E1 preosteoblasts, the activation of ERK1/2 was shown to be essential for BMP-2 stimulated osteoblastic differentiation (Gallea et al., 2001; Higuchi et al., 2002). Similar *in vitro* studies showed that constitutive expression of MEK1, the kinase upstream of ERK1, expedited the differentiation of murine calvarial cells and augmented *in vivo* bone development in mice, whilst dominant negative MEK1 impeded bone formation (Ge et al., 2007). Reports also show that ERK1/2 regulated the BMP-2-stimulated induction of osteoblast-specific genes such as Runx2, OCN and BSP as well as osteogenesis of MC3T3-E1 cells (Xiao et al., 2002). Moreover, it was reported that ERK1/2 induced osteogenesis through the phosphorylation of the master regulator of osteoblast differentiation, Runx2 (Ge et al., 2007; Xiao et al., 2002). Furthermore, a role for ERK1/2 in the expression of $\alpha\beta_1$, $\alpha_v\beta_3$ and $\alpha_v\beta_5$ integrins and adherence of human osteoblasts to the ECM has been described (Lai et al., 2001). However, it has been shown that ERK1/2 is involved in the downregulation of the type I procollagen gene in response to FGF-2, PDGF-BB (the homodimer of PDGF-B subunit) and okadaic acid (a phosphoserine/threonine-specific protein phosphatase inhibitor and ERK1/2 activator) (Chaudhary and Avioli, 2000). However, it has also been demonstrated that ERK1/2 is a negative regulator of matrix mineralization in MC3T3-E1 preosteoblasts as well as in mice (Kono et al., 2007).

In conclusion, it therefore appears that ERK1/2 regulates early events in the osteogenic differentiation program such as proliferation, Runx2 transcription and migration and adherence of osteoblastic cells to the ECM, but inhibits later differentiation events such ECM synthesis and mineralisation.

1.4.3 Regulation of ERK1/2 activity

1.4.3.1 Proliferation versus differentiation

The regulation of cell proliferation by ERK1/2 is multifaceted and intricate. Most of the work to elucidate ERK1/2 function in proliferation has been done on cells such as PC12 cells (pheochromocytoma cells) and fibroblasts (Dobrowolski et al., 1994; Gotoh et al., 1990; Nguyen et al., 1993; Marshall, 1995; Balmanno and Cook, 1999; Ebisuya et al., 2005). Not only is ERK1/2 activation a requirement for cell cycle progression and hence, cell proliferation, but the duration, magnitude and subcellular location of the ERK1/2 signal are also determinants of cellular outcome (Marshall, 1995; Ebisuya et al., 2005). An example of how the duration of ERK activation affects cellular fate is evident when quiescent fibroblasts are stimulated with thrombin or PDGF (platelet-derived growth factor); a sustained rather than transient activation of ERK1/2 is necessary for S phase entry and proliferation (Dobrowolski et al., 1994; Balmanno and Cook, 1999). In addition, EGF and thrombin-mimicking peptide (TMP) elicits transient ERK1/2 activation, which is insufficient for S phase entry and thereby inhibits cell cycle progression and proliferation (Vouret-Craviari et al., 1993; Murphy et al., 2002). In contrast to fibroblasts, when PC12 cells are treated with NGF (nerve growth factor) ERK activation is sustained and results in neuronal differentiation, whereas when they are treated with EGF, transient ERK activation is elicited, causing cells to proliferate (Gotoh et al., 1990; Nguyen et al., 1993; Marshall, 1995; Ebisuya et al., 2005).

Cell fate is also determined by the level of ERK1/2 activity (Shaul and Seger, 2007a). Modest ERK1/2 activation induces the expression of cyclin D1 and cyclin E, leading to the formation and accumulation of the active CDK complexes needed for cell cycle progression (Ebisuya et al., 2005). On the contrary, various studies have shown that strong ERK1/2 activation results in cell cycle arrest, rather than cell cycle progression (Sewing et al., 1997; Woods et al., 1997; Roovers and Assoian, 2000). A possible reason for this phenomenon is that elevated levels of ERK1/2 activity regulate the transcription and post-transcriptional modification of the CDK inhibitor, $p21^{waf}$ (Coleman et al., 2003). The induction of $p21^{waf}$ decreases CDK activity, which ultimately causes G1 arrest (Coleman et al., 2003).

The subcellular location of ERK1/2 also contributes to the cellular outcome, as ERK1/2 can move between the cytoplasm and nucleus. In quiescent cells, ERK1/2 is mostly found in the cytoplasm (Ebisuya et al., 2005; Shaul and Seger, 2007b; Yao and Seger, 2009). Although it has been reported that ERK1/2 can bind to the nuclear pore complex , ERK1/2 is mostly retained in the cytoplasm through binding to either MEK or MKP-3 (MAPK phosphatase 3) (Fukuda et al., 1996;

Matsubayashi et al., 2001; Whitehurst et al., 2002; Karlsson et al., 2004). Activated ERK1/2 dissociates from MEK or MKP-1, translocates to the nucleus and phosphorylates its nuclear targets, such as the transcription factors Elk-1 (Janknecht et al., 1993; Gille et al., 1995) and Ets1 (Yang et al., 1996; Slupsky et al., 1998; Foulds et al., 2004). It has been shown that nuclear translocation of ERK1/2 is essential for proliferation of fibroblasts and differentiation of PC12 cells (Robinson et al., 1998; Brunet et al., 1999).

Various mechanisms regulating the duration, levels as well as cellular compartmentalisation of ERK1/2 have been proposed (Marshall, 1995; Ebisuya et al., 2005). However, it is clear that different mitogens elicit different ERK1/2 activation profiles. In addition, these diverse ERK1/2 induction profiles are important in the determination of the cellular outcome elicited by these factors.

1.4.3.2 Phosphatase regulation of ERK1/2 activity

As cited before, the duration and magnitude of the ERK1/2 signal, as well as sub-cellular compartmentalisation of activated ERK1/2 are determinants of the cellular outcomes following specific stimulation (Marshall, 1995; Ebisuya et al., 2005). Therefore, attenuation of ERK1/2 activity will impede these cellular outcomes. Inactivation of activated ERK1/2, like other MAPKs, such as JNK and p38 MAPK, occurs through dephosphorylation of specific amino acids in the activation loops (Hunter, 1995; Keyse, 2000; Saxena and Mustelin, 2000; Keyse, 2008b). In the case of activated ERK1/2, the dephosphorylation of tyrosine and threonine residues in the ERK activation loop leads to inactivation of this particular MAPK (Hunter, 1995; Keyse, 2000; Saxena and Mustelin, 2000; Keyse, 2008b). This removal of phosphates from specific residues is catalysed by protein phosphatases.

ERK1/2 dephosphorylation, and consequent inactivation, is catalysed by at least two classes of phosphatase enzymes: serine/threonine phosphatases such as PP2A and PP2C (Sontag et al., 1993; Wang et al., 2003; Friedman and Perrimon, 2006) or protein tyrosine phosphatases (PTPs) such as SHP-1 and SHP-2 (Shi et al., 2000; Zhang et al., 2004; Nakata et al., 2011). In addition, a subclass of PTPs, known as the dual-specificity phosphatases (DUSPs), which include the MAP kinase phosphatases (MKPs), is also capable of phosphate removal from activated ERK1/2 (Owens and Keyse, 2007; Keyse, 2008b; Patterson et al., 2009). These MKPs particularly dephosphorylate both threonine and tyrosine residues in the ERK1/2 activation loop (Owens and Keyse, 2007; Keyse, 2008b; Patterson et al., 2009).

MKPs are capable of dephosphorylating p38 MAPK, JNK and ERK1/2 (Owens and Keyse, 2007; Keyse, 2008b; Patterson et al., 2009). However, although this dual-specificity phosphatase subclass is able to remove phosphates from the major MAPKs, MKPs vary in substrate specificity for different MAPKs (Owens and Keyse, 2007; Keyse, 2008b; Patterson et al., 2009). MKP isotypes also differ in tissue specificity, sub-cellular compartmentalisation and induction by extracellular stimuli (Keyse, 1998; Reffas, 2000). For example, MKP-3 is a cytoplasmic MKP which displays preference to ERK1/2 and ERK5 as substrates (Groom et al., 1996; Mourey et al., 1996; Muda et al., 1996a; Muda et al., 1996b). Moreover, MKP-3 shuttles between the cytoplasm and the nucleus and also serves as an anchor for ERK1/2 in the cytoplasm (Karlsson et al., 2004). It has, therefore, been suggested that MKP-3 may play a part in the regulation of the cytoplasmic localisation of ERK1/2 (Karlsson et al., 2004).

Dissimilar to MKP-3, MKP-1 is a nuclear MKP, which was first identified as an immediate early gene with a rapid induction pattern elicited by stimulation with growth factors (Charles et al., 1993; Noguchi et al., 1993), heat shock (Keyse and Emslie, 1992) and oxidative stress (Keyse and Emslie, 1992). In early *in vitro* studies done in fibroblasts, it was demonstrated that the temporal induction profile of MKP-1 after stimulation was similar to that of ERK1/2 (Alessi et al., 1993; Sun et al., 1993; Zheng and Guan, 1993). These *in vitro* studies showed that purified recombinant MKP-1 dephosphorylated and therefore attenuated ERK1/2 (Alessi et al., 1993; Sun et al., 1993; Zheng and Guan, 1993). However, the cellular regulatory role of MKP-1 appears to be complex. It was later demonstrated that MKP-1 exhibited an enhanced specificity towards JNK and p38 MAPK, instead of ERK1/2 under physiological conditions in T-cells (Chu et al., 1996; Dorfman et al., 1996; Franklin and Kraft, 1997). In addition, findings also revealed that MKP-1 inactivated JNK and p38 MAPK more efficiently than ERK1/2 *in vitro* (Chu et al., 1996; Dorfman et al., 1996; Franklin and Kraft, 1997). Furthermore, it was shown that MKP-1 deficient mice developed normally and are fertile (Dorfman et al., 1996). Moreover, ERK1/2 activation, cell growth and c-fos expression in fibroblasts from these mice lacking MKP-1 were unaltered (Dorfman et al., 1996). This is in contradiction to the general acceptance that MKP-1 is considered to be the primary phosphatase that deactivates ERK1/2 in immortalised preosteoblasts (see section 1.4.3.4) (Engelbrecht et al., 2003; Horsch et al., 2007).

1.4.3.3 Regulation of MKP-1 activity

MKP-1 expression and activity are tightly regulated at multiple levels. MKP-1 mRNA expression is up-regulated by growth factors (Charles et al., 1993; Noguchi et al., 1993; Engelbrecht et al., 2003), hormones (Clark, 2003; Sarkozi et al., 2007; Datta et al., 2010), oxidative stress (Keyse and Emslie, 1992; Tournier et al., 1997; Xu et al., 2004), hypoxia (Laderoute et al., 1999; Seta et al., 2001) and heat stress (Keyse and Emslie, 1992; Gorostizaga et al., 2004; Gorostizaga et al., 2005). Induction of MKP-1 expression after stimulation with growth factors, heat shock and oxidative stress is a result of ERK1/2 activation (Keyse and Emslie, 1992; Charles et al., 1993; Noguchi et al., 1993). In addition, transcription factors such as AP-1 (c-Fos, c-Jun and ATF2) (Laderoute et al., 1999; Casals-Casas et al., 2009; Kristiansen et al., 2010) and NF-κB (Wang et al., 2008) have been shown to associate with the MKP-1 promoter to induce MKP-1 transcription. Importantly, MKP-1 gene expression is also under control of the ligand-activated GC receptor (Kassel et al., 2001; Shipp et al., 2010). MKP-1 has thus emerged as a major molecular target of GCs in many cell types (Kassel et al., 2001; Roger et al., 2005 and Nicoletti-Carvalho et al., 2010). As with many genes, it has been found that the phosphorylation and acetylation of histone H3 leads to chromatin changes at the MKP-1 locus, resulting in heightened association of RNA polymerase II to the MKP-1 gene promoter, thereby increasing gene transcription (Li et al., 2001).

MKP-1 mRNA is regulated at a post-transcriptional stage by binding of various RNA-binding proteins such as embryonic lethal abnormal vision (ELAV) Hu-antigen R (HuR) (Kuwano et al., 2008; Lin et al., 2008), TTP (tristetraprolin or zinc finger protein 36) (Lin et al., 2008) and nuclear factor 90 (NF90) (Kuwano et al., 2008) resulting in increased mRNA stability. Moreover, HuR and NF90 have opposing effects on MKP-1 mRNA translation: whereas HuR binding leads to increased translation, NF90 is associated with translational repression of the MKP-1 transcript (Kuwano et al., 2008). Binding to substrates, such as ERK1/2, via the MAPK-binding (MKB) domain, enhances the catalytic activity of MKP-1 (Slack et al., 2001). The modulation of MKP-1 protein levels plays an important role in the sustained activation of ERK1/2 (Lin et al., 2003). It is important to note that the MKP-1 protein is directly phosphorylated by ERK1/2 (Brondello et al., 1999) and indirectly by p38 MAPK via MAPKAP (MAPK activating protein) kinase (Hu et al., 2007). This consequently leads to the stabilisation of the MKP-1 protein, which is then protected against ubiquitin-mediated degradation (Brondello et al., 1999; Hu et al., 2007). In addition, MKP-1 mRNA is also modulated post-transcriptionally by microRNA (miRNA) (Zhu et al., 2010). It was recently shown in macrophages that MKP-1 is a direct target of miRNA-101 (Zhu et al., 2010). However, this has not yet been tested in osteoblastic cells.

This tight, multi-tiered control of MKP-1 expression and activity emphasises the intricacy of this dual-specificity phosphatase in the regulation of MAPK signalling. Furthermore, it also highlights that MKP-1 should be expressed at the appropriate levels and time in response to the specific stimuli.

1.4.3.4 The action of MKP-1 in osteoblasts

Overexpression of MKP-1 resulted in the inhibition of immortalised preosteoblast proliferation (Horsch et al., 2007). In the preosteoblast cell lines, murine MBA-15.4 and human MG-63, it has been shown that Dex up-regulated MKP-1 mRNA expression by 10-fold within 30 minutes, remaining at elevated levels for up to 24 hours (Engelbrecht et al., 2003). Moreover, a correlation was found between Dex-induced MKP-1 protein expression and attenuation of ERK1/2 phosphorylation after mitogen stimulation (Engelbrecht et al., 2003; Horsch et al., 2007). Results of an *in vitro* phosphatase assay illustrated that MKP-1 dephosphorylates mitogen-induced ERK1/2 and that ERK1/2, not JNK or p38 MAPK, regulates immortalised preosteoblast proliferation (Horsch et al., 2007). Therefore, these findings offer a possible mechanism for the modulation of the proliferation of osteoblasts. However, very little is known about the effects of GCs on the proliferation of primary osteoblast precursor cells, such as MSCs and early preosteoblasts, by GCs.

1.5 Effects of GCs on bone formation and bone homeostasis

The naturally occurring GC, cortisol, regulates a number of physiological processes, such as metabolism (glucose, protein and fat), stress reactions, immune responses (anti-inflammatory and immunosuppressive) as well as bone formation (Schoneveld et al., 2004; McEwen, 2008; Chrousos and Kino, 2009). However, these responses are elicited by low, physiological levels of cortisol (McEwen, 2008; Chrousos and Kino, 2009). In contrast, continuous, elevated levels of endogenous GCs, such as cortisol, may lead to pathophysiologic conditions such as hypercorticism; as in the case of Cushing's syndrome (Cushing, 1994; Mancini et al., 2004; Kaltsas and Makras, 2010). Severe osteoporosis is a secondary clinical consequence of such hypercorticism (Cushing, 1994; Mancini et al., 2004; Kaltsas and Makras, 2010).

A variety of synthetic GCs have been developed that mimic the actions of endogenous GCs (Vayssiere et al., 1997; Newton, 2000; Simons, Jr., 2008). These include short-acting GCs such as hydrocortisone and cortisone, intermediate-acting GCs, such as prednisone and prednisolone and long-acting GCs, such as dexamethasone and betamethasone (Zoorob and Cender, 1998; Axelford,

2001). Similar to high levels of endogenous cortisol, these GC derivatives also have adverse effects on the body at high doses (Canalis, 1996; Canalis and Giustina, 2001; Dore, 2010). The long term exposure to synthetic GCs also results in pathophysiologic conditions such as osteoporosis (Canalis, 1996; Canalis and Giustina, 2001; Dore, 2010). As stated previously, the incidence of GCIO is rapidly rising, possibly due to increased prescription and use of synthetic GCs to treat numerous pathophysiologic conditions such pulmonary diseases, rheumatologic disorders and inflammatory diseases (Dore, 2010; Cohen and Adachi, 2004).

1.5.1 Synthesis of endogenous GCs

Endogenous GCs, such as cortisol, are synthesised in the adrenal glands and expression is regulated by the hypothalamic-pituitary-adrenal (HPA) axis (Chrousos, 1995; Newton, 2000): the hypothalamus is stimulated by conditions such as inflammation, pain and stress to release corticotrophic releasing hormone (CRH), which in turn stimulates the pituitary gland to synthesise and release adrenocorticotropic hormone (ACTH) (Chrousos, 1995; Newton, 2000). ACTH then provokes the adrenal cortex to produce GCs such as cortisol (Chrousos, 1995; Newton, 2000). Derived from cholesterol, GCs are lipophylic and are thus able to cross the plasma membrane of cells.

1.5.2 The mechanism of action of GCs

The action of GCs is predominantly mediated by the glucocorticoid receptor (GR), belonging to the nuclear receptor family, but is retained as a multi-protein complex in the cytoplasm (Scherrer et al., 1990; Hutchison et al., 1992; Hutchison et al., 1994; Newton, 2000). This modular protein complex consists of two heat shock protein 90 (Hsp90) molecules and other proteins acting as molecular chaperones and co-chaperones, which are dissociated after ligand binding (Scherrer et al., 1990; Hutchison et al., 1992; Hutchison et al., 1994; Newton, 2000). The cytoplasmic retention of the GR is terminated only after the ligand has diffused through the plasmamembrane and bound to the receptor, after which the ligand-receptor (GC-GR) complex translocates to the nucleus to effect changes in gene expression of GC-responsive genes (Newton, 2000; Schoneveld et al., 2004). The GC-GR complex binds to regions known as GC response elements or GREs in GC-responsive genes as homodimers and only after dimerisation of two GC-GR complexes (Newton, 2000; Schoneveld et al., 2004). Transactivation or transrepression of the gene then occurs (Newton, 2000; Schoneveld et al., 2004).

At least four types of GREs have been identified that mediate the GC transcriptional regulation: simple GREs and GRE half sites (GRE1/2s), which are involved in activation of gene expression, negative GRE (nGRE) that repress gene transcription and tethering GRE which has a dual inhibition or activation function in gene expression (Sakai et al., 1988; Schoneveld et al., 2004). These direct actions of GCs on gene expression are referred to as the genomic effects of GCs (Cato et al., 2002; Makara and Haller, 2001). Another mode of genomic effect of GCs have been described which does not involve DNA-protein interaction, but rather protein-protein interactions with proteins such as TFs, for example AP-1 (activating protein-1) (Cato et al., 1992; Konig et al., 1992) or NF-κβ (De Bosscher et al., 2000). The genomic effects of GCs are proposed to take approximately 30 minutes to 1 hour for initiation, but may last many hours, even days (Makara and Haller, 2001; Cato et al., 2002). However, GCs may have more rapid effects, which occur within a few seconds to minutes and are referred to as non-genomic effects (Croxtall et al., 2000; Liu et al., 2005). The responses elicited through this GC mechanism of action are insensitive to transcriptional inhibitors and are thus unlikely to be due to a principal transcription mechanism (Croxtall et al., 2000). It has been reported that the non-genomic effects of GCs may be mediated, at least in part, by a membrane-associated GR (Chen et al., 1999; Gametchu et al., 1993; Buttgereit et al., 2004). The described non-genomic effects of GCs include activation of phosphatidylinositol 3-kinase (PI3K) (Hafezi-Moghadam et al., 2002), MAPKs (p38, JNK and ERK1/2) (Caelles et al., 1997; Qiu et al., 2001; Li, 2001; Caelles et al., 2002) and c-src (Croxtall et al., 2000; Wong et al., 2002).

GCs action can be regulated at a pre-receptor level and involve the activation or inactivation of the circulating GC by target tissues or cells and is catalysed by two isoforms of 11β-hydroxysteroid dehydrogenase (11β-HSD) (Stewart and Krozowski, 1999). The type I isoform, 11β-HSD1, mainly catalyses the formation of the active cortisol in man and is found in tissues that express high levels of the GR, such as the liver and adipose tissue (Tannin et al., 1991). It appears that 11β-HSD1 functions to increase the concentration of cortisol in these tissues (Tannin et al., 1991). In contrast, the 11β-HSD2 isoform converts active cortisol into inactive cortisone (Albiston et al., 1995). 11β-HSD2 is mainly located in tissues with high levels of mineralocorticoid receptor (MR) such as the kidney and colon, as GCs can bind to the MR with the same specificity as aldosterone and the function of 11β-HSD2 is to prevent the binding of cortisol to the MR (Albiston et al., 1995).
GCs regulate diverse cellular functions such as bone formation (remodeling), and also regulate cell proliferation and differentiation, including that of osteoblasts (Bellows et al., 1990; Stein and Lian, 1993; Eijken et al., 2006). The effects of GCs on bone homeostasis are discussed next and will include a discussion on the role of GCs in osteoblast development.

1.5.3 Effects of GCs on bone homeostasis

In an epidemiological study, van Staa et al. (2002) demonstrated that the dose and duration of exogenous GCs treatment of patients led to changes in BMD that was accompanied by the increase incidence of bone fractures. The fracture risk, however, was decreased with cessation of GC use (van Staa et al., 2002). It was proposed that GCs targeted the bone architecture, rather than BMD, because fractures still occurred at BMDs that were considered relatively normal (van Staa et al., 2002). The micro-architecture of bone ensures maximal strength to facilitate the supportive and structural functions of bone. GCs influence remodelling of this architecture at several levels, leading to altered bone resorption by osteoclasts as well as bone formation by osteoblasts. This ultimately leads to a disturbance of bone homeostasis and bone loss as in the case of osteoporosis. Moreover, GCs affect bone remodelling through both indirect and direct actions.

1.5.3.1 Indirect actions of GCs on bone remodelling

GCs act ubiquitously in the body and therefore can affect several systems, including those regulating bone remodeling. For example, prednisone inhibits the secretion of growth hormone by the pituitary gland in response to GH-releasing hormone (Kaufmann et al., 1988). This affects the growth of a multitude of cell types which mitotically respond to GH. GCs also negatively regulate other hormones that are secreted by the pituitary gland, such as ACTH (Dallman et al., 1987; Antoni and Dayanithi, 1990; Clark et al., 1990), luteinizing hormone (LH) (Sakakura et al., 1975; D'Agostino et al., 1990) and follicle-stimulating hormone (FSH) (Hsueh and Erickson, 1978; D'Agostino et al., 1990). In addition, GCs inhibit the synthesis of oestrogen and testosterone by the gonads (Manelli and Giustina, 2000; Boling, 2004). Furthermore, GCs affect calcium and phosphorous transport, parathyroid function and vitamin D metabolism. Patients that were subjected to supra-physiological doses of GCs exhibit impaired gastrointestinal absorption of calcium, increase renal excretion of calcium and phosphorous and elevated serum levels of PTH (Luckert and Raisz, 1990; Baxter, 2000). Therefore, the impairment of the synthesis and secretion of these hormones, although indirectly, contribute to the catabolic effect of GCs on bone. However, predominantly, GCs exert direct effects on bone, through affecting the cells responsible for bone homeostasis.

1.5.3.2 Effects of GCs on osteoclasts

GCs have multiple, direct actions on osteoclasts too, by mechanisms which are not yet fully understood. It was initially postulated that GCs increase osteoclast function, since GCs stimulated

the expression of the osteoclast differentiation factors, RANKL and M-CSF, but inhibited the production of the decoy soluble RANKL receptor, OPG, by osteoblasts (Rubin et al., 1998; Hofbauer et al., 1999). Histomorphometric data shows that bone formation, as well as resorption, was affected in patients treated with GCs (Prummel et al., 1991; Weinstein, 2001). Later studies showed that Dex repressed the development of TRAP-positive multinucleated osteoclasts through the down-regulation of β3 integrin (Kim et al., 2006b). However, low levels of Dex have also been shown to be stimulatory to osteoclastogenesis, possibly through down-regulating factors that is inhibitory to osteoclast formation such as interferon–β (IFNβ) (Takuma et al., 2003). This could account for the increase in osteoclast numbers at the onset of GC-induced bone loss (Takuma et al., 2003). In addition, GCs could modulate osteoclast function via elevated recruitment or activation of quiescent pre-osteoclasts (Defranco et al., 1992). Contrary to this, *in vitro* as well as *in vivo* evidence show that GCs decrease the number of osteoclast progenitor cells, whilst promoting the survival of mature osteoclasts (Weinstein et al., 2002; Jia et al., 2006; Kim et al., 2006a). It was found that GCs inhibit the osteoclastic cytoskeletal reorganisation, essential for osteoclast function, through attenuating the activation of the guanine exchange factor, Vav3 (Kim et al., 2006a). This then leads to the inhibition of the activation of the small GTPase, Rac, an essential factor for the rearrangement of the cytoskeleton (Kim et al., 2006a). Moreover, GCs were found to repress the stability and distribution of osteoclast microtubules, which are required for the organisation of the osteoclastic cytoskeleton (Kim, 2010). Therefore, although controversial, it appears that GCs may inhibit the resorptive function of osteoclasts through several mechanisms. It has also been proposed that, in relation to bone remodelling, decreased bone resorption, caused by excess GCs, may inadvertently result in decreased recruitment and activation of osteoblasts, thus leading to reduced bone formation (Kim, 2010).

1.5.3.3 GC effects on MSCs, osteoblasts and osteocytes

Low levels of GCs are needed for the differentiation of osteoblast progenitor cells into mature osteoblasts for normal bone maintenance (Pockwinse et al., 1995; Chang et al., 2006; Kalak et al., 2009). GCs, at physiological concentrations induce the expression of certain osteoblast-specific proteins such as alkaline phosphatase, osteocalcin and osteopontin (Subramaniam et al., 1992; Pockwinse et al., 1995). Contrary to this, higher doses and sustained use of GCs have detrimental effects on osteoblastic bone formation (Chevalley et al., 1996; Engelbrecht et al., 2003; Canalis et al., 2007; Kalak et al., 2009). GCs affect osteoblast development and function in a stage-specific manner (Pockwinse et al., 1995; Ishida and Heersche, 1998; Smith et al., 2000; Pierotti et al., 2008). Findings show that osteoblasts further down the differentiation pathway are less sensitive to GCs

than immature osteoblasts (McCulloch and Tenenbaum, 1986; Tenenbaum and Heersche, 1986; Jonsson et al., 1997; Engelbrecht et al., 2003).

Numerous studies found that GCs decrease the proliferation of MSCs, the progenitor cells of osteoblasts (Fried et al., 1993; Fried and Benayahu, 1996; Shur et al., 2005; Akavia et al., 2006; Chang et al., 2006). Moreover, findings show that GCs increased the commitment of these MSCs to the osteoblastic lineage (Cooper et al., 1999; Beloti and Rosa, 2005). The lineage commitment was associated with the increased expression of osteoblastic markers such as alkaline phosphatase, (Fried and Benayahu, 1996; Akavia et al., 2006; Chang et al., 2006). FHL2 (Four and half LIM protein 2) is a LIM-domain protein which was found to regulate the early stages of osteogenic differentiation of human and murine MSCs (Hamidouche et al., 2008). It was reported that Dex upregulated the expression of FHL2 and that FHL2 interacts with β-catenin to activate the Wnt-signalling pathway, leading to increased expression of Runx2, a pivotal factor for differentiation in these cells (Hamidouche et al., 2008). Dex was also shown to potentiate the effects of BMP-2, which is an inducer of osteoblast proliferation and differentiation, by inducing the expression of osteoblast-specific mRNAs, such as ALP, Runx2, OCN, OPN and BSP, in MSCs (Rickard et al., 1994; Jager et al., 2008). These actions of GCs on MSCs thus promoted the osteogenic differentiation of MSCs.

Similar to naïve MSCs, GCs were found to decrease the proliferation of both preosteoblasts (Wong et al., 1990; Cheng et al., 1994; Jonsson et al., 1997; Engelbrecht et al., 2003) and osteoblasts (O'Brien et al., 2004). A possible mechanism for this inhibitory effect on *in vivo* osteoblast replication is that GCs may interfere with the synthesis and actions of systemic hormones and growth factors involved in bone cell development (Giustina and Wehrenberg, 1992; Giustina et al., 2008). For example, systemic hormones such as growth hormone (GH) and insulin have been shown to have anabolic effects on bone (Philippe and Missotten, 1990; Giustina and Wehrenberg, 1992; Lambillotte et al., 1997; Giustina et al., 2008) and stimulate the proliferation of various primary and immortalised osteoblastic cells (Morel et al., 1993; Kassem et al., 1993; Salles et al., 1994; Thrailkill et al., 1997; Yang et al., 2010). However, Giustina and Werhenberg (1992) showed that GCs inhibit the secretion of growth hormone by the pituitary gland. In addition, it was demonstrated that the secretion of insulin by pancreatic β-cells was also perturbed by GCs, which could lead to decreased insulin available for bone anabolism (Philippe and Missotten, 1990; Lambillotte et al., 1997). The *in vitro* actions of these systemic hormones are likely governed by the respective receptors expressed on osteoblastic cells. Evidence exist that osteoblasts express receptors for insulin (Nilsson et al., 1994; Thomas et al., 1996a) and GH (Nilsson et al., 1994;

Slootweg et al., 1997). Therefore, another possible way in which the effects of GCs on osteoblastic cells could be modulated is by the negative regulation of hormone receptor expression (Thomas et al., 1996b). An example of this is a study by Thomas *et al*. (1996b) who showed that Dex reduced the expression of insulin receptors in UMR106 osteoblasts. GCs could also attenuate osteoblastic cell proliferation by interfering with the proliferative activities of local GFs produced by osteoblasts such as IGF-I, IGF II and TGF-β (Delany et al., 2001; Canalis, 2005; Giustina et al., 2008). It was shown that GCs differentially regulate the expression and activity of IGF-I, IGF-binding proteins and TGF-β in osteoblasts (Delany et al., 2001).

GCs could also alter osteoblastic cell proliferation by influencing cellular and molecular processes distal of hormones, GFs and receptors, such as osteoblast signalling pathways. As reported earlier, the ERK1/2 MAPK pathway was shown to be the primary signalling pathway involved in modulating the proliferation of preosteoblasts and osteoblasts (Engelbrecht et al., 2003; Horsch et al., 2007). It was shown that Dex reduced the mitogen-stimulated ERK 1/2 activation in MBA 15.4 preosteoblasts and MG63 osteoblasts (Hulley et al., 1998; Engelbrecht et al., 2003; Horsch et al., 2007). Additionally, GCs could negatively affect the cell cycle of osteoblasts through modulating various cell cycle-related proteins. For example, the GC-induced attenuation of osteoblast proliferation was linked to the decreased expression of the cell cycle-related proteins: CDK4, CDK6 and cyclin D3 (Rogatsky et al., 1997). Furthermore, it was shown that increased transcription of cdk inhibitors also contributed to the decreased proliferation caused by GCs in osteoblastic cells (Rogatsky et al., 1997). Similarly, GCs could adversely impact on the transcription and translation of other proteins required for the regulation of cell proliferation such as transcription factors, like E2F-1 and c-Myc (Rogatsky et al., 1997).

GCs affect osteoblast differentiation in a number of ways as well. Administration of Dex to proliferating cultures of fetal rat calvarial cells induced various morphological changes: cells became cuboidal and differentiated cells situated within nodules, decreased in size by almost one-third compared to control cells (Pockwinse et al., 1995). The transcription and translation of several osteoblast-related proteins were also found to be affected by GCs. For instance, it was found that cortisol down-regulated the expression of Col I and β1 integrin (Delany et al., 1995). In addition, high levels of Dex (10^{-6} M) resulted in the inhibition of OCN mRNA expression through the repression of the Egr/Knox20 binding-enhancer protein in MC3T3-E1 osteoblasts (Mikami et al., 2007). In contrast, lower levels (10^{-8} M) of Dex were found to increase the expression of OCN (Stromstedt et al., 1991; Heinrichs et al., 1993; Mikami et al., 2007). Low Dex doses also upregulated the expression of other late osteoblastic markers such as BSP (Ito et al., 2007) and OPN

(Leboy et al., 1991; Shalhoub et al., 1992). This is an example of the divergent impact that different concentrations of GCs, such as Dex, might have on osteoblast differentiation. Therefore, it seems that high doses of GCs negatively regulate the expression of ECM proteins in bone cells, whilst low GCs dosages stimulate the expression of such proteins. Furthermore, the transcription of the collagenase III gene, the gene product of which is responsible for the catabolism of Col I in bone, is increased by cortisol (Delany et al., 1995). The breakdown of Col I, which is the major constituent of bone, could lead to reduced osteoblast differentiation and function by reducing calcification and thus bone formation. Moreover, it was found that GCs decreased the terminal differentiation of osteoblastic cells (Ito et al., 2007). GCs, such as cortisol, were also shown to increase the apoptosis of osteoblastic cells, including osteocytes (Weinstein et al., 1998; O'Brien et al., 2004).

In summary, these findings indicate that GCs have a negative impact on the proliferation of MSCs as well as more differentiated osteoblasts. Whilst lower concentrations of GCs induce the expression of osteoblast-related ECM protein to increase bone formation, higher doses are detrimental to the bone ECM and decrease bone formation. Attenuation of the formation and activity of these ECM proteins results in decreased osteogenic differentiation and therefore inhibit terminal osteoblast differentiation and function. Osteoblasts also negatively regulate osteoclastogenesis by producing the soluble decoy receptor of RANKL, osteoprotegerin (OPG) (Simonet et al., 1997; Tsuda et al., 1997). It was found that GCs decrease the expression of OPG, whilst increasing the levels of RANKL in human osteoblasts (Hofbauer et al., 1999). Therefore, GCs could increase bone resorption by osteoclasts as well. Although this seems contradictory to the findings in Section 1.3.3.1, it could account for the rapid initial increase in bone resorption seen in the onset of GCIO (Canalis, 1996; Canalis and Giustina, 2001; Compston, 2010).

Notably, the cellular and molecular mechanisms regulating the adverse effects of GCs on bone homeostasis has not yet been fully elucidated. As cited before, the primary targets for the negative effects of GCs on bone homeostasis, are the osteoblasts. Decreased osteoblast proliferation and differentiation, as caused by excess and prolonged treatment of GCs, ultimately leads to reduced bone formation, which then translates into diminished bone strength and development of GC-induced osteoporosis (GCIO). In the light of increased use of GCs to treat various diseases such as asthma, rheumatoid arthritis and autoimmune diseases, it is essential to investigate how early osteoblast precursor cells such as MSCs and preosteoblasts are affected under conditions that promote GCIO. Elucidation of signalling events that occur during osteoblast proliferation upon GC exposure will improve insights into the pathogenesis of GCIO and aid in the identification of novel

anti-osteoporotic agents. These could then be developed into to therapies, especially ones which are anabolic to bone, and can be used to treat GCIO.

1.6 Aims and Strategies of this study

The aim of the current research was to investigate the involvement of protein tyrosine phosphatase (PTP) activity and expression as part of the mechanism through which GCs exert their negative effects on osteoblast precursor cells. To this end, two types of osteoblast precursor cells were employed, namely: naïve rat adipose-derived mesenchymal stromal cells (rMSCs) and preosteoblasts derived from these rMSCs. Subcutaneous adipose tissue-derived mesenchymal stromal cells are very similar to bone marrow-derived stromal cells and are obtained with ease from more abundant tissue sources in higher quantities (Zuk et al., 2002; Dicker et al., 2005; Boquest et al., 2006). Moreover, these pluripotent rMSCs can be induced to differentiate, amongst other cell types, into an osteoblastic phenotype. Mesenchymal stromal cells isolated from adipose tissue can therefore be used as an experimental model to study the effects of GCs on osteoblast precursor cells.

In order to achieve the goals of this study, the strategies outlined below were followed:

- The effects of GCs on naive rMSCs and primitive preosteoblasts, by using the synthetic glucocorticoid, dexamethasone (Dex), were tested in this study by examining the mitogen-induced proliferation of cells early in the differentiated process.

- To establish the involvement of the ERK1/2 pathway in the regulation of mitogen-stimulated proliferation of rMSCs and preosteoblasts, the ERK1/2 pathway was inhibited in this study downstream of MEK1/2 using the pharmaceutical inhibitor, U0126. The activation of the ERK1/2 signalling pathway after mitogen stimulation was tested by western blot analysis. Since ERK1/2 is activated via phosphorylation, antibodies raised against phosphorylated (active) ERK1/2 (at residues Thr202 and Tyr204) were used to examine the extent of ERK1/2 phosphorylation. The degree of phosphorylation was used to infer the level of ERK1/2 activation.

- The involvement of protein tyrosine phosphatases (PTPs) in the Dex down-regulation of mitogen-induced ERK1/2 activity was investigated. This was achieved by completing phosphatase activity assays after mitogen stimulation, with and without Dex administration. It was hypothesised that by inhibiting the Dex-induced PTP activity with a PTP-specific

inhibitor such as vanadate, the contribution of PTPs to the total phosphatase activity can be determined, as it has been shown that vanadate inhibits GCIO in rats (Hulley et al., 2002). It was theorised that by inhibiting the Dex-induced PTP activities with vanadate, the attenuation of proliferation by Dex could be lifted. The possible involvement of the dual specificity phosphatase, MKP-1, in regulating the Dex responses in primary naïve rMSCs and primary preosteoblasts was investigated. MKP-1 mRNA abundance was assessed using quantitative real-time polymerase chain reaction (RT-qPCR), whilst the protein expression was examined using western blot analysis employing MKP-1-specific antibodies.

Chapter 2

Materials and Methods

2.1 Materials

Sodium pentobarbitone (Eutha-naze) was obtained from Bayer (Pty) Ltd (Isando, RSA). Fetal bovine serum (FBS) (originating from France) was purchased from Gibco™, whilst collagenase type I was bought from Worthington Biochemical Corporation (Lakewood, New Jersey, USA). Trypsin-versene mixture, penicillin and streptomycin antibiotic mixture, as well as Hank's buffered salt solution was obtained from Lonza, Biowhitaker ® (Walkersville, MD, USA). Anti-BrdU-FITC conjugated antibodies and 7-AAD were obtained from BD Biosciences (BD®, California, USA). Cell culture plasticware was purchased from either Greiner Bio-One (Cellstar ®, Frickenhausen, Germany) or Corning Incorporated (Corning ®, NY, USA). The U0126, SV Total RNA isolation system and ImProm-II™ reverse transcriptase were obtained from Promega (Madison, WI, USA). The RNAeasy Mini kit for total RNA isolation was procured from Qiagen (CA, USA). Tritiated thymidine (TRK 120 methyl-[^{3}H]-thymidine), para-nitrophenylphosphate (pNPP), horseradish peroxidase (HRP)-linked anti-rabbit IgG secondary antibody (from donkey, #NA934), enhanced chemiluminescent (ECL™) western blotting detection reagents and Hyperfilm™ ECL high performance ECL™ film were all purchased from General Electric Healthcare (Buckinghamshire, UK). Biotrace™ PVDF membrane (0.45 µM) for western blotting was purchased from Pall Life Sciences (Pensacola, Florida, USA). Primary anti-p44/42 MAPK (#9102) and anti-phospho-p44/42 (# 9101) antibodies were bought from Cell Signaling Technology (Beverly, MA, USA). LumiGLO reserve chemiluminescent substrate kit was obtained from KPL laboratories (Gaithersburg, Maryland, USA). Primers were procured from Integrated DNA Technologies Incorporated (IDT) and Metabion (Roche Diagnostics Corporation, IN, USA). Ready-gel scintillation fluid was purchased from Beckman Coulter (Chino, CA, USA). Dulbecco's modified Eagle's medium (DMEM), sodium orthovanadate (VO_4), sanguinarine chloride (SC), BrdU and all other chemicals were obtained from Sigma (St. Louis, MO, USA). Liquid solvents were procured from Merck Chemicals (Pty) Ltd (South Africa).

2.2 Methods

2.2.1 Cell culture conditions

2.2.1.1 Isolation of rat mesenchymal stromal cells (rMSCs) from adipose tissue

The protocol for isolating rat mesenchymal stromal cells (rMSCs) from adipose tissue was adapted from the method of Huang et al. (2002). Male, wild type Wistar rats, aged between 12 to 14 weeks, with average weights ranging between 250 g and 300 g were used in this study. Rats were housed in an AAALAC (Association for Assessment and Accreditation of Laboratory Animal Care) facility. Handling of laboratory animals was in accordance with the ethical guidelines of the University of Stellenbosch. The initial ethical clearance number for this project was N04/08/126 and was later changed to N08/06/163. Rats were sacrificed by intraperitoneal injection with 100 mg/kg sodium pentobarbitone. Immediately after euthanasia, subcutaneous fat from the inguinal fat pouch was excised, the surface sterilised briefly by immersion in 70 % (v/v) ethanol and placed in holding medium (Supplement A1.1.). Prior to digestion with collagenase type I, the surface area was increased by slicing fat tissue into small cubes (approximately 2 mm x 2 mm) using a sterile scalpel blade. Fat tissue cubes were divided into two equal aliquots and placed in 10 ml of collagenase type I enzyme mixture (Supplement A1.4.) and digested at 37 ^{o}C with gentle agitation for 20-30 minutes. Cells were subjected to centrifugation at 2, 500 x g for 10 minutes to separate the stromal fraction containing stromal cells (rMSCs) from non-digested adipose tissue and cellular debris. Cell pellets were then washed twice with PBS (Supplement A1.4.). These cells were designated as passage 0 (P_0) cells. P_0 cells were plated using a 1: 4 dilution in expansion media (Supplement A1.2.). Cells were grown at 37 ^{o}C with 5% CO_2 and 80%-90% humidity. At 24 and 72 hours after initial plating, media was removed, cells were rinsed briefly with PBS (Supplement A1.4.) and expansion media (Supplement A1.2.) was changed. All media used contained 10 mg/ml penicillin and 10 mg/ml streptomycin. All FBS used was heat inactivated at 56 ^{o}C for 30 minutes to inactivate the complement and stored at -20 ^{o}C for subsequent use.

2.2.1.2 Cell growth and maintenance

rMSCs were liberated from the plate for sub-culture by washing cells in pre-warmed PBS (Supplement A1.4.), followed by the addition of 1 ml of 1x trypsin -versene mixture (Lonza) per 100 mm cell culture dish for 2 minutes. Trypsin was then immediately inactivated with 2 ml of complete growth medium (Supplement A2.). Cells were plated at a 1: 5 dilution in complete growth

medium (Supplement A2.) and grown at 37 ^{o}C with 5% CO_2 and 80%-90% humidity. Passage 2 (P_2) cells were used for all experiments in this study.

2.2.1.3 Differentiation of rMSCs into an osteoblastic phenotype

Osteoblast differentiation was induced by adding osteogenic medium (OM) (Supplement A3.3.) to confluent P_2 cells which were not subjected to serum starvation. For the initial characterisation of rMSCs differentiated into an osteoblastic phenotype, cells were differentiated for a maximum of 28 days (Chapter 4). For subsequent experiments, however, rMSCs were differentiated using OM for only 7 days (Chapter 4). Osteogenic media (Supplement A3.3.) was changed every 2 to 3 days according to the methods of Jaiswal et a., 1997 and Doi et al., 2002.

2.2.1.4 Induction of mitogenesis in naïve rMSCs and preosteoblasts

Mitogenesis was induced by treating quiescent naïve rMSCs in 1% FBS with 5%; 10% and 20% (v/v) FBS. The PKC activator, PMA (100 ng/ml) was also used as a mitogen, with treatment occurring in media containing 1% (v/v) FBS. Treatment with 0.1% (v/v) DMSO served as solvent control for PMA. Mitogenic stimulation of quiescent naïve rMSCs was performed for 24 hours, 48 hours and 72 hours. Preosteoblasts were treated with mitogens for only 24 hours.

2.2.1.5 Chemical treatment and pharmaceutical inhibitors used

The synthetic glucocorticoid, dexamethasone (Dex), was used at concentrations of 1 µM, 100 nM, 10 nM, 5 nM and 1 nM. Cells were challenged with Dex for only 24 hours. Ethanol at a concentration of 0.1% (v/v) was used as a solvent control. Table 2.1 displays all inhibitors used in this study with their relevant concentrations used. Inhibitors were added to naïve rMSCs and preosteoblasts for a period of 24 hours.

Table 1: displays the pharmaceutical inhibitors used in this study.

Inhibitor	Abbreviation used	Type of inhibitor	Final concentrations used
U0126	U0126	MEK	10 µM, 5 µm and 1 µM
Sodium orthovanadate	VO_4	PTP	10 µM, 5 µM, 2.5 µM, 1 µM, 100 nM and 10 nM

2.2.2 Cell proliferation assay using [^{3}H] thymidine incorporation

Cells were cultured in 24-well plates for all proliferation assays (adapted from Hulley et al., 1998; Cave, 1966). During the last 4 hours of incubation, after mitogen or chemical treatments, 2µCi /ml of [^{3}H]-labelled thymidine (specific activity = 25 Ci/mmol) was added to each well. Cells were then incubated at 37 ^{o}C with 5% CO_2 and humidity between 80% and 90% for the remainder of the treatment period. Incorporation of [^{3}H]-labelled thymidine into newly synthesized DNA was terminated by placing the culture plate on ice for 2 minutes. After removing the medium, cells were washed twice with ice-cold PBS (Supplement A1.4) and the cell culture plate was placed at -80 ^{o}C for 1 hr to aid cell lysis. Cells were thawed at room temperature (RT) before the addition of 500 µl of lysis solution (Supplement B1.) and then incubated at room temperature for 1 hr. The cell culture plate wells were rinsed with 350 µl of lysis solution and pooled with corresponding cell lysates. Cell lysates were then transferred to 2ml microfuge tubes. In order to precipitate acid-insoluble DNA and proteins, 500 µl of ice-cold 50% (w/v) TCA (trichloroacetic acid) was added to the lysates. This was followed by incubation at 4 ^{o}C overnight. Cell precipitates were spun in a bench top centrifuge at 4 ^{o}C for 15 minutes at 15, 000 x g to pellet DNA and proteins. Pellets were washed with 500 µl of 10 % (w/v) ice-cold TCA and subjected to centrifugation at 4 ^{o}C for 5 minutes at 15,000 x g. The supernatant fractions were then discarded, ensuring that the pellets were as dry as possible. Pellets were resuspended in 500 µl of 0.1 N NaOH and incubated at RT for 1 hr with intermittent vortexing. Scintillation samples were prepared by adding 8 ml of Ready-gel scintillation (Beckman Coulter) fluid to 350 µl of each sample. These samples were clarified by the addition of 600 µl of glacial acetic acid and mixed by inversion. The amount of [^{3}H]-labelled thymidine incorporation into DNA was determined by counting radioactive decay on a LS5000TD scintillation counter (Beckman Coulter) for 5 minutes per sample. Results were displayed as values in counts per minute (cpm).

2.2.3 Cell cycle analysis using propidium iodide

The method of Vindelov et al. (1983) was adapted for cell cycle analysis of rMSCs employing flow cytometry. Culture medium was aspirated, the cells were washed twice with PBS (Supplement A1.4), followed by incubation in the presence of 1x trypsin-versene for 2 minutes. Trypsinisation was stopped using 2 ml of complete growth media (Supplement A2.). Cell suspensions were then transferred to 15 ml tubes and spun for 5 minutes at 2, 500 x g at RT. Cell pellets were washed twice with PBS (Supplement A1.4.), resuspended in 200 µl citrate buffer (Supplement B2.1.) and stored at -20 ^{o}C for subsequent use.

Cell nuclei were isolated by incubating cell suspensions in 1.8 ml of solution A (Supplement B2.3.) at RT for 10 minutes. Cell suspensions were then incubated in 1.5 ml of solution B (Supplement B2.4.) at RT for 10 minutes, with occasional inverting to inactivate trypsin and digest RNA. Isolated nuclei were subsequently stained with 1.5 ml of solution C (Supplement B2.5.) for 10 minutes on ice. Flow cytometry was performed using a FACSCalibur instrument from Beckton Dickinson Biosciences.

2.2.4 BrdU flow cytometry analysis

Cells were grown in 100 mm cell culture dishes and pulse-labelled with 20 µM 5-bromo-2'-deoxyuridine (BrdU) for the last hour of mitogenic stimulation at 37 ^{o}C and 5% CO_2. The cells were liberated from the cell culture dish by adding 1 ml of 1x trypsin-versene mixture (Lonza) to each dish for 2 minutes. To remove excess medium, cells were then washed with PBS (Supplement A1.4.) and subjected to centrifugation at 2, 500 x g for 5 minutes. The cell pellet was resuspended in 1 ml of fixative solution (Supplement B3.1.) and incubated at 4 ^{o}C overnight. Fixed cells were subjected to centrifugation at 2, 500 x g for 5 minutes and washed in 1 ml of PBS containing 1% (w/v) Glycine. So as to partially digest DNA, cells were incubated with 1 ml of DNAse I digestion solution (Supplement B3.2.) at 37 ^{o}C for 30 minutes. Subsequently, cells were washed in 1 ml PBS (Supplement A1.4.) and pelleted by centrifugation at 2, 500 x g for 5 minutes. The cell pellet was resuspended in 40 µl anti-BrdU-FITC incubation solution (Supplement B3.3.) and incubated at RT for 30 to 45 minutes. After incubation, the cells were washed with 1 ml PBS (Supplement A1.4.) containing 0.1% (w/v) BSA and pelleted by centrifugation at 2, 500 x g for 5 minutes. Cells were then resuspended in 1 ml PBS (Supplement A1.4.) and incubated with 5 µl 7-AAD (0.05 µg/µl) for 10 minutes directly before analysis by flow cytometry using a FACSCalibur instrument from Beckton Dickinson Biosciences.

2.2.5 Alkaline phosphatase (ALP) extraction and enzyme activity measurement

This protocol was adapted from Merchant-Larios et al. (1985). Cells were grown in 100 mm cell culture dishes prior to ALP enzyme extraction. After rMSCs were differentiated into an osteoblastic phenotype for 7 days, the culture medium was aspirated and cells were washed twice with PBS (Supplement A1.4.). Cells lysates were prepared by the addition of 800 µl of ice-cold ALP extraction solution (Supplement B3.1.) to each cell culture dish. After incubation at room temperature for 2 minutes, a rubber policeman was used to scrape cells off the dishes. Cell suspensions were transferred to pre-chilled 1.5 ml microfuge tubes and spun at 15, 000 x g for 15

minutes at 4 ^{o}C in a benchtop centrifuge to pellet cellular debris. Supernatants were transferred to pre-chilled 1.5 ml microfuge tubes and 1 µl of ice-cold butanol was added for every 5 µl of supernatant. After butanol addition, supernatants were vortexed for 30 sec and mixed for 45 minutes at 4 ^{o}C using a rotating wheel. Subsequent to centrifugation at 15, 000 x g for 1 hr at 4 ^{o}C, the aqueous phase was transferred to pre- chilled 2 ml microfuge tubes. A volume of 450 µl ice-cold acetone was added to 750 µl of cell lysate (aqueous phase) before centrifugation at 15, 000 x g for 30 minutes at 4 ^{o}C, to precipitate ALP fractions. Pellets were resuspended in 20 µl ALP extraction buffer without PMSF (Supplement B3.1.) and stored at -20 ^{o}C until analysis.

ALP extracts were thawed on ice for ALP enzyme activity measurements. A volume of 170 µl glycine assay buffer (Supplement B3.2.) was added into each well of a 96-well plate, followed by the addition of 10 µl of cell extract and 20 µl of pNPP (paranitrophenylphosphate) substrate solution (Supplement B3.3.) was added. The OD_{405nm} was then measured every 2 minutes for the duration of 20 minutes using a Synergy^{TM} HT microtiter plate reader and analysed with KC4 v3.3 software (Bio-Tek® Instruments, Inc., Vermont, USA). The cell extracts and BSA standards were diluted in water (1:1) for the Bradford protein determination since the ALP extraction buffer was incompatible with the Bradford reagent. The activity of ALP was calculated as:

$$A\ (U/ml) = \frac{(\Delta OD_{405nm}/min.)(assay\ volume\ in\ ml)(dilution\ factor)}{(\varepsilon\ of\ pNPP\ at\ 405\ nm)(lysate\ volume\ in\ ml)}$$, where

Δ OD_{405nm}/min. = difference in OD_{405nm} over 1 minute, here taken as:

$(OD_{405nm\ at\ 20\ min} - OD_{405nm\ at\ 4\ min})/ 16$, because the reaction was consistently linear between 4 minutes and 20 minutes,

Assay volume = 0.2 ml,

Dilution factor = 1, cell extracts are used undiluted,

ε of Pnpp at 405 nm (**millimolar extinction coefficient of Pnpp at 405 nm)** = 18.5

Lysate volume = 0.01 ml.

ALP activity was expressed as **Activity (units/ mg protein) = units per ml/mg per ml protein.**

2.2.6 Phosphatase activity assay using pNPP hydrolysis

This phosphatase activity protocol was adapted from Engelbrecht et al. (2003). After aspiration of cell growth medium, cells were washed twice with PBS (Supplement A1.4.). Cell protein lysates for the pNPP hydrolysis assay were prepared by the addition of 250 µl protein lysis buffer (Supplement B4.1.) to cells. Cells from 8 cell culture dishes (100 mm) were pooled. Following this, cell suspensions were sonicated for 3 x 10 sec (at an amplitude of 20 microns peak to peak) and spun for

10 minutes at 15, 000 x g in a benchtop centrifuge to pellet cellular debris. Supernatant fractions were placed in pre-chilled 1.5 ml microfuge tubes and stored at -20 ^{o}C for subsequent use.

Protein determination was performed using the Bradford protein assay (Supplement B4.2.) (Bradford et al., 1976). Quantities of total protein of 25, 50, 100, 150 and 200 µg were used to measure phosphatase activity, in a volume of 200 µl of pNPP assay buffer (Supplement B4.2.). A volume of 50 µl of pNPP substrate solution (Supplement B4.3.) was added to each assay well in a 96-well plate and incubated for 1 hr at 37 ^{o}C. Reactions were stopped using 50 µl of 5N NaOH and OD_{405} was measured using a Synergy^{TM} HT microtiter plate reader and analysed using KC4 v3.3 software (Bio-Tek® Instruments, Inc., Vermont, USA). One unit of phosphatase activity was defined as a change in 1 OD unit/ hour at 405 nm.

2.2.7 Senescence-associated β-galactosidase (SA-β- Gal) staining and protein activity assay

The senescence-associated β-galactosidase activity assay was adapted from the method of Dimri et al., (1995). Cells were grown in 24-well cell culture plates. Subsequent to the removal of the cell culture medium from cells, cells were washed three times with 1 x PBS (Supplement A1.4.). Cells were next fixed in 500 µl fixative solution (Supplement B6.1.) at RT for 5 minutes and washed twice with PBS (Supplement A1.4.). A volume of 2 ml SA-β-Gal staining solution (Supplement B6.2.) was added to the fixed cells. After incubation at 37 ^{o}C for 24 hr, the stain solution was removed and dishes were washed twice with PBS (Supplement A1.4.). An Olympus Cell ® system attached to an IX-81 inverted fluorescence microscope equipped with an F-view-II cooled CCD camera (Soft Imaging Systems) was used to observe cells. Image acquisition was performed using a Xenon light source (MT-20, Cell ®) with a 360 nm excitation filter and a UBG triple band pass emission filter, a 10x UPlanFLN objective and the Cell® imaging software. SA-β-Gal activity was expressed as **[number of senescent positive cells counted]/ [total number of cells counted] X 100**.

2.2.8 MTT assay

Mitochondrial activity was determined using the adapted method of Mosmann et al. (1983). Cells were cultured in 24-well plates and incubated in complete growth medium (Supplement A2.1.) containing 100 µl of 5 mg/ml MTT (3-(4, 5-dimethylthiazolyl-2)-2, 5-diphenyltetrazolium bromide) (Supplement B6.) at 37 ^{o}C for 3 hours. The medium was then removed and cells were washed with

PBS (Supplement A1.4.). The coloured formazan product was solubilised with 500 µl DMSO per well, of which 250 µl was used to measure MTT reduction at OD_{570nm}. Optical density was measured using a Synergy™ HT microtiter plate reader, utilising KC4 v3.3 software (Bio-Tek® Instruments, Inc., Vermont, USA). Results displayed are given as **[$OD570_{nm}$ of sample]/ [OD_{570nm} of basal growth control] X 100**.

2.2.9 Protein Methods

2.2.9.1 Total protein extraction

Undifferentiated rMSCs cells were grown until 80% confluent in 100 mm cell culture dishes before mitogenic stimulation for 2 minutes, 5 minutes, 10 minutes, 1 hour, 2 hours and 4 hours prior to protein extraction. Preosteoblasts were grown as indicated in Section 2.2.1.3 prior to protein lysate preparation. Cell culture plates were placed on ice and the culture medium was removed. Cells were washed once with PBS (Supplement A1.4.) and once with wash buffer (Supplement C1.1.) to remove excess medium. Total protein were extracted by the addition of 250 µl of ice-cold protein lysis buffer (Supplement C1.2.) to cells and incubated on ice for 2 minutes. A rubber policeman was used to detach cell from the plates. Cell suspensions were sonicated for 3 x 10 sec (at an amplitude of 20 microns peak to peak) and spun at 15, 000 x g at 4 ^{o}C for 10 minutes in a benchtop centrifuge to pellet cellular debris. Supernatant fractions were transferred to pre-chilled 2 ml microfuge tubes for subsequent use as protein cell lysates.

2.2.9.2 Protein gel electrophoresis

Protein concentrations were determined using the Bradford protein assay (Supplement B4.3.) (Bradford, 1976). Fifteen to eighty micrograms of total protein from cellular lysates were separated and resolved by electrophoresis on a SDS-PAGE gel (Supplement C2.; Laemmli, 1970), at 150V for 15 minutes to allow proteins to move into separating gel and then further for 2 hours at 180 V.

2.2.9.3 Western Blotting

A Bio-Rad Mini-PROTEAN® 3 (Bio-Rad Laboratories, CA, USA) tank system was used for protein transfers. Proteins were transferred onto 0.45 µM Biotrace™ PVDF membranes (Pall Life Sciences, Pall Corporation, Florida, USA) at 30 V overnight with cooling using an ice-pack. After protein transfer, membranes were briefly placed in 100% methanol and dried for 15 minutes to enhance

protein binding. Protein loading and transfer efficiency were assessed by staining membranes with Ponceau S solution (Supplement C3.2.) for 5 minutes and washing with water until the background was clear. Membranes were blocked for at least 1hr at RT with blocking buffer (Supplement C3.4.). Blocked membranes were washed three times for 10 minutes with TBS-T (Supplement C3.3.) before overnight incubation with primary antibodies (a dilution of 1: 1000 for both total p44/42 ERK and phospho-p44/42 ERK) at 4^{o}C. Prior to incubation with HRP-conjugated secondary antibodies (at a dilution of 1: 4000) membranes were washed three times for 10 minutes with TBS-T (Supplement C3.3.). Immuno-responsive proteins were visualised by incubation with enhanced chemiluminescence (ECL^{TM}) solution, after which membranes were exposed to Hyperfilm^{TM} ECL. Immuno-reactive protein bands were visualised by photographic development of the film. Films were scanned on a ScanMaker 8700 scanner using ScanWizard^{TM} Pro software (Microtek International Inc., Taiwan). ImageJ 1.42q was used for densitometry to quantify the intensity of the immuno-responsive protein bands on the scanned images. MKP-1 immuno-responsive bands were visualised using the LumiGLO reserve chemiluminescent substrate kit from KPL laboratories (Gaithersburg, Maryland, USA). For densitometry analysis, membranes were scanned with a Chemidoc imager (Bio-Rad, CA, USA) and quantification of MKP-1 and total p44/42 ERK protein levels was performed using the Quantity One® software from Bio-Rad (Ca, USA).

2.2.10 Nucleic Acid methods

2.2.10.1 Total RNA extraction

Total RNA was extracted using the Qiagen RNAeasy Mini kit (Qiagen, CA, USA) and the SV Total RNA isolation system (Promega, Madison, WI, USA) according to the manufacturer's instructions. Determination of total RNA concentrations was carried out using a ND-1000 NanoDrop® spectrophotometer (NanoDrop® Technologies, DE, USA).

2.2.10.2 RNA gel electrophoresis

Total RNA samples were subjected to electrophoresis on 1% (w/v) agarose/formaldehyde gels (Supplement D2.1.) ran in MOPS buffer (Supplement D2.3.) for 30 minutes at 70 V to assess the integrity and quality of RNA. These samples were prepared for electrophoresis by adding equal volumes of RNA sample application buffer (Supplement D2.2.) to 1 µg of total RNA. Prior to electrophoresis, RNA samples were denatured at 65 ^{o}C for 10 minutes and instantly placed on ice.

Gels were visualised and the image recorded on a Vacutec G: Box gel documentation system whilst using GeneSnap software (Syngene, Synoptics Ltd, Beacon House, Cambridge, UK).

2.2.10.3 cDNA synthesis

Possible residual genomic DNA was removed from the total RNA samples by treatment with DNase I (Promega, Madison, WI, USA) according to manufacturer's instructions. One microgram of DNase I treated total RNA was used in a two–step cDNA synthesis protocol. In the first step of the cDNA synthesis, 0.5 µg of poly-dT primers (IDT) was annealed to the RNA at 70 ^{o}C for 5 minutes in the presence of RNAsin RNAse inhibitor (according to manufacturer's recommendations; Promega, Madison, WI, USA). During the second step, Improm-II^{TM} reverse transcriptase (Promega, Madison, WI, USA) was used for first strand synthesis by incubation of the RNA/ poly-dT mixture at 42 ^{o}C for 1 hr. cDNA samples were stored at -20 ^{o}C for subsequent use.

2.2.10.4 Quantitative real time PCR (RT-qPCR) protocol

RT-qPCR was performed on a Rotor-Gene^{TM} 3000 real time thermal cycler (Corbett Research) using Rotor-Gene^{TM} version 6.1.7.1 software (Corbett Research) for data acquisition and analysis. The sequences of the primers used to amplify the reference gene (RG) and genes of interest (GOI), the sizes of expected amplicons, as well the respective annealing temperatures used to amplify each amplicon are displayed in Supplement E.

The RT- qPCR assay was carried out in three PCR parameter protocol steps:
(i) activation program at 95 ^{o}C for 10 minutes;
(ii) PCR program for 40 cycles entailing denaturation at 95 ^{o}C for 3 sec, annealing for 10 sec (see Supplement E for respective annealing temperatures) and extension at 72 ^{o}C allowing for 66 base pairs/ sec (see Table 2.2 for amplicon size); and
(iii) melting curve program with ramping from 72 ^{o}C to 95 ^{o}C, rising 1 ^{o}C/sec each step with 5 sec waiting between steps.

Each experiment employing RT-qPCR was carried out on triplicate biological samples that were each again assayed in triplicate. A dilution series was used as standard curve for each assay. The level of gene transcription of respective GOIs was quantified using the relative quantification method in which the relative abundance of GOIs was normalised to the relative expression levels of the RG, ARBP. The relative expression ratio of a GOI was calculated employing the amplification

efficiency (*E*) and quantification cycle (C_q) deviation (ΔC_q control - ΔC_q sample) of an unknown sample relative to a control (Pfaffl, 2001). The following formula was used:

Relative GOI expression ratio = $(E_{GOI})^{\Delta C_q\ (control - sample)}$ / $(E_{RG})^{\Delta C_q\ (control - sample)}$.

In addition, where indicated, the REST 2008 software program (© 2008 Corbett Research Pty Ltd and Michael W. Phaffl) was employed to calculate the relative transcript abundance of MKP-1. RT-qPCR amplicons were analysed on 1.5% (w/v) agarose gels using TBE (Supplement D2.4.) as the electrophoresis buffer and gels were run at 100 V for 1 hr. Agarose gels were visualised and photographed using a Vacutec G: Box gel documentation system (Syngene, Synoptics Ltd, Beacon House, Cambridge, UK) utilising GeneSnap Software (Syngene, Synoptics Ltd, Beacon House, Cambridge, UK).

2.2.11 Statistical analysis

Results were statistically analysed using GraphPad Prism 4 (GraphPad Software, Inc.) by a one-way ANOVA test with a Bonferroni post-hoc test to compare all groups. Lower case letters were used to denote statistical differences, that is, different letters represented significant differences between data sets, whereas the identical letters indicated no statistical differences between groups. Where indicated, a three-way ANOVA analysis was performed to correct for individual animals, time and treatments. In addition, where specified, a Student's t-test was performed when only two data sets were compared. Differences between treatment groups were considered statistically significant at $P < 0.05$.

Chapter 3

Characterisation of the mitogenic response of osteoblast precursor cells derived from rat adipose tissue

3.1. Introduction

Although various mouse, rat and human primary and immortalised cell lines have been used widely to study different aspects of osteoblastogenesis (Hughes and Aubin, 1997), the cellular mechanism governing the early proliferative phase of osteoblastogenesis, is not yet clearly understood. As outlined in Section 1.3.1.2.3.1, during the proliferative stage, osteoblast precursor cells replicate to expand cell numbers, which is crucial to form bone cell nodules. In the current section of this work, the proliferative response of primary naïve rMSCs was determined using different mitogens. This was done to establish the mitogenic conditions that induced rMSCs to proliferate, as this aspect of these primary stromal cells has not yet been characterised. Primary cells were utilised since many of the immortalised osteoblastic cell lines are osteosarcomas, which might harbour chromosomal abnormalities, cell cycle irregularities, altered gene expression, changes in receptor expression and modified signalling pathways. Standard protocols are available for isolating MSCs from murine, rat and human adipose tissue (Zuk et al., 2002; Yu et al., 2010; Lopez and Spencer, 2011; Yu et al., 2011).

Proliferating cells accurately duplicate their DNA and divide to render two daughter cells by means of a regimented, sequential process referred to as the cell cycle. This cellular process consists of four phases, namely: (i) the G1 (Gap1) phase during which cells grow and prepare for DNA synthesis, (ii) S phase where DNA synthesis occurs, (iii) G2 phase, a cell growth stage known as Gap 2 during which cells prepare for mitosis and (iv) M phase where mitosis and cell division occurs (illustrated in Fig. 1.4). At least two checkpoints exist where DNA quality is assessed before entry into the DNA synthesis and mitotic phases of the cell cycle (Fig. 1.4). If for example DNA damage occurs before these checkpoints, cells stop replicating and undergo cell cycle arrest. During this restricted stage, cells either repair the damaged DNA or undergo cell senescence or apoptosis (Schmitt et al., 2007). Cell proliferation was quantified by measuring DNA synthesis employing methyl-tritium labelled thymidine ([^{3}H]dT) incorporation into DNA. This widely used technique is

sensitive, reliable and is considered the classical, "gold standard" method for measuring proliferation.

Using flow cytometry, the cell cycle distribution of rMSCs stimulated with mitogens was also assessed. Two different methods were employed in the flow cytometric analysis evaluating the DNA content and cell cycle phase distribution of rMSCs after mitogenic stimulation for 24 hours. Firstly, the vital dye, propidium iodide (PI), was used to examine the DNA content of these cells. Secondly, to unify the [^{3}H]dT proliferation assay findings and the PI cell cycle analysis, rMSCs were pulse-labelled for the last hour of the 24 hours of mitogenic stimulation with BrdU, which was detected using FITC-labelled antibodies. In order to discern the G_0/G_1 and G_2/M phases of the cell cycle, total DNA content was determined using 7-AAD staining, as BrdU is only incorporated into actively dividing cells, that is, the S phase. The reason for choosing 7-AAD is that minimal spectral overlap occurs between 7-AAD and FITC (according to the manufacturer's notes). PI was detected using the FL-2 detector and a 585/42 filter with wavelength range of 564 nm to 606 nm. For FITC detection, the FL-1 detector was used with a 530/30 filter which detect light ranging from 515 nm to 545 nm. The FL-3 detector with a 670 LP filter which detects light up to 670 nm was used for 7-AAD detection. The recording of aggregates, defined as cells or isolated nuclei stuck to one another or which pass the flow cytometer laser simultaneously, results in distorted cell cycle data. For example, aggregates of two G1 cells, also known as doublets, may exhibit the same DNA content as one G_2/M cell which contains duplicated DNA during mitosis. The percentage of cells interpreted to be in the G_2/M phase would then be inaccurately high. Therefore, to ensure the accuracy and reproducibility of cell cycle data, cell aggregates were excluded from acquired data. Another parameter of flow cytometry data quality which must be considered is the percentage co-efficient of variation (% CV) of the G1 peak, which is specified by the ratio of $^{\text{standard deviation}}/_{\text{mean}}$ **x 100**. By convention, a low % CV is an indication of good quality data. In this study, isolated nuclei were used for PI staining, instead of whole cells, to ensure that low % CVs, minimal clumping and good quantitative staining were obtained. In order to minimise the occurrence of aggregates and to maximise the acquisition of single nuclei, recorded events were gated during acquisition using the Cell Quest Pro software. The pulse FL-2 width (FL2-W) versus FL2-area (FL2-A) dot plots were used to identify aggregates. A minimum of 25 000 gated events were recorded during flow cytometry data acquisition. The fluorescence data acquired during this study was considered acceptable because the percentage of CVs of <7% were obtained for all samples investigated (Shankey et al., 1993; Brotherick et al., 1998). In addition, the percentage aggregates as well as the amount of debris detected were overall low. These statistical parameters are indicated on the respective FL2-Area DNA histograms constructed using ModFit® and displayed in Addendum F.

Mitochondrial activity was examined using the MTT (3-(4, 5-dimethylthiazolyl)-2, 5-diphenyltetrazolium bromide) assay. MTT is reduced to a colour product, formazan, by all metabolically active cells and is therefore a measure of cell viability. Although the MTT assay is also sometimes used as a measure for cell replication, the major disadvantage of the MTT reduction assay is that it is not restricted to mitotic cells. In this application of the MTT assay, an increase in MTT staining indicates an increase in viable, active cell number, inferring that cell proliferation has occurred. However, it gives no indication of cellular turnover, as increased proliferation may be accompanied by increased apoptosis leading to a static number of viable cells. Changes in proliferation would therefore not be seen. The advantage of using [^{3}H]dT incorporation is that the isotope-labelled nucleotide will only be incorporated into actively-dividing cells, thus measuring the rate of DNA synthesis at that time. The amount of radio-labelled nucleotide incorporation during the S phase is directly proportional to the amount of actively dividing cells.

3.2 Results

3.2.1 Naïve rMSCs exhibit delayed proliferation in response to high concentrations of FBS and are non-responsive to PMA

Cellular proliferation in undifferentiated rMSCs was examined by treating cells with known mitogens, namely either the phorbol ester, PMA (phorbol 12-myristate 13-acetate) or a high concentration fetal bovine serum (FBS), which is a mixture of various growth factors (Gstraunthaler, 2003 and Brunner et al., 2010). Mitogenesis was examined every 24 hours over a course of 72 hours.

Before mitogenic induction, the concentration of serum was reduced to 1% overnight to synchronise the cell cycle in all cells. FBS concentrations lower than 1% FBS was not used, as these resulted in increased cell death by apoptosis (data not shown). Hence, 1% FBS was used as basal growth control to determine the level of proliferation elicited by mitogenic stimulation. FBS concentrations (v/v) of 5%, 10% and 20% were used to induce mitogenesis. The concentration of 100 ng/ml was used for PMA stimulation, whilst 0.1% DMSO was employed as negative control to determine whether the solvent that PMA was dissolved in had any adverse effect on cell proliferation.

It was found that rMSC proliferation decreased with increasing FBS concentration after 24 hours of mitogen treatment, with 5% FBS exhibiting the highest proliferative response of 3.1-fold after 24

hours (Fig. 3.1 A). Compared to basal growth levels, mitogenic treatment with 10% FBS elicited a 2.3-fold increase in proliferation at 24 hours, whilst 20% FBS resulted in a 1.5-fold increase.

Although phorbol esters are generally considered to be strong mitogens, PMA-induced mitogenesis was only 1.2-fold higher than that of the 1% FBS basal control (Fig. 3.1 A), and this rate persisted over the 72 hours of the experiment (Fig. 3.1 C). These were not significantly different from control. As expected, the DMSO solvent control exhibited a similar mitogenic response to the 1% FBS control at all time points (Fig. 3.1). At 48 hours after stimulation, 10% FBS produced the greatest mitogenic response (Fig. 3.1 B). The highest level of proliferation induced by 20% FBS was seen after 72 hours of stimulation (Fig. 3.1 C). It is noteworthy that after 72 hrs in culture, cells treated with 10% FBS and 20% FBS were visually confluent. Cells treated with 5% FBS were near confluent, whereas cells treated with 1% FBS and PMA did not reach confluency.

When the relative proliferation per mitogenic treatment was plotted over a timespan of 72 hours, it was seen that proliferation stimulated by 5% FBS significantly declined by 48 hours (Fig. 3.1 D), whilst that elicited by 20% FBS steadily, but significantky increased up to 72 hours (Fig. 3.1 D). Although 10% FBS had a significant effect on rMSC proliferation, maximal stimulation at this concentration was seen at 48 hours (Fig. 3.1 D). PMA showed a proliferation rate similar to that of the basal control (C) and the DMSO solvent control (Fig. 3.1 D). The decrease in proliferation observed after 72 hours of 5% FBS stimulation is not likely to be due to contact inhibition at confluency since naïve rMSCs grown for 7 days post confluency still proliferated, although beit at a slower rate (see Fig. 4.1). After careful observation, no morphological changes were seen when cells were treated with 1% FBS as serum deprivation can stimulate myoblast differentiation in stromal cells (Zhang et al., 1999; Hubé et al., 2011). This could be an indication that differentiatin into a myogenic lineage did not occur as myotubule formation was not observed.

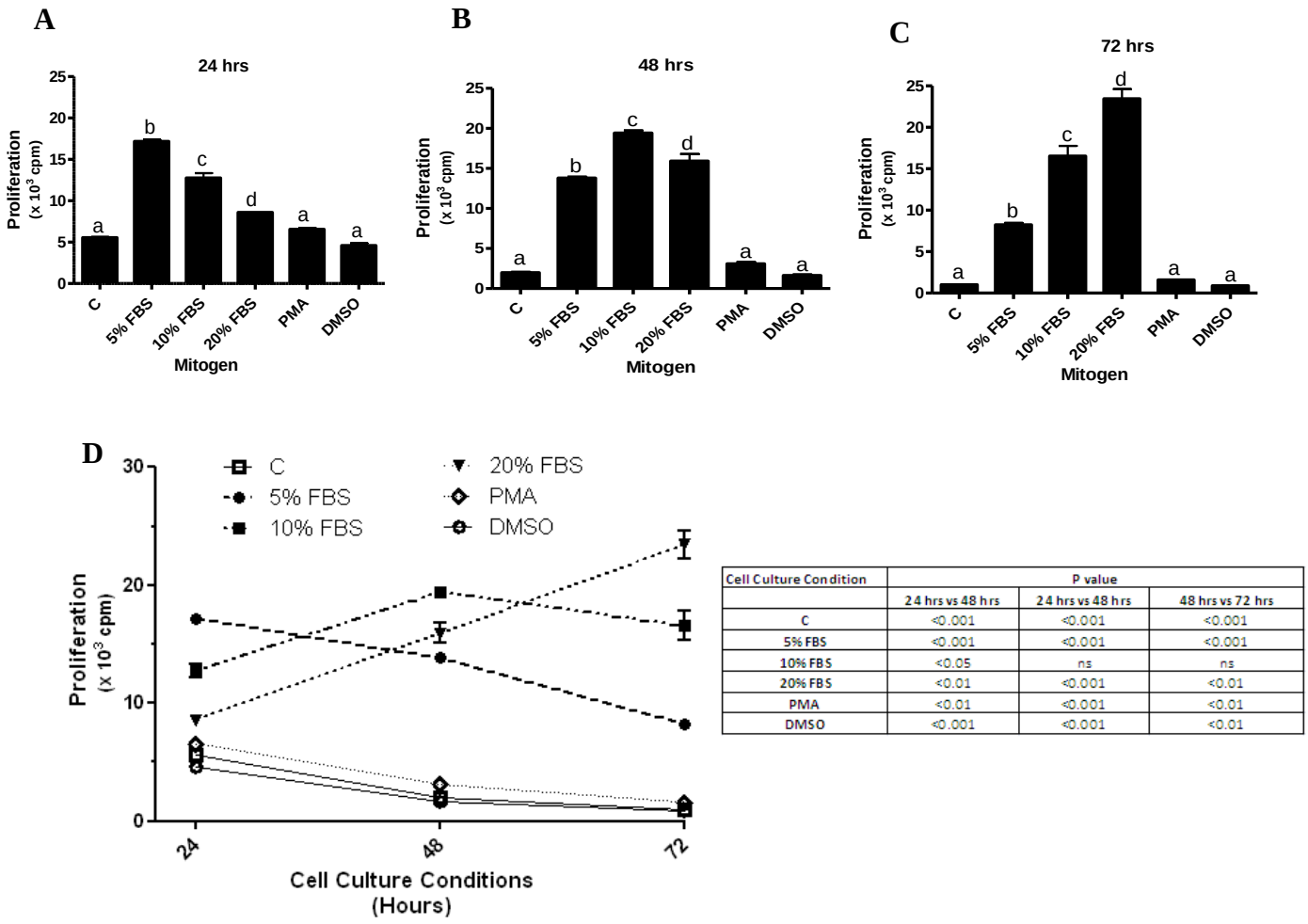

Cell Culture Condition	P value		
	24 hrs vs 48 hrs	24 hrs vs 48 hrs	48 hrs vs 72 hrs
C	<0.001	<0.001	<0.001
5% FBS	<0.001	<0.001	<0.001
10% FBS	<0.05	ns	ns
20% FBS	<0.01	<0.001	<0.01
PMA	<0.01	<0.001	<0.01
DMSO	<0.001	<0.001	<0.01

Figure 3.1.: Strong mitogenic stimulation of naïve rMSCs leads to delayed proliferation after 24 hrs.

Cells were grown to 50% confluency and serum starved in 1% FBS for 24 hrs. For mitogenic stimulation, cells were treated with either: FBS (at concentrations indicated), 100 ng/ml PMA or 0.1% DMSO for 24 (**A**), 48 (**B**) and 72 hrs (**C**). 1% FBS was used as basal growth control and is designated C. The change in proliferation over 72 hours for each of the cell treatments is shown in **D**. DNA synthesis was measured by incorporation of [^{3}H] thymidine ([^{3}H] dT) for the last 4 hrs of incubation. Data of an individual experiment is shown, where n = 3 and is representative of experiments repeated at least three times, where each repeat represents an individual animal. Results displayed are the mean cpm ± S.E.M., where P<0.05 was seen as a statistically significant difference using the One-way Anova with Bonferonni post-hoc test. Statistically significant differences are indicated by different lower case letters. Data bars with the same letter above are not statistically different. **Abbreviations**: **C** control; **cpm** counts per minute; **DMSO** dimethyl sulfoxide; **FBS** fetal bovine serum; **hrs** hours; **ns** not significant; **PMA** phorbol 12-myristate 13-acetate;**vs** versus

3.2.2 Oncogene-induced senescence and G_0/G_1 cell cycle restriction contributes to low proliferation levels after 24 hours of strong mitogenic stimulation

The weak proliferative response of undifferentiated rMSCs to strong mitogenic stimulation after a period of 24 hours may be attributed to various reasons. These could be (i) compromised cell viability, which was assessed with the MTT mitochondrial activity assay (Fig. 3.2), (ii) hypermitogenic stimulation leading to oncogene-induced senescence (OIS), which was examined using the senescence-associated β-Gal (SA-β-Gal) assay (Fig. 3.3) or (iii) cell cycle arrest as determined by propidium iodide staining of isolated nuclei (Fig. 3.7, Fig. 3.8, Table 3.1 and 3.2) or bromodeoxy- uridine (BrdU) pulse-labelling of whole cells (Fig.3.9 and Table 3.3).

3.2.2.1 Mitochondrial activity of rMSCs after 24 hours of mitogenic exposure

The MTT reduction assay revealed an increase in formazan production in naïve rMSCs to increasing concentrations of FBS; with 20% FBS exhibiting the highest formazan levels (Fig. 3.2). The 1% FBS control was set as a 100%. The low FBS concentration of 5% evoked a 27% (SD± 0.057) increase in mean formazan crystal formation compared to the control, whereas 10% FBS and 20% elicited a 44% (SD± 0.042) and 71% (SD± 0.029) increase, respectively. Contrary to FBS, PMA, although normally a powerful mitogen, did not elicit a similar response; instead, formazan levels were only increased by 5% compared to the control. However, this increase was significantly different from controls (1% FBS) (Fig. 3.2). Based on the premise that the degree of formazan conversion indicated metabolic activity levels, these results suggest that strong mitogenic stimulation resulted in higher levels of metabolic activity compared to the control. It can also be concluded that the viability of rMSC was not adversely affected by potent mitogens after 24 hours. This finding is in contrast with proliferation data (Fig 3.1 A) showing that rMSC proliferate less when stimulated with strong mitogens such as 20% FBS and PMA for 24 hours. A possible reason for this discrepancy may be that rMSCs were undergoing oncogenic-induced senescence (OIS), a cellular process characterised with an increase in metabolic activity and a decrease or cessation in cell proliferation (Dimri et al., 1995; Campisi, 2001).

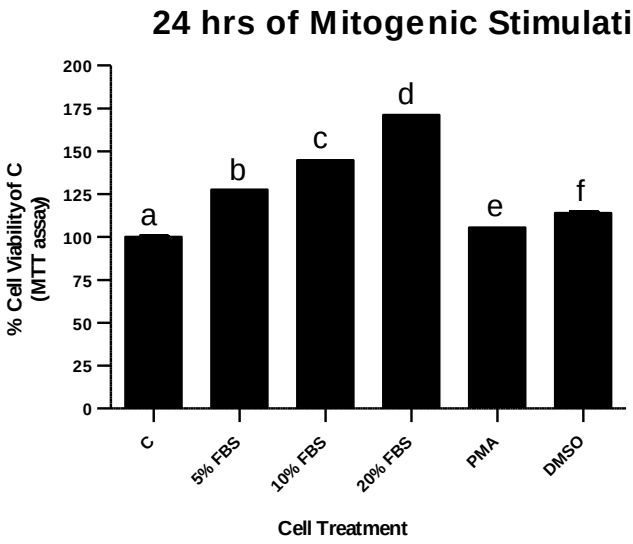

Figure 3.2: Naïve mesenchymal stromal cell mitochondrial activity is not dramatically reduced after strong mitogenic stimulation for 24 hrs.

Cells were grown until 50% confluent and serum starved in 1% FBS for 24 hrs before the addition of either FBS (at concentrations indicated), 100 ng/ml PMA or 0.1% DMSO (used as negative control) for an additional 24 hrs. Basal proliferation was elicited by treatment with 1% FBS. Mitochondrial activity was assessed using the MTT mitochondrial activity assay (2.2.7 in Methods). Data is presented as % mitochondrial activity compared to control (1% FBS). The experiment was repeated three times, with data being similar for each repeat (animal). Results displayed is a representative experiment and are shown as the mean % ± S.D, where n=3. Statistically significant differences ($P<0.05$) (One-way Anova with Bonferonni post-hoc test) are specified by different lower case letters. **Abbreviations**: **C** control; **DMSO** dimethyl sulfoxide; **FBS** fetal bovine serum; **MTT** 3-(4, 5-dimethylthiazolyl-2)-2,5-diphenyltetrazolium bromide; **PMA** phorbol 12-myristate 13-acetate

3.2.2.2 Oncogene-induced senescence is observed after rMSCs were stimulated with strong mitogens for 24 hours

Elevated β-Gal (β-galactosidase) activity is a hallmark of senescent cells (Dimri et al., 1995; Campisi, 2001) and was used to examine the level of senescence exhibited by naïve rMSCs after 24 hours of strong mitogenic stimulation (Fig. 3.3 A). Cells may undergo senescence under inadequate culture conditions such as nutrient deficiency (Mathon and Lloyd, 2001; Tang et al., 2001). These low nutrient conditions were achieved by exposing cells to 1% FBS for 48 hours (serum reduction for 24 hours and a further 24 hours while mitogenic treatments had effect). Under these conditions

of 48 hr serum depletion, 22% of cells counted exhibited elevated levels of β-Gal activity (Fig. 3.3 B). Cells stimulated with 5% FBS, the concentration which elicited the highest rMSC proliferation after 24 hours, displayed a lower level of β-Gal activity (8.3 %) compared to the 1% FBS positive control (Fig. 3.3 B). In addition, the mean percentage of β-Gal positive cells obtained with 10% FBS (7.1 %) were not significantly different from 5% FBS (8.3 %) (Fig. 3.3 B). Moreover, 20% FBS and PMA, the cell treatments which resulted in low levels of proliferation of rMSCs after 24 hours of stimulation, showed the highest levels of β-Gal activity (Fig. 3.3 B). In the case of 20% FBS, a mean percentage of 17.1% of cells showed β-Gal activity, whereas PMA treatment caused increased β-Gal activity in 24.7% of cells. These results demonstrate that strong mitogenic stimulation of naïve rMSCs led to increased β-Gal activity, suggesting that these cells exhibited cellular senescence.

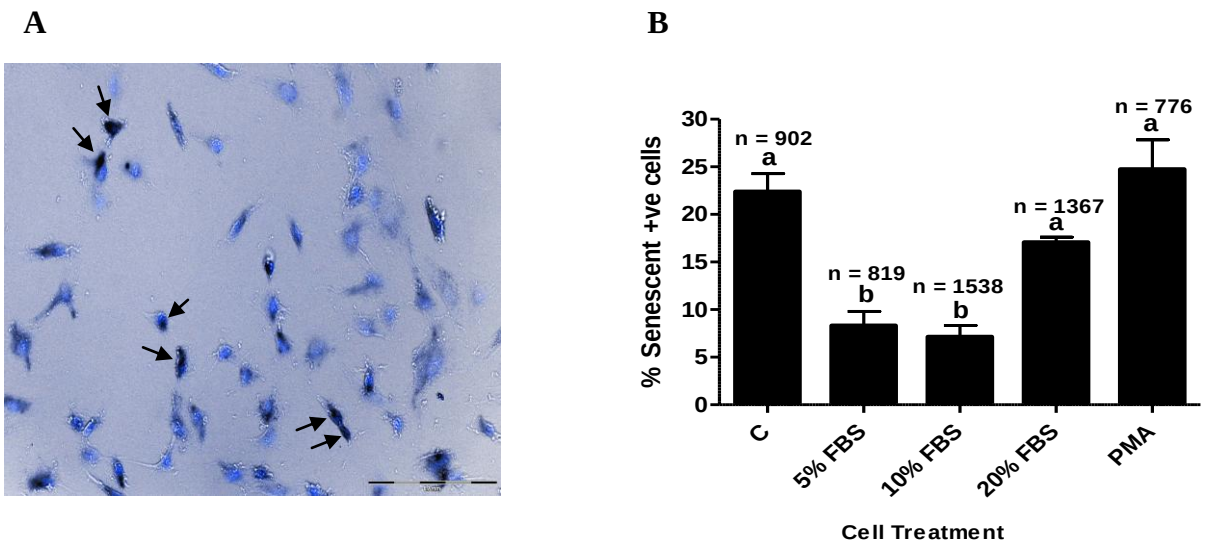

Figure 3.3: Strong mitogenic stimulation of rMSCs leads to increased SA-β-Gal activity.

Hemi-confluent cells were serum starved in 1% FBS for 24 hrs before mitogenic stimulation with either FBS (at concentrations indicated) or 100 ng/ml PMA. Oncogenic-induced senescence was examined using the SA-β-Gal activity assay. 1% FBS, which mimicked nutrient deficient conditions, was used as positive control for this assay. Cells were effectively exposed to 1% FBS for 48 hrs. Hoechst nuclear stain was used as counterstain to determine the total amount of cells per field of view. (**A**) Image overlay of transmission and counterstained images (the scale is 0.2 mm as indicated at the bottom of the image), depicting senescent positive (indicated by arrows) and negative cells (background; light blue cells). (**B**) Percentage of senescent positive cells with the total amount of cells counted specified above the columns. The experiment was repeated once (n=4), with similar trends exhibited. Statistically significant differences ($P<0.05$) (One-way Anova with Bonferonni post-hoc test) are indicated by different lower case letters. Data that were not statistically significantly different are indicated by similar lower case letters. **Abbreviations**: **C** control; **DMSO** dimethyl sulfoxide; **FBS** fetal bovine serum; **PMA** phorbol 12-myristate 13-acetate; **SA-β-Gal** senescence-associated β-galactosidase

3.2.2.3 Flow cytometric analysis of the DNA content and cell cycle phase distribution of rMSCs after 24 hour mitogenic stimulation

In order to further investigate the lack of proliferative response in naïve rMSCs to PMA and 20% FBS after 24 hr incubation (as seen in Section 3.2.1), flow cytometric analysis using propidium iodide (PI) and bromodeoxyuridine (BrdU) were used to examine the distribution of the cell cycle phases. The light scatter properties (forward scatter vs side scatter) of two independent experiments are depicted in Fig. 3.4 and Fig. 3.5. Naïve rMSCs grown in 1% FBS were used as negative growth control. Although no difference in cell size, shape and granularity was observed when using phase contrast light microscopy, analysis of the light scatter properties of the isolated nuclei indicated the presence of two nucleic populations in rMSCs cultures (Fig. 3.4 and Fig. 3.5). These two populations were identified using the autogating tool of the FlowJo® software as guideline, to reduce possible subjectivity during flow cytometry data analysis. Based on the FSC characteristics of the isolated nuclei, two main populations of different sizes were observed (Fig. 3.4 and Fig. 3.5); whereas the SSC data showed that the two major populations were also divergent in cell granularity (Fig. 3.4 and Fig. 3.5). The presence of two populations of nuclei, suggests the occurrence of two cell types in rMSC cultures of different size and complexity. These two populations were designated population 1 and population 2, respectively. Population 1 represented smaller cells with more condensed nuclei, whilst population 2 signified larger cells which have more granular nuclei (Fig. 3.4 and Fig. 3.5).

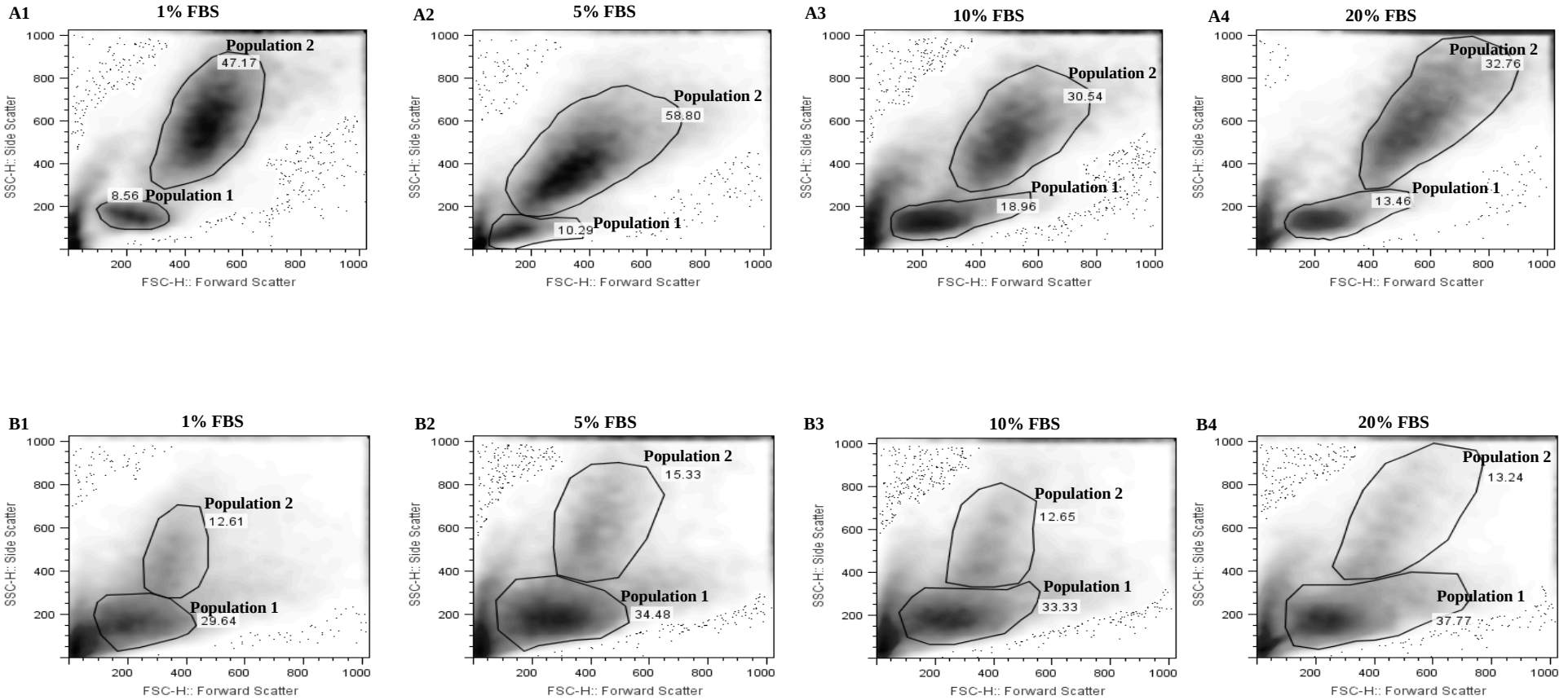

Figure 3.4: Flow cytometry analysis revealed two populations of isolated nuclei present in naïve rMSCs cultures.

Semi-confluent cells were serum starved in 1% FBS for 24 hrs before mitogenic stimulation with either FBS (at concentrations indicated) or 100 ng/ml PMA. Nuclei were isolated as described in section 2.2.7. A FACSCalibur flow cytometer was used to acquire data. FlowJo software was used for light scatter data analysis. Diagrams **A1 – A4** and **B1 – B4** specify the respective density plots of two independent experiments measuring light scatter properties (FSC vs SSC) of rMSCs stimulated for 24 hrs with mitogens, where $n_{modelled\ cells} > 25\ 000$. Cell populations were gated (populations are encircled) and the percentage of cells present in each population is specified. The respective treatments are indicated at the top of the graphs. **Abbreviations**: **FBS** fetal bovine serum; **FSC** forward scatter; **SSC** side scatter

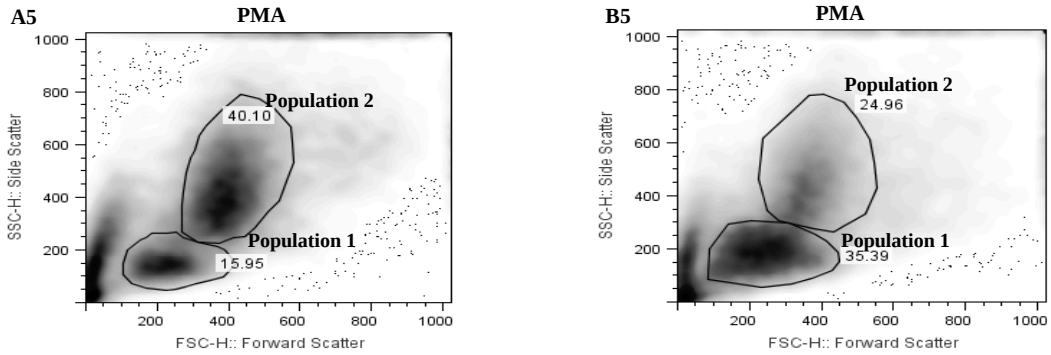

Figure 3.5: Flow cytometry analysis of the two cell populations in naïve rMSCs cultures after PMA exposure. Semi-confluent cells were subjected to serum reduction using 1% FBS for 24 hrs before stimulation with 100 ng/ml Isolated cell nuclei were stained with propidium iodide. Fluorescence data was acquired using a FACSCalibur flow cytometer. The density plots of SSC (y-axis) vs FSC (x-axis) of the two independent experiments labelled A5 and B5 are illustrated. The total modelled events were > 25 000. Cell populations were gated (populations are encircled) and the percentage of cells present in each population is marked. **Abbreviations**: **FSC** forward scatter; **PMA** phorbol 12-myristate 13-acetate; **SSC** side scatter

It was found that the rMSC cultures stained with the DNA binding dye, Hoechst 33258, under basal and mitogenic conditions, contained nuclei of two different sizes and granularity as seen microscopically, although these cells were all fibroblastic in appearance and therefore morphologically indistinguishable when viewed by phase contrast light microscopy (Fig. 3.6). This agrees with the flow cytometry light scatter results which indicated the occurrence of two populations of nuclei in rMSCs cultures, irrespective of mitogenic induction (Fig. 3.4 and Fig. 3.5). Figure 3.6 illustrates the presence of smaller, more condensed nuclei (white arrows) as well as larger, more granular nuclei (green arrows) present in rMSCs cultures. The occurrence of two types of nuclei again infers the presence of two cell populations present in rMSC cultures.

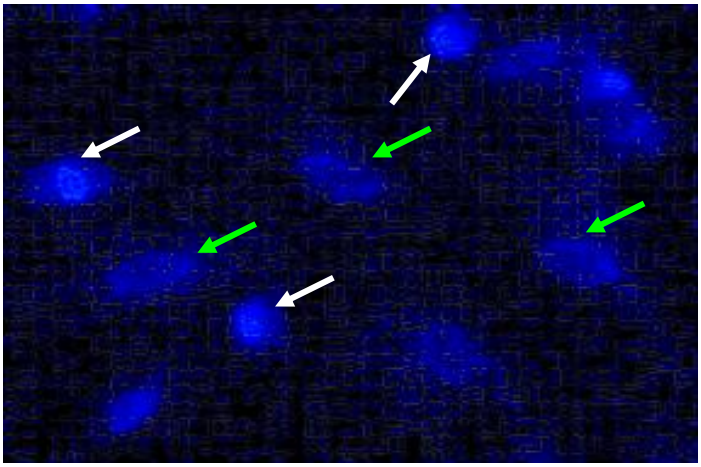

Figure 3.6: Hoechst nuclear staining of rMSC nuclei revealed the presence of large and small nuclei populations. Hemi-confluent cells were serum starved in 1% FBS for 24 hrs before mitogenic stimulation with either 20% FBS. Hoechst nuclear stain was used to examine rMSC nuclei. The white arrows specify the smaller, more condensed nuclei, whilst the green arrows represent the larger, more granular nuclei. Images were obtained using an Olympus Cell ® system attached to an IX-81 inverted fluorescence microscope equipped with an F-view-II cooled CCD camera (Soft Imaging Systems). Image acquisition was performed using a Xenon light source (MT-20, Cell ®) with a 360 nm excitation filter and a UBG triple band pass emission filter, a 10x UPlanFLN objective and the Cell® imaging software.

In order to determine whether the cells in populations 1 and 2 were undergoing cell division, the FL2 area (channel for PI fluorescence) was plotted against the side scatter (SSC; indication of granularity), specifically to identify the G_0/G_1 and G_2/M phases in these populations (Fig. 3.7 and Fig.3.8). In accordance with the results shown in Fig 3.4 and Fig. 3.5, two discrete populations were again identified (Fig. 3.7 and Fig. 3.8). Analysis of the FL-2 area versus SSC area density plots revealed that both populations, irrespective of mitogenic stimulation, were undergoing cell cycle events and were not just quiescent (Fig. 3.7 and Fig. 3.8). Figures 3.7 (A1 – A4; B1 – B4) and Fig. 3.8 (A5; B5), illustrates the G_0/G_1-, S- and G_2/M cell cycle phases, respectively designated as regions i, ii and iii, of each of the identified populations. For closer examination of the cell cycle phase distribution of the nuclei present in populations 1 and -2, cell cycle analysis was performed using ModFit® software and gated (addenda F1 – F20). Importantly, the relevant debris areas were included in the gated regions to ensure accurate modelling using Modfit®. For example, upon gating the smaller, less granular population, the debris surrounding the smaller population was included for accurate cell cycle modelling using the Modfit® software (as shown in addendum F). Similarly, the debris surrounding the bigger, more granular population was included in the relevant regions to ensure accurate cell cycle modelling as exclusion of the debris region would lead to inaccurate data interpretation (addendum F). The relevant statistical parameters are shown in the colour coded tables, with the colour coding keys indicate at the bottom of the tables (addenda F1 – F20).

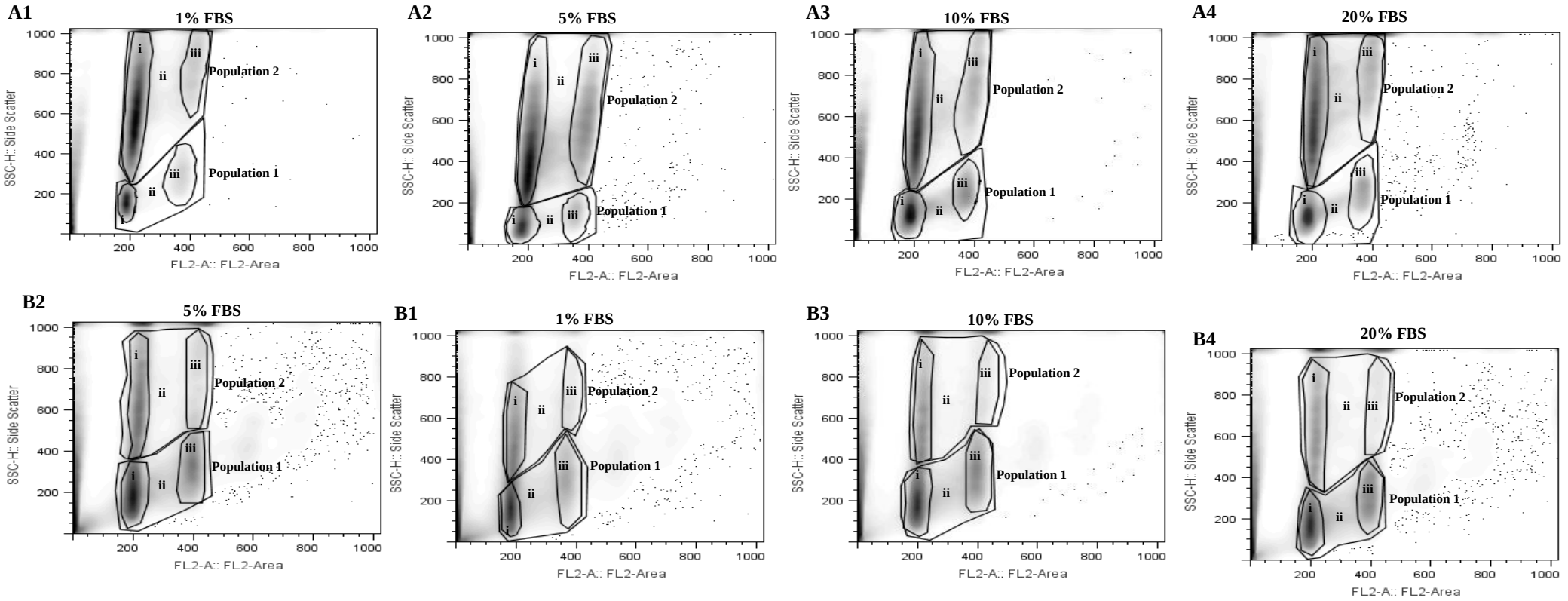

Figure 3.7: Flow cytometry analysis revealed two cell populations with different cell cycle phase distributions present in naïve rMSCs cultures.

Semi-confluent cells were serum starved with 1% FBS for 24 hrs before mitogenic stimulation with either FBS (at concentrations indicated) or 100 ng/ml PMA. Isolated cell nuclei were stained with propidium iodide and fluorescence data was acquired using a FACSCalibur flow cytometer. In figures **A1 – A5** and **B1 –B5** the density plots of SSC (y-axis) vs FL-2 area (x-axis) of two independent experiments, where $n_{\text{modelled events}} > 25\,000$, are illustrated. The respective treatments are indicated at the top of the graphs. Regions specified as i, ii, and iii represent the **G_0/G_1**, **S** and **G_2/M** phases of the cell cycle, respectively. **Abbreviations**: **FBS** fetal bovine serum; **SSC** side scatter; **FL-2 area** fluorescence channel for PI

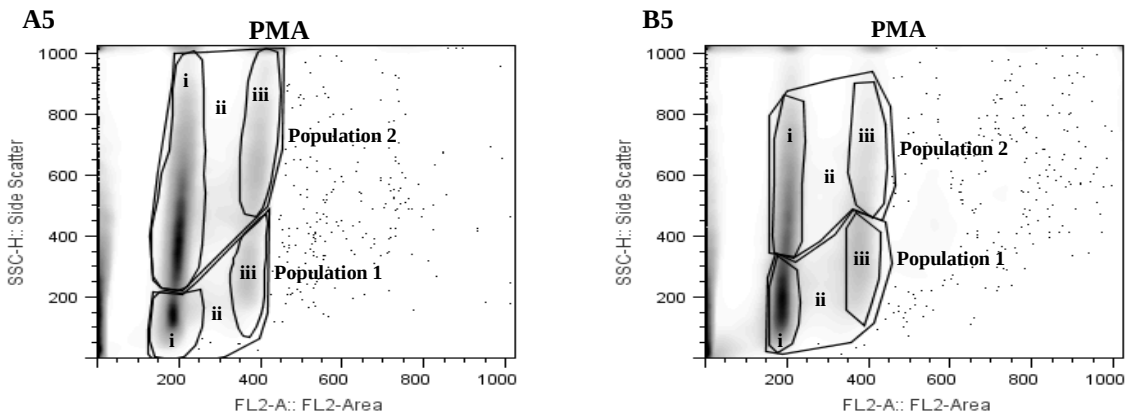

Figure 3.8: Flow cytometry analysis revealed two cell populations with different cell cycle phase distributions present in naive rMSCs cultures after PMA exposure.

Hemi-confluent cells were subjected to serum reduction using 1% FBS for 24 hrs before stimulation with 100 ng/ml PMA. Isolated cell nuclei were stained with propidium iodide. Fluorescence data was acquired using a FACSCalibur flow cytometer. The density plots of SSC (y-axis) vs FL-2 area (x-axis) of the two independent experiments labelled A5 abnd B5 are illustrated. The total modelled events were > 25 000. Regions indicated as i, ii, and iii represent the **G_0/G_1**, **S** and **G_2/M** phases of the cell cycle, respectively. **Abbreviations**: **PMA** phorbol 12-myristate 13-acetate; **SSC** side scatter; **FL-2 area** fluorescence channel for PI

The cell cycle analysis of rMSCs subjected to mitogenic stimulation for 24 hours, using Modfit®, revealed that each of the observed populations in rMSC cultures displayed different cell cycle distributions (Addenda F1–F20). The greatest percentage of cells in population 1, irrespective of mitogenic induction, was observed in the G_0/G_1 phase of the cell cycle (Table 3.1). This suggests that these cells are either in a quiescent state or perhaps undergoing senescence. rMSCs subjected to limited GFs (1% FBS) and the potent mitogen, PMA, in both experiments, exhibited the highest percentages of cells in the G_0/G1. In addition, cells grown in the presence of high concentrations of GFs, like 20% FBS, displayed the least amount of cells in this phase (Table 3.1). All treatments resulted in a portion of population 1 cells in S phase, with 20% FBS showing the highest number of cells present in this phase (Table 3.1). A fraction of cells in population 1, irrespective of treatment, were also observed in G_2/M, again with 20% FBS treatment resulting in the highest percentage of cells in the G_2/M phase (Table 3.1). These results suggest that treatment of rMSCs with 20% FBS may possibly be restricted at the G_2/M block in the cell cycle, because proliferation is low in these cells (as seen in Section 3.2.1; Fig. 3.1 A).

Table 3.1 displays the cell cycle phase distribution of Population 1 (% cells).

Cell Treatment	Experiment A (% cells)			Experiment B (% cells)		
	G_0/G_1	S	G_2/M	G_0/G_1	S	G_2/M
1% FBS	76.31	13.00	10.70	78.95	12.36	8.69
5% FBS	68.78	19.51	11.72	71.03	16.35	12.62
10% FBS	60.54	26.24	13.22	75.78	20.25	3.97
20% FBS	56.87	27.23	15.89	63.27	21.92	14.81
PMA	74.41	14.49	11.10	88.50	7.36	4.14

Like cells in population 1, the majority of cells in population 2 were also restricted in the G_0/G_1 cell cycle phase (Table 3.2), suggesting that these cells are either quiescent or possibly in a senescent state. As seen in Table 3.2, a lesser amount of rMSCs in population 2 were observed in the S phase and G_2/M phase of the cell cycle. Although the amount of cells observed in the S phase after 20% FBS stimulation were similar in both experiments, the percentage of cells in the G_2/M phase differed considerably (12.79 vs 0.58) (Table 3.2). The reason for the discrepancy is unknown.

Table 3.2 displays the cell cycle phase distribution of Population 2 (% cells).

Cell Treatment	Experiment A (% cells)			Experiment B (% cells)		
	G_0/G_1	S	G_2/M	G_0/G_1	S	G_2/M
1% FBS	78.39	14.46	7.15	82.72	17.28	0.00
5% FBS	63.13	25.68	11.19	69.28	17.45	13.26
10% FBS	62.13	26.75	11.13	67.14	17.73	15.13
20% FBS	60.10	27.11	12.79	71.42	27.99	0.58
PMA	78.24	11.37	10.39	82.60	12.15	5.24

These findings indicate that after 24 hours of mitogen stimulation (for all mitogens tested), the majority of cells, irrespective of size and granularity, are in the G_0/G_1 cell cycle phase. In addition, under all experimental conditions, a portion of rMSCs were found to be in the S-phase of the cell cycle. This indicates the percentage of cells that are actively undergoing DNA replication after 24 hours of basal growth and mitogenic stimulation. Therefore, it is the DNA synthesis and hence proliferation of this portion of cells that is measured during the [^{3}H]dT proliferation assay. However, the cell cycle distributions of rMSCs subjected to 20% FBS treatment do not correlate with the [^{3}H]dT proliferation assay results obtained after 24 hours. Although the highest portion of cells were seen in the S phase after 20% FBS stimulation, rMSCs stimulated with 20% FBS mounted a weak proliferative response (50% of the control) after 24 hours, but this increased after

72 hours (Fig. 3.1 A and C). This thus indicates that these cells could be restricted at the G_1/S boundary of the cell cycle.

In order to reconcile the [^{3}H]dT proliferation assay findings with the PI DNA content analysis, rMSCs were pulse-labelled with BrdU for 1 hr. The BrdU fluorescence data are displayed in Fig. 3.9 as density plots where FL3-H was plotted against the FL1-H using the FlowJo® software. Since BrdU is only incorporated into DNA of actively dividing cells, that is cells in the S phase, the DNA binding dye, 7-AAD (7-Aminoactinomycin D), was also used to measure total DNA content in order to identify the G_0/G_1 and G_2/M cell populations. To accurately analyse the distribution of the cell cycle phases using the FL3-H (anti-BrdU-FITC channel) versus FL1-H (7-AAD channel) zebra plots, the debris regions were excluded from the analysis by gating the area surrounding the G_0/G_1-, S- and G_2/M cell cycle phases. This debris region was designated as R (Fig. 3.7 and Fig. 3.8). The cell cycle phases were demarcated as regions i, ii and iii, corresponding in that order to the G_0/G_1-, S- and G_2/M cell cycle phases (Fig. 3.7 and Fig. 3.8).

The amount of cells present in each cell cycle phase was expressed as percentages of the gated region, R and displayed in Table 3.3.It is noteworthy that because the total number of cells in the gated region R was used as opposed to the amount of the cells in the regions i, ii and iii, the total percentage of the cell phases for each treatment does not amount to 100%. Since 1% FBS was used to synchronise the cell cycle of naïve rMSCs prior to mitogenic stimulation, cells subjected to 1% FBS showed the largest amount of cells in G_0/G_1 and almost none in the S phase. This is in agreement with the [^{3}H]dT proliferation results where 1% FBS was used as basal growth condition (Fig. 3.1 A). rMSCs were treated with 10% FBS to simulate normal growth conditions and results revealed that 52% of these cells were found in the G_0/G_1, with moderate amounts observed in the S – and G_2/M phases. Although the majority of cells for all treatments were found in the G_0/G_1 cell cycle phase, cells subjected to 5% FBS treatment had the least amount of cells in G_0/G_1 (Table 3.3). In addition, cells treated with 5% FBS exhibited a modest amount of cells in S phase and the highest percentage of cells in the G_2/M cell cycle phase (Table 3.3), suggesting that this portion of cells are actively synthesising DNA and undergoing mitosis. This finding is in agreement with the [^{3}H]dT proliferation data in Fig. 3.1 A, where 5% FBS elicited the greatest proliferative response after 24 hours of stimulation.

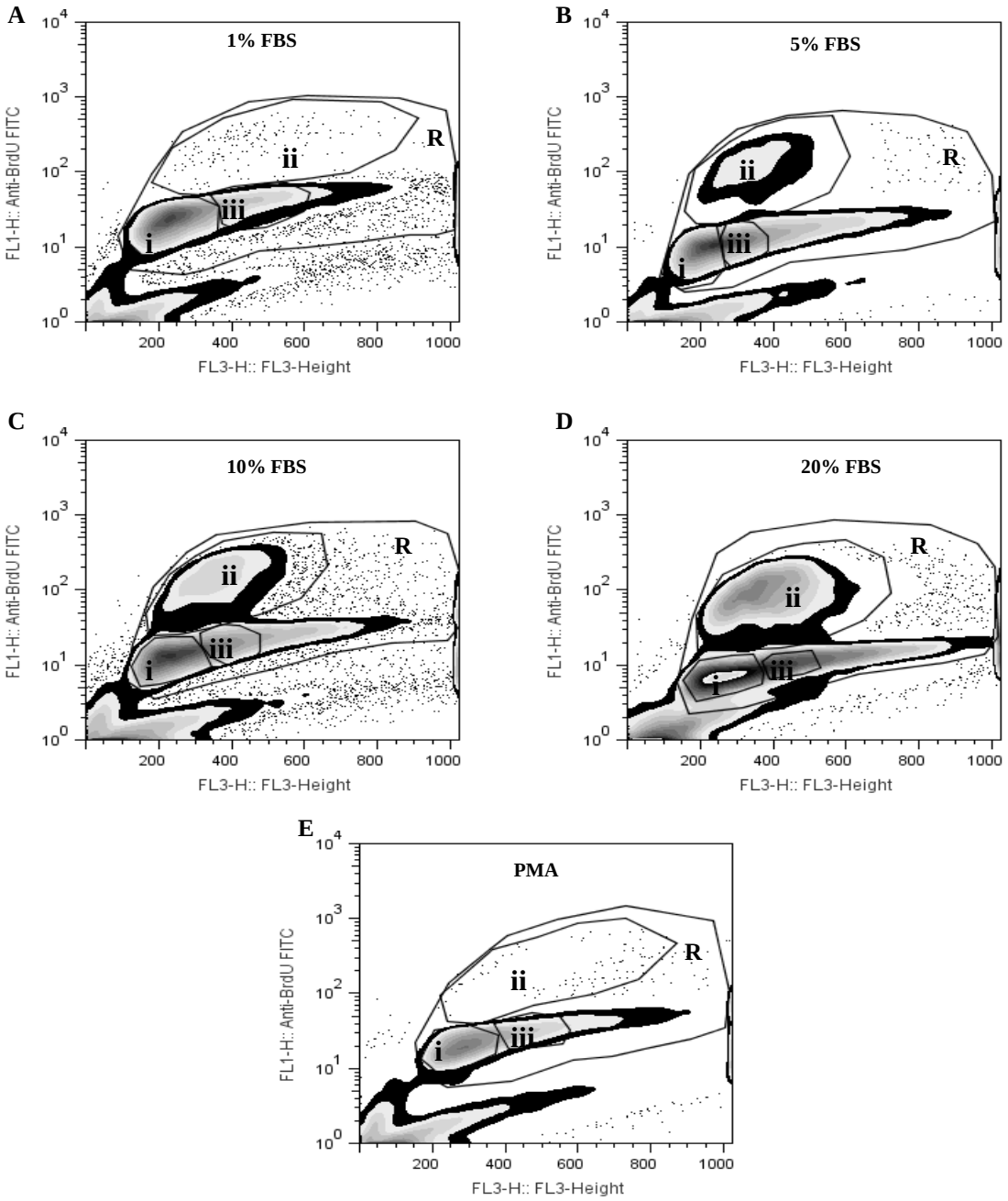

Figure 3.9: BrdU pulse-labelling of mitogen-stimulated rMSCs shows different cell cycle phase distributions.
Semi-confluent cells were serum starved in 1% FBS for 24 hrs before mitogenic stimulation with either FBS (at concentrations indicated) or 100 ng/ml PMA. Cells were then pulse-labelled with BrdU for 1 hr before cell fixation. Fixed cells were stained with 7-AAD for 5 min before fluorescence data acquisition using a FACSCalibur flow cytometer. Figures **A – E** display the zebra density plots of FL3-(H) area (x-axis) versus FL1-H (y-axis), where $n_{\text{modelled events}} > 25\,000$, are illustrated. The respective treatments are indicated at the top of the graphs. Regions specified as i, ii, and iii represent the G_0/G_1, S and G_2/M phases of the cell cycle, respectively and was gated using FlowJo® software. **Abbreviations**: **BrdU** bromodeoxyuridine; **FBS** fetal bovine serum; **FITC** Fluorescein isothiocyanate; **FL1** fluorescence channel for BrdU-FITC; **FL1** fluorescence channel for 7-AAD; **H** height; **PMA** phorbol 12-myristate 13-acetate; **7-AAD** 7-Aminoactinomycin D; **R** debris region

Table 3.3 displays the cell cycle phase distribution (% cells) of rMSCs using BrdU staining.

Cell Treatment	BrdU (%)		
	G_0/G_1	S	G_2/M
1% FBS	73	1	16
5% FBS	40	11	28
10% FBS	52	16	17
20% FBS	46	24	13
PMA	61	2	17

Compared to the PI cell cycle data, BrdU pulse-labelling revealed that 20% FBS also exhibited the highest percentage of cells in the S phase of the cell cycle (Table 3.3). In addition, the amount of cells observed in the G_2/M phase after 20% FBS stimulation, was the least, compared to other cell treatments (Tale 3.3). In accordance with the PI cell cycle data, these findings suggest that naïve rMSCs may experience S-phase restriction after 24 hours of stimulation with 20% FBS and not progressing to the mitotic phase of G_2/M. A possible reason for this could be that these cells were under the restriction of the intra-S-phase checkpoint (Kastan and Bartek, 2004; Houtgraaf et al., 2006).

Cells treated with PMA also had most of the cells in G_0/G_1, virtually none in S phase and a moderate amount in G_2/M (Table 3.3). It appears that 1% FBS and PMA elicited comparable cell cycle phase distributions and this is in agreement with proliferation data where these treatments resulted in similar proliferation levels (Fig. 3.1 A). In contrast to PMA, 20% FBS elicited slight, but significant proliferation when compared to the 1% FBS negative growth control (Fig. 3.1 A). However, this small response of cells to 20% FBS was much lower than that evoked by 5% FBS (Fig. 3.1 A). In conjunction with this proliferation data, it appears that the cell cycle phase distribution of cells treated with 20% FBS were also considerably different to 1% FBS and PMA (Table 3.3), suggesting a possible difference in mechanism of senescence between these treatments.

In addition, even though the levels of senescence elicited by 1% FBS, 20% FBS and PMA were not statistically significantly different, the level of senescence caused by 20% FBS was slightly less than that of 1% FBS and PMA (Fig. 3.3). This illustrates a possible difference between the cellular mechanism resulting in reduced proliferation and senescence elicited by 1% FBS, 20% FBS and PMA. Moreover, 1% FBS and PMA were observed to be stronger inducers of senescence than 20% FBS (Fig. 3.3).

3.3 Discussion

Mesenchymal stromal cells derived from adipose tissue present an original model to study various aspects of bone cell development. Analysis of the light scatter properties of whole rMSCs using flow cytometry has shown that the isolation method used in this thesis produces a homogenous cell population of rMSCs (Dr. H Sadie- van Gisjen, unpublished data). Moreover, it was also found that these cells were positive for the stromal cell surface marker, CD90 and negative for the haematopoietic cell surface antigen, CD45 (personal communication, Dr. H Sadie- van Gisjen). These results, together with the ability of these adherent rMSCs to form calcified bone nodules (see Fig. 4.3) and adipocytes (Ogawa et al., 2004; Lopez and Spencer, 2011), suggests that the rMSCs used in this study were multipotent, mesenchymal stromal cells. Although the presence and absence of more cell surface antigen markers still needs to be tested, these findings are in accordance with the minimum criteria for classification of multipotent MSC as outlined by Dominici et al. (2006).

Since little is known about the proliferation of these adipose-derived stromal cells, various mitogenic conditions were used to ascertain the proliferative response of rMSCs to known mitogens such as fetal bovine serum (FBS) and PMA (Fig. 3.1 A, B and C). It was hypothesised that stimulation of rMSCs with increasing concentrations of FBS would result in an increased proliferative cellular response. The results obtained was contrary to this hypothesis, in that the lower FBS concentration of 5% elicited the greatest proliferative response in naïve rMSCs, whilst the higher FBS concentration of 20% FBS and PMA resulted in proliferation similar to the 1% FBS growth control after 24 hours (Fig. 3.1 A). These findings suggest that potent mitogenic stimulation, such as 20% FBS and PMA, hindered the proliferation of naïve rMSCs. In the case of 20% FBS, proliferation is only increased after 72 hours compared to the other mitogenic treatments, whilst PMA remained unchanged at this time (Fig. 3.1 C). A number of possibilities could explain the lack of proliferation seen after strong mitogenic stimulation in Fig. 3.1. One such suggestion is that the mitogens present in FBS such as FGF-1 (Lee and Blaber), IGF-I (Goodrich et al., 2006) and VEGF (Kleinheinz et al., 2010) have relatively short biological half lives. This could lead to stunted signaling events and end responses such as proliferation due to the metabolisation of mitogens during extended time in culture. PMA, on the other hand, has a half life ranging between 8 hours to 24 hours, depending on cell type and dosage (Berry et al., 1978; O'Brien et al., 1980). Earlier results have shown that even if FBS was replaced daily over a 72 hour period, 5% FBS still elicited the highest rate of proliferation and that 20% still showed decreased proliferation in rMSCs up to 48 hours (data not shown). PMA is known to cause inactivation of biological responses (Berry et al., 1978; O'Brien and Saladik, 1978) and the inhibition of rMSCs proliferation after PMA treatment is in accordance with these findings. Another possibility is decreased cellular sensitivity due to

receptor downregulation, since these high concentrations of mitogens persisted for long time periods (Bouvier et al., 1989; Dale et al., 2002).

It is also known that hypermitogenic stimulation of some cell types could result in stunted growth in an anti-oncogenic response known as oncogenic-induced senescence (OIS) (Dimri et al., 1995; Campisi, 2001). This response could likely explain the attenuated rMSC proliferation after strong mitogenic stimulation like 20% FBS and PMA. Several findings corroborate this deduction. Firstly, the increase in formazan formation by enhanced metabolic activity, as seen in the MTT assay, suggests that strong mitogenic stimulation of rMSCs result in heightened mitochondrial activity and metabolism (Fig. 3.2). The increased metabolic activity evoked by 5% FBS and 10% FBS (proliferating conditions) after 24 hours may be ascribed to the increase in metabolism associated with mitotic cell division (Chambard et al., 2007). Seeing that PMA provoked a metabolic response similar to the 1% FBS control, but dissimilar to that of 20% FBS, it is likely that the mechanism responsible for low proliferation after 20% FBS and that elicited by PMA could be different. Secondly, the senescence-associated β-gal (SA-β-Gal) assay showed that the portion of cells undergoing senescence after 24 hours of strong mitogenic stimulation were significantly increased, with 17% and 25% senescent positive cells being present after 20% FBS and 100 ng/ml PMA treatment, respectively (Fig. 3.3 B). Taken together, the lack of proliferation and increased metabolic activity observed in naïve rMSCs suggest that OIS could be a contributing factor to the lack of cell growth seen after 24 hours of incubation with excessive quantities of mitogens. Thirdly, closer investigation using flow cytometry showed two populations within the cultures of distinct size and granularity (Fig. 3.4 and Fig. 3.5). Flow cytometry histograms showed a shoulder on the G_0/G_1 and G_2/M peaks of in rMSCs preparations (data not shown). This profile of DNA content is characteristic of senescent cells. Lastly, heterochromatin is a chromatin form in which the DNA is extremely condensed and is a hallmark of senescent cells (Narita et al., 2003). The analysis of the fluorescence intensity of Hoechst 33258 stained cells also suggests the presence of two cell populations in rMSCs preparations (Fig. 3.6). Although differences in the morphology of unstained cells could not be distinguished using phase contrast microscopy, the difference in fluorescence intensity seen in Fig. 3.6 could indicate differential uptake of the Hoechst 33258 stain by these nuclei, possibly reflecting different DNA condensation states. As the Hoechst 33258 stain binds to the minor groove of the DNA double helix, especially AT rich sequences (Cesarone et al., 1979), it is probable that the brightly stained nuclei represent a cell population of which the DNA backbone is more accessible to the DNA dye. Consequently, the diffusely stained nuclei would represent a cell population with more compacted DNA, thereby making the DNA basepairs less accessible to

the Hoechst 33258 stain and resulting in weak staining. Therefore, it is likely that the cells of these nuclei were possibly undergoing OIS, characterised by nuclear condensation.

DNA content analysis revealed that, for all mitogenic conditions tested, the majority of cells, regardless of size and granularity, are in the G_0/G_1 cell cycle phase, thereby suggesting that these cells were either in a quiescent state or conceivably undergoing senescence (Tables 3.1 to 3.3). Findings indicate that treatment with 20% FBS possibly hindered the S phase transition into G_2/M of rMSCs after 24 hours, since this cell treatment exhibited the highest S-phase content compared to other cell stimulants (Table 3.3). This indicates that these cells were restricted to these cell cycle phases. Since quantification of cells in the S phase represent the percentage of cells that are undergoing DNA synthesis after 24 hours of mitogenic stimulation, it is therefore the proliferation of this fraction of cells that is measured during the [^{3}H]dT proliferation assay. Flow cytometry results also suggest that the mechanisms by which 20% FBS and PMA induce senescence in rMSCs after 24 hr could be different. A likely means could be that PMA might induce cell growth arrest at the G_0/G_1 mitotic checkpoint before entry into the S-phase, thus explaining the G_0/G_1 restriction of rMSCs treated with PMA (Fig. 3.9 E). In addition, G_0/G_1 restriction could also possibly also indicate cell differentiation or apoptosis. In contrast, 20% FBS stimulation could lead to a cell cycle arrest before the commencement of mitosis, thereby possibly justifying the moderate amount of cells restricted to the S-phase of the cell cycle (Fig. 3.9 D). This could conceivably be due to blockage at the intra-S-phase checkpoint as part of a DNA damage response (Schmitt et al., 2007), possibly caused by reactive oxygen species due to the high concentration of FBS (20%) used (Chen and Ames, 1994; Brar et al., 1999; Chae et al., 2000). The mechanism underlying this S-phase blockage could possibly include delayed replication fork progression; replicarion fork stalling or collapse as well as abberent DNA repair systems (Sancar et al., 2004; Ben-Yehoyada et al., 2007).

To conclude, mild mitogenic stimulation such as 5% FBS elicited a good proliferative response in these cells. On the contrary, strong mitogens such as 20% FBS and PMA did not stimulate the proliferation of naïve rMSCs over 24 hours as 5% FBS, possibly due to some cells undergoing senescence. However, increased proliferation after 20% FBS was seen after 72 hours, indicating that this mitogenic stimulation had a delayed replication period. Hence, the conditions that stimulate mitogenesis in naïve rMSCs were established. The following section of the current work will cover the characterisation of preosteoblasts derived from these naïve stromal cells.

Chapter 4

Characterisation of rMSCs differentiated into an osteoblastic phenotype

4.1 Introduction

The aim of this section of the research was to identify cells in an early osteoblastic stage in order to study the effects of GCs on mitogen-induced proliferation of preosteoblasts. Differentiation of naïve rMSCs was induced using osteogenic media (OM) containing ascorbic acid, β-glycerophosphate and dexamethasone (Supplement A3.3) (Digirolamo et al., 1999; Colter et al., 2001; Deliloglu-Gurhan et al., 2006a; Deliloglu-Gurhan et al., 2006b). The inclusion of ascorbic acid in the osteogenic media is necessary for the stimulation of collagen synthesis and maturation (Franceschi, 1999). It is an important co-factor for the hydroxylation of the pro-collagen chains and subsequent triple helix formation, secretion and collagen fibril assembly (Franceschi, 1999). β-glycerophosphate is employed as an exogenous phosphate source to aid mineralization, whereas GCs, in this case dexamethasone, are required in low doses to promote bone nodule formation (Bellows et al., 1990). GCs regulate nodule formation by modulating the expression of gene-products necessary for the maturation, organisation and mineralisation of the ECM (Leboy et al., 1991; Stromstedt et al., 1991; Shalhoub et al., 1992; Subramaniam et al., 1992; Heinrichs et al., 1993; Ito et al., 2007; Mikami et al., 2007). The selection criteria for preosteoblasts were that these cells must still proliferate and express early osteoblastic phenotype markers. Consequently, rMSCs were differentiated for 7 days in osteogenic medium before proliferation and the expression of early osteoblastic markers were assessed. In addition, to assess the ability of these adipose tissue-derived rMSCs to form mineralized bone nodules and therefore osteogenesis, was assessed by staining for calcium deposition using Alizarin Red after 28 days in culture.

The ability of early osteoblast precursor cells such as preosteoblasts to proliferate and replenish depleted osteoblasts in the BMU is paramount to the maintenance of a balanced osteoblastic population and hence maintenance of healthy bone. The cell cycle is progressively down-regulated as MSCs differentiate into mature bone forming cells, which leads to a reduction in the proliferative potential in more differentiated cells (Aubin and Liu, 1996; Franceschi, 1999). Down-regulation of the cell cycle is due to a reduction in the expression of cell cycle-regulating proteins as well cell growth related genes such as CDKI, c-fos and c-jun (Aubin and Liu, 1996; Franceschi, 1999). This

post-proliferative stage is also characterised by the synthesis and maturation of the collagen-containing extracellular matrix and the accompanied expression of osteoblast-related proteins (Aubin and Triffitt, 2002), which marks the attainment of the osteoblastic phenotype. Furthermore, the response of these osteoblastic cells to growth factors diminishes, which could be attributed to the decrease in the expression of specific growth factor receptors, decreasing the proliferative capacity of these cells (Chien et al., 2000; Picton et al., 2000; Mizuno et al., 2005). This is seen in MC 3T3 E1 cells where the amount of EGF receptors decreased during the differentiation into mature osteoblasts (Chien et al., 2000). These authors also showed that the more mature ROS osteoblastic cell line, which highly expressed the late osteoblast markers Col I, ALP, BSP and OCN, did not respond to EGF treatment (Chien et al., 2000). Therefore, an objective of this part of the study was also to test whether preosteoblasts derived from rMSCs were capable of responding to growth factor stimulation. FBS is a cocktail of growth factors and was used at a concentration of 20% (v/v) to induce preosteoblast proliferation. This FBS concentration was determined by a dose response, where 20% FBS elicited the highest cell proliferation of partially osteogenic differentiated cells compared to 5% FBS and 10% FBS (data not shown).

4.2 Results

4.2.1 Characterisation of early osteoblastic phenotype marker expression in rMSCs differentiated for 7 days

Naïve rMSCs were grown to confluency and differentiated with osteogenic medium (described in Section 2.2.1.3 and Supplement A3.3.) before total RNA was extracted and converted into cDNA (explained in Section 2.2.10) to serve as template for RT-qPCR to study the relative mRNA expression of early osteogenic markers. The early osteoblast-related genes used to assess the development of the preosteoblast phenotype in rMSCs differentiated with OM for 7 days were Runx2, Msx2, Osx and ALP. Runx2 (Ducy et al., 1997; Komori et al., 1997; Otto et al., 1997; Mundlos et al., 1997), Msx2 (Dodig et al., 1999; Liu et al., 1999; Satokata et al., 2000; Wilkie et al., 2000) and osterix (Nakashima et al., 2002) are transcription factors that controls the restriction of mesenchymal stromal cells to the osteogenic lineage, whereas ALP is needed for bone mineralisation (Stein et al., 1990; Stein and Lian, 1993). To determine the relative gene expression of the respective genes of interest (GOIs), the relative abundance of these GOIs was normalised to the expression levels of the ARBP reference gene and expressed using arbitrary units.

Results showed that all of the early transcripts studied were present 7 days after the induction of osteogenic differentiation (Fig. 4.1 A-C). In addition, the relative transcript abundance of Msx2 and ALP osteogenic markers were significantly increased after 7 days of osteogenic differentiation (Fig. 4.1 B and D). These results suggest that early osteogenic markers are present at varying quantities in rMSCs differentiated into an osteogenic phenotype for 7 days and that these cells may be classified as preosteoblasts.

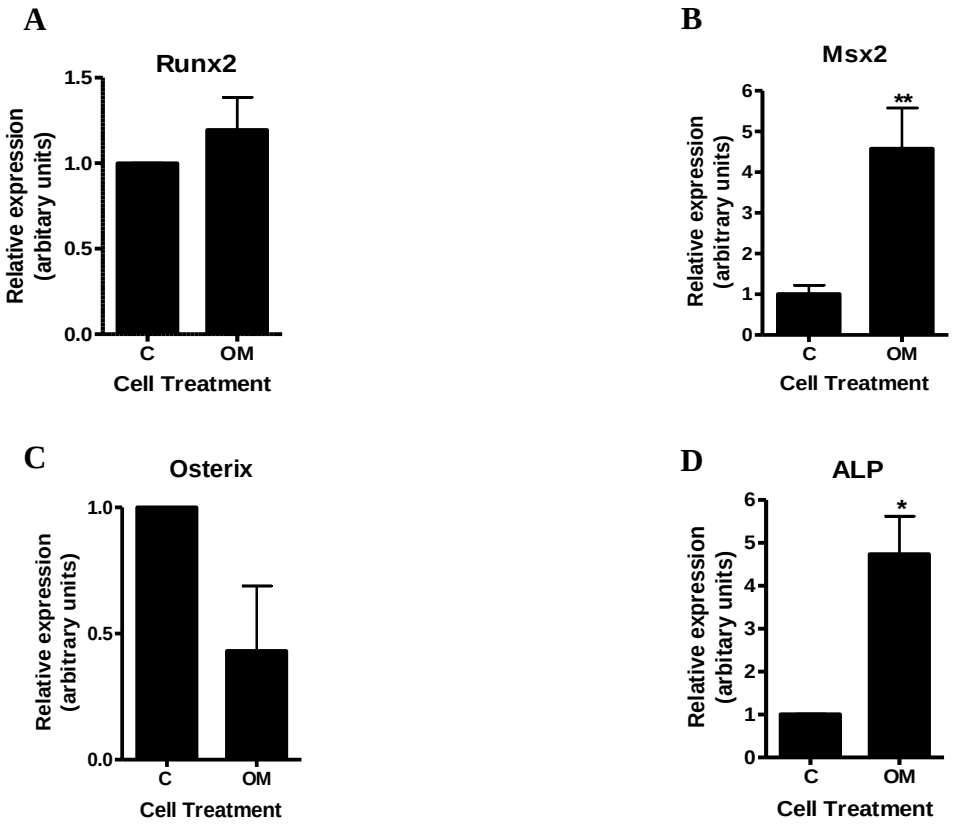

Figure 4.1: rMSCs differentiated for 7 days with osteogenic medium express genes associated with early osteogenic stages.

Cells were grown to confluency before induction of osteoblastic differentiation using OM (10 mM glycerol-2-phosphate, 50 µM ascorbic acid and 10 nM Dex) for 7 days. Confluent naïve rMSCs grown in DMEM/10% FBS for 7 days were used as a growth control. The transcript abundance of Runx2 (**A**), Msx 2 (**B**), Osx (**C**) and ALP (**D**) was measured using RT-qPCR. Data of three independent experiments are given. For RT-qPCR analysis, three biological replicates per experiment (N=3) were assayed in triplicate. Results displayed are the mean ± S.D and are shown relative to the control, which was set to 1. Statistically significant differences were calculated using the Student t-test and are indicated by * ($P<0.01$) and ** ($P<0.001$) above the bar graph. **Abbreviations**: **ALP** alkaline phosphatase; **C** control; **Dex** dexamethasone; **Msx 2** muscle segment homeobox 2; **OM** osteogenic medium; **Osx** osterix; **Runx2** runt-related transcription factor 2

4.2.2 ALP enzyme activity is increased in preosteoblasts after 7 days

To further assess the preosteoblast phenotype of rMSCs differentiated for 7 days in OM, the activity of the ALP protein was assessed. In accordance with the literature (Lian and Stein, 1995; Aubin, 1998; Aubin and Triffitt, 2002), ALP protein activity was significantly increased in differentiated preosteoblasts compared to the undifferentiated growth control (Fig. 4.2). This result demonstrates that rMSCs cultured in OM for 7 days display a preosteoblast phenotype with the increase in ALP activity being indicative of differentiation.

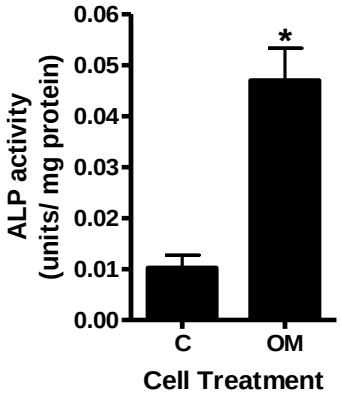

Figure 4.2: rMSCs differentiated for 7 days with osteogenic medium exhibits increased ALP protein activity. Cells were grown to confluency before induction of osteoblastic differentiation using OM (10 mM glycerol-2-phosphate, 50 µM ascorbic acid and 10 nM Dex) for 7 days. Confluent naïve rMSCs grown in growth medium for 7 days were used as growth control. ALP activity was measured using the Pnpp hydrolysis assays (refer to Section 2.2.5). Data of six independent experiments are given, with each sample done in triplicate. Results displayed are the mean ± S.D., where $P<0.001$ was seen as a statistically significant difference using the paired Student t-test. Statistically significant differences are indicated by * above the bar graph. **Abbreviations**: **ALP** alkaline phosphatase; **C** control; **OM** osteogenic medium

4.2.3 Naïve rMSCs differentiated into an osteoblastic phenotype forms mineralised bone nodules after 28 days in culture

The endpoint of the osteogenic differentiation pathway is the formation of calcified bone nodules. To determine whether stromal cells derived from rat adipose tissue could differentiate into a mature bone phenotype and thus form calcified nodules, naïve rMSCs were grown until confluent, after which osteogenic differentiation was induced using osteogenic medium (refer to Section 2.2.1.3 and Supplement A3.3.) for 28 days with media changes occurring every 2 to 3 days.

Cells grown in complete growth medium (Supplement A2.) were employed as negative calcification controls (Fig.4.3). Employing light microscopy, nodule formation was observed 28 days after induction of osteogenic differentiation and nodules were stained with Alizarin Red to detect calcification. The presence of calcified bone cell nodules were observed in cells cultured in osteogenic medium for 28 days (Fig.4.3 B), but not in cells grown in complete growth medium (Supplement A2.) (Fig.4.3 A). These results indicate that upon osteogenic induction, naïve rMSCs differentiate into mineralised bone cell nodules, which is a feature of functional, mature osteoblasts.

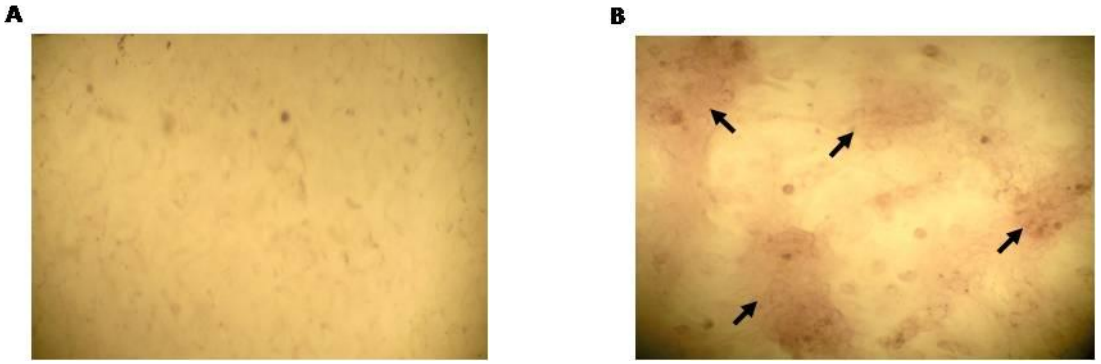

Figure 4.3: Osteogenic differentiation of naïve rMSCs culminates in calcified nodules after 28 days *ex vivo*. Confluent naïve rMSCs grown in complete growth medium for 28 days were used as a negative calcification control (**A**). Naïve rMSCs were grown to confluency before induction of osteoblastic differentiation using OM (10 mM glycerol-2-phosphate, 50 µM ascorbic acid and 10 nM Dex) for 28days (**B**). Calcified nodules were detected by staining cells with Alizarin Red. Mineralised nodules are indicated with black arrows. This image was kindly provided by Dr. H. Sadie- van Gijsen from the Endocrinology and Metabolism Unit at University of Stellenbosch. **Abbreviations**: **OM** osteogenic medium

4.2.4 rMSCs differentiated with osteogenic medium for 7 days exhibits reduced cell proliferation

In order to investigate the degree of proliferation exhibited by rMSCs differentiated into a preosteoblast phenotype, confluent naïve MSCs were treated with osteogenic medium for 7 days. Although the proliferation of these preosteoblasts was significantly decreased in comparison to the growth and ethanol solvent controls, preosteoblasts proliferation was not ablated (Fig. 4.4). This decrease in proliferation after induction of osteogenic differentiation is in agreement with findings from Aubin and Liu (1996) and Franceschi (1999).

After 7 days post-confluency rMSCs were able to replicate (Fig. 4.4), demonstrating the high proliferative capability of these osteoblast precursor cells. Since the osteogenic medium contained Dex dissolved in ethanol, confluent naïve rMSCs were subjected to growth medium containing 0.1% (v/v) ethanol for 7 days, as a solvent control. It was found that the proliferative response elicited by the ethanol solvent control was not significantly different from the growth control (Fig. 4.4). Therefore, naïve rMSCs differentiated in osteogenic medium for 7 days express early osteoblastic markers and are still able to proliferate after induction of osteogenic differentiation.

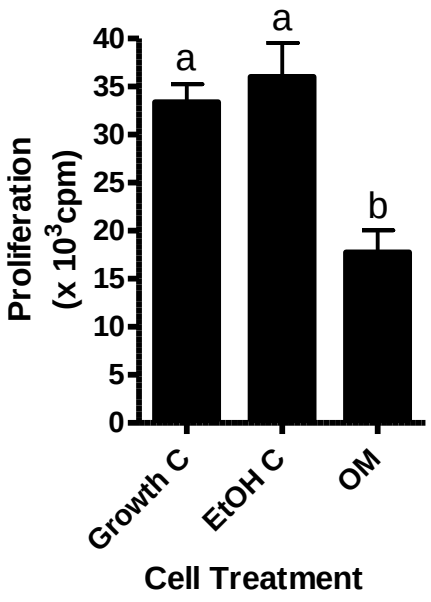

Figure 4.4: rMSCs differentiated for 7 days with osteogenic medium display decreased cell proliferation.
Cells were grown to confluency before induction of osteoblastic differentiation using OM (10 mM glycerol-2-phosphate, 50 µM ascorbic acid and 10 nM Dex) for 7 days. Confluent naïve rMSCs grown in growth medium for 7 days were used as growth control. As solvent control, confluent naïve rMSCs were grown in the presence of 0.1% (v/v) EtOH for 7 days. DNA synthesis was measured by incorporation of [^{3}H] thymidine ([^{3}H]dT) for the last 4 hrs of incubation. Data shown is representative of an individual experiment, where n = 3. The experiment was repeated at least four times, where each repeat represents an individual animal. Results displayed are the mean cpm ± S.E.M., where $P<0.05$ was seen as a statistically significant difference using the One-way Anova with Bonferonni post-hoc test. Statistically significant differences are indicated by different lower case letters. Data bars with the same letter above are not statistically different. **Abbreviations**: **C** control; **cpm** counts per minute; **d** day/s; **EtOH** ethanol; **OM** osteogenic medium

4.2.5 Preosteoblasts display a modest increase in proliferation after 24 hours of mitogenic stimulation

Confluent naïve rMSCs were differentiated in osteogenic medium for 7 days before 24 hours of mitogenic stimulation using 20% FBS. As the osteogenic medium contained 10 nM Dex that was dissolved in 0.1% (v/v) ethanol, naïve rMSCs were cultured in complete growth medium (Supplement A.2.) containing this concentration of ethanol and was used as solvent control. In addition, these cells were also used as negative differentiation control. After 7 days in culture, cells exposed to ethanol in the growth medium still proliferated (Fig. 4.5). The proliferative ability of preosteoblasts differentiated in osteogenic medium for 7 days was dramatically reduced and was employed as a control of basal growth (Fig. 4.5). It was found that preosteoblasts stimulated with 20% FBS for 24 hours exhibited a statistically significant increase in proliferation compared to cells grown in osteogenic medium alone (Fig. 4.5). This finding indicates that preosteoblasts, differentiated for 7 days, can be driven to proliferate by a strong mitogenic stimulant, such as 20% FBS.

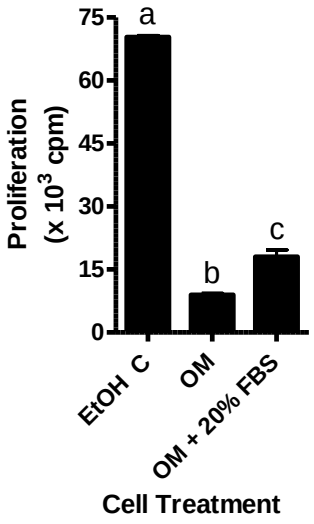

Figure 4.5: rMSCs differentiated with osteogenic medium for 7 days exhibit increased proliferation upon stimulation with 20% FBS.

Cells were grown to confluency before induction of osteoblastic differentiation using OM (10 mM glycerol-2-phosphate, 50 µM ascorbic acid and 10 nM Dex) for 7 days. The proliferative potential of confluent rMSCs was monitored by growing naïve stem cells in complete growth medium for 7 days. Confluent naïve rMSCs were grown in the presence of 0.1% (v/v) ethanol for 7 days and was used as solvent control. Mitogenesis of differentiated cells was induced by 24 hour stimulation with 20% FBS. DNA synthesis was measured by incorporation of [^{3}H] thymidine ([^{3}H]dT) for the last 4 hrs of incubation. Data shown is representative of an individual experiment, where n = 3. The experiment was repeated at least four times. Each repeat experiment represents an individual animal. Results displayed are the mean cpm ± S.E.M., where $P<0.05$ was seen as a statistically significant difference using the One-way Anova with Bonferonni post-hoc test. Statistically significant differences are indicated by different lower case letters. **Abbreviations**: **C** control; **cpm** counts per minute; **d** day/s; **EtOH** ethanol; **OM** osteogenic medium

4.3 Discussion

The aim of this chapter was to differentiate primary naïve rMSCs into a preosteoblastic phenotype and to characterise the mitogenic potential of such cells. The selection criteria for preosteoblasts were that cells should still exhibit proliferative capacity, although early bone markers are expressed. Naïve rMSCs differentiated for 7 days in osteogenic medium expressed the early osteoblasts markers Run x2, Msx 2, osterix and ALP (Fig. 4.1 A – D). In addition, ALP protein activity was significantly elevated in these cells (Fig. 4.2). Moreover, these osteogenic differentiated cells still proliferated when stimulated with mitogens. Therefore, naïve rMSCs differentiated for 7 days using osteogenic medium fulfilled the requirements for preosteoblasts, and Fig.4.4). The mitogenic potential of 7 day differentiated preosteoblasts diminished along the differentiation program as seen in Fig. 4.4, but however, these cells could be stimulated using a high concentration of FBS (20% FBS) (Fig. 4.5). This suggests that these preosteoblasts still express the relevant growth factor receptors needed to mount such a proliferative response, even though this proliferation is considerably stunted. The degree of [^{3}H] thymidine ([^{3}H]dT) incorporation varied between experiments and is particularly evident when comparing Fig. 4.4 and Fig.4.5. This discrepancy could be attributed to biological differences as the cells originated from different animals for these experiments. Technical reasons such as batch variations of [^{3}H] thymidine ([^{3}H]dT) could also be plausible.

The biological endpoint of osteoblast differentiation is the formation of mineralised bone nodules. It was fundamental to discern whether these naïve rMSCs could develop into mature, functioning osteoblasts. Results demonstrate that the differentiated cells used in this part of the study were preosteoblasts, which are capable of forming calcified bone nodules (Fig. 4.3). In agreement with the literature, findings showed that the proliferative ability of rMSCs diminished upon induction of osteogenic differentiation (Fig. 4.4) (Aubin and Liu, 1996; Franceschi, 1999).

In summary, osteogenic differentiation of naïve rMSCs for 7 days was sufficient to obtain preosteoblasts that could still proliferate; a prerequisite for this work. The next section of the current investigation will deal with the effects of GCs on the mitogen-induced proliferation of naïve rMSCs and preosteoblasts.

Chapter 5

Glucocorticoid regulation of mitogen-induced proliferation in osteoblast precursor cells

5.1 Introduction

Together with apoptosis, osteoblastogenesis ensures that a healthy population of osteoblast precursors exist that can differentiate into osteoblasts to counteract the bone resorption by osteoclasts. The balanced actions of osteoclasts and osteoblasts, in turn, govern bone homeostasis. Any disturbance in this balance could lead to irregular bone formation such as decreased bone density, as in the case of osteoporosis after prolonged and high doses of GCs.

The effect of GC exposure on the proliferation of mitogen-stimulated osteoblast precursor cells, such as primary rMSCs and early preosteoblasts, was studied. It was previously found that Dex inhibited the mitogen-induced proliferation of immortalised MBA 15.4 preosteoblasts and MG 63 osteoblasts (Hulley et al., 1998; Engelbrecht et al., 2003; Horsch et al., 2007). However, the effects of GCs have not been fully tested in primary osteoblast precursor cells, such as naïve rMSCs and early preosteoblasts.

The synthetic GC, Dex was used in this study because other synthetic GC derivatives, like the more widely prescribed prednisolones, exhibit less specificity to the GC receptor (GR) (Buttgereit et al., 1999). Furthermore, Dex has negligible binding to the mineralocorticoid receptor (MR) compared to other GCs and the relative potency of Dex is higher at equivalent doses than prednisolone, prednisone and methylprednisolone, *in vivo* and *in vitro* (Buttgereit et al., 1999). Dexamethasone is classified as a long-acting GC with a biological half life of 36 to 54 hours (Singh et al., 1994; Zoorob and Cender, 1998; Axelford, 2001). However, little is known about the *in vitro* kinetics of this GC. As a result of a long half life, Dex could effect chronic activation of signaling pathways rather than acute signaling mechanisms (Lasa et al., 2002). Pharmacological doses of Dex, such as 1µM and 100 nM, were used to emulate *in vivo* serum concentrations which occur during GC-induced osteoporosis (Ishida and Heersche, 1998).

5.2 Results

5.2.1 Dex dramatically retards mitogen-stimulated rMSC proliferation

Naïve rMSCs were initially pre-treated with 1 µM Dex for 24 hours, prior to mitogenic stimulation using 5% FBS (48 hours Dex) (Fig. 5.1 A). However, the proliferation of these rMSC was severely impaired by 1 µM Dex pre-treatment with a mean percentage decrease in proliferation of more than 90% was observed under both basal (1% FBS, Fig. 5.1 A) and mitogenic conditions (5% FBS) (Fig. 5.1 A), indicating that naïve rMSCs are extremely sensitive to proliferative inhibition by Dex. Due to the high sensitivity of rMSCs to 1 µM Dex pre-treatment, a dose response was performed where Dex was concomitantly administered with mitogens to rMSCs (Fig. 5.1 C and D). It was found that the mean percentage drop in proliferation was not statistically different for Dex pre-treated cells and cells concomitantly treated with both 5% FBS and 1 µM Dex (Fig. 5.1 A and C). Therefore, for subsequent proliferation experiments using Dex, Dex was simultaneously added with other treatments to rMSCs (for example 5% FBS).

Under basal proliferative conditions, all Dex concentrations used, severely impaired rMSC proliferation compared to both control media (1% FBS and EtOH C, where ethanol is added to the media to compensate for the addition of solvent to the Dex treated samples) (Fig. 5.1 B). Even the low Dex concentration of 1 nM resulted in a significant decrease in the proliferation of slow growing rMSCs. Contrary to expectation, the EtOH solvent control elicited a statistically significant increase in proliferation compared to the 1% FBS control (Fig. 5.1 B).

In order to examine the effect of Dex on mitogen-stimulated proliferation, mitogenesis was induced with either 5% FBS treatment for 24 hours or 20% FBS for 72 hours (Fig. 5.1 C and D). These concentrations induced the highest mitogenic response for their respective time points (Fig. 3.1 A and C). All Dex concentrations used caused a statistically significant drop in 5% FBS-induced proliferation compared to both the control media (5% FBS and 0.1% EtOH) (Fig. 5.1 C). Dex at 1 nM evoked a 50 % decrease in mitogen-induced proliferation (Fig. 5.1 C) and, therefore, this concentration was used in subsequent experiments since the reduction in proliferation caused by the higher Dex concentrations was too excessive to see subtle changes during subsequent co-incubation experiments. As expected, the EtOH solvent control displayed a statistically equivalent proliferation response to the 5% FBS control media, while a very strong mitogenic response was elicited by 20% FBS after 72 hours (Fig. 5.1 D). Although incubation with 1 µM, 100 nM and 10 nM Dex caused a decrease in 20% FBS-induced rMSC proliferation, 1 nM Dex did not exhibit a statistically

significant decrease (Fig. 5.1 D). The EtOH vector control exhibited a similar proliferative response as the 20% FBS control media (Fig. 5.1 D). These results indicate that Dex dramatically decrease mitogen-induced proliferation in rMSCs. In addition, the magnitude of reduction in proliferation caused by Dex is less upon stronger mitogenic stimulation such as 20% FBS (Fig. 5.1 D).

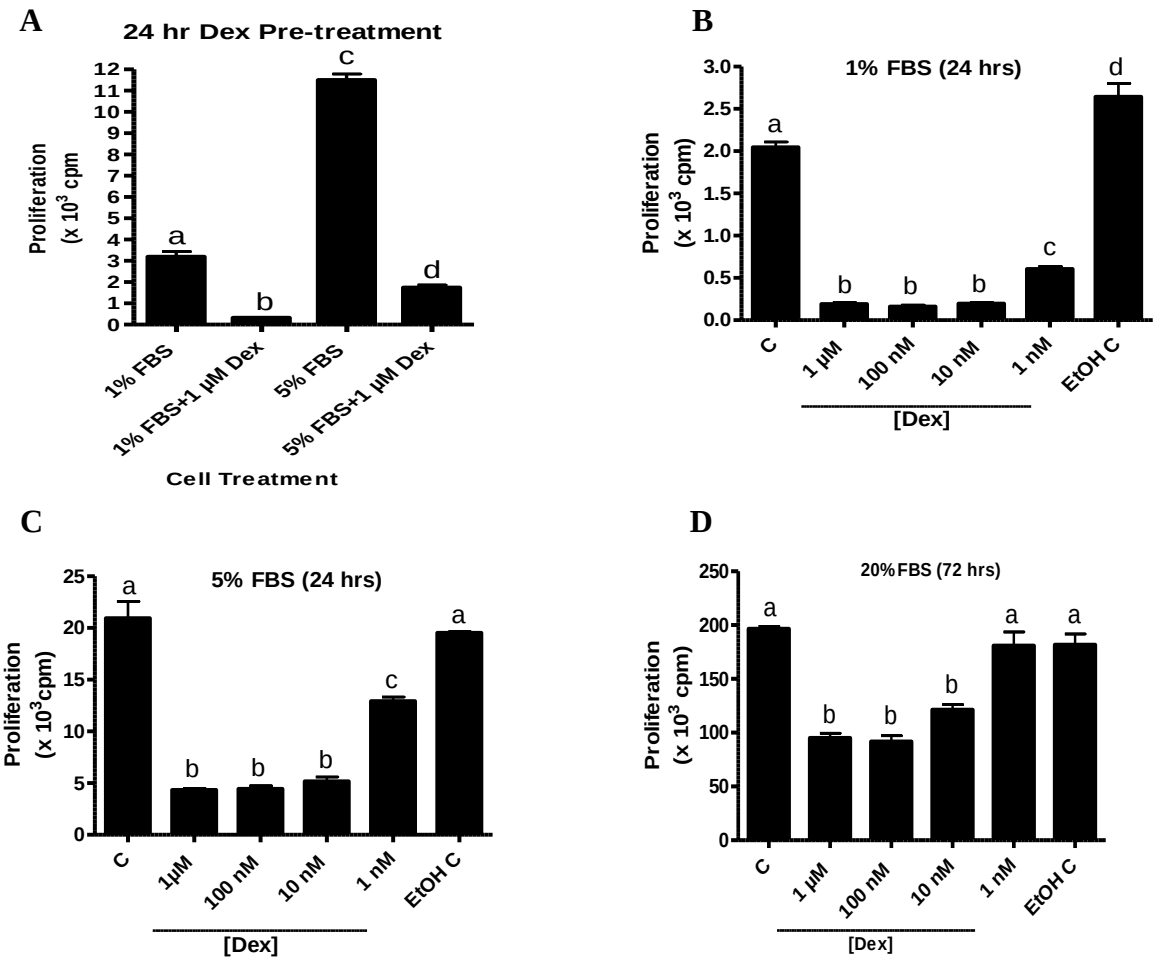

Figure 5.1: **Dex impairs naïve rMSC proliferation under basal and mitogenic conditions.**

rMSCs were grown to 50% confluency and serum starved in 1% FBS for 24 hrs. Cell proliferation was assessed using [^{3}H] dT incorporation during DNA synthesis. (**A**) rMSCs were pre-treated 1 µM Dex for 24 hrs before 24 hr mitogenic stimulation with 5% FBS. 1% FBS served as negative control. (**B**) Naïve rMSCs were treated with either 1% FBS or simultaneous with 1% FBS and Dex for an additional 24 hrs. C denotes 1% FBS as control media. (**C**) rMSCs were treated with either 5% FBS or concomitantly with 5% FBS and Dex for an additional 24 hrs where C denotes 5% FBS as control. (**D**) rMSCs were treated with 20% FBS for 72 hrs prior to challenge with Dex for another 24 hrs, where C denotes 20% FBS as control. 0.1% ethanol was used as solvent control. [^{3}H]dT was incorporated into DNA for the last 4 hrs of incubation. Results displayed are the mean cpm ± S.E.M., where $P<0.05$ was seen as a statistically significant difference using the One-way Anova with Bonferoni post-hoc test. Statistically significant differences are specified by different lower case letters. These experiments were repeated at least three times. Each experimental replicate represents an individual animal. **Abbreviations**: **C** control; **cpm** counts per minute; **Dex** dexamethasone; **EtOH** ethanol; **FBS** fetal bovine serum

5.2.2 Mitogen-induced proliferation of preosteoblasts is reduced by dexamethasone

In order to assess the effect of GCs on mitogen-stimulated growth of preosteoblasts, 1 µM of Dex was administered concomitantly with mitogenic exposure of preosteoblasts, since lower Dex concentrations, such as 1 nM, did not reduce preosteoblast proliferation sufficiently (Fig. 5.1 B, C and D). A concentration of 20% FBS was used to mitogenically stimulate preosteoblast cells for 24 hours as this concentration elicited a significant increase in preosteoblast proliferation compared to 5% FBS and 10% FBS (data not shown). As ethanol was the solvent for Dex, confluent naïve rMSCs were cultured in growth medium containing 0.1% (v/v) ethanol for 7 days and was designated a solvent control (Fig. 5.2). These cells still proliferated (Fig. 5.2). Preosteoblasts displayed the characteristic reduction in proliferation and were used as negative growth control (Fig. 5.2). Dex decreased the proliferation of cells differentiated in OM by 45% (Fig. 5.2). The proliferation of mitogen-stimulated preosteoblasts was reduced by 33% after Dex administration for 24 hours (Fig. 5.2). These results show that Dex markedly reduces the proliferation of preosteoblastic cells grown under osteogenic and mitogen conditions (Fig. 5.2).

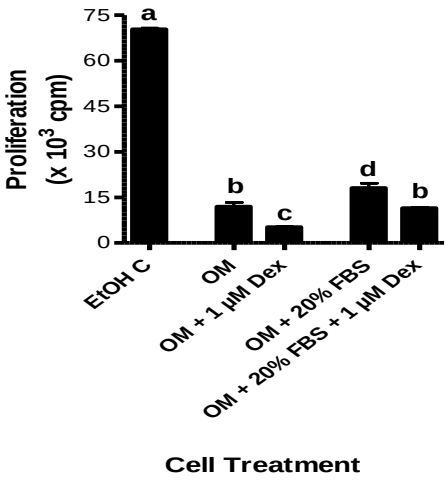

Figure 5.2: Dex markedly reduced mitogen-stimulated proliferation of preosteoblasts after 24 hours.
Confluent rMSCs were induced to differentiate into osteoblasts using OM (DMEM containing 10% FBS, 10 mM glycerol-2-phosphate, 50 µM ascorbic acid and 10 nM Dex) for 7 days. The proliferative potential of confluent rMSCs was tested by growing rMSCs in complete growth medium (Supplement A2.) and EtOH for 7 days. A concentration of 1 µM Dex was used to treat cells grown under basal conditions (OM containing 10% FBS) or mitogenic stimulation (OM supplemented with 20% FBS). DNA synthesis was measured by incorporation of [^{3}H] thymidine ([^{3}H]dT) for the last 4 hrs of incubation. Data shown is representative of an individual experiment, where n = 3. The experiment was repeated at least four times where each repeat represents an individual animal. Results displayed are the mean cpm ± S.E.M. $P<0.05$ was seen as a statistically significant difference using the One-way Anova with Bonferonni post-hoc test. Statistically significant differences are indicated by different lower case letters. Results that are not statistically different are indicated by the same letter above the data bars. **Abbreviations**: **C** control; **cpm** counts per minute; **Dex** dexamethasone; **DMEM** Dulbecco's minimal essential medium; **EtOH** ethanol; **OM** osteogenic medium

Also, comparing concomitant OM plus Dex with OM only and OM plus Dex and 20% FBS, it can be seen that the addition of 20% FBS to Dex treated cells attenuates the GC-induced inhibition of proliferation (Fig. 5.2). Therefore, 1 µM Dex does not totally inhibit the capacity of preosteoblasts to respond to mitogenic stimuli.

5.3 Discussion

The objective of the research outlined in this chapter was to examine how GCs affect mitogen-induced proliferation in early osteoblast precursor cells. The mitogenic conditions for naïve rMSCs were established in Chapter 3, whereas that of preosteoblasts derived from these stromal cells were determined in Chapter 4.

The results of this study indicate that Dex attenuates the mitogen-stimulated proliferation of both primary naïve rMSCs and preosteoblasts. Pre-treatment of primary naïve rMSCs with 1 µM Dex for 24 hours severely impaired mitogen-stimulated proliferation in these cells. Basal (1% FBS) rMSC proliferation was also attenuated by all Dex concentrations tested. Mitogen-stimulated proliferation was significantly decreased in naïve rMSCs after concomitant Dex and mitogen stimulation (5% FBS for 24 hours and 20% FBS for 72 hours). Basal (OM) and mitogen-stimulated (20% FBS) proliferation of preosteoblasts were also significantly decreased by 24 hour administration of 1 µM Dex. This is in accordance with the response of immortalised preosteoblastic cell lines to this pharmacological dose of Dex (Hulley et al., 1998; Engelbrecht et al., 2003 and Horsch et al., 2007). When confluent naïve rMSCs were grown for 7 days in ethanol, significant proliferation was still observed; suggesting that these cells were not undergoing contact inhibition at this stage. Additionally, the concentration of Dex which elicited a 50% inhibition of proliferation was identified. This Dex concentration of 1 nM is considered to be near a physiological dose of glucocorticoids (Ishida et al., 1995; Naves et al., 2011) and was used in subsequent phosphatase experiments (see Chapter 7, Fig. 7.2). It was hypothesised that the fraction of phosphatases active during a 50% proliferative response would be sufficient for the subsequent phosphatase inhibitory studies to avoid possible toxic levels at which the phosphatase inhibitor vanadate would be used (see Chapter 7).

The inhibition of mitogen-induced proliferation of these cells due to Dex was ascertained. The next section of the current work deals with the signal transduction events, specifically the role of the

ERK 1/2 MAPK signalling cascade, in the Dex inhibition of proliferation in naïve rMSCs and preosteoblasts.

Chapter 6

The ERK1/2 MAPK signalling pathway regulates the mitogen-induced proliferation in osteoblast precursor cells and is attenuated by Dexamethasone

6.1 Introduction

The importance of osteoblast precursor cell proliferation in osteoblastogenesis is discussed in Section 1.1.2.3.1. It is known that the ERK1/2 signalling pathway regulates growth factor and -mitogen-induced cell proliferation in various cell types including osteoblasts (Zhang and Liu, 2002; Katz et al., 2007; Assoian and Schwartz, 2001). With the use of pharmaceutical inhibitors to the ERK1/2, JNK and p38 MAPK pathways, it has been demonstrated that ERK1/2 is the main proliferative pathway in immortalised human MG-63 and mouse MBA-15.4 and MC3T3-E1 preosteoblast cell lines (Mehrotra et al., 2004; Horsch et al., 2007). Under proliferative conditions, ERK1/2 was found the be induced in two phases; a rapid peak phase lasting between 2 minutes and 30 minutes and a prolonged, sustained phase persisting for several hours in a number of cell types, including preosteoblasts (Meloche et al., 1992; Meloche, 1995; Talarmin et al., 1999; Engelbrecht et al., 2003). This biphasic induction of ERK1/2 activity is considered a proliferative profile for most cell types (Marshall, 1995; Ebisuya et al., 2005). The aim of this current research was to establish whether the ERK1/2 signal transduction cascade plays a role in the regulation of mitogen-induced proliferation in naïve rMSCs and primary preosteoblasts. This was achieved by testing the effect of the pharmaceutical MEK1/2 inhibitor, U0126, on mitogen-induced proliferation in these cells. The mitogenic conditions established in Chapter 3 (see Fig. 3.1) and Chapter 4 (see Fig. 4.5), were used to elicit cellular proliferation. To determine the ERK1/2 activation profile after mitogenic stimulation in naïve rMSCs and preosteoblasts, western blot analysis was performed employing antibodies raised against phosphorylated ERK1/2 protein. Examination of the expression of total ERK1/2 protein was used to ensure equal loading of protein samples.

GCs, including synthetic derivatives such as Dex, have been shown to be anti-mitogenic in osteoblasts (Hulley et al., 1998; Smith et al., 2002; Engelbrecht et al., 2003; Horsch et al., 2007). It has been shown that Dex reduces the mitogen-induced proliferation in MBA-15.4, MC 3T3-E1 and MG-63 preosteoblasts (Hulley et al., 1998; Smith et al., 2002; Engelbrecht et al., 2003; Horsch et

al., 2007). The mechanism of GC action involves both transcriptional-dependent as well as transcriptional–independent events (Schoneveld et al., 2004; Liu et al., 2005). GCs such as Dex exert their anti-proliferative effects through the modulating the expression of genes that either activate or inactivate mitogenic signalling pathways such as ERK1/2. This also provides a possible mechanism for the deleterious effects of GCs on bone. The effect of Dex on ERK1/2 activation was assessed by looking at the ERK1/2 phosphorylation levels after 1 hour pre-treatment with 1 µM Dex, followed by mitogenic stimulation (Engelbrecht et al., 2003). A time period of 1 hour pre-treatment was used to allow the effects of Dex on gene expression. Densitometry was used to quantify the level of ERK1/2 phosphorylation and thus ERK1/2 activation.

6.2 Results

6.2.1 U0126 treatment of rMSCs and primary preosteoblasts results in decreased mitogen-induced proliferation

In order to investigate the involvement of ERK1/2 in the regulation of rMSC and primary preosteoblast proliferation, the pharmaceutical MEK1/2 inhibitor, U0126, was used to block the ERK1/2 pathway downstream of MEK. Naïve rMSCs were grown until 50% confluent and serum starved for 24 hours. Mitogenesis in naïve rMSCs was induced by using 5% FBS (24 hours) and 20% FBS (72 hours). These conditions were used because 5% FBS evoked maximal proliferation in naïve rMSCs after 24 hours, whilst 20% FBS (strong stimulant) showed delayed proliferation and elicited maximal growth only at 72 hours (as seen in Section 3.2.1; Fig. 3.1). Therefore, to assess the effect of U0126 on mitogen-induced naïve rMSC proliferation, mitogen and U0126 treatment were done concomitantly: 5% FBS plus U0126 for 24 hours and 20% FBS along with U0126 for 72 hours. For the stimulation with 20% FBS for 72 hours, culture medium containing U0126 was replenished after 48 hours to ensure that U0126 was active. Preosteoblasts were obtained by differentiating confluent rMSCs for 7 days in osteogenic medium (Supplement A3.3.) and mitogenesis was evoked by stimulation with 20% FBS for 24 hours. U0126 was used at concentrations of 10 µM, 5 µM, 1 µM and 100 nM. Cells grown in DMSO at a concentration of 0.1% (v/v) served as a solvent control.

Results showed that treatment of naïve rMSCs with high U0126 concentrations (10 µM and 1 µM) led to a significant decreased in proliferation under basal (1% FBS) and mitogenic conditions (5% FBS) after 24 hours of stimulation (Fig. 6.1 A and B).

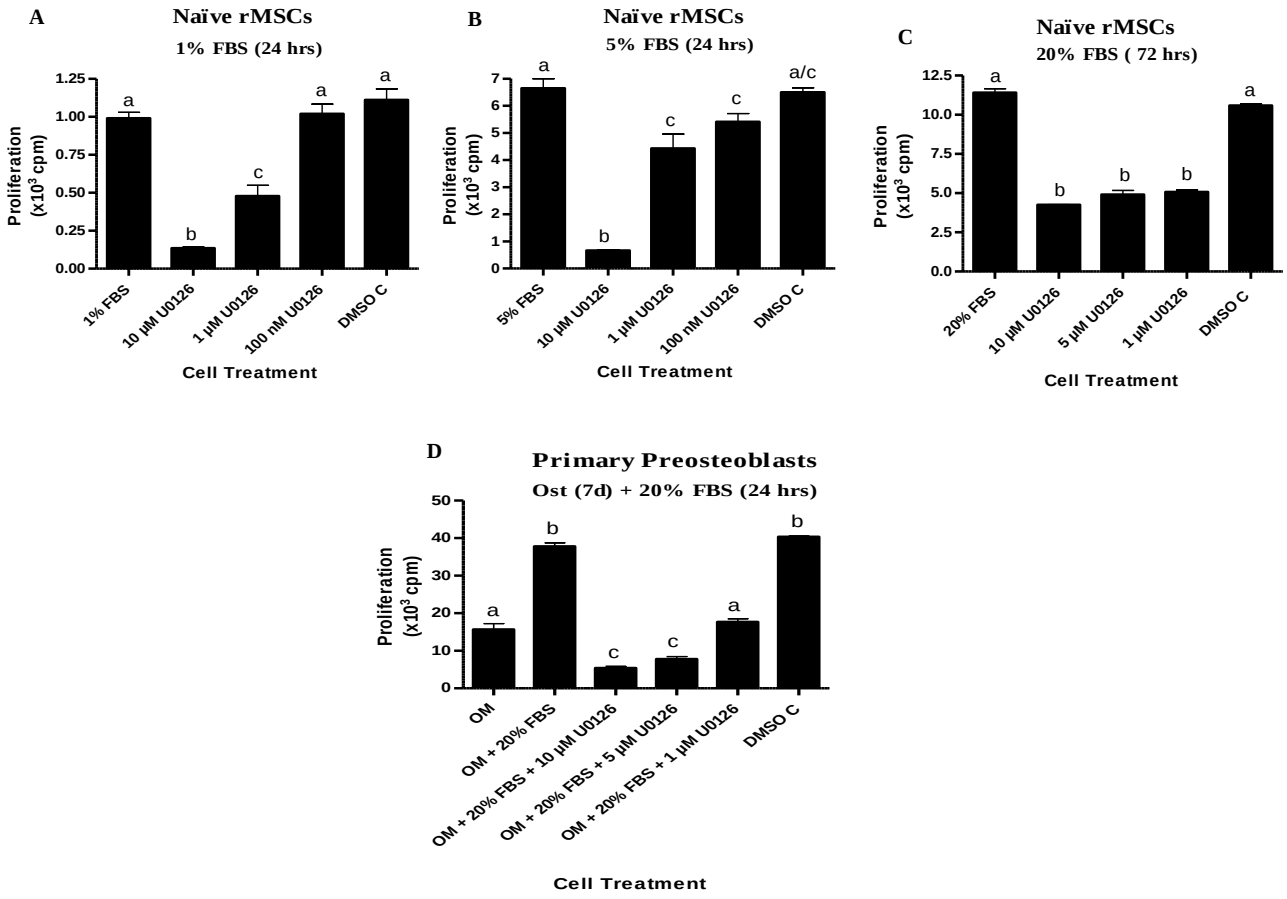

Figure 6.1: The pharmaceutical inhibitor of MEK 1/2, U0126, blocks mitogen-induced proliferation of naïve rMSCs and primary preosteoblasts.

Cells were grown to 50% confluency, serum starved in medium containing 1% FBS (**A**). Mitogenesis was elicited using 5% FBS for 24 hrs (**B**) and 20% FBS for 72 hrs (**C**) (as indicated above bar graphs). Alternatively, cells were differentiated for 7 days in OM media (Supplement A3.3.) and stimulated for with 20% FBS (**D**). U0126 treatment occurred concurrently with mitogenic stimulation at indicated concentrations and time. 0.1% DMSO was used as solvent control. DNA synthesis was measured by incorporation of [^{3}H] thymidine ([^{3}H]dT) for the last 4 hrs of incubation. Data of an individual experiment is shown, where n = 3 and is representative of experiments repeated at least three times, with similar results obtained in the different experiments. Results displayed are the mean cpm ± S.E.M., where $P<0.05$ was seen as a statistically significant difference using the One-way Anova with Bonferonni post-hoc test. Statistically significant differences are indicated by different lower case letters. Data bars with the same letter above are not statistically different. **Abbreviations**: **C** control; **cpm** counts per minute; **DMSO** dimethyl sulfoxide; **FBS** fetal bovine serum; **hrs** hours; **OM** osteogenic medium

Conversely, a lower concentration of U0126 (100 nM) had no pronounced effect (Fig. 4.1 A and B). U0126 significantly attenuated naïve rMSCs proliferation after strong mitogenic stimulation (20% FBS) for 72 hours (Fig. 6.1 C). However, the different doses of U0126 (10 µM, 5 µM and 1 µM) used concomitantly with 20% FBS for 72 hours did not elicit a dose response as no difference was found between these treatments.

Proliferation of preosteoblasts cultured for 24 hours in 20% FBS with U0126 was significantly reduced compared to cells solely cultured in media containing 20% FBS (Fig. 6.1 D). These results suggest that U0126 effectively reduced naïve rMSCs and preosteoblasts mitogen-induced proliferation, thereby indicating the involvement of the ERK1/2 signalling pathway in this process.

6.2.2 U0126 effectively blocks mitogen-induced ERK1/2 activation in rMSCs

In order to determine the extent of inhibition caused by U0126 on mitogen-induced ERK1/2 activation, semi-confluent naïve rMSCs were serum starved for 24 hours and subjected to 30 minutes of 10 µM U0126 pre-treatment prior to mitogenic stimulation using 5% FBS. Engelbrecht et al. (2003) showed that mitogen-induced proliferation of MBA 15.4 preosteoblasts was accompanied by ERK1/2 activation. Furthermore, peak ERK1/2 activation in mitogen-stimulated MBA 15.4 preosteoblasts with 20% FBS occurred between 2 minutes and 30 minutes, after which activity declined to a plateau after 1 hour (Engelbrecht et al., 2003). To represent the peak-and shoulder stages of ERK1/2 activation, cells were stimulated with 5% FBS for 5 minutes and 1 hour. In order to confirm the MEK1/2 inhibitory effects of U0126 on both the peak-and plateau, cells were also treated concomitantly with 5% FBS and 10 µM U0126 for 24 hours.

It was found that U0126 effectively attenuates both 5 minutes and 1 hour ERK1/2 phosphorylation in naïve rMSCs after stimulation with 5% FBS (Fig. 6.2 A), thereby suggesting that under these conditions, U0126 effectively inhibits ERK1/2 peak and shoulder activity. U0126 also effectively blocked ERK1/2 phosphorylation after 24 hours of mitogen stimulation (Fig. 6.2 B). Therefore, in conjunction with the ablation of mitogen-induced rMSC proliferation by U0126 (Fig. 6.1), these results indicate the possible involvement of ERK1/2 in mediating proliferation in these cells.

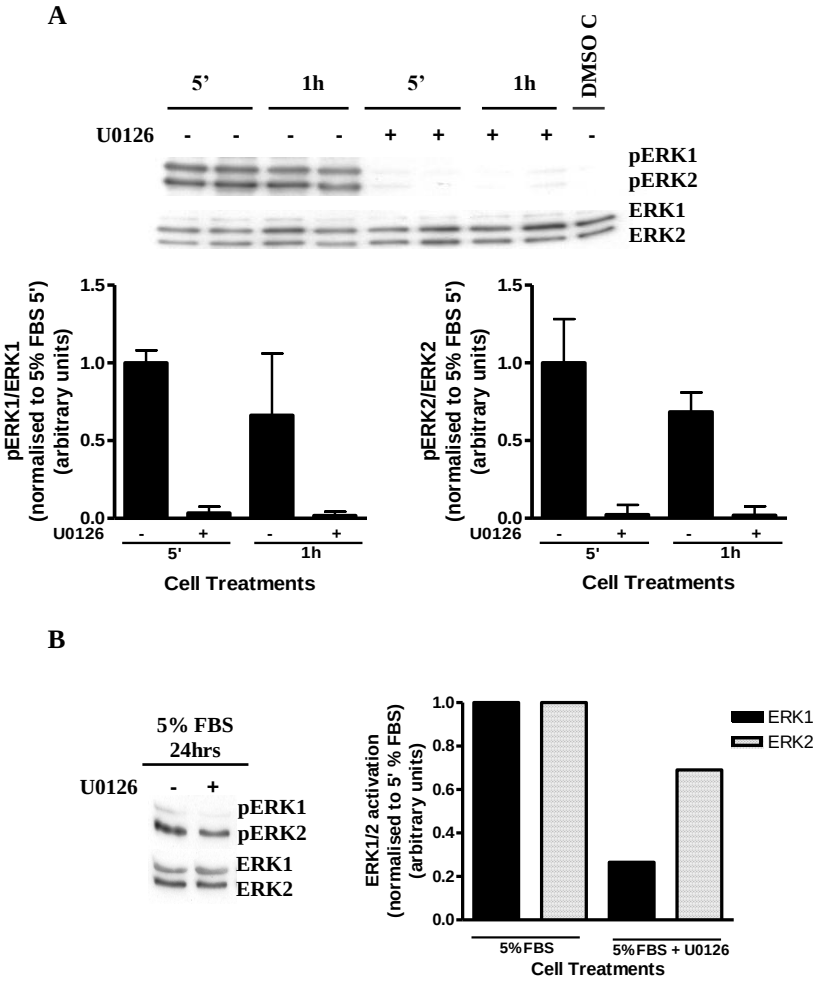

Figure 6.2: U0126 attenuates mitogen-induced ERK1/2 activation efficiently.

Naïve rMSCs were grown until 80% confluent and serum starved in 1% FBS for 24 hrs. (A) Cells were pretreated with 10 µM U0126 prior to mitogenic stimulation with 5% FBS or (B) concomitantly treated with 5% FBS and 10 µM U0126. Cell lysates (as outlined in Materials and Methods, Section 2.2.8.1) were prepared at indicated times. An amount of 20 µg of total proteins was resolved by SDS PAGE after which proteins were transferred onto a PVDF membrane. The degree of ERK phosphorylation/ activation was examined by using anti-phospho-ERK1/2 (active ERK1/2) antibodies. To ensure equal protein loading, duplicate membranes were blotted using anti-ERK1/2 (total ERK1/2) antibodies. Densitometry was used to analyse ERK1/2 phosphorylation and quantified utilising the ImageJ software. A representative blot of two experimental repeats is shown. Each repeat experiment represents an individual animal. Similar trends were observed between repeat experiments. Results are expressed as ratios of pERK1 integrated intensity/ERK1 integrated intensity (left graph) or pERK2 integrated intensity/ERK2 integrated intensity (right graph). The product of the mean pixel intensity and the band area was termed integrated intensity. Data is expressed in arbitrary units which was normalised to the time points specified on the respective graphs and set at 1.

6.2.3 A typical proliferative ERK1/2 induction profile is obtained upon growth factor stimulation of naïve rMSCs and preosteoblasts

To further investigate the involvement of the ERK1/2 MAPK cascade in the regulation of mitogen-induced proliferation of naïve rMSCs and preosteoblasts, the level of ERK1/2 phosphorylation and hence ERK1/2 activation was investigated after addition of mitogens. Cells were cultured until 80% confluent with subsequent serum reduction (1% FBS) for 24 hours for cell cycle synchronisation (Fig. 6.3 A) or grown until confluent before induction of differentiation using OM (Supplement A3.3.) for 7days (Fig. 6.3 B). Since 5% FBS stimulation resulted in increased proliferation in naïve rMSCs after 24 hours (Fig. 3.1), this concentration of FBS was used as a mitogen in these cells. Proliferation of preosteoblasts was stimulated when treated with 20% FBS, as seen in Fig. 4.2. Consequently this concentration of FBS was used to examine the proliferative induction profile of ERK1/2 in preosteoblasts (Fig. 6.3 B).

Basal ERK1/2 levels were assessed using the unstimulated controls, designated as time 0 (Fig. 6.3 A and B). Total ERK1/2 and phospho-ERK1/2 levels were compared in order to determine ERK activation (Fig. 6.3 A and B). The results showed that peak phosphorylation after mitogenic induction using 5% FBS was obtained between 2 minutes to 30 minutes for both ERK isoforms in naïve rMSCs (Fig. 6.3 A). Although a decrease in ERK1/2 phosphorylation was observed from 30 minutes until the end of the assay after stimulation with 5% FBS, ERK1/2 remained phosphorylated up to 4 hours (Fig. 6.3 A). In the case of preosteoblasts, maximum ERK1/2 activation occurred at 5 minutes, dropping further at 30 minutes (Fig. 6.3 B). ERK1/2 remained phosphorylated at reduced levels up to 4 hours (Fig. 6.3 B). A slight difference in the ERK1/2 activation profile was observed when comparing naïve rMSCs and preosteoblasts. This difference in ERK1/2 induction could be ascribed to the presence of differentiating factors in preosteoblast cell cultures upon mitogenic stimulation. No observable basal ERK1 phosphorylation was found and barely discernable levels of phospho-ERK2 were seen under basal conditions. Furthermore, the magnitude of peak ERK1 and ERK2 phosphorylation was similar whereas ERK2 showed slightly higher phosphorylation levels at 1h, 2h and 4h following mitogenic induction. These findings indicate that ERK1/2 is phosphorylated and hence, activated, after mitogenic stimulation of naïve rMSCs and primary preosteoblasts.

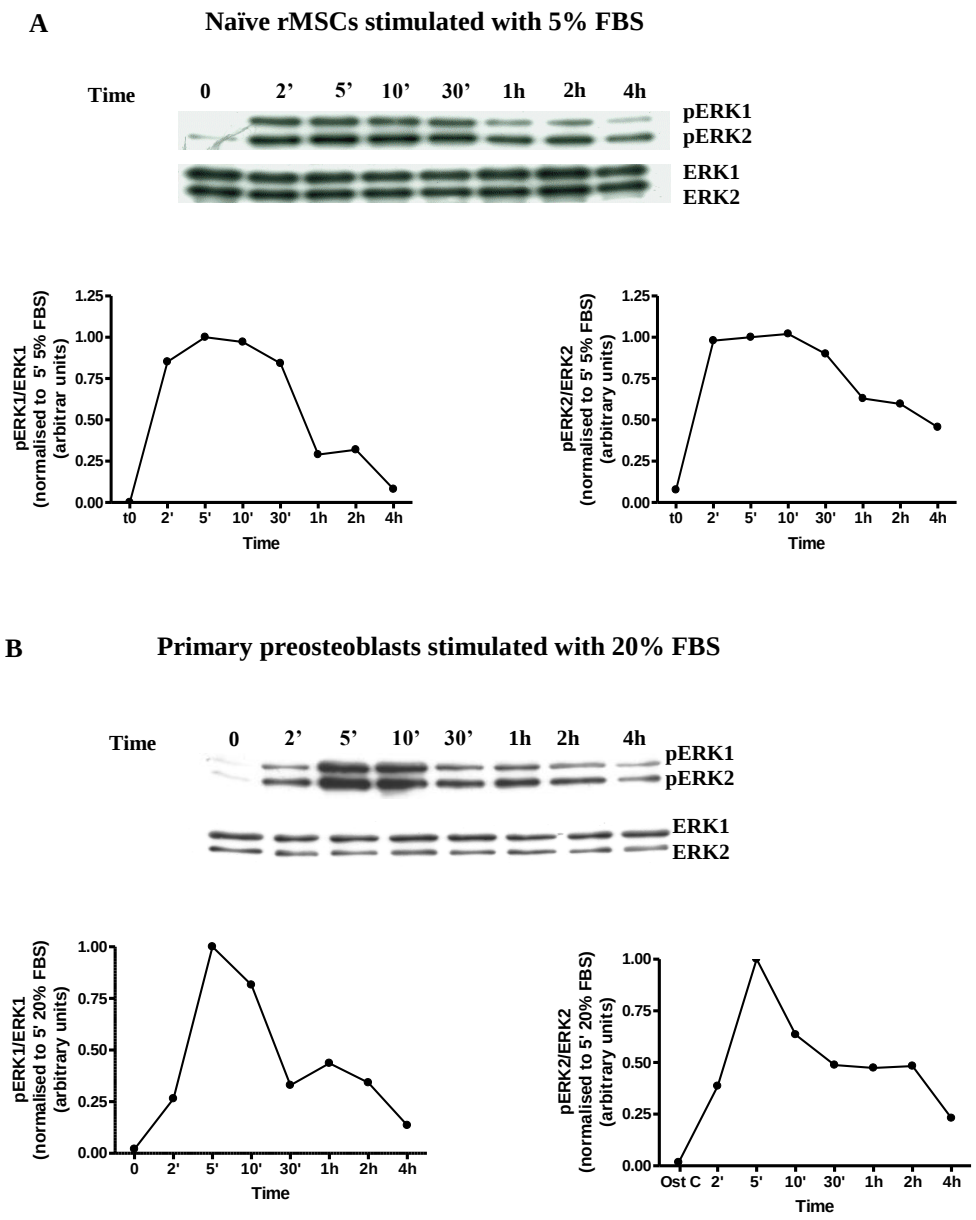

Figure 6.3: An ERK1/2 activation profile characteristic of proliferating cells is observed in naïve rMSCs and preosteoblasts after 5% FBS and 20% FBS stimulation.

Naïve rMSCs were cultured to 80% confluence, serum starved in 1% FBS for 24 hrs and treated with 5% FBS to elicit mitogenesis (A). Alternatively, confluent rMSCs were differentiated in OM (Supplement A3.3.) for 7 days prior to mitogenic stimulation with 20% FBS (B). Cell lysates were prepared (see Materials and Methods, Section 2.2.8.1) at indicated times after the addition of mitogen and 20 µg of total proteins was resolved by SDS polyacrylamide gel by electrophoresis. Proteins were then transferred onto a PVDF membrane. To determine the extent of ERK phosphorylation and thus activation, membranes were probed with anti-phospho-ERK1/2 (active ERK1/2) antibodies and compared to bands seen using antibodies against total ERK1/2 proteins. ERK1/2 phosphorylation was quantified by densitometry and ImageJ 1.42q software. The blot shown is representative of at least three (for rMSCs) and two (for preosteoblasts) independent experiments, where each experiment represents an individual animal which showed similar trends of ERK1/2 activation. Results are expressed as ratios of pERK1 integrated intensity/total ERK1 integrated intensity (left graph) or pERK2 integrated intensity/total ERK2 integrated intensity (right graph) and normalised to the 5 min time point, which was set at 1. Integrated density was calculated as the product of mean pixel intensity and area of the immunoresponsive band.

6.2.4 Strong mitogenic stimulation leads to elevated ERK1/2 phosphorylation levels

As strong mitogenic stimulation elicited only a weak proliferative response in naïve rMSCs (Fig. 3.1 A) and strong ERK1/2 activation has previously been associated with cell cycle arrest (Sewing et al., 1997; Woods et al., 1997; Roovers and Assoian, 2000), the ERK1/2 phosphorylation profile was examined after stimulation of rMSCs with 20% FBS or PMA. Cells were grown until 80% confluent and the serum was reduced until 1% FBS before cultures were subjected to concentrations of mitogens that results in proliferation (5% FBS) and growth arrest (20% FBS and 100 ng/ml PMA). In order to directly compare the results, lysates were blotted on the same membranes. Phospho-ERK1/2 was compared to total ERK1/2 to assess ERK1/2 activation.

The results showed that 5% FBS elicited a similar proliferative ERK1/2 activation profile as observed in Fig. 6.2 B, with peak ERK1/2 activity seen between 2 minutes and 30 minutes and reduced, but sustained activity after 30 minutes (Fig. 6.4 A and B). Contrary to 5% FBS stimulation, ERK1 activation peaked between 10 minutes and 30 minutes, after which decreased but sustained ERK1 activation was seen, following 20% FBS treatment (Fig. 6.4 A). In addition, the magnitude of ERK1 phosphorylation observed at 30 minutes, 2h and 4h was higher than that elicited by 5% FBS (Fig. 6.4 B).When comparing the level of activation of ERK2 elicited by 20% FBS to that of 5% FBS, ERK2 levels only dropped after 4h subsequent to 20% FBS treatment, but was still higher than that of 5% FBS (Fig 6.4 B). In addition, maximum ERK1 activity brought about by PMA was seen between 2 minutes to 5 minutes, dropping at 10 minutes and then again at 2h and 4h (Fig. 6.4 A and B). Maximum ERK2 phosphorylation was found at 5 minutes, decreasing after 30 minutes. These findings indicate that 5% FBS, 20% FBS and PMA may elicit different ERK1/2 activation profile, thereby providing a possible explanation for the divergent cellular proliferation obtained (Fig. 3.1.1). The ERK2 phosphorylation profile elicited by 20% FBS was found to be significantly ($P < 0.0211$) higher than that of 5% FBS and PMA. Overall, the 20% FBS response was 1.54 times higher (SE=0.58) than that of 5% FBS and 1.3 times higher (SE=0.58) than that of PMA. However, ERK1 phosphorylation was higher for 20% FBS than 5% FBS and PMA, but did not reach significance ($P < 0.7$) over the time period.

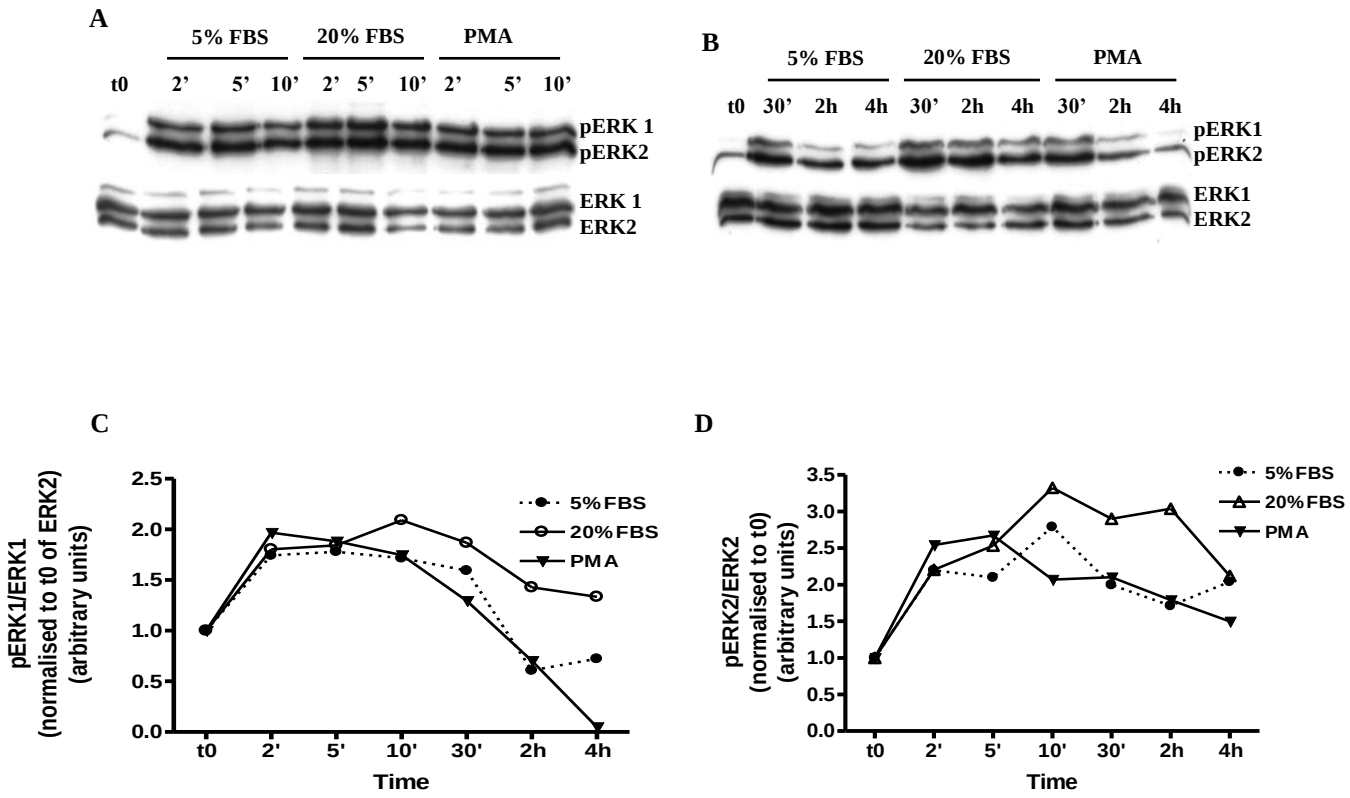

Figure 6.4: The magnitude of ERK1/2 phosphorylation is increased after strong mitogenic stimulation of naïve rMSCs.

Naïve rMSCs were grown until 80% confluent and serum starved in 1% FBS for 24 hrs. Cells were then stimulated with mitogens as indicated and cell lysates (as outlined in Materials and Methods, Section 2.2.8.1) were prepared at specified times. An amount of 20 µg of total proteins was resolved by electrophoresis on a SDS polyacrylamide gel and then transferred onto a PVDF membrane. The amount of ERK phosphorylation/ activation was examined by using anti-phospho-ERK1/2 (active ERK1/2) antibodies, followed by stripping the membrane to compare to total ERK1/2 . The short mitogenic treatments are shown in (**A**), whilst the longer stimulations are exhibited in (**B**). Analysis of ERK1/2 phosphorylation was performed using densitometry with ImageJ software to quantify the intensity of immunoresponsive bands. A representative blot of three experimental repeats is shown. Each repeat experiment represents an individual animal. Similar trends were observed between repeat experiments. A three-way ANOVA statistical analysis was done to determine the effects of 5% FBS, 20% FBS and PMA on ERK1/2 phosphorylation in naïve rMSCs over a time span of 4h in the three repeats experiments. The test was corrected for time, treatment and independent repeats. Results were considered significantly different at $(P < 0.05)$. Results are expressed as ratios of pERK1 integrated intensity/total ERK1 integrated intensity (**C**) or pERK2 integrated intensity/total ERK2 integrated intensity (**D**). Integrated density is defined as mean pixel intensity X area of bands. Data is expressed in arbitrary units, which were normalised to the time points specified on the respective graphs and set at 1.

6.2.5 Dexamethasone decreases mitogen-induced ERK activation

In order to determine the effect of Dex on mitogen-induced ERK1/2 activation in rMSCs and primary preosteoblasts, cells were pre-treated with 1 µM Dex for 1h prior to mitogenic stimulation with 5% FBS or 20% FBS, respectively. Before experimental treatments, rMSCs were grown until 80% confluent and serum starved in 1% FBS, whereas confluent cells were differentiated with OM media (Supplement A3.3.) for 7 days and designated as time 0 (t0).

ERK1/2 was phosphorylated to a greater extent in naïve cells pre-treated with 1 µM Dex for 1h and stimulated with 5% FBS for 2 minutes and 5 minutes compared to cells stimulated with mitogen only (Fig. 6.5.1 A). Even though a drop in the levels of phospho-ERK1/2 was observed at 10 minutes in cultures treated with 5% FBS, an even greater drop in ERK1/2 phosphorylation was seen in Dex pre-treated cells at this time point (Fig. 6.5.1 A and B). This decrease in ERK1/2 phosphorylation persisted up to 4h, after which ERK1/2 activity diminished further (Fig. 6.5.1 B). Although mitogen-stimulated ERK activity was clearly decreased after the addition of Dex, it did not reach significance (three-was ANOVA statistical analysis, which corrected for time, treatment and individual experimental repeats, N=2, where $P<0.9$ and $P<0.2$ for ERK1 and ERK2, respectively). This is most likely due to the low number of repeat experiments; however, due to time constraints, no additional experiments could be undertaken.

The mitogen-induced ERK1/2 activation profile of preosteoblasts is different from naïve rMSCs (Fig. 6.5.1 and Fig. 6.5.2). A decrease in ERK1 activity was observed after 10 minutes of mitogenic stimulation in the Dex treated cells. The lower actitivity after Dex treatment was further sustained in ERK2 (Fig. 6.5.2). Therefore, a general decrease in ERK1/2 activity was seen when preosteoblasts are treated with GCs, however, significance (three-way ANOVA statistical analysis, N=2, where $P<0.8$ and $P<0.6$ for ERK1 and ERK2, respectively) was not obtained over a time span of 4 hours. Similar to rMSCs, this could possibly be attributed to the low number of replicate experiments, which, due to time constraints, could not be repeated.

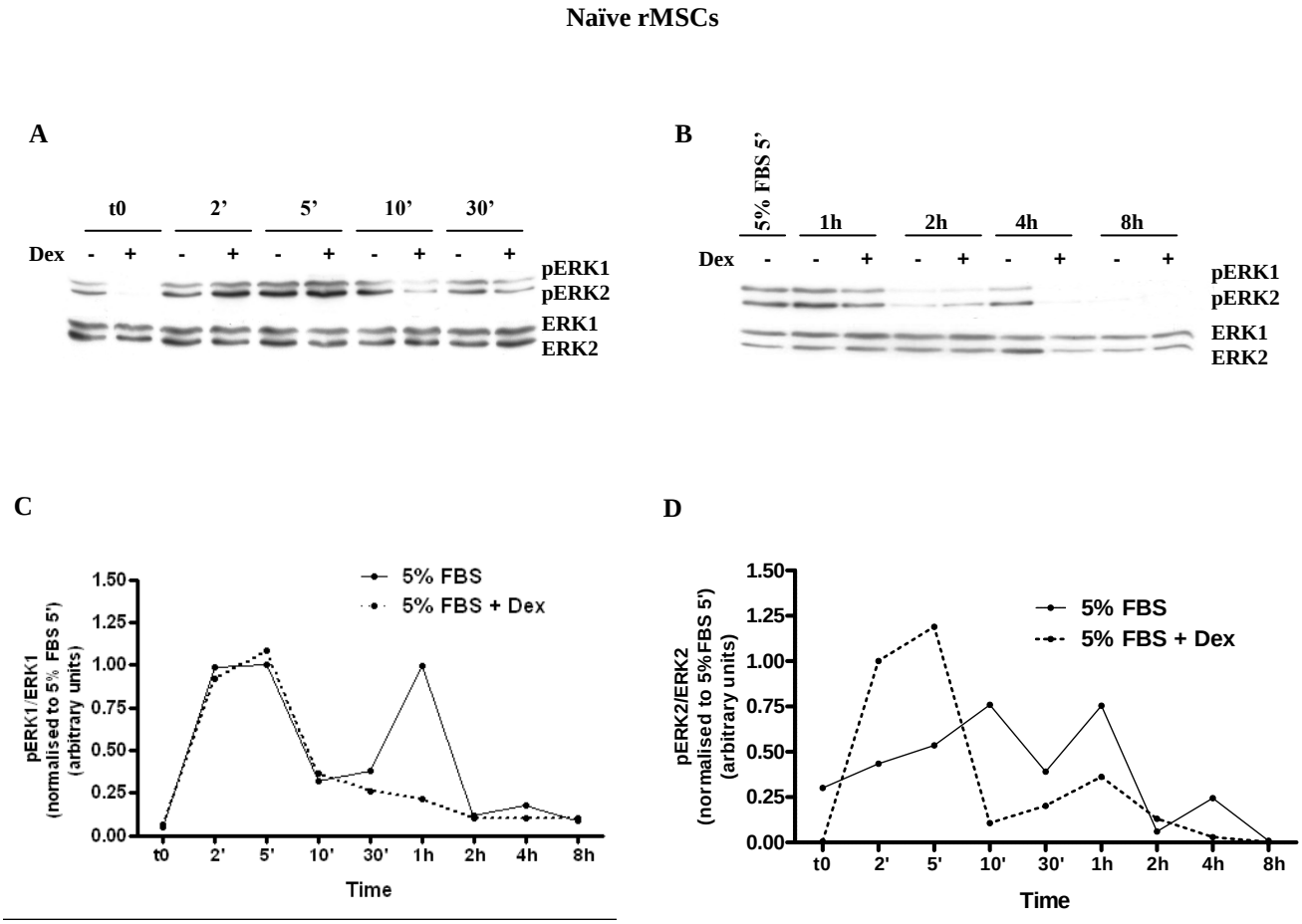

Figure 6.5.1: rMSCs pre-treated with 1 µM Dex for 1h exhibits reduced prolonged ERK1/2 activity.

Semi-confluent naïve rMSCs were serum starved in 1% FBS for 24 hrs. Cells were stimulated with 5% FBS as indicated and lysates prepared at indicated times (as outlined in Materials and Methods, Section 2.2.8.1). Cells incubated in 1% FBS were used as negative control and designated as t0. An amount of 20 µg of total proteins was resolved by electrophoresis on a SDS polyacrylamide gel. Proteins were subsequently transferred onto a PVDF membrane. The degree of ERK phosphorylation/ activation was examined by using anti-phospho-ERK1/2 (active ERK1/2) antibodies. The short mitogenic treatments are shown in (**A**), whilst the longer stimulations are exhibited in (**B**). To ensure equal protein loading, stripped membranes were blotted using anti-ERK1/2 (inactive ERK1/2) antibodies. Densitometry was used to analyse ERK1/2 phosphorylation and quantified utilising the ImageJ software. A representative blot of two experimental repeats (N=2) is shown. Each repeat experiment represents an individual animal. Similar trends were observed between repeat experiments. Results are expressed as ratios of pERK1 intensity/ERK1 intensity (**C**) or pERK2 intensity/ERK2 intensity (**D**). Data is expressed in arbitrary units which was normalised to the time points specified on the respective graphs and set at 1.

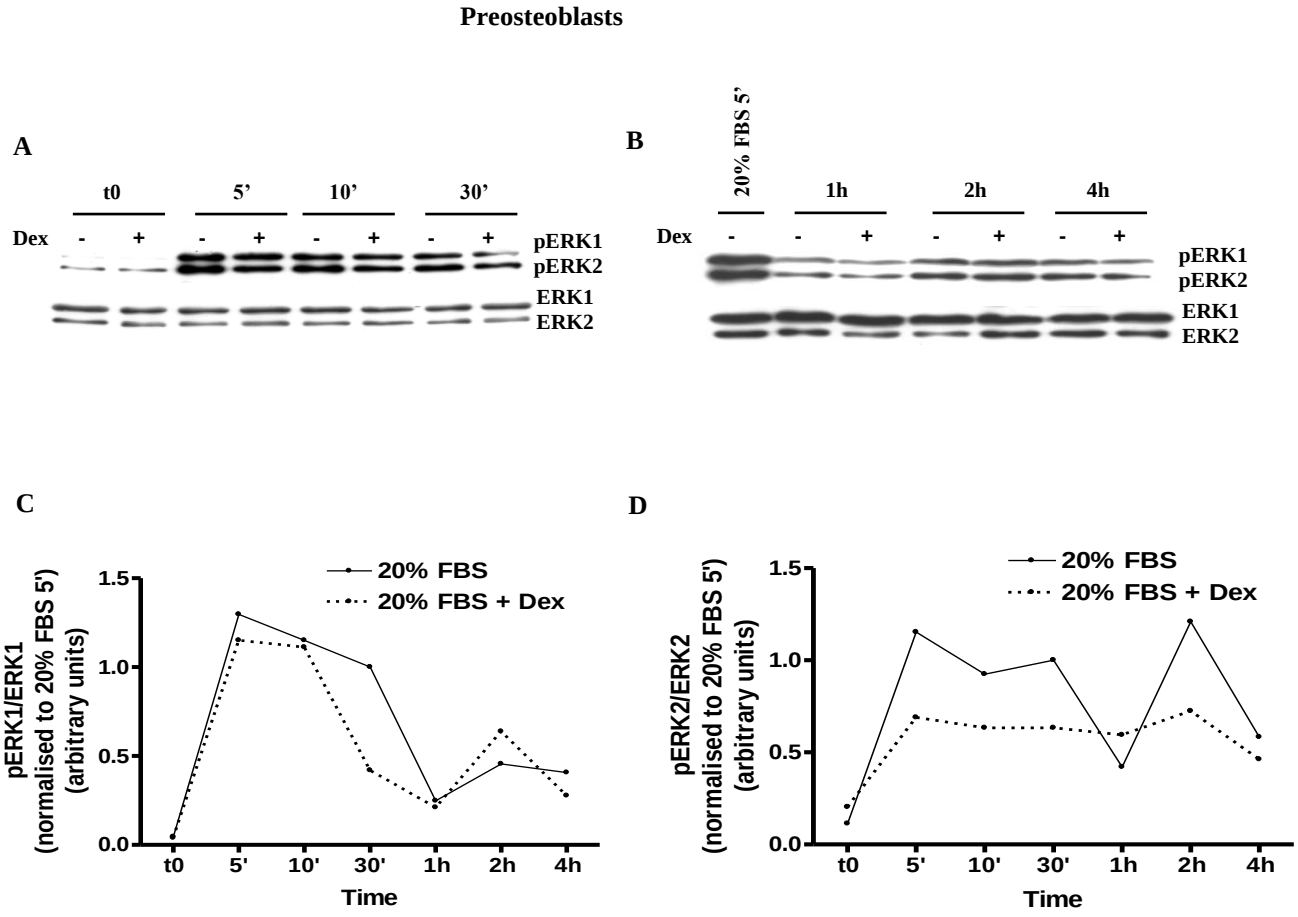

Figure 6.5.2: Preosteoblasts pre-treated with 1 µM Dex for 1h shows decreased ERK1/2 activity.

Confluent rMSCs were cultured in OM (Supplement A3.3.) for 7 days before 1h pre-treatment with 1 µM Dex. Cells were then stimulated with 20% FBS as indicated and cell lysates were prepared at the indicated times (see Materials and Methods, Section 2.2.8.1). An amount of 20 µg of total proteins was resolved by SDS PAGE, after which proteins were transferred onto a PVDF membrane. The amount of ERK phosphorylation/ activation was examined by using anti-phospho-ERK1/2 (active ERK1/2) antibodies. The western blots of the short mitogenic treatments are shown in (**A**), whereas the longer stimulations are displayed in (**B**). Stripped membranes were blotted using anti-ERK1/2 (inactive ERK1/2) antibodies to check that proteins were loaded in equal amounts. ERK1/2 phosphorylation was analysed using densitometry and quantified using ImageJ software. A representative blot of two experimental repeats (N=2) is shown. Each repeat experiment represents an individual animal. Similar trends were observed between repeat experiments. Results are expressed graphically as ratios of pERK1 integrated intensity/ total ERK1 integrated intensity (**C**) or pERK2 integrated intensity/ total ERK2 integrated intensity (**D**). Integrated intensity was defined as the product of the mean pixel intensity and the area of the immunoresponsive bands. Data was normalised to the 5 min time point and then set at 1 in arbitrary units.

6.3 Discussion

It was previously shown that mitogen-induced proliferation of osteoblastic cells like the MBA 15.4, MG63 and RobC26 cell lines, was mainly regulated by the ERK1/2 signalling cascade (Mehrotra et al., 2004; Horsch et al., 2007). An increase in ERK1/2 activity followed by enhanced proliferation was observed in these osteoblastic cell lines (Hulley et al., 1998; Engelbrecht et al., 2003; Horsch et al., 2007). Therefore, the aim of the research outlined in this chapter was to examine whether the ERK1/2 signal transduction pathway plays a role in the regulation of the mitogenic response of naïve rMSCs and primary preosteoblasts originating from these stromal cells. Furthermore, it was previously observed that Dex decreased the mitogen-induced proliferation of the MBA 15.4, MG63 and RobC26 cell lines and that this reduction was likely to be caused by a reduction in ERK1/2 activation (Hulley et al., 1998; Engelbrecht et al., 2003; Horsch et al., 2007). In consequence, the effect of Dex on the mitogenic activation of ERK 1/2 in rMSCs and preosteoblasts was investigated.

The involvement of the ERK1/2 signalling pathway in the modulation of growth factor-stimulated cell growth was established using the pharmaceutical inhibitor, U0126, which blocks signal transduction downstream of MEK1/2. U0126 successfully blocked the mitogen-induced proliferation of rMSCs and preosteoblasts, thereby indicating that ERK1/2 activation is required for the proliferative response of these cells (Fig 6.1). The ERK1/2 activation profile after mitogenic stimulation was also ascertained. A typical proliferative profile, with a swift peak, persisting between 2 minutes and 30 minutes and a prolonged lower-activity shoulder stage, lasting for a few hours, were obtained for both rMSCs and preosteoblasts after growth factor stimulation (Fig. 6.3 A and B) (Meloche et al., 1992; Meloche, 1995; Talarmin et al., 1999; Engelbrecht et al., 2003). The degree of U0126 (10 µM, 5 µM and 1 µM) inhibition was assessed in order to examine the relationship between ERK activity and proliferation. It was observed that U0126 effectively diminishes ERK1/2 activity during peak (5 minutes) as well as shoulder (1 hr) activity (Fig. 6.2). Moreover, U0126 attenuated the mitogen-stimulated proliferation in both rMSCs and preosteoblasts (Fig. 6.1), suggesting that ERK1/2 is essential for proliferation in these cells.

Marshall et al. (1995) suggested that both the duration and magnitude of ERK1/2 activation contributes to cellular fate. Since 20% FBS and PMA, which are considered powerful proliferative agents, did not elicit the expected mitogenic response in naïve rMSCs, the extent of ERK1/2 phosphorylation and hence activation was determined (Fig. 6.4 A). Subsequent to incubation with these mitogens, it was found that stimulation resulted in strong ERK1/2 activation (20% FBS; Fig. 6.4 A and B) as well as lasting ERK1/2 induction (PMA, Fig. 6.4 A and B). It has previously been

found that over-stimulation of ERK1/2 could lead to cell growth arrest and oncogenic senescence (Tuveson et al., 2004; DeNicola and Tuveson, 2009). This mechanism of strong ERK1/2 activation without proliferation could also be due to oncogenic-induced senescence in naïve rMSCs after incubation with 20% FBS and PMA.

As mitogenic stimulation of rMSCs and preosteoblasts has previously been associated with elevated ERK1/2 activation (Hulley et al., 1998; Engelbrecht et al., 2003; Horsch et al., 2007; Smith et al., 2002), which was abrogated by GCs, the effect of Dex on the ERK1/2 activation profile was assessed. rMSCs and preosteoblasts were pre-treated with a pharmaceutical dose of Dex (1 µM) for 1 hr before mitogenic stimulation. This pre-incubation was done to allow time for transcription to occur, propagating the non-genomic and the genomic effects of Dex. In accordance with the literature, Dex swiftly decreased the activity of both ERK isoforms starting at 10 minutes after mitogenic stimulation (therefore Dex exposure was 1h 10 minutes) and lasting up to 4 hours (that is total Dex exposure was 5 hours; Fig. 6.5.1). This time period is in agreement with the findings of Engelbrecht et al. (2003), where ERK1/2 activity was reduced within 2 hours. In addition, the genomic effects of GCs are seen only after approximately 30 minutes to 1 hour and could last up to several hours and days (Makara and Haller, 2001; Cato et al., 2002). Therefore, these findings suggest that a plausible mechanism for the anti-proliferative effect of Dex on rMSCs and preosteoblasts could be the transcriptional regulation of protein expression in the ERK1/2 pathway, other than the ERK1 and ERK2 proteins (Engelbrecht et al., 2003). Possible candidates for such transcriptional regulation could be proteins located upstream or downstream from the ERK1/2 proteins.

The MAPK signalling pathway is regulated through phosphorylation. Phosphorylation of constituent proteins in this cascade, by protein kinases, leads to the activation of ERK1/2. Therefore, induction of protein kinase activity regulates the ERK1/2 protein signalling cascade. Conversely, the inactivation of ERK1/2 is executed by phosphatases via dephosphorylation of various key kinases in this specific pathway. Hence, up-regulation of protein phosphatases could be a potential mechanism by which GCs down-regulates the activity of ERK1/2. In the next chapter the role of phosphatases, in particular protein tyrosine phosphatases, in the regulation of the ERK1/2 signal transduction pathway after activation by mitogens is examined.

Chapter 7

The role of the protein tyrosine phosphatase, MKP-1, in the Dex-regulation of mitogen-induced proliferation in osteoblast progenitor cells

7.1 Introduction

As seen in Section 6.3.1, ERK1/2 was found to regulate mitogen-stimulated osteoblast precursor replication. Seeing that the ERK1/2 signalling pathway is regulated through phosphorylation, the degree of phosphatase activity induced upon mitogen and concomitant mitogen and Dex administration was determined. Phosphatase activity was assessed using a p-Nitrophenyl phosphate (pNPP) hydrolysis assay. This colorimetric assay is based on the catalytic ability of phosphatases to hydrolyze the pNPP substrate to the product, *p*-nitrophenol. The chromogenic product is then detected spectrophotometrically at A_{405nm}, with an increase in the yellow colour product of the pNPP hydrolysis reaction being indicative of increased phosphatase activity. Mitogen-activated ERK1/2 phosphorylation and hence activation has previously been shown to be attenuated by Dex in immortalised cell lines (Hulley et al., 1998; Engelbrecht et al., 2003; Horsch et al., 2007). Since ERK1/2 inactivation occurs via tyrosine and threonine dephosphorylation, the contribution of protein tyrosine phosphatases to the induction of total (gross) phosphatase activity after mitogenic and Dex stimulation was determined in rMSCs and preosteoblasts. To achieve this, vanadate was used to block PTP activity whilst the residual phosphatase activity, which could possibly be ascribed to serine/threonine phosphatases, was measured using pNPP hydrolysis. It was hypothesised that because ERK activation is essential for proliferation and ERK is exquisitely regulated by tyrosine phosphorylation, that, if the PTP activity induced by concomitant mitogen and Dex stimulation was inhibited by vanadate, the Dex-induced impairment of osteoblast precursor cell proliferation would be restored. Therefore, the effect of vanadate on the Dex-induced attenuation of proliferation in naïve rMSCs and preosteoblast proliferation was assessed. As MKP-1 was previously shown to regulate ERK1/2 activity in immortalised MBA 15.4 preosteoblasts (Horsch et al., 2007), the mRNA and protein abundance of MKP-1 was examined in rMSCs and primary preosteoblasts using quantitative real-time PCR (RT-qPCR) and western blot analysis, respectively.

7.2 Results

7.2.1 Vanadate decreases protein tyrosine phosphatase activity induced after mitogen and Dex treatment

In order to examine the induction of phosphatase activity in rMSCs, cells were first grown until 80% confluent and then subjected to 24 hr serum deprivation at 1% FBS to synchronise the cell cycle of cells before the pNPP assay. In the case of preosteoblasts, confluent rMSCs were differentiated with osteogenic medium (OM) for 7 days to induce the osteoblastic phenotype. Mitogenic cell treatments with 5% FBS (Fig. 7.1 B and C) or 20% FBS (Fig. 7.1 D) and concomitant mitogen and Dex lasted for 24 hours, before protein lysates were prepared. Cells treated with 1% FBS (Fig. 7.1 A and C) or osteogenic medium (designated as OM C) (Fig. 7.1 D) were used to determine basal phosphatase activity levels. This work was based on the premise that increased formation of the yellow *p*-nitrophenol product of the pNPP hydrolysis reaction indicates elevated phosphatase activity. Before inhibitor studies were performed, various concentrations of the phosphatase-containing lysates were used to determine the reaction limiting conditions, such as the amount of enzyme and substrate used (Fig. 7.1 A and B). It was found that the hydrolysis reaction peaked at 150 µg of protein lysates under both basal and mitogen-stimulated conditions and reached a plateau thereafter (Fig. 7.1 A and B). Therefore, 150 µg of protein was used in subsequent phosphatase assays.

A considerable amount of *p*-nitrophenol and hence phosphatase activity was observed under basal (1% FBS) and mitogenic conditions (5% FBS and 20% FBS), which was increased after the addition of 1 µM Dex (Fig. 7.1 C and D). These findings indicate the presence of Dex-inducible phosphatases in non-stimulated (1% FBS) as well as mitogenic treated rMSCs and preosteoblasts. Vanadate at 10 µM and 1 µM was then used to examine the contribution of PTPs to the total phosphatase activity. Basal and mitogen-induced phosphatase activity was reduced by 80% at 10 mM vanadate, whereas 1 mM caused a 50% drop in phosphatase activity under these conditions (Fig. 7.1 C and D). Since the degree of vanadate inhibition was so severe, it can be postulated that PTPs constitute the main fraction of phosphatases active under these basal and mitogenic condition.

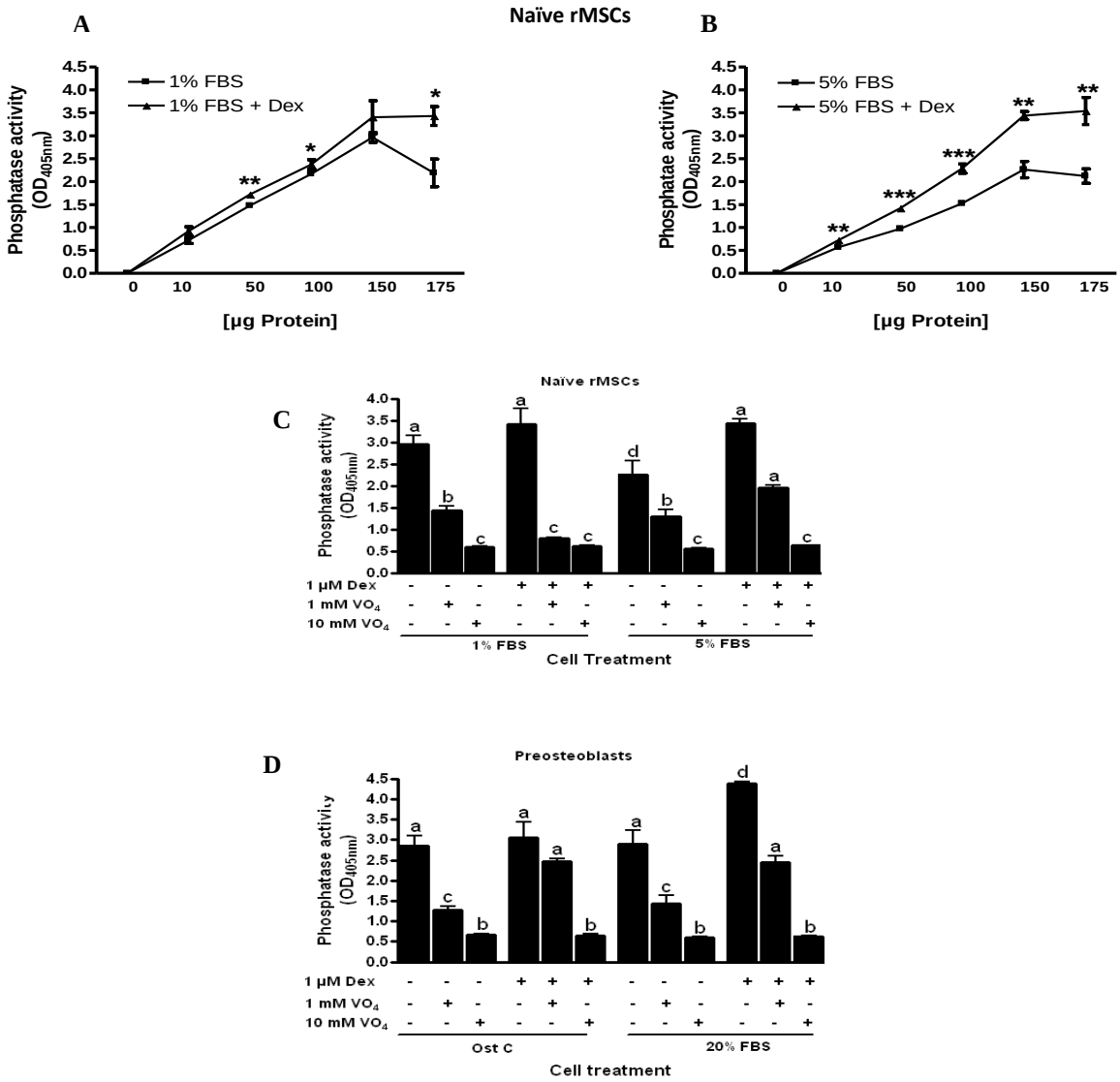

Figure 7.1: Protein tyrosine phosphatases are the major class of phosphatases present after mitogenic induction and are up-regulated by Dex in naïve rMSCs and preosteoblasts.

Semi-confluent rMSCs which were serum starved for 24 hrs (**A** and **B**) or confluent rMSCs differentiated into an osteoblastic phenotype for 7 days (**C**) were used for the pNPP hydrolysis assay to measure phosphatase activity at pH 7 (as outlined in Materials and Methods, Section 2.2.5). Protein lysates were prepared (see Materials and Methods, Section 2.2.5). The limiting enzymatic conditions for optimal phosphatase activity after 24 hrs of incubation in 1% FBS (**A**) and 5% FBS (**B**) was then established. Cells were treated with 1% FBS (**A** and **C**) or osteogenic medium (OM C) (**D**) to determine basal phosphatase levels. A concentration of 150 µg of total protein was consequently used to assess phosphatase activity (**C** and **D**). The optical density was measured at 405 nm using a Synergy™ HT microtiter plate reader and data was analysed with KC4 v3.3 software (Bio-Tek® Instruments, Inc., Vermont, USA). Data shown are the means± standard deviation of two independent experiments where n=3. Statistically significant differences are indicated as * ($P<0.05$), ** ($P<0.005$) and *** ($P<0.0005$) on the line graphs or as lower case letters on the bar graphs. **Abbreviations**: **Dex** dexamethasone; **OD** optical density; **mM** millimolar; **nM** nanomolar; **OM C** osteogenic control; **pNPP** paranitrophenylphosphate; **VO_4** vanadate

7.2.2 Vanadate partially rescues the Dex-induced inhibition of proliferation in rMSCs and preosteoblasts

As seen in Sections 5.2.1 and 5.2.4, respectively, Dex inhibits mitogen-induced proliferation in rMSCs and preosteoblasts, and is accompanied by a Dex-induced decrease in mitogen-stimulated ERK1/2 activity (Section 6.3.3). Since ERK1/2 activity is regulated by protein tyrosine phosphatases (PTPs) (Section 1.4.3.2) and vanadate decreased PTP activity in Dex-stimulated fractions (Fig. 7.1), the effect of vanadate on the Dex-induced reduction of proliferation in rMSCs and preosteoblasts was assessed. Naïve rMSCs were grown until 50% confluent and serum starved with 1% FBS for cell cycle synchronisation or confluent cells were differentiated into preosteoblasts using OM (as described in Section 2.2.1.3 and Supplement A3.3.). Cell proliferation was stimulated using 5% FBS (naïve rMSCs) or 20% FBS (preosteoblasts) as a mitogenic treatment, whilst basal growth conditions were assessed with 1% FBS or OM (Supplement A3.3.).

A proliferation assay was done to assess the dose response of vanadate under basal and mitogenic conditions to determine the effect of vanadate on rMSCs proliferation. It was found that 10 µM and 5 µM vanadate, reduced rMSC proliferation even after mitogenic stimulation with 5% FBS; this could possibly be attributed to cytotoxicity (data not shown). Cells treated with 10 µM vanadate detached from the culture dish and had a blebbed appearance, typical of cells undergoing cell death, when examined using light microscopy (data not shown). Under basal conditions, 1 µM vanadate was proliferative compared to the 1% FBS control (Fig. 7.2 A and B), whereas after 5% FBS stimulation, cells exhibited similar proliferation levels (Fig. 7.2 C and D). Therefore, 1 µM of vanadate was used subsequently. To accurately assess the effect of vanadate on the Dex-inhibition of proliferation in rMSCs, a 50% drop in proliferation was required. This allowed any small change in proliferation to easily be noticed as extreme inhibition might require high concentrations of vanadate to alleviate the effects of high Dex doses; these concentrations of vanadate, in turn, may be cytotoxic. Since naïve rMSCs are extremely sensitive to Dex (Fig. 5.1), two low Dex concentrations (1 nM and 5 nM) were tested to elicit a 50% decrease in proliferation. In non-stimulated rMSCs, that is under basal proliferation, administration of 1 nM and 5 nM Dex resulted in severely reduced mitogenesis (Fig. 7.2 A and B), whilst an approximately 50% reduction was obtained under mitogenic conditions (Fig. 7.2 C and D). It was shown that 1 µM vanadate partially, but significantly, restored the Dex-induced inhibition of rMSC proliferation to basal growth control levels (Fig. 7.2 A, B, C and D).

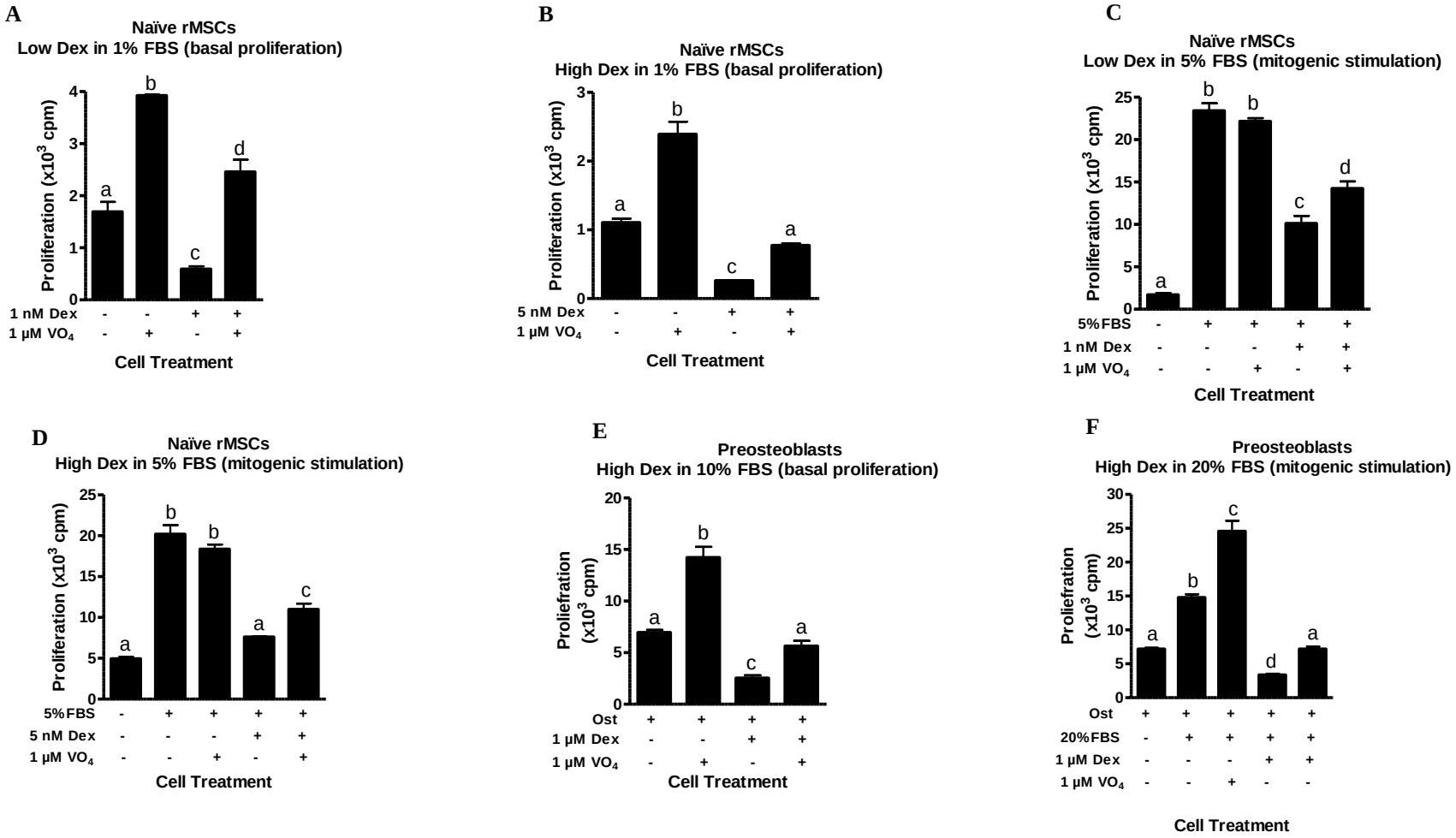

Figure 7.2: Vanadate moderately restores the Dex-mediated impairment of proliferation in naïve rMSCs and preosteoblasts.

Hemi-confluent rMSCs were serum deprived using 1% FBS or confluent rMSCs were differentiated into an osteoblastic phenotype using OM (Supplement A3.3.). For mitogenic stimulation, cells were treated with either 5% FBS (**C**, **D**) or 20% FBS (**F**) for 24 hrs. 1% FBS (**A**, **B**) or OM (**E**, **F**) were used as basal growth controls. Cells were treated with either: 1 nM or 5 nM for rMSCs and 1 µM Dex for preosteoblasts to diminish cell proliferation. Vanadate was used at a dose of 1 µM. DNA synthesis was measured by incorporation of [^{3}H] thymidine ([^{3}H] dT) for the last 4hrs of incubation. Data of an individual experiment is shown, where n = 3 and is representative of experiments repeated at least three times. Each repeat represents an individual animal. Results displayed are the mean cpm ± S.E.M., where $P<0.05$ was seen as a statistically significant difference using the One-way Anova with Bonferonni post-hoc test. Statistically significant differences are indicated by different lower case letters. Data bars with the same letter above are not statistically different. **Abbreviations**: **C** control; **cpm** counts per minute; **Dex** dexamethasone; **FBS** fetal bovine serum; **VO_4** vanadate

Similar to rMSCs, 1 µM vanadate also significantly increased the proliferation of preosteoblasts under basal (OM) and mitogen-induced (20% FBS) conditions (Fig. 7.2 E and F). Furthermore, 1 µM Dex caused a significant decrease in preosteoblast proliferation under both basal and mitogenic conditions and vanadate was found to partially, but significantly; restore this Dex-induced inhibition (Fig. 7.2 E and F). Therefore, taken together, these results suggest that vanadate-sensitive phosphatases, possibly PTPs, are partly responsible for the Dex-induced reduction of proliferation in rMSCs and preosteoblasts. One other plausible explanation for the vanadate stimulated proliferation could be that vanadate might induce kinase activity as well inhibits PTPs (Kadota et al., 1987a; Kadota et al., 1987b; Fantus et al., 1989; Heffetz et al., 1990; Elberg et al., 1994).

7.2.3 Vanadate elicits a typical proliferative ERK1/2 activation profile in rMSCs

Since 1 µM vanadate treatment of osteoblast precursors caused a significant increase in proliferation (Fig. 7.2) and ERK1/2 activation is essential for proliferation (Fig. 6.1), the involvement of the ERK1/2 mitogenic pathway in vanadate-induced proliferation was assessed. The MEK1/2 inhibitor, U0126, was employed to block the ERK1/2 cascade in order to discern the involvement of ERK1/2 in vanadate-stimulated proliferation. The activation profile of the ERK1/2 proteins was also examined using western blotting after vanadate. rMSCs were grown to a density of 80% and serum starved for 24 hours to synchronise the cell cycle of these cells, before vanadate stimulation. For the proliferation assay, cells were treated with 1 µM vanadate for 24 hours, cells lysed and proteins analysed at specified time points.

Results showed that 1 µM vanadate evoked significantly more rMSC proliferation under basal and mitogenic conditions, compared to the controls (Fig. 7.3.1). U0126 inhibited vanadate-induced proliferation to control levels, thereby indicating the involvement of ERK1/2 in regulating this response. Moreover, vanadate induced an ERK1/2 activation profile that is characteristic of proliferating cells (Fig. 7.3.2), further demonstrating the involvement of ERK1/2 in regulating rMSCs proliferation as stimulated by vanadate.

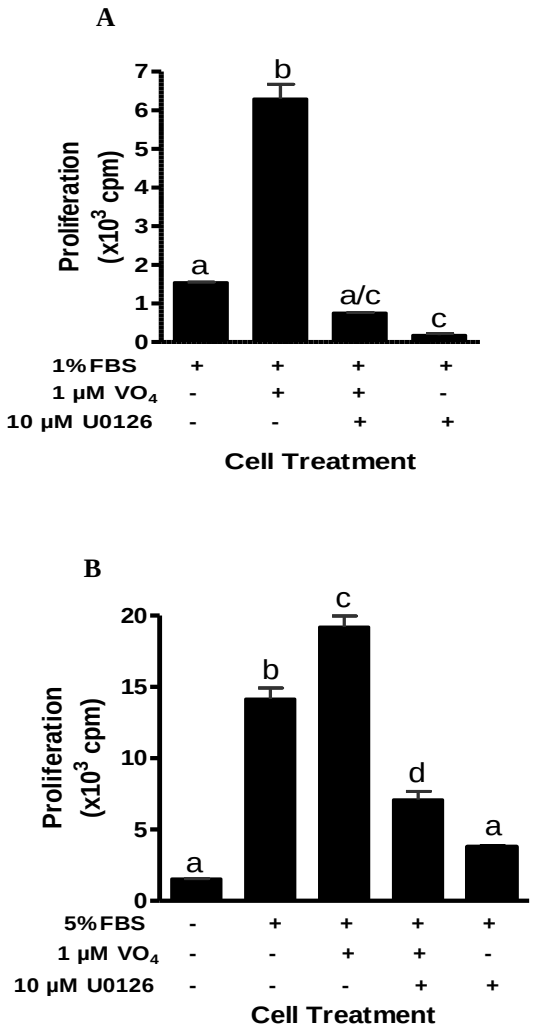

Figure 7.3.1: ERK1/2 activity is required for vanadate-induced rMSCs proliferation.

Cells were grown to 50% confluency, serum starved in medium containing 1% FBS for 24 hrs. U0126 treatment occurred concurrently with VO_4 stimulation. 1% FBS was used as basal growth controls (**A**) and 5% FBS was used as mitogenic stimulation (**B**). DNA synthesis was measured by incorporation of [^{3}H] thymidine ([^{3}H] dT) for the last 4 hrs of incubation. Data of an individual experiment is shown, where n = 3 and is representative of experiments repeated at least three times, where each repeat represents an individual animal. Results displayed are the mean cpm ± S.E.M., where $P<0.05$ was seen as a statistically significant difference using the One-way Anova with Bonferonni post-hoc test. Statistically significant differences are indicated by different lower case letters. Data bars with the same letter above are not statistically different. **Abbreviations**: **cpm** counts per minute; **FBS** fetal bovine serum; **VO_4** vanadate

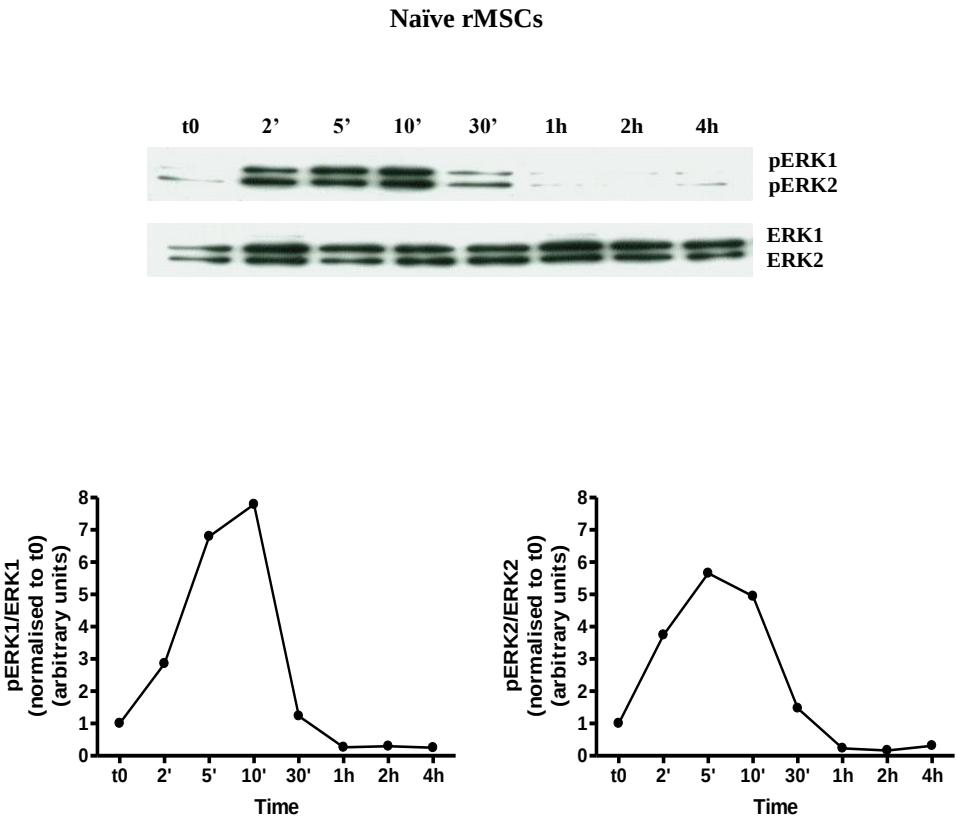

Figure 7.3.2: A characteristic proliferative ERK1/2 activation pattern is evoked by vanadate in naïve rMSCs.

Naïve rMSCs were grown until a cell density of 80% and serum starved in 1% FBS for 24 hrs. Cells were then incubated with 1µM VO_4 and cell lysates were prepared at specified times (as outlined in Materials and Methods, Section 2.2.8.1). 1% FBS was used as a negative control and designated as t0. An amount of 20 µg of total proteins was resolved by electrophoresis on a SDS polyacrylamide gel. Proteins were transferred onto a PVDF membrane. The amount of ERK phosphorylation/ activation was determined by using anti-phospho-ERK1/2 (active ERK1/2) antibodies. To ensure equal protein loading, stripped membranes were probed using anti-ERK1/2 (inactive ERK1/2) antibodies. Analysis of ERK1/2 phosphorylation was performed using densitometry. ImageJ software was used to quantify the intensity of immunoresponsive bands. A representative blot of three experimental repeats is shown. Each repeat experiment represents an individual animal. Similar trends were observed between repeat experiments. Results are expressed as ratios of pERK1 integrated intensity/ERK1 integrated intensity (left graph) or pERK2 integrated intensity/ERK2 integrated intensity (right graph). Integrated density is defined as the mean pixel intensity multiplied by the area of bands. Data is given in arbitrary units which was normalised to t0 and set at 1.

7.2.4 The mRNA of the dual-specific phosphatase, MKP-1, is up-regulated by FBS and Dex in rMSCs and preosteoblasts

As determined in Section 7.1, the predominant phosphatase class active under basal and mitogenic conditions in rMSCs and preosteoblasts were sensitive to vanadate, thereby suggesting the involvement of protein tyrosine phosphatases (Fig. 7.1). Moreover, vanadate enhanced cell growth as well as moderately restored the Dex-induced attenuation of mitogen-stimulated cell proliferation (Fig. 7.2). In addition, it was shown that ERK1/2 was required for the proliferative response of vanadate and that vanadate elicited a characteristic proliferative ERK1/2 activation profile (Fig. 7.3). These results suggest that one or more vanadate responsive phosphatases are most likely involved in the Dex regulation of rMSC and preosteoblast proliferation under mitogenic conditions.

Previous it has been found that the mRNA and protein of the nuclear dual-specificity PTP, MKP-1, are up-regulated by Dex and inhibit preosteoblast proliferation after mitogen stimulation. Furthermore, overexpression of recombinant MKP-1 in these immortalised cells led to decreased preosteoblast proliferation (Engelbrecht et al., 2003; Horsch et al., 2007). This indicates the involvement of MKP-1 in the Dex regulation of preosteoblast proliferation. A further role for MKP-1 in the modulation of preosteoblast proliferation was illustrated when it was found that MKP-1 dephosphorylated mitogen-induced ERK1/2 after Dex treatment (Horsch et al., 2007), thereby leading to ERK1/2 inactivation and resulting in decreased cell proliferation. The expression profile of MKP-1 was therefore examined in naïve rMSCs and preosteoblasts.

Naïve rMSCs were grown until 80% confluent and serum starved in 1% FBS for cell cycle synchronisation. Preosteoblasts were generated by differentiating confluent rMSCs with OM (Supplement A3.3.) for 7 days. Cell treatments involved the mitogenic stimulation of naïve rMSCs with 5% FBS and preosteoblast cells with 20% FBS, or concomitant mitogen and 1 µM Dex administration to both cell types. RNA was isolated and reverse transcribed into cDNA, which was used as a template in the RT-qPCR to examine the relative abundance of MKP-1 transcripts. ARBP was used as reference gene.

Data showed that serum stimulation and 1 µM Dex in combination with serum rapidly increased the abundance of MKP-1 mRNA in naïve rMSCs and preosteoblastic cells, although to different magnitudes (Fig. 7.4.1 A, B and Fig. 7.4.2 A, B). A decrease in the amount of serum-and Dex-induced MKP-1 mRNA was generally observed after 30 min in both cell types (Fig. 7.4.1 A, B and Fig. 5.4.2 A, B). When examining the effect of Dex alone in naïve rMSCs, it was seen that MKP-1 mRNA slightly increased at 30 min. However, at 1h and 2h, MKP-1 mRNA levels significantly different ($P<0.001$) compared to the control were observed, peaking at 2h (Fig. 7.4.1 C). Contrary to this, in preosteoblasts, Dex caused an elevation in MKP-1 mRNA levels between 1h and 4h, reaching a maximum at 2h, which was significantly different ($P<0.001$) compared to the control (Fig. 7.4.2 C). These results suggest that Dex treatment results in an increase in MKP-1 mRNA in naïve rMSCs and preosteoblasts.

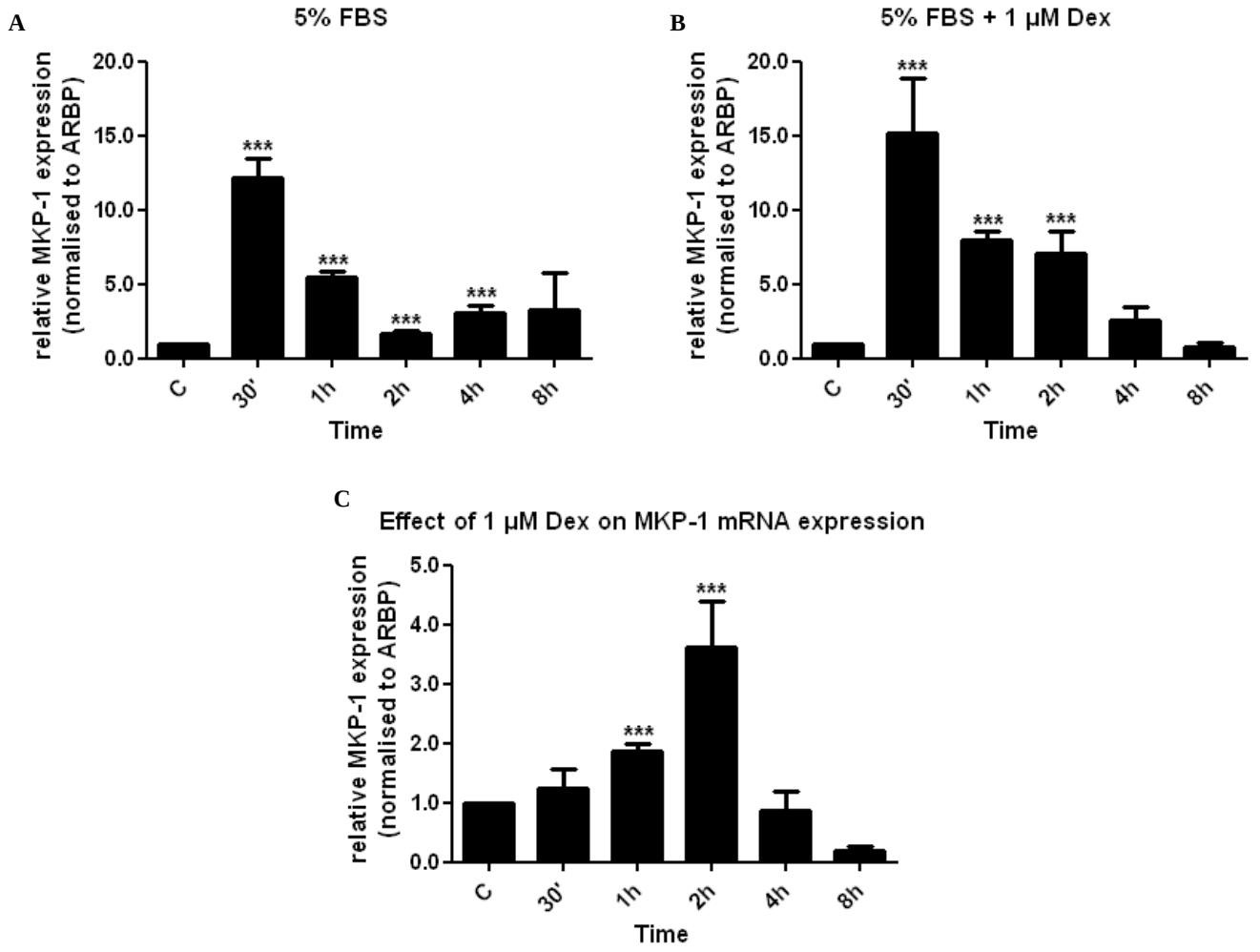

Figure 7.4.1: MKP-1 mRNA is rapidly up-regulated by 5% FBS and 1 µM Dex in naïve rMSCs.

Semi-confluent rMSCs were serum starved by using 1% FBS before mitogenic stimulation. Cell stimulation entailed treatment with 5% FBS (**A**) or simultaneous 5% FBS and 1 µM Dex (**B, C**) treatment at specified times. 1% FBS were used as negative induction control and used as untreated control for transcript abundance determination. Total RNA was isolated at the given times and converted into cDNA using reverse transcription with ImpromII reverse transcriptase. cDNA was used as RT-qPCR templates to determine the relative abundance of MKP-1 transcripts. ARBP was utilised as reference gene for data normalisation. Data of an individual experiment is displayed as mean ± standard error, where n = 3 and is representative of experiments repeated at least three times, where each repeat represents an individual animal. Results displayed are the relative expression as determined using the REST 2008 software program and expressed as $\mathbf{[MKP\text{-}1]_{treated}}$/ $\mathbf{[MKP\text{-}1]_{untreated}}$. *** denotes statistical significant different data ($P<0.001$) compared to controls, which were set to 1. It is worthy to note that (C) depicts a bar graph where the data is expressed as a ratio of $\mathbf{[MKP\text{-}1]_{5\%\ FBS\ and\ 1\ \mu M\ Dex\ (treated)}}$ / $\mathbf{[MKP\text{-}1]_{5\%FBS\ (untreated)}}$ to determine the effect of Dex on MKP-1 mRNA expression. **Abbreviations**: **ARBP** acidic ribosomal phosphoprotein; **C** control; **h** hour

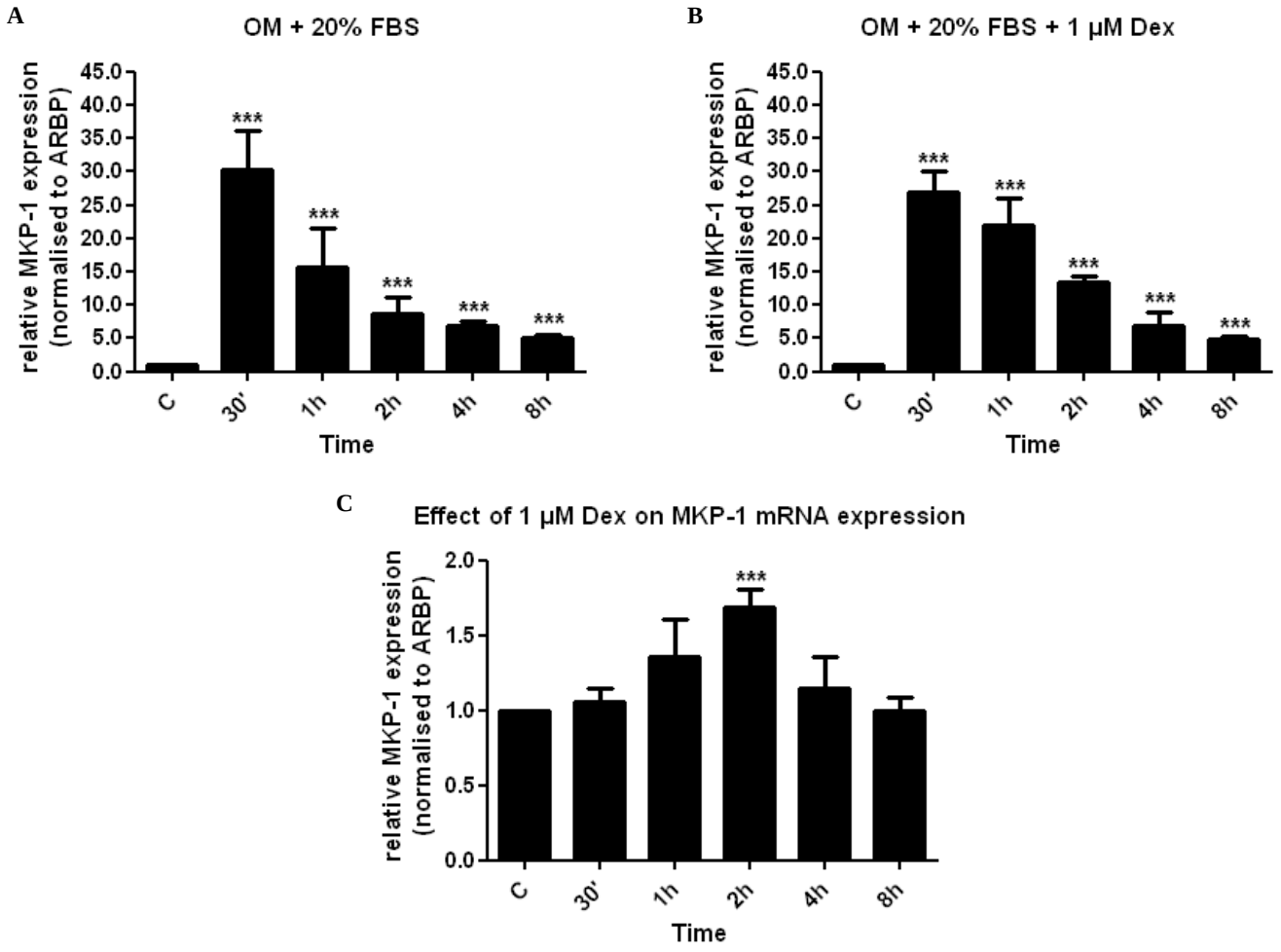

Figure 7.4.2: MKP-1 mRNA is up-regulated by 20% FBS and 1 µM Dex in preosteoblasts.

Confluent rMSCs were differentiated into an osteoblastic phenotype for 7 days using OM. Cell stimulation entailed treatment with 20% FBS (**A**) or concomitant 20% FBS and 1 µM Dex (**B, C**) treatment at indicated times. Osteogenic medium was used as negative induction control and used as untreated control to determine the relative transcript quantity of MKP-1 transcripts. Total RNA was isolated at the specified times. cDNA templates were produced using ImpromII reverse transcriptase. ARBP was employed as reference gene for RT-qPCR data normalisation. Data of an individual experiment, where n = 3, is displayed. This data is representative of experiments repeated at least three times and is expressed as mean ± standard error. Each repeat corresponds to an individual animal. Results displayed are the relative expression as determined using the REST 2008 software program. Data is expressed as $\mathbf{[MKP\text{-}1]_{treated}}$/ $\mathbf{[MKP\text{-}1]_{untreated}}$. *** denotes statistical significant different data ($P<0.001$) compared to controls, which were set to 1. Please note that (**C**) illustrates a graph where the data is expressed as a ratio of $\mathbf{[MKP\text{-}1]_{20\%\ FBS\ and\ 1\ \mu M\ Dex\ (treated)}}$ / $\mathbf{[MKP\text{-}1]_{20\%FBS\ (untreated)}}$ to determine the effect of Dex on MKP-1 mRNA expression.

7.2.5 MKP-1 protein is up-regulated by FBS and Dex

The aim of this investigation was to determine the effect of Dex on the MKP-1 protein expression levels in naïve rMSCs and preosteoblasts. Hence, 80% confluent naïve rMSCs were serum starved using 1% FBS before mitogenic and Dex exposure commenced. In addition, confluent rMSCs were treated with osteogenic medium for 7 days to induce osteogenic differentiation, prior to exposure to mitogen and Dex.

To fully activate the genomic responses of Dex, cells were pre-treated with 1 µM Dex for 1h prior to mitogenic stimulation with 5% FBS (naïve rMSCs) and 20% FBS (preosteoblasts) for 5 minutes, 30 minutes, 2 hours and 4 hours, after which whole cell protein lysates were prepared. The short time periods (5 minutes and 30 minutes) represented peak ERK1/2 activity, whereas the longer time (2 hr and 4 hr) points represented the shoulder of ERK1/2 activity. MKP-1 levels from non-stimulated cells were examined utilising 1% FBS and osteogenic medium as negative controls, which were designated as t0.

In order to determine MKP-1 protein levels, MKP-1 densitometry data were normalised to both total ERK1/2 isoforms. Findings showed that in naïve rMSCs, Dex caused a slight, although not statistically significant, increase in MKP-1 protein expression levels compared to the 5% FBS treatment, irrespective of the ERK1/2 isoform used for normalisation. This increase occurred at 30 minutes after mitogenic exposure (hence 1 hour and 30 minutes exposure to Dex) and continued up to 4 hours (that is 5 hours exposure to Dex; Fig. 7.5 A). In contrast, MKP-1 protein abundance was elevated after 2 hours of mitogenic stimulation (that is 3h of Dex exposure) and lasted up to 4 hours in preosteoblasts (Fig. 7.5 B). In addition, Dex did not have a major effect after 5 minutes of mitogenic stimulation in either cell type (Fig. 7.5). A three-way ANOVA analysis showed that Dex has no statistical effect ($P<0.9$ for both total ERK1 and total ERK2) on mitogen-stimulated MKP-1 protein expression in naïve rMSCs and preosteoblasts.

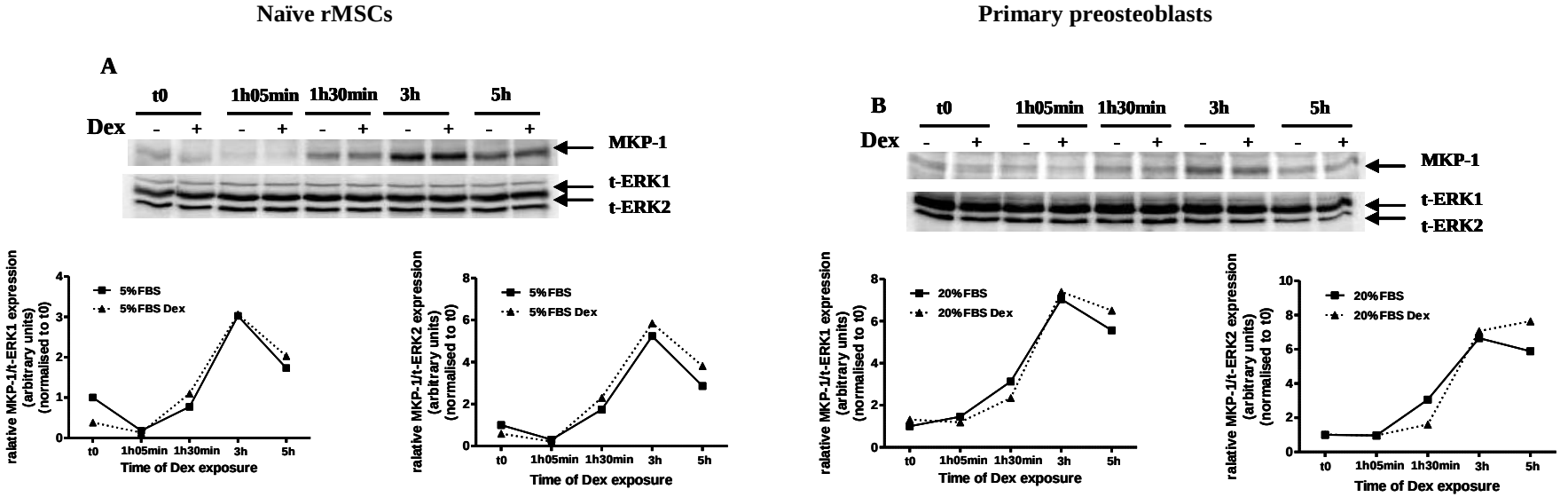

Figure 7.5: FBS and Dex increases the MKP-1 protein abundance in naïve rMSCs and preosteoblasts.

(**A**) Naïve rMSCs were grown until 80% confluent and serum starved in 1% FBS for 24 hrs. Cells were pre-treated with 1 µM Dex for 1 hr prior to mitogenic stimulation with 5% FBS or (**B**) Confluent rMSCs were induced to differentiate into preosteoblasts using osteogenic medium. After 7 days of culturing in OM, preosteoblasts were pre-treated with 1 µM Dex before exposure to 20% FBS as mitogenic stimulation. Cell lysates (as outlined in Materials and Methods, Section 2.2.8.1) were prepared at t0, 5', 30', 2 hrs and 4hrs after mitogen administration. An amount of 80 µg of total proteins was resolved by SDS PAGE and proteins were subsequently transferred onto a PVDF membrane. The level of MKP-1 protein was determined by using anti-MKP-1 antibodies. To ensure equal protein loading, membranes were stripped using 0.2 N NaOH and reprobed with anti-total ERK1/2 antibodies. Immuno-responsive bands were visualised using the LumiGLO reserve chemiluminescent substrate kit from KPL laboratories (Gaithersburg, Maryland, USA). For densitometry, blots were photographed using a ChemiDoc Universal Hood II imager (Bio-Rad, CA, USA). Quantification of MKP-1 and t-ERK1/2 protein levels was performed utilising the Quantity One® software from Bio-Rad (Ca, USA). A representative blot of at least four experimental repeats is shown. Each repeat experiment represents an individual animal. Similar trends were observed between repeat experiments. Results are expressed as ratios of MKP-1 integrated intensity/tERK1 and MKP-1 integrated intensity/tERK2. A three-way ANOVA was done to determine the effect of Dex over a time span of 5 hours on mitogen-induced MKP-1 expression and statistical significance was considered at ($P<0.05$). This analysis was adjusted for the four individual experiments. Data is expressed in arbitrary units which was normalised to the time points specified on the respective graphs and set at 1.

7.3 Discussion

The purpose of this work was to determine if protein tyrosine phosphatase (PTP) expression and activity may play a role in the Dex modulation of mitogen-induced proliferation resulting from ERK1/2 activation. It has previously been found that preosteoblast proliferation evoked by mitogens was mainly regulated by the ERK1/2 pathway in immortalised osteoblastic cell lines (Hulley et al., 1998; Horsch et al., 2007). This MAPK signalling cascade is regulated by phosphorylation (Marshall, 1995; Ebisuya et al., 2005), with activation of the ERK1/2 protein being via kinase-mediated phosphorylation, whereas inactivation arises from dephosphorylation executed by phosphatases (Hunter, 1995; Keyse, 2000; Saxena and Mustelin, 2000; Keyse, 2008b).

ERK1/2 dephosphorylation and therefore, inactivation, is regulated by two types of phosphatases: Serine/Threonine (Ser/Thr) phosphatases, which remove phosphates from serine and threonine residues, and Protein Tyrosine Phosphatases (PTPs) which dephosphorylate tyrosine residues. An *in vitro* phosphatase assay based on pNPP hydrolysis to *p*-nitrophenol was used to measure total phosphatase activity. A substantial amount of *p*-nitrophenol, the hydrolysis product of phosphatase activity, was detected under basal (1% FBS) and mitogenic (5% FBS) conditions (Fig. 7.1 A), indicating that there is phosphatase activity under these conditions in rMSCs. Moreover, following Dex exposure of rMSCs under basal and growth factor stimulated conditions, a significant additional increase in phosphatase activity was observed (Fig.7.1 A). This result suggests the presence of Dex-inducible phosphatases (proteins) under these conditions. Furthermore, the amount of 150 µg of total protein lysate was determined to be the optimal concentration to use in this assay before the reaction becomes limiting (Fig. 7.1 A).

The protein tyrosine phosphatase inhibitor, vanadate (sodium orthovanadate), was used to determine the proportion of protein tyrosine phosphatases active after mitogen and concomitant mitogen and Dex exposure in rMSCs and preosteoblasts (Fig. 7.1 C and D). The concentrations of vanadate used in the *in vitro* phosphatase assay were either high (10 mM) or moderate (1 mM). Higher concentrations of vanadate was used in the *in vitro* phosphatase assays to ensure efficient inhibition of PTPs, because unlike proliferation assays where high doses were toxic to osteoblast precursor cells, the phosphatase assay used cell lysates and cytotoxic effects are irrelevant (Fig. 7.2 A and D). It was found that 10 mM vanadate effectively prevented the formation of *p-nitrophenol* in naïve rMSCs and preosteoblasts, thereby suggesting that phosphatase activity in these cell types after mitogenic stimulation, as well as after Dex exposure, was inhibited (Fig. 7.1 B and C). In addition, 1 mM vanadate inhibited approximately 50% of phosphatase activity under both basal and

mitogenic conditions, in naïve rMSCs and preosteoblasts (Fig. 7.1 B and C). These results indicate that vanadate-sensitive phosphatases are present and active in rMSCs and preosteoblasts under these conditions and that a large proportion of these phosphatases are protein tyrosine phosphatases. This result is in accordance with the findings of Engelbrecht et al. (2003), where vanadate inhibited up to 70% of cytosolic phosphatases in fast growing immortalised MBA 15.4 preosteoblasts, thereby indicating that PTPs are the main active phosphatase group in these cells.

Table 7.1: Dex inhibition of naïve rMSCs and preosteoblasts proliferation rescue by vanadate.

Cell Type	Cell Culture Conditions	% Dex inhibition compared to control	% VO_4 rescue compared to control
Naïve rMSCs	1% FBS/ 1 nM Dex	65 %	110 %
	1% FBS/ 5 nM Dex	76 %	46 %
	5% FBS/ 1 nM Dex	57 %	18 %
	5% FBS/ 5 nM Dex	38 %	16 %
Preosteoblasts	Ost/ 1 µM Dex	37 %	44%
	20% FBS/ Ost/ 1 µM Dex	75 %	21 %

Osteoblast precursor proliferation elicited by mitogens is attenuated by Dex in immortalised cells (Hulley et al., 1998; Engelbrecht et al., 2003). This reduction in proliferation was linked to increased inactivation of ERK1/2 via dephosphorylation by protein tyrosine phosphatases (PTPs) (Engelbrecht et al., 2003; Horsch et al., 2007). It was therefore hypothesised that by inhibiting PTP activity using vanadate, the attenuation of rMSC and primary preosteoblast growth factor-stimulated proliferation by Dex may be lifted. The percentages of Dex inhibition on the proliferation in naïve rMSCs and preosteoblasts together with the percentage vanadate rescue are shown in Table 7.1. It was found that vanadate significantly, though not necessarily totally, reversed the Dex-induced inhibition of proliferation in naïve rMSCs and preosteoblasts (Fig. 7.2 and Table 7.1). The largest percentage recovery by vanadate (110%) was seen when Dex inhibition of the proliferation of naïve rMSCs was restored by 65%. Moreover, 1 µM vanadate was shown to elicit a proliferative response compared to basal growth controls in both rMSCs and preosteoblasts, which might account for the ‘rescued’ proliferation exerted by vanadate (Fig. 7.2). Closer investigation into the resulting proliferative response by vanadate revealed that this response was dependent on ERK1/2, since U0126 abolished naïve rMSCs proliferation after 1 µM vanadate under basal and mitogenic conditions (Fig. 7.3.1). Moreover, when the effect of vanadate on the activation of ERK1/2 was investigated, a characteristic proliferative ERK1/2 activation pattern was obtained in rMSCs (Fig. 7.3.2).

It was previously found that Dex up-regulated the mRNA and protein expression of the dual-specificity MAPK phosphatase, MKP-1 in human and mouse immortalised osteoblast cell lines (Engelbrecht et al., 2003; Horsch et al., 2007). The importance of MKP-1 in the negative regulation of mitogen-induced osteoblast proliferation and concurrent ERK activation was illustrated by Horsch et al. (2007): this investigation showed that MKP-1 is an exclusive Dex-inducible PTP, which is capable of preferentially dephosphorylating ERK1/2 in MBA 15.4 and MG-63 cell lines (Horsch et al., 2007). Moreover, it was found that overexpression of MKP-1 not only leads to ERK1/2 dephosphorylation, but also inhibits osteoblast proliferation (Horsch et al., 2007). Additionally, in human MG-63 preosteoblasts, knock-down of MKP-1 blocked Dex-stimulated ERK1/2 dephosphorylation (Horsch et al., 2007); therefore the abundance of MKP-1 mRNA and protein after mitogen and Dex exposure was examined to compare the effect of Dex on MKP-1 expression in naïve rMSCs and preosteoblasts.

In rMSCs, both Dex and 5% FBS caused a significant increase in MKP-1 mRNA at 30 minutes (Fig. 7.4.1 A and B). This early mRNA induction is in accordance with the postulation that MKP-1 is an immediate early gene (Kwak and Dixon, 1995; Brondello et al., 1997; Brondello et al., 1999). Moreover, a significant decline in the abundance of MKP-1 mRNA was observed after 1 h, to near basal levels at 8 hours for both mitogen –and –Dex stimulation in rMSCs (Fig. 7.4.2 A and B). However, when the net effect of Dex on MKP-1 mRNA expression was determined by subtracting the 5% FBS from the 5% FBS + 1 µM Dex response, that is $[MKP\text{-}1]_{5\%\ FBS+Dex}$ - $[MKP\text{-}1]_{5\%\ FBS,}$ it was observed that MKP-1 mRNA was significantly elevated at 1h after exposure of Dex (Fig. 7.4.1 C). MKP-1 mRNA levels peaked 2 hours after Dex administration, after which a steady decline was observed up to 8 hours (Fig. 7.4.1 C). Similarly to rMSCs, MKP-1 mRNA was also increased at 30 minutes after 20% FBS mitogenic stimulation, as well as after concurrent Dex and mitogen treatment in preosteoblasts (Fig. 7.4.2 A and B). Yet, the net effect of Dex on MKP-1 mRNA in preosteoblasts was different to that in rMSCs (Fig. 7.4.2 C). Although MKP-1 mRNA levels were raised at 1hr, a significant increase compared to controls was only seen 2 hours after Dex administration in preosteoblasts (Fig. 7.4.2 C). These results suggest that the Dex regulation of MKP-1 mRNA expression in rMSCs and preosteoblasts is temporally different. Moreover, these results are in agreement with the findings of Engelbrecht et al. (2003), where MKP-1 mRNA was elevated at 30 minutes post-Dex administration and is expressed up to 24 hours in mouse and human immortalised preosteoblast cell lines.

The effect of Dex on MKP-1 protein expression was subsequently examined. rMSCs and preosteoblasts were pre-treated for 1 hr with 1 µM Dex to induce the genomic response elicited by

Dex, giving time for protein expression. MKP-1 protein levels were normalised to both isoforms of total ERK1/2 and similar induction patterns were obtained regardless of the ERK1/2 isoform used for normalisation, in naïve rMSCs and preosteoblasts (Fig. 7.5 A and B). Results showed that, similarly to the mRNA levels, MKP-1 protein expression was induced by both FBS and Dex in rMSCs as well as preosteoblasts, reaching peak levels at 3 hours post Dex exposure (Fig. 7.5 A and B). In rMSCs, Dex exposure caused a slight raise in MKP-1 protein levels after 1 hour and 30 minutes compared to 5% FBS (Fig. 7.5 A). However, there was no significant difference between 5% FBS and 5% FBS + Dex at any time point again. A similar expression profile was elicited by Dex in preosteoblasts and maximum expression only occurred at 3 hours (Fig. 7.5 B).

As expected there is a lag between MKP-1 mRNA and protein expression elicited by Dex (Fig. 7.4.1; Fig 7.4.2 and Fig. 7.5). In naïve rMSCs, Dex caused a gradual increase in MKP-1 mRNA, which peaked at 2 hours and drastically declined to below baseline levels after 4 hours (Fig. 7.4.1 C), whereas protein expression reached maximal levels at 3 hours, declining sharply after 6 hours (Fig. 7.5). Consequently, it is likely that Dex regulates MKP-1 expression through transcriptional mechanisms.

The MKP-1 protein induction pattern of Dex did not differ from that elicited by 5% FBS, with the expected Dex-induced MKP-1 protein levels not being more pronounced compared to the 5% FBS stimulation in naïve rMSCs. One possible explanation for this phenomenon is that Dex not only enhances the protein synthesis but also the degradation of the MKP-1 protein. The MKP-1 protein is normally swiftly degraded by the 26S proteasome and consequently MKP-1 has been designated as a high turnover protein (Brondello et al., 1997). Inhibition of proteosomal degradation increased MKP-1 protein levels by 10 to 20 fold in human and mouse preosteoblasts (Engelbrecht et al., 2003) and these more stable proteins then lead to better detection. Moreover, phosphorylation of MKP-1 on Ser^{359} and Ser^{364} increases protein stability (Brondello et al., 1995; Brondello et al., 1999) and it is thus likely that MKP-1 phosphorylation is attenuated by Dex. Indeed, MKP-1 is a target of ERK1/2 phosphorylation (Brondello et al., 1995; Brondello et al., 1999). Since ERK1/2 activation is inhibited by Dex, especially the shoulder activity (after 1 hour) (Fig. 6.5.1), this could explain the lack of MKP-1 protein detection in naïve rMSCs after 1 hour of pre-incubation with Dex (Fig. 7.5 A). Moreover, a sharp decline in MKP-1 protein levels was also seen after 3 hours, which corresponds to the decrease in ERK1/2 shoulder activity (Fig. 6.5.1).

Similar Dex-induced MKP-1 mRNA and protein expression profiles were obtained for preosteoblasts compared to that of naïve rMSCs (Fig. 7.5). In comparison to naïve rMSCs, Dex

rapidly induced MKP-1 mRNA in preosteoblasts, with peak levels seen after 1 hour and then gradually declining. Peak MKP-1 protein was also exhibited after 3 hours of Dex stimulation, which sharply decreased up to 6 hours (Fig. 7.5 B). Even though a slightly dissimilar mRNA expression profile was obtained for preosteoblasts in comparison to naïve rMSCs, the discrepancy between mRNA and protein expression could also be attributed to post-transcriptional mechanisms and protein instability.

The elucidation of a possible role for MKP-1 in the GC regulation of the proliferation of naïve rMSCs and preosteoblasts using specific pharmacological MKP-1 inhibitors such as sanguinarine chloride and triptolide was attempted (data not shown). Low concentrations (1 nM to 5 nM) of sanguinarine chloride and triptolide did not have any effects on basal and mitogen-induced proliferation in naïve rMSCs and preosteoblasts. Contrary to this, both these MKP-1 inhibitors were extremely toxic to naïve rMSCs and preosteoblasts above these concentrations resulting in extensive cell death (data not shown).

In summary, the vanadate inhibition studies revealed that PTPs are involved in the Dex regulation of mitogen-induced proliferation in naïve rMSCs and preosteoblasts. MKP-1 was identified as the likely candidate in immortalised preosteoblast cell lines. Therefore, the expression of MKP-1 mRNA and protein was examined in naïve rMSCs and preosteoblasts. Ultimately, no difference in protein expression elicited by mitogens and Dex was observed in both cell types. It is thus probable that MKP-1 does not mediate the Dex-induced decrease in rMSCs-and preosteoblast proliferation. However, MKP-1 is a high turnover protein and the true effect of Dex on MKP-1 protein expression needs to be determined by using proteosomal inhibitors to prevent protein breakdown. Furthermore, it appears that the negative effects of Dex on rMSC and preosteoblast proliferation could also be regulated by another PTP/s.

Chapter 8

Conclusion and Future Work

The rMSC experimental model used in this study is unique. These naïve stromal cells can be differentiated into preosteoblasts and can effectively be used to study the effects of GCs on early osteoblast precursor cell proliferation.

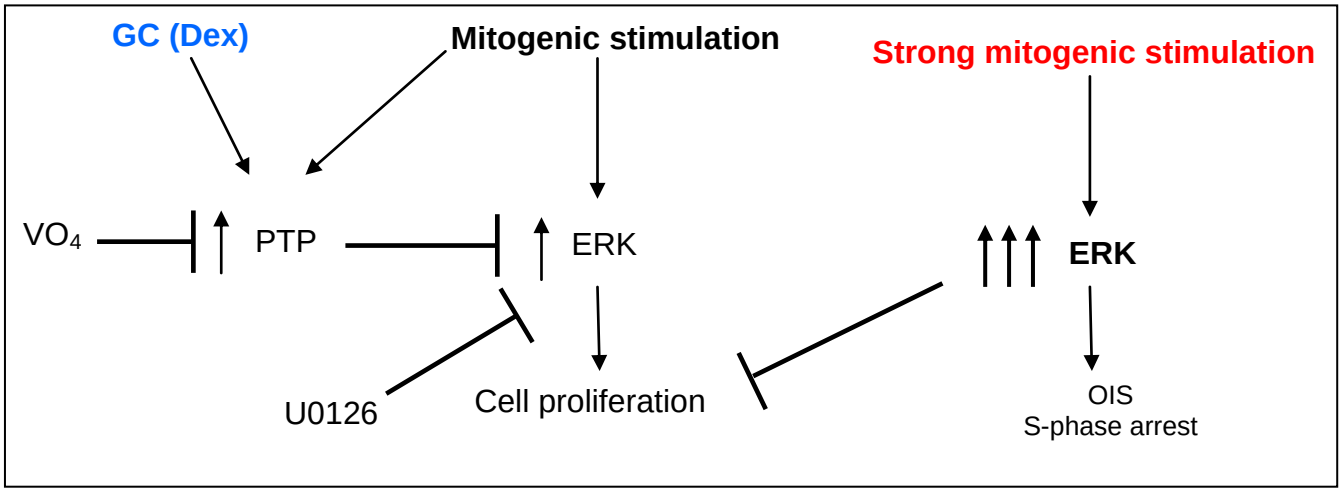

Figure 8.1: Proposed model for the Dex regulation of mitogen-induced proliferation in naïve rMSCs and preosteoblasts. Arrows depict activation and blunt arrows specify inhibition.

A proposed mechanism of action for the GC regulation of naïve rMSCs and preosteoblast proliferation is depicted in Fig. 8.1. Moderate concentrations of mitogens, such as 5% FBS and 10% FBS, led to cell proliferation in naïve rMSCs and preosteoblasts, whereas high concentration of 20% FBS was observed to be predominantly mitogenic in preosteoblasts. The ERK1/2 signalling pathway was found to be integrally involved in the regulation of mitogen-induced proliferation in rMSCs and preosteoblasts, as cell proliferation was effectively blocked by U0126 and mitogen-induced proliferation coincided with the activation of the ERK1/2 mitogenic pathway in both cell types. However, strong mitogenic stimulation of naïve rMSCs resulted in inhibition of proliferation, possibly due to oncogene-induced senescence (OIS) and led to hyperactivation of ERK1/2, which is a hallmark of OIS. In addition, two cell populations were identified in the rMSCs preparations after incubation in 20% FBS and it is likely that the smaller population of cells with condensed chromatin were undergoing OIS. In order to circumvent the possible occurrence of senescent cells in the initial stage of MSC preparation, isolation could in future be performed using 5% FBS or 10% FBS instead of 20% FBS. Alternatively, cells that were expanded in culture medium

containing 20% FBS could be sorted according to size and granularity using FACS before being subcultured into higher cell passages or commencement of experiments.

After rMSC isolation, pharmacological doses of GCs administered to naïve cells and preosteoblasts caused a drastic decrease in mitogen-induced proliferation. It was hypothesised that a possible molecular mechanism for this GC action could be that Dex hinders naïve rMSC and preosteoblast proliferation by inhibiting the mitogen-induced activation of ERK1/2, through the function of MKP-1. The presence of Dex-inducible phosphatases under basal and mitogenic conditions was demonstrated, the majority of which were likely to be PTPs, since VO_4 inhibited a considerable fraction of the phosphatase activities under these conditions. Vanadate marginally rescued the Dex-inhibition of mitogen-induced osteoblast precursor cell proliferation, a response which was dependent on ERK1/2 and again suggested the involvement of PTPs in the Dex regulation of osteoblast precursor cell proliferation. Dex was shown to differentially regulate MKP-1 mRNA expression in naïve rMSCs and preosteoblasts, which increased after 30 minutes and lasted up to 2 hours in the respective cell types post Dex administration. This finding suggests that Dex could regulate MKP-1 expression through transcriptional mechanisms. Dex was then found to increase MKP-1 protein abundance after 1 and a half hours in naive rMSCs and preosteoblasts. However, contrary to expectations, Dex did not significantly increase MKP-1 protein expression above that of mitogenic stimulation. This could possibly be explained by the rapid degradation of the MKP-1 protein by the 26S proteasome, where a negative feedback loop exist between ERK1/2 and MKP-1 with MKP-1 phosphorylation by ERK1/2 stabilising the MKP-1 protein. Decreased ERK1/2 protein phosphorylation would destabilise the MKP-1 protein, rendering detection of changes in expression difficult. However, another explanation is that one or more other PTPs mediate the dephosphorylation of ERK1/2 protein after the administration of GCs, resulting in the subsequent reduction in proliferation. Interestingly, the effects of mitogen stimulation on MKP-1 mRNA and protein induction over time were not taken into account previously (Engelbrecht et al., 2003); even though it was known that MKP-1 mRNA is induced by growth factors (Charles et al., 1993; Noguchi et al., 1993; Engelbrecht et al., 2003) and hormones (Clark, 2003; Sarkozi et al., 2007; Datta et al., 2010). Engelbrecht et al (2003) only looked at a single point of MKP-1 mRNA and protein induction in immortalised MBA 15.4 preosteoblasts after stimulation with 10% FBS, which is the standard growth condition of these cells. Therefore, the effect of Dex on the mitogen-stimulated induction of MKP-1 mRNA and protein could be similar to the results in the present study, although this still needs to be determined.

Studies have shown that stimulation of mesenchymal stromal cells with mitogens such as EGF and basic FGF resulted in increased proliferation, which was linked to the activation of the ERK1/2 signalling pathway (Tamama et al., 2006; Solmesky et al., 2010). However, little is known about the mechanism of the ERK1/2 regulation in MSCs, especially protein deactivation by phosphatases. Even though MKP-1 was identified as the prime candidate for regulating ERK1/2 activity after mitogenic stimulation in the MBA 15.4 and MC3T3-E1 immortalised preosteoblast cell lines (Engelbrecht et al., 2003; Horsch et al., 2007; Datta et al., 2010), results of the present study indicate that this is not likely in naïve rMSCs and suggests the involvement of other PTPs. MKP isoforms, such as MKP-2,-3,-4 and MKP-X, have been shown to also dephosphorylate ERK1/2 (Owens and Keyse, 2007; Junttila et al., 2008; Keyse, 2008a). Moreover, MKP-2 and MKP-3 are expressed in MBA 15.4 and UMR106 osteoblastic cells (Engelbrecht et al., 2003; Homme et al., 2004), suggesting that these MKPs could potentially regulate ERK1/2 activity and osteoblast precursor cell proliferation. In addition, PTPs, such as the neuronal PTP-SL and STEP (Pulido et al., 1999; Zuniga et al., 1999) as well as the hematopoietic PTP, LC-PTP/He-PTP (Oh-hora et a., 1999; Saxena et al, 1999), are capable of dephosphorylating ERK1/2. Homologues of these tissue-specific PTPs could possibly be present in osteoblastic cells, which could then regulate ERK1/2 and thus proliferation of osteoblast precursor cells. Therefore, it is evident that redundancy exists in the PTP regulation of ERK1/2 activity and hence in osteoblast precursor cell proliferation that is modulated by GCs. This thus warrants further investigation into the molecular mechanisms employed by GCs to regulate early osteoblast proliferation.

Chapter 9

References

The reference list was compiled using Reference Manager 12 and is in accordance with the specifications of the scientific journal, Cell.

Reference List

Aarden,E.M., Burger,E.H., and Nijweide,P.J. (1994). Function of osteocytes in bone. J. Cell Biochem. *55*, 287-299.

Acampora,D., Merlo,G.R., Paleari,L., Zerega,B., Postiglione,M.P., Mantero,S., Bober,E., Barbieri,O., Simeone,A., and Levi,G. (1999). Craniofacial, vestibular and bone defects in mice lacking the Distal-less-related gene Dlx5. Development *126*, 3795-3809.

Ajubi,N.E., Klein-Nulend,J., Nijweide,P.J., Vrijheid-Lammers,T., Alblas,M.J., and Burger,E.H. (1996). Pulsating fluid flow increases prostaglandin production by cultured chicken osteocytes--a cytoskeleton-dependent process. Biochem. Biophys. Res. Commun. *225*, 62-68.

Akavia,U.D., Shur,I., Rechavi,G., and Benayahu,D. (2006). Transcriptional profiling of mesenchymal stromal cells from young and old rats in response to Dexamethasone. BMC. Genomics *7*, 95.

Albiston,A.L., Smith,R.E., Obeyesekere,V.R., and Krozowski,Z.S. (1995). Cloning of the 11 beta HSD type II enzyme from human kidney. Endocr. Res. *21*, 399-409.

Alessi,D.R., Smythe,C., and Keyse,S.M. (1993). The human CL100 gene encodes a Tyr/Thr-protein phosphatase which potently and specifically inactivates MAP kinase and suppresses its activation by oncogenic ras in Xenopus oocyte extracts. Oncogene *8*, 2015-2020.

Anderson,D.M., Maraskovsky,E., Billingsley,W.L., Dougall,W.C., Tometsko,M.E., Roux,E.R., Teepe,M.C., DuBose,R.F., Cosman,D., and Galibert,L. (1997). A homologue of the TNF receptor and its ligand enhance T-cell growth and dendritic-cell function. Nature *390*, 175-179.

Anderson,H.C. (1995). Molecular biology of matrix vesicles. Clin. Orthop. Relat Res. 266-280.

Anderson,H.C. (2003). Matrix vesicles and calcification. Curr. Rheumatol. Rep. *5*, 222-226.

Antoni,F.C. and Dayanithi,G.O.V.I. (1990). Evidence for Distinct Glucocorticoid and Guanine 3',5'-Monophosphate-Effected Inhibition of Stimulated Adrenocorticotropin Release in Vitro. Endocrinology *126*, 1355-1360.

Aronheim,A., Engelberg,D., Li,N., al-Alawi,N., Schlessinger,J., and Karin,M. (1994). Membrane targeting of the nucleotide exchange factor Sos is sufficient for activating the Ras signaling pathway. Cell *78*, 949-961.

Assoian,R.K. and Schwartz,M.A. (2001). Coordinate signaling by integrins and receptor tyrosine kinases in the regulation of G1 phase cell-cycle progression. Curr. Opin. Genet. Dev. *11*, 48-53.

Aubin,J. and Liu,F. (1996). The osteoblast lineage. In Principles of Bone Biology, J.P.Bilezikian, L.G.Raisz, and G.A.Rodan, eds. (New York: Academic Press), pp. 51-67.

Aubin,J.E. (1998). Advances in the osteoblast lineage. Biochem. Cell Biol. *76*, 899-910.

Aubin,J.E. (2001). Regulation of osteoblast formation and function. Rev. Endocr. Metab Disord. *2*, 81-94.

Aubin,J.E. and Triffitt,J.T. (2002). Mesenchymal stem cells and the osteoblast lineage. In Principles of Bone Biology, J.P.Bilezikian, L.G.Raisz, and G.A.Rodan, eds. (New York: Academic Press), pp. 59-81.

Avruch,J., Zhang,X.F., and Kyriakis,J.M. (1994). Raf meets Ras: completing the framework of a signal transduction pathway. Trends Biochem. Sci. *19*, 279-283.

Axelford,L. (2001). Corticosteroid Therapy. In Principles and Practice of Endocrinology and Metabolism, K.C.Becker, ed. (Philadelphia: Lippincott Williams and Wilkins), pp. 751-764.

Balcerzak,M., Hamade,E., Zhang,L., Pikula,S., Azzar,G., Radisson,J., Bandorowicz-Pikula,J., and Buchet,R. (2003). The roles of annexins and alkaline phosphatase in mineralization process. Acta Biochim. Pol. *50*, 1019-1038.

Balmanno,K. and Cook,S.J. (1999). Sustained MAP kinase activation is required for the expression of cyclin D1, p21Cip1 and a subset of AP-1 proteins in CCL39 cells. Oncogene *18*, 3085-3097.

Barberis,L., Wary,K.K., Fiucci,G., Liu,F., Hirsch,E., Brancaccio,M., Altruda,F., Tarone,G., and Giancotti,F.G. (2000). Distinct roles of the adaptor protein Shc and focal adhesion kinase in integrin signaling to ERK. J Biol. Chem. *275*, 36532-36540.

Baron,R. (1995). Molecular mechanisms of bone resorption. An update. Acta Orthop. Scand. Suppl *266*, 66-70.

Baud,C.A. (1968). [Structure and functions of osteocytes in normal conditions and under the influence of parathyroid extract]. Schweiz. Med. Wochenschr. *98*, 717-720.

Baxter,J.D. (2000). Advances in glucocorticoid therapy. Adv. Intern. Med. *45*, 317-349.

Bellows,C.G., Heersche,J.N., and Aubin,J.E. (1990). Determination of the capacity for proliferation and differentiation of osteoprogenitor cells in the presence and absence of dexamethasone. Dev. Biol. *140*, 132-138.

Beloti,M.M. and Rosa,A.L. (2005). Osteoblast differentiation of human bone marrow cells under continuous and discontinuous treatment with dexamethasone. Braz. Dent. J. *16*, 156-161.

Ben-Yehoyada,M., Gautier,J., and Dupre,A. (2007). The DNA damage response during an unperturbed S-phase. DNA Repair (Amst) *6*, 914-922.

Berry,D.L., Bracken,W.M., Fischer,S.M., Viaje,A., and Slaga,T.J. (1978). Metabolic conversion of 12-O-tetradecanoylphorbol-13-acetate in adult and newborn mouse skin and mouse liver microsomes. Cancer Res. *38*, 2301-2306.

Betsholtz,C., Johnsson,A., Heldin,C.H., Westermark,B., Lind,P., Urdea,M.S., Eddy,R., Shows,T.B., Philpott,K., Mellor,A.L., and . (1986). cDNA sequence and chromosomal localization of human platelet-derived growth factor A-chain and its expression in tumour cell lines. Nature *320*, 695-699.

Bodine,P.V., Zhao,W., Kharode,Y.P., Bex,F.J., Lambert,A.J., Goad,M.B., Gaur,T., Stein,G.S., Lian,J.B., and Komm,B.S. (2004). The Wnt antagonist secreted frizzled-related protein-1 is a negative regulator of trabecular bone formation in adult mice. Mol. Endocrinol. *18*, 1222-1237.

Boivin,G., Farlay,D., Bala,Y., Doublier,A., Meunier,P.J., and Delmas,P.D. (2009). Influence of remodeling on the mineralization of bone tissue. Osteoporos. Int. *20*, 1023-1026.

Boling,E.P. (2004). Secondary osteoporosis: underlying disease and the risk for glucocorticoid-induced osteoporosis. Clin. Ther. *26*, 1-14.

Bonewald,L.F. (1999). Establishment and characterization of an osteocyte-like cell line, MLO-Y4. J. Bone Miner. Metab *17*, 61-65.

Boquest,A.C., Shahdadfar,A., Brinchmann,J.E., and Collas,P. (2006). Isolation of stromal stem cells from human adipose tissue. Methods Mol. Biol. *325*, 35-46.

Bouvier,M., Collins,S., O'Dowd,B.F., Campbell,P.T., de,B.A., Kobilka,B.K., MacGregor,C., Irons,G.P., Caron,M.G., and Lefkowitz,R.J. (1989). Two distinct pathways for cAMP-mediated down-regulation of the beta 2-adrenergic receptor. Phosphorylation of the receptor and regulation of its mRNA level. J. Biol. Chem. *264*, 16786-16792.

Bouxsein,M.L. and Seeman,E. (2009). Quantifying the material and structural determinants of bone strength. Best. Pract. Res. Clin. Rheumatol. *23*, 741-753.

Boyan,B.D., Schwartz,Z., and Swain,L.D. (1990). Matrix vesicles as a marker of endochondral ossification. Connect. Tissue Res. *24*, 67-75.

Bradford,M.M. (1976). A rapid and sensitive method for the quantitation of microgram quantities of protein utilizing the principle of protein-dye binding. Anal. Biochem. *72*, 248-254.

Brar,S.S., Kennedy,T.P., Whorton,A.R., Murphy,T.M., Chitano,P., and Hoidal,J.R. (1999). Requirement for Reactive Oxygen Species in Serum-induced and Platelet-derived Growth Factor-induced Growth of Airway Smooth Muscle. Journal of Biological Chemistry *274*, 20017-20026.

Bringhurst,F.R. and Strewler,G.J. (2002). Renal and skeletal actions of parathyroid hormone (PTH) and PTH-related protein. In Principle of Bone Biology, J.P.Bilezikian, L.G.Raisz, and G.A.Rodan, eds. (San Diego: Academic Press), pp. 483-514.

Brondello,J.M., Brunet,A., Pouyssegur,J., and McKenzie,F.R. (1997). The dual specificity mitogen-activated protein kinase phosphatase-1 and -2 are induced by the p42/p44MAPK cascade. J. Biol. Chem. *272*, 1368-1376.

Brondello,J.M., Pouyssegur,J., and McKenzie,F.R. (1999). Reduced MAP kinase phosphatase-1 degradation after p42/p44MAPK-dependent phosphorylation. Science *286*, 2514-2517.

Brotherick,I., Robson,C.N., Browell,D.A., Shenfine,J., White,M.D., Cunliffe,W.J., Shenton,B.K., Egan,M., Webb,L.A., Lunt,L.G., Young,J.R., and Higgs,M.J. (1998). Cytokeratin expression in breast cancer: phenotypic changes associated with disease progression. Cytometry *32*, 301-308.

Brunet,A., Roux,D., Lenormand,P., Dowd,S., Keyse,S., and Pouyssegur,J. (1999). Nuclear translocation of p42/p44 mitogen-activated protein kinase is required for growth factor-induced gene expression and cell cycle entry. EMBO J *18*, 664-674.

Brunner,D., Frank,J., Appl,H., Schoffl,H., Pfaller,W., and Gstraunthaler,G. (2010). Serum-free cell culture: the serum-free media interactive online database. ALTEX. *27*, 53-62.

Buday,L. and Downward,J. (1993). Epidermal growth factor regulates p21ras through the formation of a complex of receptor, Grb2 adapter protein, and Sos nucleotide exchange factor. Cell *73*, 611-620.

Bueno E and Glowacki,J. (2011). Structure and Function of Bone and Cartilage Tissue. In Biological Foundations for Skeletal Tissue Engineering., Athanasiou K, ed. (California: Morgan and Claypool Publishers), pp. 3-39.

Buenzli,P.R., Pivonka,P., and Smith,D.W. (2010). Spatio-temporal structure of cell distribution in cortical Bone Multicellular Units: A mathematical model. Bone.

Burger,E.H. and Klein-Nulend,J. (1999). Mechanotransduction in bone--role of the lacuno-canalicular network. FASEB J. *13 Suppl*, S101-S112.

Burgess,T.L., Qian,Y., Kaufman,S., Ring,B.D., Van,G., Capparelli,C., Kelley,M., Hsu,H., Boyle,W.J., Dunstan,C.R., Hu,S., and Lacey,D.L. (1999). The ligand for osteoprotegerin (OPGL) directly activates mature osteoclasts. J. Cell Biol. *145*, 527-538.

Buttgereit,F., Brand,M.D., and Burmester,G.R. (1999). Equivalent doses and relative drug potencies for non-genomic glucocorticoid effects: a novel glucocorticoid hierarchy. Biochem. Pharmacol. *58*, 363-368.

Caelles,C., Bruna,A., Morales,M., Gonzalez-Sancho,J.M., Gonzalez,M.V., Jimenez,B., and Munoz,A. (2002). Glucocorticoid receptor antagonism of AP-1 activity by inhibition of MAPK family. Ernst. Schering. Res. Found. Workshop 131-152.

Caelles,C., Gonzalez-Sancho,J.M., and Munoz,A. (1997). Nuclear hormone receptor antagonism with AP-1 by inhibition of the JNK pathway. Genes Dev. *11*, 3351-3364.

Campisi,J. (2001). Cellular senescence as a tumor-suppressor mechanism. Trends Cell Biol. *11*, S27-S31.

Canalis,E. (1996). Clinical review 83: Mechanisms of glucocorticoid action in bone: implications to glucocorticoid-induced osteoporosis. J. Clin. Endocrinol. Metab *81*, 3441-3447.

Canalis,E. (2005). Mechanisms of glucocorticoid action in bone. Curr. Osteoporos. Rep. *3*, 98-102.

Canalis,E. and Giustina,A. (2001). Glucocorticoid-induced osteoporosis: summary of a workshop. J. Clin. Endocrinol. Metab *86*, 5681-5685.

Canalis,E. and Rydziel,S. (2002). Platelet-derived growth factor and the skeleton. In Principles of Bone Biology., J.P.Bilezikian, L.G.Raisz, and G.A.Rodan, eds. (San Diego: Academic Press), pp. 817-824.

Canalis,E., Bilezikian,J.P., Angeli,A., and Giustina,A. (2004). Perspectives on glucocorticoid-induced osteoporosis. Bone *34*, 593-598.

Canalis,E., Mazziotti,G., Giustina,A., and Bilezikian,J.P. (2007). Glucocorticoid-induced osteoporosis: pathophysiology and therapy. Osteoporos. Int. *18*, 1319-1328.

Candeliere,G.A., Rao,Y., Floh,A., Sandler,S.D., and Aubin,J.E. (1999). cDNA fingerprinting of osteoprogenitor cells to isolate differentiation stage-specific genes. Nucleic Acids Res. *27*, 1079-1083.

Cappellen,D., Luong-Nguyen,N.H., Bongiovanni,S., Grenet,O., Wanke,C., and Susa,M. (2002). Transcriptional program of mouse osteoclast differentiation governed by the macrophage colony-stimulating factor and the ligand for the receptor activator of NFkappa B. J. Biol. Chem. *277*, 21971-21982.

Casals-Casas,C., +ülvarez,E., Serra,M., de la Torre,C., Farrera,C., S+ínchez-Till+¦,E., Caelles,C., Lloberas,J., and Celada,A. (2009). CREB and AP-1 activation regulates MKP-1 induction by LPS or M-CSF and their kinetics correlate with macrophage activation versus proliferation. Eur. J. Immunol. *39*, 1902-1913.

Cato,A.C.B., Nestl,A., and Mink,S. (2002). Rapid Actions of Steroid Receptors in Cellular Signaling Pathways. Sci. STKE .

Cave,M.D. (1966). Incorporation of tritium-labeled thymidine and lysine into chromosomes of cultured human leukocytes. J. Cell Biol. *29*, 209-222.

Cesarone,C.F., Bolognesi,C., and Santi,L. (1979). Improved microfluorometric DNA determination in biological material using 33258 Hoechst. Anal. Biochem. *100*, 188-197.

Chae,H.J., Kang,J.S., Han,J.I., Bang,B.G., Chae,S.W., Kim,K.W., Kim,H.M., and Kim,H.R. (2000). Production of hydrogen peroxide by serum and its involvement in cell proliferation in ROS 17/2.8 osteoblasts. Immunopharmacol. Immunotoxicol. *22*, 317-337.

Chambard,J.C., Lefloch,R., Pouyssegur,J., and Lenormand,P. (2007). ERK implication in cell cycle regulation. Biochim. Biophys. Acta *1773*, 1299-1310.

Chang,P.L., Blair,H.C., Zhao,X., Chien,Y.W., Chen,D., Tilden,A.B., Chang,Z., Cao,X., Faye-Petersen,O.M., and Hicks,P. (2006). Comparison of fetal and adult marrow stromal cells in osteogenesis with and without glucocorticoids. Connect. Tissue Res. *47*, 67-76.

Chang,P.L., Blair,H.C., Zhao,X., Chien,Y.W., Chen,D., Tilden,A.B., Chang,Z., Cao,X., Faye-Petersen,O.M., and Hicks,P. (2006). Comparison of fetal and adult marrow stromal cells in osteogenesis with and without glucocorticoids. Connect. Tissue Res. *47*, 67-76.

Chang,S.F., Chang,T.K., Peng,H.H., Yeh,Y.T., Lee,D.Y., Yeh,C.R., Zhou,J., Cheng,C.K., Chang,C.A., and Chiu,J.J. (2009). BMP-4 induction of arrest and differentiation of osteoblast-like cells via p21 CIP1 and p27 KIP1 regulation. Mol. Endocrinol. *23*, 1827-1838.

Charles,C.H., Sun,H., Lau,L.F., and Tonks,N.K. (1993). The growth factor-inducible immediate-early gene 3CH134 encodes a protein-tyrosine-phosphatase. Proc. Natl. Acad. Sci. U. S. A *90*, 5292-5296.

Chaudhary,L.R. and Avioli,L.V. (2000). Extracellular-signal regulated kinase signaling pathway mediates downregulation of type I procollagen gene expression by FGF-2, PDGF-BB, and okadaic acid in osteoblastic cells. J Cell Biochem. *76*, 354-359.

Chavassieux,P., Pastoureau,P., Chapuy,M.C., Delmas,P.D., and Meunier,P.J. (1993). Glucocorticoid-induced inhibition of osteoblastic bone formation in ewes: a biochemical and histomorphometric study. Osteoporos. Int. *3*, 97-102.

Chen,Q. and Ames,B.N. (1994). Senescence-like growth arrest induced by hydrogen peroxide in human diploid fibroblast F65 cells. Proceedings of the National Academy of Sciences of the United States of America *91*, 4130-4134.

Chen,Y.Z. and Qiu,J. (1999). Pleiotropic signaling pathways in rapid, nongenomic action of glucocorticoid. Mol. Cell Biol. Res. Commun. *2*, 145-149.

Cheng,S.L., Yang,J.W., Rifas,L., Zhang,S.F., and Avioli,L.V. (1994). Differentiation of human bone marrow osteogenic stromal cells in vitro: induction of the osteoblast phenotype by dexamethasone. Endocrinology *134*, 277-286.

Chevalley,T., Strong,D.D., Mohan,S., Baylink,D., and Linkhart,T.A. (1996). Evidence for a role for insulin-like growth factor binding proteins in glucocorticoid inhibition of normal human osteoblast-like cell proliferation. Eur. J. Endocrinol. *134*, 591-601.

Chien,H.H., Lin,W.L., and Cho,M.I. (2000). Down-regulation of osteoblastic cell differentiation by epidermal growth factor receptor. Calcif. Tissue Int. *67*, 141-150.

Chrousos,G.P. (1995). The hypothalamic-pituitary-adrenal axis and immune-mediated inflammation. N. Engl. J. Med. *332*, 1351-1362.

Chrousos,G.P. and Kino,T. (2009). Glucocorticoid signaling in the cell. Expanding clinical implications to complex human behavioral and somatic disorders. Ann. N. Y. Acad. Sci. *1179*, 153-166.

Chu,Y., Solski,P.A., Khosravi-Far,R., Der,C.J., and Kelly,K. (1996). The mitogen-activated protein kinase phosphatases PAC1, MKP-1, and MKP-2 have unique substrate specificities and reduced activity in vivo toward the ERK2 sevenmaker mutation. J. Biol. Chem. *271*, 6497-6501.

Clark,A.J., STEWART,M.F., LAVENDER,P.M., FARRELL,W., CROSBY,S.R., REES,L.H., and WHITE,A. (1990). Defective glucocorticoid regulation of proopiomelanocortin gene expression and peptide secretion in a small cell lung cancer cell line. J Clin Endocrinol Metab *70*, 485-490.

Clark,A.R. (2003). MAP kinase phosphatase 1: a novel mediator of biological effects of glucocorticoids? J Endocrinol. *178*, 5-12.

Clarke,B. (2008). Normal bone anatomy and physiology. Clin. J. Am. Soc. Nephrol. *3 Suppl 3*, S131-S139.

Cohen,D. and Adachi,J.D. (2004). The treatment of glucocorticoid-induced osteoporosis. J. Steroid Biochem. Mol. Biol. *88*, 337-349.

Coleman,M.L., Marshall,C.J., and Olson,M.F. (2003). Ras promotes p21(Waf1/Cip1) protein stability via a cyclin D1-imposed block in proteasome-mediated degradation. EMBO J *22*, 2036-2046.

Collart,D., Romain,P.L., Huebner,K., Pockwinse,S., Pilapil,S., Cannizzaro,L.A., Lian,J.B., Croce,C.M., Stein,J.L., and Stein,G.S. (1992). A human histone H2B.1 variant gene, located on chromosome 1, utilizes alternative 3' end processing. J. Cell Biochem. *50*, 374-385.

Colter,D.C., Sekiya,I., and Prockop,D.J. (2001). Identification of a subpopulation of rapidly self-renewing and multipotential adult stem cells in colonies of human marrow stromal cells. Proc. Natl. Acad. Sci. U. S. A *98*, 7841-7845.

Compston,J. (2006). Bone quality: what is it and how is it measured? Arq Bras. Endocrinol Metabol. *50*, 579-585.

Compston,J. (2010). Management of glucocorticoid-induced osteoporosis. Nat. Rev. Rheumatol. *6*, 82-88.

Conover,C.A. and Rosen,C. (2002). The role of insulin-like growth factors and bindgig proteins in bone cell biology. In Principles of Bone Biology, J.P.Bilezikian, L.G.Raisz, and G.A.Rodan, eds. (San Diego: Academic Press), pp. 801-815.

Cooper,M.S., Hewison,M., and Stewart,P.M. (1999). Glucocorticoid activity, inactivity and the osteoblast. J. Endocrinol. *163*, 159-164.

Crews,C.M. and Erikson,R.L. (1992). Purification of a murine protein-tyrosine/threonine kinase that phosphorylates and activates the Erk-1 gene product: relationship to the fission yeast byr1 gene product. Proceedings of the National Academy of Sciences of the United States of America *89*, 8205-8209.

Crews,C.M., Alessandrini,A., and Erikson,R.L. (1992). The primary structure of MEK, a protein kinase that phosphorylates the ERK gene product. Science *258*, 478-480.

Crews,C.M., Alessandrini,A.A., and Erikson,R.L. (1991). Mouse Erk-1 gene product is a serine/threonine protein kinase that has the potential to phosphorylate tyrosine. Proc. Natl. Acad. Sci. U. S. A *88*, 8845-8849.

Croxtall,J.D., Choudhury,Q., and Flower,R.J. (2000). Glucocorticoids act within minutes to inhibit recruitment of signalling factors to activated EGF receptors through a receptor-dependent, transcription-independent mechanism. Br. J. Pharmacol. *130*, 289-298.

Cushing,H. (1994). The basophil adenomas of the pituitary body and their clinical manifestations (pituitary basophilism). 1932. Obes. Res. *2*, 486-508.

D'Agostino,J., Valadka,R.J., and Schwartz,N.B. (1990). Differential effects of in vitro glucocorticoids on luteinizing hormone and follicle-stimulating hormone secretion: dependence on sex of pituitary donor. Endocrinology *127*, 891-899.

Dale,L.B., Babwah,A.V., and Ferguson,S.S. (2002). Mechanisms of metabotropic glutamate receptor desensitization: role in the patterning of effector enzyme activation. Neurochem. Int *41*, 319-326.

Dalle,C.L., Arlot,M.E., Chavassieux,P.M., Roux,J.P., Portero,N.R., and Meunier,P.J. (2001). Comparison of trabecular bone microarchitecture and remodeling in glucocorticoid-induced and postmenopausal osteoporosis. J. Bone Miner. Res. *16*, 97-103.

Dallman,M.F., Akana,S.F., Cascio,C.S., Darlington,D.N., Jacobson,L., and Levin,N. (1987). Regulation of ACTH secretion: variations on a theme of B. Recent Prog. Horm. Res. *43*, 113-173.

Datta,N.S., Kolailat,R., Fite,A., Pettway,G., and Abou-Samra,A.B. (2010). Distinct roles for mitogen-activated protein kinase phosphatase-1 (MKP-1) and ERK-MAPK in PTH1R signaling during osteoblast proliferation and differentiation. Cell Signal. *22*, 457-466.

De Bosscher,K., Vanden Berghe,W., Vermeulen,L., Plaisance,S., Boone,E., and Haegeman,G. (2000). Glucocorticoids repress NF-kappaB-driven genes by disturbing the interaction of p65 with

the basal transcription machinery, irrespective of coactivator levels in the cell. Proc. Natl. Acad. Sci. U. S. A *97*, 3919-3924.

Defranco,D.J., Lian,J.B., and Glowacki,J. (1992). Differential effects of glucocorticoid on recruitment and activity of osteoclasts induced by normal and osteocalcin-deficient bone implanted in rats. Endocrinology *131*, 114-121.

Delany,A.M., Durant,D., and Canalis,E. (2001). Glucocorticoid suppression of IGF I transcription in osteoblasts. Mol. Endocrinol. *15*, 1781-1789.

Delany,A.M., Gabbitas,B.Y., and Canalis,E. (1995). Cortisol downregulates osteoblast alpha 1 (I) procollagen mRNA by transcriptional and posttranscriptional mechanisms. J. Cell Biochem. *57*, 488-494.

Deliloglu-Gurhan,I., Tuglu,I., Vatansever,H.S., Ozdal-Kurt,F., Ekren,H., Taylan,M., and Sen,B.H. (2006a). The effect of osteogenic medium on the adhesion of rat bone marrow stromal cell to the hydroxyapatite. Saudi. Med. J. *27*, 305-311.

Deliloglu-Gurhan,S.I., Vatansever,H.S., Ozdal-Kurt,F., and Tuglu,I. (2006b). Characterization of osteoblasts derived from bone marrow stromal cells in a modified cell culture system. Acta Histochem. *108*, 49-57.

DeNicola,G.M. and Tuveson,D.A. (2009). RAS in cellular transformation and senescence. Eur. J. Cancer *45 Suppl 1*, 211-216.

Dicker,A., Le,B.K., Astrom,G., van,H., V, Gotherstrom,C., Blomqvist,L., Arner,P., and Ryden,M. (2005). Functional studies of mesenchymal stem cells derived from adult human adipose tissue. Exp. Cell Res. *308*, 283-290.

Digirolamo,C.M., Stokes,D., Colter,D., Phinney,D.G., Class,R., and Prockop,D.J. (1999). Propagation and senescence of human marrow stromal cells in culture: a simple colony-forming assay identifies samples with the greatest potential to propagate and differentiate. Br. J. Haematol. *107*, 275-281.

Dimri,G.P., Lee,X., Basile,G., Acosta,M., Scott,G., Roskelley,C., Medrano,E.E., Linskens,M., Rubelj,I., Pereira-Smith,O., and . (1995). A biomarker that identifies senescent human cells in culture and in aging skin in vivo. Proc. Natl. Acad. Sci. U. S. A *92*, 9363-9367.

Dobnig,H. and Turner,R.T. (1995). Evidence that intermittent treatment with parathyroid hormone increases bone formation in adult rats by activation of bone lining cells. Endocrinology *136*, 3632-3638.

Dobrowolski,S., Harter,M., and Stacey,D.W. (1994). Cellular ras activity is required for passage through multiple points of the G0/G1 phase in BALB/c 3T3 cells. Mol. Cell Biol. *14*, 5441-5449.

Dodig,M., Tadic,T., Kronenberg,M.S., Dacic,S., Liu,Y.H., Maxson,R., Rowe,D.W., and Lichtler,A.C. (1999). Ectopic Msx2 overexpression inhibits and Msx2 antisense stimulates calvarial osteoblast differentiation. Dev. Biol. *209*, 298-307.

Doi,M., Nagano,A., and Nakamura,Y. (2002). Genome-wide screening by cDNA microarray of genes associated with matrix mineralization by human mesenchymal stem cells in vitro. Biochem. Biophys. Res. Commun. *290*, 381-390.

Dominici,M., Le,B.K., Mueller,I., Slaper-Cortenbach,I., Marini,F., Krause,D., Deans,R., Keating,A., Prockop,D., and Horwitz,E. (2006). Minimal criteria for defining multipotent mesenchymal stromal cells. The International Society for Cellular Therapy position statement. Cytotherapy. *8*, 315-317.

Dore,R.K. (2010). How to prevent glucocorticoid-induced osteoporosis. Cleve. Clin. J. Med. *77*, 529-536.

Dorfman,K., Carrasco,D., Gruda,M., Ryan,C., Lira,S.A., and Bravo,R. (1996). Disruption of the erp/mkp-1 gene does not affect mouse development: normal MAP kinase activity in ERP/MKP-1-deficient fibroblasts. Oncogene *13*, 925-931.

Doty,S.B. (1981). Morphological evidence of gap junctions between bone cells. Calcif. Tissue Int. *33*, 509-512.

Drissi,H., Hushka,D., Aslam,F., Nguyen,Q., Buffone,E., Koff,A., van,W.A., Lian,J.B., Stein,J.L., and Stein,G.S. (1999). The cell cycle regulator p27kip1 contributes to growth and differentiation of osteoblasts. Cancer Res. *59*, 3705-3711.

Ducy,P., Zhang,R., Geoffroy,V., Ridall,A.L., and Karsenty,G. (1997). Osf2/Cbfa1: a transcriptional activator of osteoblast differentiation. Cell *89*, 747-754.

Durham,S.K., Kiefer,M.C., Riggs,B.L., and Conover,C.A. (1994). Regulation of insulin-like growth factor binding protein 4 by a specific insulin-like growth factor binding protein 4 proteinase in normal human osteoblast-like cells: implications in bone cell physiology. J Bone Miner Res *9*, 111-117.

Eapen,A., Sundivakkam,P., Song,Y., Ravindran,S., Ramachandran,A., Tiruppathi,C., and George,A. (2010). Calcium-mediated stress kinase activation by DMP1 promotes osteoblast differentiation. J Biol. Chem. *285*, 36339-36351.

Ebisuya,M., Kondoh,K., and Nishida,E. (2005). The duration, magnitude and compartmentalization of ERK MAP kinase activity: mechanisms for providing signaling specificity. J Cell Sci. *118*, 2997-3002.

Egan,S.E., Giddings,B.W., Brooks,M.W., Buday,L., Sizeland,A.M., and Weinberg,R.A. (1993). Association of Sos Ras exchange protein with Grb2 is implicated in tyrosine kinase signal transduction and transformation. Nature *363*, 45-51.

Eijken,M., Koedam,M., van,D.M., Buurman,C.J., Pols,H.A., and van Leeuwen,J.P. (2006). The essential role of glucocorticoids for proper human osteoblast differentiation and matrix mineralization. Mol. Cell Endocrinol. *248*, 87-93.

Elberg,G., Li,J., and Shechter,Y. (1994). Vanadium activates or inhibits receptor and non-receptor protein tyrosine kinases in cell-free experiments, depending on its oxidation state. Possible role of endogenous vanadium in controlling cellular protein tyrosine kinase activity. J. Biol. Chem. *269*, 9521-9527.

Engelbrecht,Y., de,W.H., Horsch,K., Langeveldt,C.R., Hough,F.S., and Hulley,P.A. (2003). Glucocorticoids induce rapid up-regulation of mitogen-activated protein kinase phosphatase-1 and dephosphorylation of extracellular signal-regulated kinase and impair proliferation in human and mouse osteoblast cell lines. Endocrinology *144*, 412-422.

Engsig,M.T., Chen,Q.J., Vu,T.H., Pedersen,A.C., Therkidsen,B., Lund,L.R., Henriksen,K., Lenhard,T., Foged,N.T., Werb,Z., and Delaisse,J.M. (2000). Matrix metalloproteinase 9 and vascular endothelial growth factor are essential for osteoclast recruitment into developing long bones. J Cell Biol. *151*, 879-889.

Everts,V., Delaisse,J.M., Korper,W., Jansen,D.C., Tigchelaar-Gutter,W., Saftig,P., and Beertsen,W. (2002). The bone lining cell: its role in cleaning Howship's lacunae and initiating bone formation. J. Bone Miner. Res. *17*, 77-90.

Fantus,I.G., Kadota,S., Deragon,G., Foster,B., and Posner,B.I. (1989). Pervanadate [peroxide(s) of vanadate] mimics insulin action in rat adipocytes via activation of the insulin receptor tyrosine kinase. Biochemistry *28*, 8864-8871.

Fedde,K.N., Blair,L., Silverstein,J., Coburn,S.P., Ryan,L.M., Weinstein,R.S., Waymire,K., Narisawa,S., Millan,J.L., MacGregor,G.R., and Whyte,M.P. (1999). Alkaline phosphatase knock-out mice recapitulate the metabolic and skeletal defects of infantile hypophosphatasia. J. Bone Miner. Res. *14*, 2015-2026.

Felix,R., Cecchini,M.G., and Fleisch,H. (1990). Macrophage colony stimulating factor restores in vivo bone resorption in the op/op osteopetrotic mouse. Endocrinology *127*, 2592-2594.

Felsenberg,D. and Boonen,S. (2005). The bone quality framework: determinants of bone strength and their interrelationships, and implications for osteoporosis management. Clin. Ther. *27*, 1-11.

Fernley,H.N. (1971). Mammalian alkaline phosphatase. In The Enzymes, Boyer P.D., ed. (New Yok, London: Academic Press), pp. 417-447.

Fisher,L.W. and Termine,J.D. (1985). Noncollagenous proteins influencing the local mechanisms of calcification. Clin. Orthop. Relat Res 362-385.

Fisher,L.W., Termine,J.D., and Young,M.F. (1989). Deduced protein sequence of bone small proteoglycan I (biglycan) shows homology with proteoglycan II (decorin) and several nonconnective tissue proteins in a variety of species. J Biol. Chem. *264*, 4571-4576.

Foulds,C.E., Nelson,M.L., Blaszczak,A.G., and Graves,B.J. (2004). Ras/mitogen-activated protein kinase signaling activates Ets-1 and Ets-2 by CBP/p300 recruitment. Mol Cell Biol. *24*, 10954-10964.

Fox,S.W., Fuller,K., and Chambers,T.J. (2000). Activation of osteoclasts by interleukin-1: divergent responsiveness in osteoclasts formed in vivo and in vitro. J. Cell Physiol *184*, 334-340.

Franceschi,R.T. (1999). The Developmental Control of Osteoblast-Specific Gene Expression: Role of Specific Transcription Factors and the Extracellular Matrix Environment. Critical Reviews in Oral Biology & Medicine *10*, 40-57.

Franklin,C.C. and Kraft,A.S. (1997). Conditional expression of the mitogen-activated protein kinase (MAPK) phosphatase MKP-1 preferentially inhibits p38 MAPK and stress-activated protein kinase in U937 cells. J Biol. Chem. *272*, 16917-16923.

Fremin,C. and Meloche,S. (2010). From basic research to clinical development of MEK1/2 inhibitors for cancer therapy. J. Hematol. Oncol. *3*, 8.

Fried,A. and Benayahu,D. (1996). Dexamethasone regulation of marrow stromal-derived osteoblastic cells. J Cell Biochem. *62*, 476-483.

Fried,A., Benayahu,D., and Wientroub,S. (1993). Marrow stroma-derived osteogenic clonal cell lines: putative stages in osteoblastic differentiation. J. Cell Physiol *155*, 472-482.

Friedenstein,A.J. (1990). Osteogenic stem cells in the bone marrow. In Bone and Mineral Research, J.N.Heersche and J.A.Kanis, eds. (Amsterdam: Elsevier Science Publishers B.V. (Biochemical division)), pp. 243-270.

Friedman,A. and Perrimon,N. (2006). A functional RNAi screen for regulators of receptor tyrosine kinase and ERK signalling. Nature *444*, 230-234.

Frost,H.M. (1963). Bone remodelling dynamics. C.C.Thomas, ed. (Springfield, IL.

Frost,H.M. (1964). Dynamics of bone remodelling. In Bone Biodynamics, H.M.Frost, ed. Little, Brown and Co), pp. 315-333.

Fu,Q., Jilka,R.L., Manolagas,S.C., and O'Brien,C.A. (2002). Parathyroid Hormone Stimulates Receptor Activator of NF+¦B Ligand and Inhibits Osteoprotegerin Expression via Protein Kinase A Activation of cAMP-response Element-binding Protein. Journal of Biological Chemistry *277*, 48868-48875.

Fukuda,M., Gotoh,I., Gotoh,Y., and Nishida,E. (1996). Cytoplasmic Localization of Mitogen-activated Protein Kinase Kinase Directed by Its NH2-terminal, Leucine-rich Short Amino Acid Sequence, Which Acts as a Nuclear Export Signal. Journal of Biological Chemistry *271*, 20024-20028.

Fuller,K., Wong,B., Fox,S., Choi,Y., and Chambers,T.J. (1998). TRANCE Is Necessary and Sufficient for Osteoblast-mediated Activation of Bone Resorption in Osteoclasts. The Journal of Experimental Medicine *188*, 997-1001.

Gallea,S., Lallemand,F., Atfi,A., Rawadi,G., Ramez,V., Spinella-Jaegle,S., Kawai,S., Faucheu,C., Huet,L., Baron,R., and Roman-Roman,S. (2001). Activation of mitogen-activated protein kinase cascades is involved in regulation of bone morphogenetic protein-2-induced osteoblast differentiation in pluripotent C2C12 cells. Bone *28*, 491-498.

Gametchu,B., Watson,C.S., and Wu,S. (1993). Use of receptor antibodies to demonstrate membrane glucocorticoid receptor in cells from human leukemic patients. FASEB J. *7*, 1283-1292.

Ge,C., Xiao,G., Jiang,D., and Franceschi,R.T. (2007). Critical role of the extracellular signal-regulated kinase-MAPK pathway in osteoblast differentiation and skeletal development. J. Cell Biol. *176*, 709-718.

Gerstenfeld,L.C., Chipman,S.D., Glowacki,J., and Lian,J.B. (1987). Expression of differentiated function by mineralizing cultures of chicken osteoblasts. Dev. Biol. *122*, 49-60.

Gilbert,S. (2010). Osteoclast commitment, differentiation and function. S.Gilbert, ed. Sinauer Associates, Inc.).

Gil-Henn,H., Destaing,O., Sims,N.A., Aoki,K., Alles,N., Neff,L., Sanjay,A., Bruzzaniti,A., De Camilli,P., Baron,R., and Schlessinger,J. (2007). Defective microtubule-dependent podosome organization in osteoclasts leads to increased bone density in Pyk2□êÆ/□êÆ mice. The Journal of Cell Biology *178*, 1053-1064.

Gille,H., Kortenjann,M., Thomae,O., Moomaw,C., Slaughter,C., Cobb,M.H., and Shaw,P.E. (1995). ERK phosphorylation potentiates Elk-1-mediated ternary complex formation and transactivation. EMBO J. *14*, 951-962.

Girasole,G., Passeri,G., Jilka,R.L., and Manolagas,S.C. (1994). Interleukin-11: a new cytokine critical for osteoclast development. J. Clin. Invest *93*, 1516-1524.

Giustina,A. and Wehrenberg,W.B. (1992). The role of glucocorticoids in the regulation of Growth Hormone secretion: mechanisms and clinical significance. Trends Endocrinol. Metab *3*, 306-311.

Giustina,A., Mazziotti,G., and Canalis,E. (2008). Growth hormone, insulin-like growth factors, and the skeleton. Endocr. Rev. *29*, 535-559.

Glaser,J.H. and Conrad,H.E. (1981). Formation of matrix vesicles by cultured chick embryo chondrocytes. J. Biol. Chem. *256*, 12607-12611.

Glimcher,M.J. (1981). On the form and function of bone: from molecules to organs. Wollf's law revisited. In The Chemistry and Biology of Mineralised Connective Tissues., A.Veis, ed. (New York: Elsevier North Holland Inc.), pp. 617-673.

Globus,R.K., Plouet,J., and Gospodarowicz,D. (1989). Cultured bovine bone cells synthesize basic fibroblast growth factor and store it in their extracellular matrix. Endocrinology *124*, 1539-1547.

Golub,E.E. (2009). Role of matrix vesicles in biomineralization. Biochim. Biophys. Acta *1790*, 1592-1598.

Gordon,J.A., Tye,C.E., Sampaio,A.V., Underhill,T.M., Hunter,G.K., and Goldberg,H.A. (2007). Bone sialoprotein expression enhances osteoblast differentiation and matrix mineralization in vitro. Bone *41*, 462-473.

Gorostizaga,A., Brion,L., Maloberti,P., Maciel,F.C., Podesta,E.J., and Paz,C. (2005). Heat shock triggers MAPK activation and MKP-1 induction in Leydig testicular cells. Biochem. Biophys. Res Commun. *327*, 23-28.

Gorostizaga,A., Brion,L., Maloberti,P., Poderoso,C., Podesta,E.J., Maciel,F.C., and Paz,C. (2004). Molecular events triggered by heat shock in Y1 adrenocortical cells. Endocr. Res *30*, 655-659.

Gotoh,Y., Nishida,E., Yamashita,T., Hoshi,M., Kawakami,M., and Sakai,H. (1990). Microtubule-associated-protein (MAP) kinase activated by nerve growth factor and epidermal growth factor in PC12 cells. Identity with the mitogen-activated MAP kinase of fibroblastic cells. Eur. J Biochem. *193*, 661-669.

Graves,D.T., Valentin-Opran,A., Delgado,R., Valente,A.J., Mundy,G., and Piche,J. (1989). The potential role of platelet-derived growth factor as an autocrine or paracrine factor for human bone cells. Connect. Tissue Res *23*, 209-218.

Grigoriadis,A.E., Wang,Z.Q., Cecchini,M.G., Hofstetter,W., Felix,R., Fleisch,H.A., and Wagner,E.F. (1994). c-Fos: a key regulator of osteoclast-macrophage lineage determination and bone remodeling. Science *266*, 443-448.

Groom, L. A., Sneddon, A. A., Alessi, A. A., Dowd, S., and Keyse, S. M. Differential regulation of MAP, SAP and RK/p38 kinases by Pyst1, a novel cytosolic dual-specificity phosphatase. EMBO J 15[14], 3621-3632. 1996.

Gudermann,T., Grosse,R., and Schultz,G. (2000). Contribution of receptor/G protein signaling to cell growth and transformation. Naunyn Schmiedebergs Arch. Pharmacol. *361*, 345-362.

Gstraunthaler,G. (2003). Alternatives to the use of fetal bovine serum: serum-free cell culture. ALTEX. *20*, 275-281.

Gudermann,T., Schoneberg,T., and Schultz,G. (1997). Functional and structural complexity of signal transduction via G-protein-coupled receptors. Annu. Rev. Neurosci. *20*, 399-427.

Guicheux,J., Lemonnier,J., Ghayor,C., Suzuki,A., Palmer,G., and Caverzasio,J. (2003). Activation of p38 mitogen-activated protein kinase and c-Jun-NH2-terminal kinase by BMP-2 and their implication in the stimulation of osteoblastic cell differentiation. J Bone Miner Res *18*, 2060-2068.

Guo,X. and Wang,X.F. (2009). Signaling cross-talk between TGF-beta/BMP and other pathways. Cell Res *19*, 71-88.

Hafezi-Moghadam,A., Simoncini,T., Yang,Z., Limbourg,F.P., Plumier,J.C., Rebsamen,M.C., Hsieh,C.M., Chui,D.S., Thomas,K.L., Prorock,A.J., Laubach,V.E., Moskowitz,M.A., French,B.A., Ley,K., and Liao,J.K. (2002). Acute cardiovascular protective effects of corticosteroids are mediated by non-transcriptional activation of endothelial nitric oxide synthase. Nat. Med. *8*, 473-479.

Hamidouche,Z., Hay,E., Vaudin,P., Charbord,P., Schule,R., Marie,P.J., and Fromigue,O. (2008). FHL2 mediates dexamethasone-induced mesenchymal cell differentiation into osteoblasts by activating Wnt/beta-catenin signaling-dependent Runx2 expression. FASEB J. *22*, 3813-3822.

Harada,S.i. and Rodan,G.A. (2003). Control of osteoblast function and regulation of bone mass. Nature *423*, 349-355.

Harris,H. (1989). The human alkaline phosphatases: what we know and what we don't know. Clinica Chimica Acta *186*, 133-150.

Hauschka,P.V., Mavrakos,A.E., Iafrati,M.D., Doleman,S.E., and Klagsbrun,M. (1986). Growth factors in bone matrix. Isolation of multiple types by affinity chromatography on heparin-Sepharose. J Biol. Chem. *261*, 12665-12674.

Hay,E., Nouraud,A., and Marie,P.J. (2009). N-cadherin negatively regulates osteoblast proliferation and survival by antagonizing Wnt, ERK and PI3K/Akt signalling. PLoS. One. *4*, e8284.

Hayashi,Y. and Nagasawa,H. (1990). Matrix vesicles isolated from apical pulp of rat incisors: crystal formation in low Ca x Pi ion-product medium containing beta-glycerophosphate. Calcif. Tissue Int. *47*, 365-372.

Hedbom,E. and Heinegard,D. (1989). Interaction of a 59-kDa connective tissue matrix protein with collagen I and collagen II. J. Biol. Chem. *264*, 6898-6905.

Heffetz,D., Bushkin,I., Dror,R., and Zick,Y. (1990). The insulinomimetic agents H2O2 and vanadate stimulate protein tyrosine phosphorylation in intact cells. J. Biol. Chem. *265*, 2896-2902.

Heino,T.J., Hentunen,T.A., and Vaananen,H.K. (2002). Osteocytes inhibit osteoclastic bone resorption through transforming growth factor-beta: enhancement by estrogen. J. Cell Biochem. *85*, 185-197.

Heinrichs,A.A., Bortell,R., Rahman,S., Stein,J.L., Alnemri,E.S., Litwack,G., Lian,J.B., and Stein,G.S. (1993). Identification of multiple glucocorticoid receptor binding sites in the rat osteocalcin gene promoter. Biochemistry *32*, 11436-11444.

Henkel,G.W., McKercher,S.R., Yamamoto,H., Anderson,K.L., Oshima,R.G., and Maki,R.A. (1996). PU.1 but not ets-2 is essential for macrophage development from embryonic stem cells. Blood *88*, 2917-2926.

Hickman,J. and McElduff,A. (1989). Insulin promotes growth of the cultured rat osteosarcoma cell line UMR-106-01: an osteoblast-like cell. Endocrinology *124*, 701-706.

Higuchi,C., Myoui,A., Hashimoto,N., Kuriyama,K., Yoshioka,K., Yoshikawa,H., and Itoh,K. (2002). Continuous inhibition of MAPK signaling promotes the early osteoblastic differentiation and mineralization of the extracellular matrix. J Bone Miner Res *17*, 1785-1794.

Hock,J.M., Fitzpatrick,L.A., and Bilezikian,J.P. (2002). Actions of parathyroid hormone. In Principles of Bone Biology, J.P.Bilezikian, L.G.Raisz, and G.A.Rodan, eds. (San Diego: Academic Press), pp. 463-481.

Hock,J.M., Hummert,J.R., Boyce,R., Fonseca,J., and Raisz,L.G. (1989). Resorption is not essential for the stimulation of bone growth by hPTH-(1-34) in rats in vivo. J Bone Miner Res *4*, 449-458.

Hofbauer,L.C., Gori,F., Riggs,B.L., Lacey,D.L., Dunstan,C.R., Spelsberg,T.C., and Khosla,S. (1999). Stimulation of osteoprotegerin ligand and inhibition of osteoprotegerin production by glucocorticoids in human osteoblastic lineage cells: potential paracrine mechanisms of glucocorticoid-induced osteoporosis. Endocrinology *140*, 4382-4389.

Homme,M., Schmitt,C.P., Mehls,O., and Schaefer,F. (2004). Mechanisms of mitogen-activated protein kinase inhibition by parathyroid hormone in osteoblast-like cells. J Am. Soc. Nephrol. *15*, 2844-2850.

Horne,W.C., Sanjay,A., Bruzzaniti,A., and Baron,R. (2005). The role(s) of Src kinase and Cbl proteins in the regulation of osteoclast differentiation and function. Immunol. Rev. *208*, 106-125.

Horsch,K., de,W.H., Schuurmans,M.M., Allie-Reid,F., Cato,A.C., Cunningham,J., Burrin,J.M., Hough,F.S., and Hulley,P.A. (2007). Mitogen-activated protein kinase phosphatase 1/dual specificity phosphatase 1 mediates glucocorticoid inhibition of osteoblast proliferation. Mol. Endocrinol. *21*, 2929-2940.

Hoshi,K., Amizuka,N., Oda,K., Ikehara,Y., and Ozawa,H. (1997). Immunolocalization of tissue non-specific alkaline phosphatase in mice. Histochem. Cell Biol. *107*, 183-191.

Houtgraaf,J.H., Versmissen,J., and van der Giessen,W.J. (2006). A concise review of DNA damage checkpoints and repair in mammalian cells. Cardiovasc. Revasc. Med. *7*, 165-172.

Hsu,H., Lacey,D.L., Dunstan,C.R., Solovyev,I., Colombero,A., Timms,E., Tan,H.L., Elliott,G., Kelley,M.J., Sarosi,I., Wang,L., Xia,X.Z., Elliott,R., Chiu,L., Black,T., Scully,S., Capparelli,C., Morony,S., Shimamoto,G., Bass,M.B., and Boyle,W.J. (1999). Tumor necrosis factor receptor family member RANK mediates osteoclast differentiation and activation induced by osteoprotegerin ligand. Proc. Natl. Acad. Sci. U. S. A *96*, 3540-3545.

Hsueh,A.J. and Erickson,G.F. (1978). Glucocorticoid inhibition of FSH-induced estrogen production in cultured rat granulosa cells. Steroids *32*, 639-648.

Hu,J.H., Chen,T., Zhuang,Z.H., Kong,L., Yu,M.C., Liu,Y., Zang,J.W., and Ge,B.X. (2007). Feedback control of MKP-1 expression by p38. Cell Signal. *19*, 393-400.

Huang,J.I., Beanes,S.R., Zhu,M., Lorenz,H.P., Hedrick,M.H., and Benhaim,P. (2002). Rat extramedullary adipose tissue as a source of osteochondrogenic progenitor cells. Plast. Reconstr. Surg. *109*, 1033-1041.

Hube,F., Velasco,G., Rollin,J., Furling,D., and Francastel,C. (2011). Steroid receptor RNA activator protein binds to and counteracts SRA RNA-mediated activation of MyoD and muscle differentiation. Nucleic Acids Res. *39*, 513-525.

Hughes,F.J. and Aubin,J.E. (1997). Culture of cells of the osteoblast lineage. In Methods in Bone biology, Springer), pp. 1-49.

Hulley,P.A., Conradie,M.M., Langeveldt,C.R., and Hough,F.S. (2002). Glucocorticoid-induced osteoporosis in the rat is prevented by the tyrosine phosphatase inhibitor, sodium orthovanadate. Bone *31*, 220-229.

Hulley,P.A., Gordon,F., and Hough,F.S. (1998). Inhibition of mitogen-activated protein kinase activity and proliferation of an early osteoblast cell line (MBA 15.4) by dexamethasone: role of protein phosphatases. Endocrinology *139*, 2423-2431.

Hunter,T. (1995). Protein kinases and phosphatases: the yin and yang of protein phosphorylation and signaling. Cell *80*, 225-236.

Hurley,M.M., Abreu,C., Gronowicz,G., Kawaguchi,H., and Lorenzo,J. (1994). Expression and regulation of basic fibroblast growth factor mRNA levels in mouse osteoblastic MC3T3-E1 cells. J Biol. Chem. *269*, 9392-9396.

Hurrell,D.J. (1937). The Nerve Supply of Bone. J. Anat. *72*, 54-61.

Hutchison,K.A., Brott,B.K., De Leon,J.H., Perdew,G.H., Jove,R., and Pratt,W.B. (1992). Reconstitution of the multiprotein complex of pp60src, hsp90, and p50 in a cell-free system. J. Biol. Chem. *267*, 2902-2908.

Hutchison,K.A., Dittmar,K.D., Czar,M.J., and Pratt,W.B. (1994). Proof that hsp70 is required for assembly of the glucocorticoid receptor into a heterocomplex with hsp90. J. Biol. Chem. *269*, 5043-5049.

Ishida,Y. and Heersche,J.N. (1998). Glucocorticoid-induced osteoporosis: both in vivo and in vitro concentrations of glucocorticoids higher than physiological levels attenuate osteoblast differentiation. J. Bone Miner. Res. *13*, 1822-1826.

Ito,S., Suzuki,N., Kato,S., Takahashi,T., and Takagi,M. (2007). Glucocorticoids induce the differentiation of a mesenchymal progenitor cell line, ROB-C26 into adipocytes and osteoblasts, but fail to induce terminal osteoblast differentiation. Bone *40*, 84-92.

Jager,M., Fischer,J., Dohrn,W., Li,X., Ayers,D.C., Czibere,A., Prall,W.C., Lensing-Hohn,S., and Krauspe,R. (2008). Dexamethasone modulates BMP-2 effects on mesenchymal stem cells in vitro. J. Orthop. Res. *26*, 1440-1448.

Jaiswal,N., Haynesworth,S.E., Caplan,A.I., and Bruder,S.P. (1997). Osteogenic differentiation of purified, culture-expanded human mesenchymal stem cells in vitro. J. Cell Biochem. *64*, 295-312.

Jaiswal,R.K., Jaiswal,N., Bruder,S.P., Mbalaviele,G., Marshak,D.R., and Pittenger,M.F. (2000). Adult human mesenchymal stem cell differentiation to the osteogenic or adipogenic lineage is regulated by mitogen-activated protein kinase. J Biol. Chem. *275*, 9645-9652.

Janknecht,R., Ernst,W.H., Pingoud,V., and Nordheim,A. (1993). Activation of ternary complex factor Elk-1 by MAP kinases. EMBO J. *12*, 5097-5104.

Jia,D., O'Brien,C.A., Stewart,S.A., Manolagas,S.C., and Weinstein,R.S. (2006). Glucocorticoids act directly on osteoclasts to increase their life span and reduce bone density. Endocrinology *147*, 5592-5599.

Jilka,R.L. (2003). Biology of the basic multicellular unit and the pathophysiology of osteoporosis. Med. Pediatr. Oncol. *41*, 182-185.

Jilka,R.L., Weinstein,R.S., Bellido,T., Parfitt,A.M., and Manolagas,S.C. (1998). Osteoblast programmed cell death (apoptosis): modulation by growth factors and cytokines. J. Bone Miner. Res. *13*, 793-802.

Jonsson,K.B., Frost,A., Larsson,R., Ljunghall,S., and Ljunggren,O. (1997). A new fluorometric assay for determination of osteoblastic proliferation: effects of glucocorticoids and insulin-like growth factor-I. Calcif. Tissue Int. *60*, 30-36.

Junttila,M.R., Li,S.P., and Westermarck,J. (2008). Phosphatase-mediated crosstalk between MAPK signaling pathways in the regulation of cell survival. FASEB J. *22*, 954-965.

Kadota,S., Fantus,I.G., Deragon,G., Guyda,H.J., and Posner,B.I. (1987b). Stimulation of insulin-like growth factor II receptor binding and insulin receptor kinase activity in rat adipocytes. Effects of vanadate and H2O2. Journal of Biological Chemistry *262*, 8252-8256.

Kadota,S., Fantus,I.G., Deragon,G., Guyda,H.J., Hersh,B., and Posner,B.I. (1987a). Peroxide(s) of vanadium: a novel and potent insulin-mimetic agent which activates the insulin receptor kinase. Biochem. Biophys. Res. Commun. *147*, 259-266.

Kaiser,E. and Chandrasekhar,S. (2003). Distinct pathways of extracellular signal-regulated kinase activation by growth factors, fibronectin and parathyroid hormone 1-34. Biochem. Biophys. Res Commun. *305*, 573-578.

Kalak,R., Zhou,H., Street,J., Day,R.E., Modzelewski,J.R., Spies,C.M., Liu,P.Y., Li,G., Dunstan,C.R., and Seibel,M.J. (2009). Endogenous glucocorticoid signalling in osteoblasts is necessary to maintain normal bone structure in mice. Bone *45*, 61-67.

Kaltsas,G. and Makras,P. (2010). Skeletal diseases in Cushing's syndrome: osteoporosis versus arthropathy. Neuroendocrinology *92 Suppl 1*, 60-64.

Kamioka,H., Honjo,T., and Takano-Yamamoto,T. (2001). A three-dimensional distribution of osteocyte processes revealed by the combination of confocal laser scanning microscopy and differential interference contrast microscopy. Bone *28*, 145-149.

Kanis,J.A. (1994a). Assessment of fracture risk and its application to screening for postmenopausal osteoporosis: synopsis of a WHO report. WHO Study Group. Osteoporos. Int. *4*, 368-381.

Kanis,J.A., Melton,L.J., III, Christiansen,C., Johnston,C.C., and Khaltaev,N. (1994b). The diagnosis of osteoporosis. J. Bone Miner. Res. *9*, 1137-1141.

Karlsson,M., Mathers,J., Dickinson,R.J., Mandl,M., and Keyse,S.M. (2004). Both Nuclear-Cytoplasmic Shuttling of the Dual Specificity Phosphatase MKP-3 and Its Ability to Anchor MAP Kinase in the Cytoplasm Are Mediated by a Conserved Nuclear Export Signal. Journal of Biological Chemistry *279*, 41882-41891.

Kassel,O., Sancono,A., Kratzschmar,J., Kreft,B., Stassen,M., and Cato,A.C. (2001). Glucocorticoids inhibit MAP kinase via increased expression and decreased degradation of MKP-1. EMBO J *20*, 7108-7116.

Kassem,M., Blum,W., Ristelli,J., Mosekilde,L., and Eriksen,E.F. (1993). Growth hormone stimulates proliferation and differentiation of normal human osteoblast-like cells in vitro. Calcif. Tissue Int. *52*, 222-226.

Kastan,M.B. and Bartek,J. (2004). Cell-cycle checkpoints and cancer. Nature *432*, 316-323.

Kato,K., Tokuda,H., Adachi,S., Matsushima-Nishiwaki,R., Natsume,H., Yamakawa,K., Gu,Y., Otsuka,T., and Kozawa,O. (2010). AMP-activated protein kinase positively regulates FGF-2-stimulated VEGF synthesis in osteoblasts. Biochem. Biophys. Res Commun. *400*, 123-127.

Kato,M., Patel,M.S., Levasseur,R., Lobov,I., Chang,B.H., Glass,D.A., Hartmann,C., Li,L., Hwang,T.H., Brayton,C.F., Lang,R.A., Karsenty,G., and Chan,L. (2002). Cbfa1-independent decrease in osteoblast proliferation, osteopenia, and persistent embryonic eye vascularization in mice deficient in Lrp5, a Wnt coreceptor. J. Cell Biol. *157*, 303-314.

Katz,M., Amit,I., and Yarden,Y. (2007). Regulation of MAPKs by growth factors and receptor tyrosine kinases. Biochim. Biophys. Acta *1773*, 1161-1176.

Kaufmann,S., Jones,K.L., Wehrenberg,W.B., and Culler,F.L. (1988). Inhibition by prednisone of growth hormone (GH) response to GH-releasing hormone in normal men. J. Clin. Endocrinol. Metab *67*, 1258-1261.

Kaunitz,J.D. and Yamaguchi,D.T. (2008). TNAP, TrAP, ecto-purinergic signaling, and bone remodeling. J. Cell Biochem. *105*, 655-662.

Kerby,J.A., Hattersley,G., Collins,D.A., and Chambers,T.J. (1992). Derivation of osteoclasts from hematopoietic colony-forming cells in culture. J Bone Miner Res *7*, 353-362.

Keshet,Y. and Seger,R. (2010). The MAP kinase signaling cascades: a system of hundreds of components regulates a diverse array of physiological functions. Methods Mol. Biol. *661*, 3-38.

Keyse,S.M. (1998). Protein phosphatases and the regulation of MAP kinase activity. Semin. Cell Dev. Biol. *9*, 143-152.
Keyse,S.M. (2000). Protein phosphatases and the regulation of mitogen-activated protein kinase signalling. Curr. Opin. Cell Biol. *12*, 186-192.

Keyse,S.M. (2008a). Dual-specificity MAP kinase phosphatases (MKPs) and cancer. Cancer Metastasis Rev. *27*, 253-261.

Keyse,S.M. (2008b). Protein phosphatases and cancer. Preface. Cancer Metastasis Rev. *27*, 121-122.

Keyse,S.M. and Emslie,E.A. (1992). Oxidative stress and heat shock induce a human gene encoding a protein-tyrosine phosphatase. Nature *359*, 644-647.

Kilian,K.A., Bugarija,B., Lahn,B.T., and Mrksich,M. (2010). Geometric cues for directing the differentiation of mesenchymal stem cells. Proc. Natl. Acad. Sci. U. S. A *107*, 4872-4877.

Kim,H.J. (2010). New understanding of glucocorticoid action in bone cells. BMB. Rep. *43*, 524-529.

Kim,Y.H., Jun,J.H., Woo,K.M., Ryoo,H.M., Kim,G.S., and Baek,J.H. (2006). Dexamethasone inhibits the formation of multinucleated osteoclasts via down-regulation of beta3 integrin expression. Arch. Pharm. Res. *29*, 691-698.

Kitazawa,R. and Kitazawa,S. (2002). Vitamin D3 Augments Osteoclastogenesis via Vitamin D-Responsive Element of Mouse RANKL Gene Promoter. Biochemical and Biophysical Research Communications *290*, 650-655.

Kitazawa,S., Kajimoto,K., Kondo,T., and Kitazawa,R. (2003). Vitamin D3 supports osteoclastogenesis via functional vitamin D response element of human RANKL gene promoter. J. Cell Biochem. *89*, 771-777.

Knothe Tate,M.L. (2003). "Whither flows the fluid in bone?" An osteocyte's perspective. J. Biomech. *36*, 1409-1424.

Knothe Tate,M.L., Adamson,J.R., Tami,A.E., and Bauer,T.W. (2004). The osteocyte. Int. J. Biochem. Cell Biol. *36*, 1-8.

Komori,T., Yagi,H., Nomura,S., Yamaguchi,A., Sasaki,K., Deguchi,K., Shimizu,Y., Bronson,R.T., Gao,Y.H., Inada,M., Sato,M., Okamoto,R., Kitamura,Y., Yoshiki,S., and Kishimoto,T. (1997). Targeted disruption of Cbfa1 results in a complete lack of bone formation owing to maturational arrest of osteoblasts. Cell *89*, 755-764.

Konig,H., Ponta,H., Rahmsdorf,H.J., and Herrlich,P. (1992). Interference between pathway-specific transcription factors: glucocorticoids antagonize phorbol ester-induced AP-1 activity without altering AP-1 site occupation in vivo. EMBO J. *11*, 2241-2246.

Kono,S.J., Oshima,Y., Hoshi,K., Bonewald,L.F., Oda,H., Nakamura,K., Kawaguchi,H., and Tanaka,S. (2007). Erk pathways negatively regulate matrix mineralization. Bone *40*, 68-74.

Krens,S.F., Spaink,H.P., and Snaar-Jagalska,B.E. (2006). Functions of the MAPK family in vertebrate-development. FEBS Lett. *580*, 4984-4990.

Kristiansen,M., Hughes,R., Patel,P., Jacques,T.S., Clark,A.R., and Ham,J. (2010). Mkp1 Is a c-Jun Target Gene That Antagonizes JNK-Dependent Apoptosis in Sympathetic Neurons. J. Neurosci. *30*, 10820-10832.

Kurihara,N. (1990). The origin of osteoclasts. Bull. Kanagawa. Dent. Coll. *18*, 161-164.

Kurihara,N., Civin,C., and Roodman,G.D. (1991). Osteotropic factor responsiveness of highly purified populations of early and late precursors for human multinucleated cells expressing the osteoclast phenotype. J Bone Miner Res *6*, 257-261.

Kuwano,Y., Kim,H.H., Abdelmohsen,K., Pullmann,R., Jr., Martindale,J.L., Yang,X., and Gorospe,M. (2008). MKP-1 mRNA stabilization and translational control by RNA-binding proteins HuR and NF90. Mol. Cell Biol. *28*, 4562-4575.

Kwak,S.P. and Dixon,J.E. (1995). Multiple dual specificity protein tyrosine phosphatases are expressed and regulated differentially in liver cell lines. J. Biol. Chem. *270*, 1156-1160.

Kwon,O.H., Lee,C.K., Lee,Y.I., Paik,S.G., and Lee,H.J. (2005). The hematopoietic transcription factor PU.1 regulates RANK gene expression in myeloid progenitors. Biochem. Biophys. Res. Commun. *335*, 437-446.

Kyriakis,J.M., App,H., Zhang,X.F., Banerjee,P., Brautigan,D.L., Rapp,U.R., and Avruch,J. (1992). Raf-1 activates MAP kinase-kinase. Nature *358*, 417-421.

Lacey,D.L., Erdmann,J.M., Teitelbaum,S.L., Tan,H.L., Ohara,J., and Shioi,A. (1995). Interleukin 4, interferon-gamma, and prostaglandin E impact the osteoclastic cell-forming potential of murine bone marrow macrophages. Endocrinology *136*, 2367-2376.

Lacey,D.L., Timms,E., Tan,H.L., Kelley,M.J., Dunstan,C.R., Burgess,T., Elliott,R., Colombero,A., Elliott,G., Scully,S., Hsu,H., Sullivan,J., Hawkins,N., Davy,E., Capparelli,C., Eli,A., Qian,Y.X., Kaufman,S., Sarosi,I., Shalhoub,V., Senaldi,G., Guo,J., Delaney,J., and Boyle,W.J. (1998). Osteoprotegerin ligand is a cytokine that regulates osteoclast differentiation and activation. Cell *93*, 165-176.

Laderoute,K.R., Mendonca,H.L., Calaoagan,J.M., Knapp,A.M., Giaccia,A.J., and Stork,P.J. (1999). Mitogen-activated protein kinase phosphatase-1 (MKP-1) expression is induced by low oxygen conditions found in solid tumor microenvironments. A candidate MKP for the inactivation of hypoxia-inducible stress-activated protein kinase/c-Jun N-terminal protein kinase activity. J Biol. Chem. *274*, 12890-12897.

Lai,C.F., Chaudhary,L., Fausto,A., Halstead,L.R., Ory,D.S., Avioli,L.V., and Cheng,S.L. (2001). Erk is essential for growth, differentiation, integrin expression, and cell function in human osteoblastic cells. J. Biol. Chem. *276*, 14443-14450.

Lakkakorpi,P.T. and Vaananen,H.K. (1991). Kinetics of the osteoclast cytoskeleton during the resorption cycle in vitro. J. Bone Miner. Res. *6*, 817-826.

Lambillotte,C., Gilon,P., and Henquin,J.C. (1997). Direct glucocorticoid inhibition of insulin secretion. An in vitro study of dexamethasone effects in mouse islets. J. Clin. Invest *99*, 414-423.

Lamp,E.C. and Drexler,H.G. (2000). Biology of tartrate-resistant acid phosphatase. Leuk. Lymphoma *39*, 477-484.

Langlois,J.A., Rosen,C.J., Visser,M., Hannan,M.T., Harris,T., Wilson,P.W., and Kiel,D.P. (1998). Association between insulin-like growth factor I and bone mineral density in older women and men: the Framingham Heart Study. J Clin. Endocrinol. Metab *83*, 4257-4262.

Lasa,M., Abraham,S.M., Boucheron,C., Saklatvala,J., and Clark,A.R. (2002). Dexamethasone causes sustained expression of mitogen-activated protein kinase (MAPK) phosphatase 1 and phosphatase-mediated inhibition of MAPK p38. Mol. Cell Biol. *22*, 7802-7811.

Leaffer,D., Sweeney,M., Kellerman,L.A., Avnur,Z., Krstenansky,J.L., Vickery,B.H., and Caulfield,J.P. (1995). Modulation of osteogenic cell ultrastructure by RS-23581, an analog of human parathyroid hormone (PTH)-related peptide-(1-34), and bovine PTH-(1-34). Endocrinology *136*, 3624-3631.

Lean,J.M., Jagger,C.J., Chambers,T.J., and Chow,J.W. (1995). Increased insulin-like growth factor I mRNA expression in rat osteocytes in response to mechanical stimulation. Am. J. Physiol *268*, E318-E327.

Leboy,P.S., Beresford,J.N., Devlin,C., and Owen,M.E. (1991). Dexamethasone induction of osteoblast mRNAs in rat marrow stromal cell cultures. J. Cell Physiol *146*, 370-378.

Lee,K.S., Kim,H.J., Li,Q.L., Chi,X.Z., Ueta,C., Komori,T., Wozney,J.M., Kim,E.G., Choi,J.Y., Ryoo,H.M., and Bae,S.C. (2000). Runx2 is a common target of transforming growth factor beta1 and bone morphogenetic protein 2, and cooperation between Runx2 and Smad5 induces osteoblast-specific gene expression in the pluripotent mesenchymal precursor cell line C2C12. Mol. Cell Biol. *20*, 8783-8792.

Lee,M.H., Kwon,T.G., Park,H.S., Wozney,J.M., and Ryoo,H.M. (2003). BMP-2-induced Osterix expression is mediated by Dlx5 but is independent of Runx2. Biochem. Biophys. Res. Commun. *309*, 689-694.

Lee,S.K. and Lorenzo,J.A. (1999). Parathyroid hormone stimulates TRANCE and inhibits osteoprotegerin messenger ribonucleic acid expression in murine bone marrow cultures: correlation with osteoclast-like cell formation. Endocrinology *140*, 3552-3561.

Lee,T.H., Fevold,K.L., Muguruma,Y., Lottsfeldt,J.L., and Lee,M.Y. (1994). Relative roles of osteoclast colony-stimulating factor and macrophage colony-stimulating factor in the course of osteoclast development. Exp. Hematol. *22*, 66-73.

Lees,S. (1981). A model for bone hardness. J. Biomech. *14*, 561-567.

Li, J., Sarisu, I, Yan, X., McCabe, S, Tan, H. L., Capparelli, C., Morony, S., Elliott, R., Van, G., and Kaufman, S. Absolute requirement for the TNFR-related protein RANK during osteoclastogenesis and in the regulation of bone mass and calcium metabolism. Journal of Bone and Mineral Research Supplement 1[14], S149. 1999.

Li,J., Gorospe,M., Hutter,D., Barnes,J., Keyse,S.M., and Liu,Y. (2001). Transcriptional induction of MKP-1 in response to stress is associated with histone H3 phosphorylation-acetylation. Mol. Cell Biol. *21*, 8213-8224.

Li,J., Sarosi,I., Yan,X.Q., Morony,S., Capparelli,C., Tan,H.L., McCabe,S., Elliott,R., Scully,S., Van,G., Kaufman,S., Juan,S.C., Sun,Y., Tarpley,J., Martin,L., Christensen,K., McCabe,J., Kostenuik,P., Hsu,H., Fletcher,F., Dunstan,C.R., Lacey,D.L., and Boyle,W.J. (2000). RANK is the intrinsic hematopoietic cell surface receptor that controls osteoclastogenesis and regulation of bone mass and calcium metabolism. Proceedings of the National Academy of Sciences of the United States of America *97*, 1566-1571.

Li,N., Batzer,A., Daly,R., Yajnik,V., Skolnik,E., Chardin,P., Bar-Sagi,D., Margolis,B., and Schlessinger,J. (1993). Guanine-nucleotide-releasing factor hSos1 binds to Grb2 and links receptor tyrosine kinases to Ras signalling. Nature *363*, 85-88.

Li,X.Y. (2001). Rapid activation of p38 mitogen-activated protein kinase by corticosterone in PC12 cells. Sheng Li Xue. Bao. *53*, 414-418.

Li,Y.P., Alexander,M., Wucherpfennig,A.L., Yelick,P., Chen,W., and Stashenko,P. (1995). Cloning and complete coding sequence of a novel human cathepsin expressed in giant cells of osteoclastomas. J. Bone Miner. Res. *10*, 1197-1202.

Lian, J. B. and Stein, G. S. (1995). Development of the osteoblast phenotype: molecular mechanisms mediating osteoblast growth and differentiation. The Iowa Ortopaedic Journal 15, 118-140.

Lian,J.B. and Stein,G.S. (1993). The developmental stages of osteoblast growth and differentiation exhibit selective responses of genes to growth factors (TGF beta 1) and hormones (vitamin D and glucocorticoids). J. Oral Implantol. *19*, 95-105.

Lin,N.Y., Lin,C.T., and Chang,C.J. (2008). Modulation of immediate early gene expression by tristetraprolin in the differentiation of 3T3-L1 cells. Biochem. Biophys. Res Commun. *365*, 69-74.

Lin,Y.W., Chuang,S.M., and Yang,J.L. (2003). ERK1/2 achieves sustained activation by stimulating MAPK phosphatase-1 degradation via the ubiquitin-proteasome pathway. J. Biol. Chem. *278*, 21534-21541.

Liu,F., Malaval,L., and Aubin,J.E. (2003). Global amplification polymerase chain reaction reveals novel transitional stages during osteoprogenitor differentiation. J. Cell Sci. *116*, 1787-1796.

Liu,L., Wang,Y.X., Zhou,J., Long,F., Sun,H.W., Liu,Y., Chen,Y.Z., and Jiang,C.L. (2005). Rapid non-genomic inhibitory effects of glucocorticoids on human neutrophil degranulation. Inflamm. Res. *54*, 37-41.

Liu,Y.H., Tang,Z., Kundu,R.K., Wu,L., Luo,W., Zhu,D., Sangiorgi,F., Snead,M.L., and Maxson,R.E. (1999). Msx2 gene dosage influences the number of proliferative osteogenic cells in growth centers of the developing murine skull: a possible mechanism for MSX2-mediated craniosynostosis in humans. Dev. Biol. *205*, 260-274.

Lloyd,R.V., Erickson,L.A., Jin,L., Kulig,E., Qian,X., Cheville,J.C., and Scheithauer,B.W. (1999). p27kip1: a multifunctional cyclin-dependent kinase inhibitor with prognostic significance in human cancers. Am. J. Pathol. *154*, 313-323.

Lo,C., V, Kanis,J.A., Beneton,M.N., Bertoldo,F., Adami,S., Poggi,G., and Zanolin,M.E. (1995). Acute effects of deflazacort and prednisone on rates of mineralization and bone formation. Calcif. Tissue Int. *56*, 109-112.

Lopez,M.J. and Spencer,N.D. (2011). In vitro adult rat adipose tissue-derived stromal cell isolation and differentiation. Methods Mol. Biol. *702*, 37-46.

Lorenzo,J.A., Sousa,S.L., Fonseca,J.M., Hock,J.M., and Medlock,E.S. (1987). Colony-stimulating factors regulate the development of multinucleated osteoclasts from recently replicated cells in vitro. J. Clin. Invest *80*, 160-164.

Loveridge,N. (1999). Bone: more than a stick. J. Anim Sci. *77 Suppl 2*, 190-196.

Lukert,B.P. and Raisz,L.G. (1990). Glucocorticoid-induced osteoporosis: pathogenesis and management. Ann. Intern. Med. *112*, 352-364.

Mackie,E.J. (2003). Osteoblasts: novel roles in orchestration of skeletal architecture. Int. J. Biochem. Cell Biol. *35*, 1301-1305.

Makara,G.B. and Haller,J. (2001). Non-genomic effects of glucocorticoids in the neural system. Evidence, mechanisms and implications. Prog. Neurobiol. *65*, 367-390.

Malaval,L., Liu,F., Roche,P., and Aubin,J.E. (1999). Kinetics of osteoprogenitor proliferation and osteoblast differentiation in vitro. J. Cell Biochem. *74*, 616-627.

Mancini,T., Doga,M., Mazziotti,G., and Giustina,A. (2004). Cushing's syndrome and bone. Pituitary. *7*, 249-252.

Manelli,F. and Giustina,A. (2000). Glucocorticoid-induced osteoporosis. Trends Endocrinol. Metab *11*, 79-85.

Manolagas,S.C. (2000). Birth and death of bone cells: basic regulatory mechanisms and implications for the pathogenesis and treatment of osteoporosis. Endocr. Rev. *21*, 115-137.

Marks,S. and Odgren,P.R. (2002). Structure and development of the skeleton. In Principles of bone biology, J.P.Bilezikian, L.G.Raisz, and G.A.Rodan, eds. (New York: Academic Press), pp. 3-15.

Marshall,C.J. (1995). Specificity of receptor tyrosine kinase signaling: transient versus sustained extracellular signal-regulated kinase activation. Cell *80*, 179-185.

Mathon,N.F. and Lloyd,A.C. (2001). Cell senescence and cancer. Nat. Rev. Cancer *1*, 203-213.

Matsuguchi,T., Chiba,N., Bandow,K., Kakimoto,K., Masuda,A., and Ohnishi,T. (2009). JNK activity is essential for Atf4 expression and late-stage osteoblast differentiation. J. Bone Miner. Res. *24*, 398-410.

Matsumoto,M., Kogawa,M., Wada,S., Takayanagi,H., Tsujimoto,M., Katayama,S., Hisatake,K., and Nogi,Y. (2004). Essential role of p38 mitogen-activated protein kinase in cathepsin K gene expression during osteoclastogenesis through association of NFATc1 and PU.1. J. Biol. Chem. *279*, 45969-45979.

Matsuo,K. and Irie,N. (2008). Osteoclast-osteoblast communication. Arch. Biochem. Biophys. *473*, 201-209.

Matsuo,K., Owens,J.M., Tonko,M., Elliott,C., Chambers,T.J., and Wagner,E.F. (2000). Fosl1 is a transcriptional target of c-Fos during osteoclast differentiation. Nat. Genet. *24*, 184-187.

Matsuzaki,K., Udagawa,N., Takahashi,N., Yamaguchi,K., Yasuda,H., Shima,N., Morinaga,T., Toyama,Y., Yabe,Y., Higashio,K., and Suda,T. (1998). Osteoclast differentiation factor (ODF) induces osteoclast-like cell formation in human peripheral blood mononuclear cell cultures. Biochem. Biophys. Res. Commun. *246*, 199-204.

Mazziotti,G., Angeli,A., Bilezikian,J.P., Canalis,E., and Giustina,A. (2006). Glucocorticoid-induced osteoporosis: an update. Trends Endocrinol. Metab *17*, 144-149.

McCulloch,C.A. and Tenenbaum,H.C. (1986). Dexamethasone induces proliferation and terminal differentiation of osteogenic cells in tissue culture. Anat. Rec. *215*, 397-402.

McEwen,B.S. (2008). Central effects of stress hormones in health and disease: Understanding the protective and damaging effects of stress and stress mediators. Eur. J. Pharmacol. *583*, 174-185.

Mehrara,B.J., Mackool,R.J., McCarthy,J.G., Gittes,G.K., and Longaker,M.T. (1998). Immunolocalization of basic fibroblast growth factor and fibroblast growth factor receptor-1 and receptor-2 in rat cranial sutures. Plast. Reconstr. Surg. *102*, 1805-1817.

Mehrotra,M., Krane,S.M., Walters,K., and Pilbeam,C. (2004). Differential regulation of platelet-derived growth factor stimulated migration and proliferation in osteoblastic cells. J. Cell Biochem. *93*, 741-752.

Meloche,S. (1995). Cell cycle reentry of mammalian fibroblasts is accompanied by the sustained activation of p44mapk and p42mapk isoforms in the G1 phase and their inactivation at the G1/S transition. J. Cell Physiol *163*, 577-588.

Meloche,S. and Pouyssegur,J. (2007). The ERK1/2 mitogen-activated protein kinase pathway as a master regulator of the G1- to S-phase transition. Oncogene *26*, 3227-3239.

Meloche,S., Seuwen,K., Pages,G., and Pouyssegur,J. (1992). Biphasic and synergistic activation of p44mapk (ERK1) by growth factors: correlation between late phase activation and mitogenicity. Mol Endocrinol *6*, 845-854.

Menaa,C., Barsony,J., Reddy,S.V., Cornish,J., Cundy,T., and Roodman,G.D. (2000). 1,25-Dihydroxyvitamin D3 hypersensitivity of osteoclast precursors from patients with Paget's disease. J. Bone Miner. Res. *15*, 228-236.

Merchant-Larios,H., Mendlovic,F., and Alvarez-Buylla,A. (1985). Characterization of alkaline phosphatase from primordial germ cells and ontogenesis of this enzyme in the mouse. Differentiation *29*, 145-151.

Miao,D. and Scutt,A. (2002). Histochemical localization of alkaline phosphatase activity in decalcified bone and cartilage. J. Histochem. Cytochem. *50*, 333-340.

Mikami,Y., Omoteyama,K., Kato,S., and Takagi,M. (2007). Inductive effects of dexamethasone on the mineralization and the osteoblastic gene expressions in mature osteoblast-like ROS17/2.8 cells. Biochem. Biophys. Res. Commun. *362*, 368-373.

Miraoui,H., Oudina,K., Petite,H., Tanimoto,Y., Moriyama,K., and Marie,P.J. (2009). Fibroblast growth factor receptor 2 promotes osteogenic differentiation in mesenchymal cells via ERK1/2 and protein kinase C signaling. J. Biol. Chem. *284*, 4897-4904.

Mistry A.S and Mikos,A.G. (2005). Anatomy and Physiology of bone. In Regenerative medicine, Clinical and Preclinical Applications, Tissue Engineering Strategies for Bone Regeneration, Yannas I, ed. Springer-Verlag Berlin Heidelberg), pp. 4-22.

Miyazono,A., Yamada,A., Morimura,N., Takami,M., Suzuki,D., Kobayashi,M., Tezuka,K., Yamamoto,M., and Kamijo,R. (2007). TGF-beta suppresses POEM expression through ERK1/2 and JNK in osteoblasts. FEBS Lett. *581*, 5321-5326.

Mizuno,E., Iura,T., Mukai,A., Yoshimori,T., Kitamura,N., and Komada,M. (2005). Regulation of epidermal growth factor receptor down-regulation by UBPY-mediated deubiquitination at endosomes. Mol Biol. Cell *16*, 5163-5174.

Mohan,S. and Baylink,D.J. (1991). Bone growth factors. Clin. Orthop. Relat Res 30-48.

Mohan,S., Bautista,C.M., Herring,S.J., Linkhart,T.A., and Baylink,D.J. (1990). Development of valid methods to measure insulin-like growth factors-I and -II in bone cell-conditioned medium. Endocrinology *126*, 2534-2542.

Montessuit,C., Caverzasio,J., and Bonjour,J.P. (1991). Characterization of a Pi transport system in cartilage matrix vesicles. Potential role in the calcification process. J. Biol. Chem. *266*, 17791-17797.

Moodie,S.A., Willumsen,B.M., Weber,M.J., and Wolfman,A. (1993). Complexes of Ras.GTP with Raf-1 and mitogen-activated protein kinase kinase. Science *260*, 1658-1661.

Morel,G., Chavassieux,P., Barenton,B., Dubois,P.M., Meunier,P.J., and Boivin,G. (1993). Evidence for a direct effect of growth hormone on osteoblasts. Cell Tissue Res. *273*, 279-286.

Mosmann,T. (1983). Rapid colorimetric assay for cellular growth and survival: application to proliferation and cytotoxicity assays. J. Immunol. Methods *65*, 55-63.

Mourey,R.J., Vega,Q.C., Campbell,J.S., Wenderoth,M.P., Hauschka,S.D., Krebs,E.G., and Dixon,J.E. (1996). A Novel Cytoplasmic Dual Specificity Protein Tyrosine Phosphatase Implicated in Muscle and Neuronal Differentiation. Journal of Biological Chemistry *271*, 3795-3802.

Muda,M., Boschert,U., Dickinson,R., Martinou,J.C., Martinou,I., Camps,M., Schlegel,W., and Arkinstall,S. (1996b). MKP-3, a Novel Cytosolic Protein-tyrosine Phosphatase That Exemplifies a New Class of Mitogen-activated Protein Kinase Phosphatase. Journal of Biological Chemistry *271*, 4319-4326.

Muda,M., Theodosiou,A., Rodrigues,N., Boschert,U., Camps,M., Gillieron,C., Davies,K., Ashworth,A., and Arkinstall,S. (1996a). The dual specificity phosphatases M3/6 and MKP-3 are highly selective for inactivation of distinct mitogen-activated protein kinases. J Biol. Chem. *271*, 27205-27208.

Mundlos,S., Otto,F., Mundlos,C., Mulliken,J.B., Aylsworth,A.S., Albright,S., Lindhout,D., Cole,W.G., Henn,W., Knoll,J.H., Owen,M.J., Mertelsmann,R., Zabel,B.U., and Olsen,B.R. (1997). Mutations involving the transcription factor CBFA1 cause cleidocranial dysplasia. Cell *89*, 773-779.

Murphy,L.O. and Blenis,J. (2006). MAPK signal specificity: the right place at the right time. Trends Biochem. Sci. *31*, 268-275.

Murphy,L.O., Smith,S., Chen,R.H., Fingar,D.C., and Blenis,J. (2002). Molecular interpretation of ERK signal duration by immediate early gene products. Nat. Cell Biol. *4*, 556-564.

Nakagawa,N., Kinosaki,M., Yamaguchi,K., Shima,N., Yasuda,H., Yano,K., Morinaga,T., and Higashio,K. (1998). RANK is the essential signaling receptor for osteoclast differentiation factor in osteoclastogenesis. Biochem. Biophys. Res. Commun. *253*, 395-400.

Nakashima,A., Katagiri,T., and Tamura,M. (2005). Cross-talk between Wnt and bone morphogenetic protein 2 (BMP-2) signaling in differentiation pathway of C2C12 myoblasts. J Biol. Chem. *280*, 37660-37668.

Nakashima,K., Zhou,X., Kunkel,G., Zhang,Z., Deng,J.M., Behringer,R.R., and de,C.B. (2002). The novel zinc finger-containing transcription factor osterix is required for osteoblast differentiation and bone formation. Cell *108*, 17-29.

Nakata,K., Suzuki,Y., Inoue,T., Ra,C., Yakura,H., and Mizuno,K. (2011). Deficiency of SHP1 leads to sustained and increased ERK activation in mast cells, thereby inhibiting IL-3-dependent proliferation and cell death. Molecular Immunology *48*, 472-480.

Narisawa,S., Frohlander,N., and Millan,J.L. (1997). Inactivation of two mouse alkaline phosphatase genes and establishment of a model of infantile hypophosphatasia. Dev. Dyn. *208*, 432-446.

Narita,M., Nunez,S., Heard,E., Narita,M., Lin,A.W., Hearn,S.A., Spector,D.L., Hannon,G.J., and Lowe,S.W. (2003). Rb-mediated heterochromatin formation and silencing of E2F target genes during cellular senescence. Cell *113*, 703-716.

Nesbitt,S.A. and Horton,M.A. (1997). Trafficking of matrix collagens through bone-resorbing osteoclasts. Science *276*, 266-269.

Newberry,E.P., Latifi,T., and Towler,D.A. (1998). Reciprocal regulation of osteocalcin transcription by the homeodomain proteins Msx2 and Dlx5. Biochemistry *37*, 16360-16368.

Newton,R. (2000). Molecular mechanisms of glucocorticoid action: what is important? Thorax *55*, 603-613.

Nguyen,T.T., Scimeca,J.C., Filloux,C., Peraldi,P., Carpentier,J.L., and Van,O.E. (1993). Co-regulation of the mitogen-activated protein kinase, extracellular signal-regulated kinase 1, and the 90-kDa ribosomal S6 kinase in PC12 cells. Distinct effects of the neurotrophic factor, nerve growth factor, and the mitogenic factor, epidermal growth factor. J Biol. Chem. *268*, 9803-9810.

Nicoletti-Carvalho,J.E., Lellis-Santos,C., Yamanaka,T.S., Nogueira,T.C., Caperuto,L.C., Leite,A.R., Anhe,G.F., and Bordin,S. (2010). MKP-1 mediates glucocorticoid-induced ERK1/2 dephosphorylation and reduction in pancreatic ss-cell proliferation in islets from early lactating mothers. Am. J Physiol Endocrinol. Metab *299*, E1006-E1015.

Nijweide,P.J., Burger,E.H., and Klein-Nulend,J. (2002). The osteocyte. In Principles of bone biology, J.P.Bilezikian, L.G.Raisz, and G.A.Rodan, eds. (New York: Academic Press), pp. 93-107.

Nilsson,A., Ohlsson,C., Isaksson,O.G., Lindahl,A., and Isgaard,J. (1994). Hormonal regulation of longitudinal bone growth. Eur. J. Clin. Nutr. *48 Suppl 1*, S150-S158.

Noble,B. (2003). Bone microdamage and cell apoptosis. Eur. Cell Mater. *6*, 46-55.

Noble,B.S. (2008). The osteocyte lineage. Arch. Biochem. Biophys. *473*, 106-111.

Noguchi,T., Metz,R., Chen,L., Mattei,M.G., Carrasco,D., and Bravo,R. (1993). Structure, mapping, and expression of erp, a growth factor-inducible gene encoding a nontransmembrane protein tyrosine phosphatase, and effect of ERP on cell growth. Mol. Cell Biol. *13*, 5195-5205.

Nohe,A., Keating,E., Knaus,P., and Petersen,N.O. (2004). Signal transduction of bone morphogenetic protein receptors. Cell Signal. *16*, 291-299.

Nohe,A., Keating,E., Underhill,T.M., Knaus,P., and Petersen,N.O. (2003). Effect of the distribution and clustering of the type I A BMP receptor (ALK3) with the type II BMP receptor on the activation of signalling pathways. J. Cell Sci. *116*, 3277-3284.

O'Brien,T.G. and Diamond,L. (1978). Metabolism of tritium-labeled 12-O-tetradecanoylphorbol-13-acetate by cells in culture. Cancer Res. *38*, 2562-2566.

O'Brien,T.G. and Saladik,D. (1980). Differences in the metabolism of 12-O-[3H]tetradecanoylphorbol-13-acetate and [3H]phorbol-12,13-didecanoate by cells in culture. Cancer Res. *40*, 4433-4437.

O'Brien,C.A., Jia,D., Plotkin,L.I., Bellido,T., Powers,C.C., Stewart,S.A., Manolagas,S.C., and Weinstein,R.S. (2004). Glucocorticoids act directly on osteoblasts and osteocytes to induce their apoptosis and reduce bone formation and strength. Endocrinology *145*, 1835-1841.

Ogawa,R., Mizuno,H., Watanabe,A., Migita,M., Shimada,T., and Hyakusoku,H. (2004). Osteogenic and chondrogenic differentiation by adipose-derived stem cells harvested from GFP transgenic mice. Biochem. Biophys. Res. Commun. *313*, 871-877.

Oh-hora,M., Ogata,M., Mori,Y., Adachi,M., Imai,K., Kosugi,A., and Hamaoka,T. (1999). Direct suppression of TCR-mediated activation of extracellular signal-regulated kinase by leukocyte protein tyrosine phosphatase, a tyrosine-specific phosphatase. J. Immunol. *163*, 1282-1288.

Oleksik,A., Ott,S.M., Vedi,S., Bravenboer,N., Compston,J., and Lips,P. (2000). Bone structure in patients with low bone mineral density with or without vertebral fractures. J. Bone Miner. Res. *15*, 1368-1375.

Orimo,H. (2010). The mechanism of mineralization and the role of alkaline phosphatase in health and disease. J. Nippon Med. Sch *77*, 4-12.

Ortuno,M.J., Ruiz-Gaspa,S., Rodriguez-Carballo,E., Susperregui,A.R., Bartrons,R., Rosa,J.L., and Ventura,F. (2010). p38 regulates expression of osteoblast-specific genes by phosphorylation of osterix. J Biol. Chem. *285*, 31985-31994.

Otto,F., Thornell,A.P., Crompton,T., Denzel,A., Gilmour,K.C., Rosewell,I.R., Stamp,G.W., Beddington,R.S., Mundlos,S., Olsen,B.R., Selby,P.B., and Owen,M.J. (1997). Cbfa1, a candidate gene for cleidocranial dysplasia syndrome, is essential for osteoblast differentiation and bone development. Cell *89*, 765-771.

Owen,M.E. (1998). The marrow stromal cells system. In Marrow stromal cells in culture., J.N.Beresford and M.E.Owen, eds. (Cambridge: Cambridge University Press), pp. 88-110.

Owen,T.A., Bortell,R., Yocum,S.A., Smock,S.L., Zhang,M., Abate,C., Shalhoub,V., Aronin,N., Wright,K.L., van Wijnen,A.J., and . (1990). Coordinate occupancy of AP-1 sites in the vitamin D-responsive and CCAAT box elements by Fos-Jun in the osteocalcin gene: model for phenotype suppression of transcription. Proc. Natl. Acad. Sci. U. S. A *87*, 9990-9994.

Owens,D.M. and Keyse,S.M. (2007). Differential regulation of MAP kinase signalling by dual-specificity protein phosphatases. Oncogene *26*, 3203-3213.

Ozawa,H., Hoshi,K., and Amizuka,N. (2008). Current concepts of bone mineralization. Journal of Oral Bioscience *50*, 1-14.

Palmqvist,P., Persson,E., Conaway,H.H., and Lerner,U.H. (2002). IL-6, Leukemia Inhibitory Factor, and Oncostatin M Stimulate Bone Resorption and Regulate the Expression of Receptor Activator of NF-+¦B Ligand, Osteoprotegerin, and Receptor Activator of NF-+¦B in Mouse Calvariae. The Journal of Immunology *169*, 3353-3362.

Palumbo,C. (1986). A three-dimensional ultrastructural study of osteoid-osteocytes in the tibia of chick embryos. Cell Tissue Res. *246*, 125-131.

Palumbo,C., Palazzini,S., Zaffe,D., and Marotti,G. (1990). Osteocyte differentiation in the tibia of newborn rabbit: an ultrastructural study of the formation of cytoplasmic processes. Acta Anat. (Basel) *137*, 350-358.

Parfitt,A.M. (1982). The coupling of bone formation to bone resorption: a critical analysis of the concept and of its relevance to the pathogenesis of osteoporosis. Metab Bone Dis. Relat Res. *4*, 1-6.

Parfitt,A.M. (1984). The cellular basis of bone remodeling: the quantum concept reexamined in light of recent advances in the cell biology of bone. Calcif. Tissue Int. *36 Suppl 1*, S37-S45.

Parfitt,A.M. (1994). Osteonal and hemi-osteonal remodeling: the spatial and temporal framework for signal traffic in adult human bone. J. Cell Biochem. *55*, 273-286.

Parfitt,A.M. (2000). The mechanism of coupling: a role for the vasculature. Bone *26*, 319-323.

Parfitt,A.M. (2002). Targeted and nontargeted bone remodeling: relationship to basic multicellular unit origination and progression. Bone *30*, 5-7.

Parfitt,A.M., Mundy,G.R., Roodman,G.D., Hughes,D.E., and Boyce,B.F. (1996). A new model for the regulation of bone resorption, with particular reference to the effects of bisphosphonates. J. Bone Miner. Res. *11*, 150-159.

Partington,G.A., Fuller,K., Chambers,T.J., and Pondel,M. (2004). Mitf-PU.1 interactions with the tartrate-resistant acid phosphatase gene promoter during osteoclast differentiation. Bone *34*, 237-245.

Patterson,K.I., Brummer,T., O'Brien,P.M., and Daly,R.J. (2009). Dual-specificity phosphatases: critical regulators with diverse cellular targets. Biochem. J. *418*, 475-489.

Payne,D.M., Rossomando,A.J., Martino,P., Erickson,A.K., Her,J.H., Shabanowitz,J., Hunt,D.F., Weber,M.J., and Sturgill,T.W. (1991). Identification of the regulatory phosphorylation sites in pp42/mitogen-activated protein kinase (MAP kinase). EMBO J. *10*, 885-892.

Peng,S., Zhou,G., Luk,K.D., Cheung,K.M., Li,Z., Lam,W.M., Zhou,Z., and Lu,W.W. (2009). Strontium promotes osteogenic differentiation of mesenchymal stem cells through the Ras/MAPK signaling pathway. Cell Physiol Biochem. *23*, 165-174.

Peress,N.S., Anderson,H.C., and Sajdera,S.W. (1974). The lipids of matrix vesicles from bovine fetal epiphyseal cartilage. Calcif. Tissue Res. *14*, 275-281.

Philippe,J. and Missotten,M. (1990). Dexamethasone inhibits insulin biosynthesis by destabilizing insulin messenger ribonucleic acid in hamster insulinoma cells. Endocrinology *127*, 1640-1645.

Phimphilai,M., Zhao,Z., Boules,H., Roca,H., and Franceschi,R.T. (2006). BMP signaling is required for RUNX2-dependent induction of the osteoblast phenotype. J. Bone Miner. Res. *21*, 637-646.

Phinney,D.G., Kopen,G., Isaacson,R.L., and Prockop,D.J. (1999). Plastic adherent stromal cells from the bone marrow of commonly used strains of inbred mice: variations in yield, growth, and differentiation. J. Cell Biochem. *72*, 570-585.

Picton,M.L., Moore,P.R., Mawer,E.B., Houghton,D., Freemont,A.J., Hutchison,A.J., Gokal,R., and Hoyland,J.A. (2000). Down-regulation of human osteoblast PTH/PTHrP receptor mRNA in end-stage renal failure. Kidney Int *58*, 1440-1449.

Pierotti,S., Gandini,L., Lenzi,A., and Isidori,A.M. (2008). Pre-receptorial regulation of steroid hormones in bone cells: insights on glucocorticoid-induced osteoporosis. J. Steroid Biochem. Mol. Biol. *108*, 292-299.

Plotkin,L.I., Manolagas,S.C., and Bellido,T. (2002). Transduction of cell survival signals by connexin-43 hemichannels. J Biol. Chem. *277*, 8648-8657.

Pockwinse,S.M., Stein,J.L., Lian,J.B., and Stein,G.S. (1995). Developmental stage-specific cellular responses to vitamin D and glucocorticoids during differentiation of the osteoblast phenotype: interrelationship of morphology and gene expression by in situ hybridization. Exp. Cell Res. *216*, 244-260.

Pockwinse,S.M., Wilming,L.G., Conlon,D.M., Stein,G.S., and Lian,J.B. (1992). Expression of cell growth and bone specific genes at single cell resolution during development of bone tissue-like organization in primary osteoblast cultures. J. Cell Biochem. *49*, 310-323.

Prockop,D.J. (1997). Marrow stromal cells as stem cells for nonhematopoietic tissues. Science *276*, 71-74.

Proff,P. and Romer,P. (2009). The molecular mechanism behind bone remodelling: a review. Clin. Oral Investig. *13*, 355-362.

Prummel,M.F., Wiersinga,W.M., Lips,P., Sanders,G.T., and Sauerwein,H.P. (1991). The course of biochemical parameters of bone turnover during treatment with corticosteroids. J. Clin. Endocrinol. Metab *72*, 382-386.

Pulido,R., Zuniga,A., and Ullrich,A. (1998). PTP-SL and STEP protein tyrosine phosphatases regulate the activation of the extracellular signal-regulated kinases ERK1 and ERK2 by association through a kinase interaction motif. EMBO J. *17*, 7337-7350.

Qiao,M., Shapiro,P., Kumar,R., and Passaniti,A. (2004). Insulin-like growth factor-1 regulates endogenous RUNX2 activity in endothelial cells through a phosphatidylinositol 3-kinase/ERK-dependent and Akt-independent signaling pathway. J. Biol. Chem. *279*, 42709-42718.

Qiu,J., Wang,P., Jing,Q., Zhang,W., Li,X., Zhong,Y., Sun,G., Pei,G., and Chen,Y. (2001). Rapid activation of ERK1/2 mitogen-activated protein kinase by corticosterone in PC12 cells. Biochem. Biophys. Res. Commun. *287*, 1017-1024.

Rawlinson,S.C., Mosley,J.R., Suswillo,R.F., Pitsillides,A.A., and Lanyon,L.E. (1995). Calvarial and limb bone cells in organ and monolayer culture do not show the same early responses to dynamic mechanical strain. J. Bone Miner. Res. *10*, 1225-1232.

Reffas,S. and Schlegel,W. (2000). Compartment-specific regulation of extracellular signal-regulated kinase (ERK) and c-Jun N-terminal kinase (JNK) mitogen-activated protein kinases (MAPKs) by ERK-dependent and non-ERK-dependent inductions of MAPK phosphatase (MKP)-3 and MKP-1 in differentiating P19 cells. Biochem. J. *352 Pt 3*, 701-708.
Reya,T. and Clevers,H. (2005). Wnt signalling in stem cells and cancer. Nature *434*, 843-850.

Rho,J.Y., Kuhn-Spearing,L., and Zioupos,P. (1998). Mechanical properties and the hierarchical structure of bone. Med. Eng Phys. *20*, 92-102.

Rice,D.P., Aberg,T., Chan,Y., Tang,Z., Kettunen,P.J., Pakarinen,L., Maxson,R.E., and Thesleff,I. (2000). Integration of FGF and TWIST in calvarial bone and suture development. Development *127*, 1845-1855.

Rickard,D.J., Sullivan,T.A., Shenker,B.J., Leboy,P.S., and Kazhdan,I. (1994). Induction of rapid osteoblast differentiation in rat bone marrow stromal cell cultures by dexamethasone and BMP-2. Dev. Biol. *161*, 218-228.

Roberts,S., Narisawa,S., Harmey,D., Millan,J.L., and Farquharson,C. (2007). Functional involvement of PHOSPHO1 in matrix vesicle-mediated skeletal mineralization. J. Bone Miner. Res. *22*, 617-627.

Robinson,M.J. and Cobb,M.H. (1997). Mitogen-activated protein kinase pathways. Curr. Opin. Cell Biol. *9*, 180-186.

Robinson,M.J., Stippec,S.A., Goldsmith,E., White,M.A., and Cobb,M.H. (1998). A constitutively active and nuclear form of the MAP kinase ERK2 is sufficient for neurite outgrowth and cell transformation. Curr. Biol. *8*, 1141-1150.

Robling,A.G., Castillo,A.B., and Turner,C.H. (2006). Biomechanical and molecular regulation of bone remodeling. Annu. Rev. Biomed. Eng *8*, 455-498.

Rodan, G. A. and Martin, T. J. (1981). Role of osteoblasts in hormonal control of bone resorption: A hypothesis. Calcif.Tissue Int. [33], 349-351.

Rogatsky,I., Trowbridge,J.M., and Garabedian,M.J. (1997). Glucocorticoid receptor-mediated cell cycle arrest is achieved through distinct cell-specific transcriptional regulatory mechanisms. Mol. Cell Biol. *17*, 3181-3193.

Roger,T., Chanson,A.L., Knaup-Reymond,M., and Calandra,T. (2005). Macrophage migration inhibitory factor promotes innate immune responses by suppressing glucocorticoid-induced expression of mitogen-activated protein kinase phosphatase-1. Eur. J Immunol. *35*, 3405-3413.

Roodman,G.D. (1992). Interleukin-6: an osteotropic factor? J Bone Miner Res *7*, 475-478.

Roodman,G.D. (2006). Regulation of osteoclast differentiation. Ann. N. Y. Acad. Sci. *1068*, 100-109.

Roovers,K. and Assoian,R.K. (2000). Integrating the MAP kinase signal into the G1 phase cell cycle machinery. Bioessays *22*, 818-826.

Rosen,C.J. and Bilezikian,J.P. (2001). Clinical review 123: Anabolic therapy for osteoporosis. J. Clin. Endocrinol Metab *86*, 957-964.

Rosen,C.J. and Rackoff,P.J. (2001). Emerging anabolic treatments for osteoporosis. Rheum. Dis. Clin. North Am. *27*, 215-33, viii.

Rosen,V. and Wozney,J.M. (2002). Bone morphogenetic proteins. In Principles of Bone Biology, J.P.Bilezikian, L.G.Raisz, and G.A.Rodan, eds. (San Diego: Academic Press), pp. 919-928.

Ross,F.P. and Teitelbaum,S.L. (2005). alphavbeta3 and macrophage colony-stimulating factor: partners in osteoclast biology. Immunol. Rev. *208*, 88-105.

Rossert,J. and de Combrugghe,B. (2002). Type I Collagen. In Principles of Bone Biology, J.P.Bilezikian, L.G.Raisz, and G.A.Rodan, eds. (San Diego: Academic Press), pp. 189-210.

Rubin,J. and Rubin,C.T. (2009). Biology, physiology and morphology of bone. In Kelley's Textbook of Rheumatology., G.S.Firestein, ed. (Philadelphia: Elsevier Incorporated), p. 71.

Rubin,J., Biskobing,D.M., Jadhav,L., Fan,D., Nanes,M.S., Perkins,S., and Fan,X. (1998). Dexamethasone promotes expression of membrane-bound macrophage colony-stimulating factor in murine osteoblast-like cells. Endocrinology *139*, 1006-1012.

Rydziel,S., Ladd,C., McCarthy,T.L., Centrella,M., and Canalis,E. (1992). Determination and expression of platelet-derived growth factor-AA in bone cell cultures. Endocrinology *130*, 1916-1922.

Ryoo,H.M., Hoffmann,H.M., Beumer,T., Frenkel,B., Towler,D.A., Stein,G.S., Stein,J.L., van Wijnen,A.J., and Lian,J.B. (1997). Stage-specific expression of Dlx-5 during osteoblast differentiation: involvement in regulation of osteocalcin gene expression. Mol. Endocrinol. *11*, 1681-1694.

Sakai,D.D., Helms,S., Carlstedt-Duke,J., Gustafsson,J.A., Rottman,F.M., and Yamamoto,K.R. (1988). Hormone-mediated repression: a negative glucocorticoid response element from the bovine prolactin gene. Genes Dev. *2*, 1144-1154.

Sakakura,M., Takebe,K., and Nakagawa,S. (1975). Inhibition of luteinizing hormone secretion induced by synthetic LRH by long-term treatment with glucocorticoids in human subjects. J. Clin. Endocrinol. Metab *40*, 774-779.

Salles,J.P., De Vries,C.P., Netelenbos,J.C., and Slootweg,M.C. (1994). Dexamethasone increases and serum decreases growth hormone receptor binding to UMR-106.01 rat osteosarcoma cells. Endocrinology *134*, 1455-1459.

Salo,J., Lehenkari,P., Mulari,M., Metsikko,K., and Vaananen,H.K. (1997). Removal of osteoclast bone resorption products by transcytosis. Science *276*, 270-273.

Sancar,A., Lindsey-Boltz,L.A., Unsal-Kacmaz,K., and Linn,S. (2004). Molecular mechanisms of mammalian DNA repair and the DNA damage checkpoints. Annu. Rev. Biochem. *73*, 39-85.

Sarkozi,R., Miller,B., Pollack,V., Feifel,E., Mayer,G., Sorokin,A., and Schramek,H. (2007). ERK1/2-driven and MKP-mediated inhibition of EGF-induced ERK5 signaling in human proximal tubular cells. J Cell Physiol *211*, 88-100.

Satokata,I., Ma,L., Ohshima,H., Bei,M., Woo,I., Nishizawa,K., Maeda,T., Takano,Y., Uchiyama,M., Heaney,S., Peters,H., Tang,Z., Maxson,R., and Maas,R. (2000). Msx2 deficiency in mice causes pleiotropic defects in bone growth and ectodermal organ formation. Nat. Genet. *24*, 391-395.

Saxena,M. and Mustelin,T. (2000). Extracellular signals and scores of phosphatases: all roads lead to MAP kinase. Semin. Immunol. *12*, 387-396.

Saxena,M., Williams,S., Brockdorff,J., Gilman,J., and Mustelin,T. (1999). Inhibition of T cell signaling by mitogen-activated protein kinase-targeted hematopoietic tyrosine phosphatase (HePTP). J. Biol. Chem. *274*, 11693-11700.

Scherrer,L.C., Dalman,F.C., Massa,E., Meshinchi,S., and Pratt,W.B. (1990). Structural and functional reconstitution of the glucocorticoid receptor-hsp90 complex. J. Biol. Chem. *265*, 21397-21400.

Scheven,B.A., Kawilarang-de Haas,E.W., Wassenaar,A.M., and Nijweide,P.J. (1986). Differentiation kinetics of osteoclasts in the periosteum of embryonic bones in vivo and in vitro. Anat. Rec. *214*, 418-423.

Schindeler,A. and Little,D.G. (2006). Ras-MAPK signaling in osteogenic differentiation: friend or foe? J Bone Miner Res *21*, 1331-1338.

Schmitt,E., Paquet,C., Beauchemin,M., and Bertrand,R. (2007). DNA-damage response network at the crossroads of cell-cycle checkpoints, cellular senescence and apoptosis. J. Zhejiang. Univ Sci. B *8*, 377-397.

Schneider,G.B. and Relfson,M. (1988). A bone marrow fraction enriched for granulocyte-macrophage progenitors gives rise to osteoclasts in vitro. Bone *9*, 303-308.

Schoneveld,O.J., Gaemers,I.C., and Lamers,W.H. (2004). Mechanisms of glucocorticoid signalling. Biochim. Biophys. Acta *1680*, 114-128.

Seeman,E. and Delmas,P.D. (2006). Bone quality--the material and structural basis of bone strength and fragility. N. Engl. J. Med. *354*, 2250-2261.

Seger,R. and Krebs,E.G. (1995). The MAPK signaling cascade. FASEB J *9*, 726-735.

Seta,K.A., Kim,R., Kim,H.W., Millhorn,D.E., and Beitner-Johnson,D. (2001). Hypoxia-induced regulation of MAPK phosphatase-1 as identified by subtractive suppression hybridization and cDNA microarray analysis. J Biol. Chem. *276*, 44405-44412.

Sewing,A., Wiseman,B., Lloyd,A.C., and Land,H. (1997). High-intensity Raf signal causes cell cycle arrest mediated by p21Cip1. Mol. Cell Biol. *17*, 5588-5597.

Shalhoub,V., Conlon,D., Tassinari,M., Quinn,C., Partridge,N., Stein,G.S., and Lian,J.B. (1992). Glucocorticoids promote development of the osteoblast phenotype by selectively modulating expression of cell growth and differentiation associated genes. J. Cell Biochem. *50*, 425-440.

Shankey,T.V., Rabinovitch,P.S., Bagwell,B., Bauer,K.D., Duque,R.E., Hedley,D.W., Mayall,B.H., Wheeless,L., and Cox,C. (1993). Guidelines for implementation of clinical DNA cytometry. International Society for Analytical Cytology. Cytometry *14*, 472-477.

Shaul,Y.D. and Seger,R. (2007a). The MEK/ERK cascade: from signaling specificity to diverse functions. Biochim. Biophys. Acta *1773*, 1213-1226.

Shaul,Y.D. and Seger,R. (2007b). The MEK/ERK cascade: From signaling specificity to diverse functions. Biochimica et Biophysica Acta (BBA) - Molecular Cell Research *1773*, 1213-1226.

Shi,Z.Q., Yu,D.H., Park,M., Marshall,M., and Feng,G.S. (2000). Molecular mechanism for the Shp-2 tyrosine phosphatase function in promoting growth factor stimulation of Erk activity. Mol. Cell Biol. *20*, 1526-1536.

Shioi,A., Teitelbaum,S.L., Ross,F.P., Welgus,H.G., Suzuki,H., Ohara,J., and Lacey,D.L. (1991). Interleukin 4 inhibits murine osteoclast formation in vitro. J. Cell Biochem. *47*, 272-277.

Shur,I., Socher,R., and Benayahu,D. (2005). Dexamethasone regulation of cFos mRNA in osteoprogenitors. J Cell Physiol *202*, 240-245.

Siegel,R.C. (1974). Biosynthesis of Collagen Crosslinks: Increased Activity of Purified Lysyl Oxidase with Reconstituted Collagen Fibrils. Proceedings of the National Academy of Sciences of the United States of America *71*, 4826-4830.

Simonet,W.S., Lacey,D.L., Dunstan,C.R., Kelley,M., Chang,M.S., Luthy,R., Nguyen,H.Q., Wooden,S., Bennett,L., Boone,T., Shimamoto,G., DeRose,M., Elliott,R., Colombero,A., Tan,H.L., Trail,G., Sullivan,J., Davy,E., Bucay,N., Renshaw-Gegg,L., Hughes,T.M., Hill,D., Pattison,W., Campbell,P., Sander,S., Van,G., Tarpley,J., Derby,P., Lee,R., and Boyle,W.J. (1997).

Osteoprotegerin: a novel secreted protein involved in the regulation of bone density. Cell *89*, 309-319.

Simons,S.S., Jr. (2008). What goes on behind closed doors: physiological versus pharmacological steroid hormone actions. Bioessays *30*, 744-756.

Sims,N.A. and Gooi,J.H. (2008). Bone remodeling: Multiple cellular interactions required for coupling of bone formation and resorption. Semin. Cell Dev. Biol. *19*, 444-451.

Singh,H., Singh,J.R., Dhillon,V.S., Bali,D., and Paul,H. (1994). In vitro and in vivo genotoxicity evaluation of hormonal drugs. II. Dexamethasone. Mutat. Res. *308*, 89-97.

Sipos,W., Pietschmann,P., Rauner,M., Kerschan-Schindl,K., and Patsch,J. (2009). Pathophysiology of osteoporosis. Wien. Med. Wochenschr. *159*, 230-234.

Skolnik,E.Y., Batzer,A., Li,N., Lee,C.H., Lowenstein,E., Mohammadi,M., Margolis,B., and Schlessinger,J. (1993). The function of GRB2 in linking the insulin receptor to Ras signaling pathways. Science *260*, 1953-1955.

Slack,D.N., Seternes,O.M., Gabrielsen,M., and Keyse,S.M. (2001). Distinct binding determinants for ERK2/p38alpha and JNK map kinases mediate catalytic activation and substrate selectivity of map kinase phosphatase-1. J. Biol. Chem. *276*, 16491-16500.

Slootweg,M.C., Swolin,D., Netelenbos,J.C., Isaksson,O.G., and Ohlsson,C. (1997). Estrogen enhances growth hormone receptor expression and growth hormone action in rat osteosarcoma cells and human osteoblast-like cells. J. Endocrinol. *155*, 159-164.

Slupsky,C.M., Gentile,L.N., Donaldson,L.W., Mackereth,C.D., Seidel,J.J., Graves,B.J., and McIntosh,L.P. (1998). Structure of the Ets-1 pointed domain and mitogen-activated protein kinase phosphorylation site. Proc. Natl. Acad. Sci. U. S. A *95*, 12129-12134.

Smith,E., Coetzee,G.A., and Frenkel,B. (2002). Glucocorticoids inhibit cell cycle progression in differentiating osteoblasts via glycogen synthase kinase-3beta. J. Biol. Chem. *277*, 18191-18197.

Smith,E., Redman,R.A., Logg,C.R., Coetzee,G.A., Kasahara,N., and Frenkel,B. (2000). Glucocorticoids inhibit developmental stage-specific osteoblast cell cycle. Dissociation of cyclin A-cyclin-dependent kinase 2 from E2F4-p130 complexes. J. Biol. Chem. *275*, 19992-20001.

Solmesky,L., Lefler,S., Jacob-Hirsch,J., Bulvik,S., Rechavi,G., and Weil,M. (2010). Serum free cultured bone marrow mesenchymal stem cells as a platform to characterize the effects of specific molecules. PLoS. One. *5*.

Sontag,E., Fedorov,S., Kamibayashi,C., Robbins,D., Cobb,M., and Mumby,M. (1993). The interaction of SV40 small tumor antigen with protein phosphatase 2A stimulates the map kinase pathway and induces cell proliferation. Cell *75*, 887-897.

Sowa,H., Kaji,H., Yamaguchi,T., Sugimoto,T., and Chihara,K. (2002). Activations of ERK1/2 and JNK by transforming growth factor beta negatively regulate Smad3-induced alkaline phosphatase activity and mineralization in mouse osteoblastic cells. J Biol. Chem. *277*, 36024-36031.

Stein,G.S. and Lian,J.B. (1993). Molecular mechanisms mediating proliferation/differentiation interrelationships during progressive development of the osteoblast phenotype. Endocr. Rev. *14*, 424-442.

Stein,G.S., Lian,J.B., and Owen,T.A. (1990). Relationship of cell growth to the regulation of tissue-specific gene expression during osteoblast differentiation. FASEB J. *4*, 3111-3123.

Stein,G.S., Lian,J.B., Stein,J.L., van Wijnen,A.J., and Montecino,M. (1996). Transcriptional control of osteoblast growth and differentiation. Physiol Rev. *76*, 593-629.

Stewart,P.M. and Krozowski,Z.S. (1999). 11 beta-Hydroxysteroid dehydrogenase. Vitam. Horm. *57*, 249-324.

Strauss,P.G., Closs,E.I., Schmidt,J., and Erfle,V. (1990). Gene expression during osteogenic differentiation in mandibular condyles in vitro. J Cell Biol. *110*, 1369-1378.

Stromstedt,P.E., Poellinger,L., Gustafsson,J.A., and Carlstedt-Duke,J. (1991). The glucocorticoid receptor binds to a sequence overlapping the TATA box of the human osteocalcin promoter: a potential mechanism for negative regulation. Mol. Cell Biol. *11*, 3379-3383.

Subramaniam,M., Colvard,D., Keeting,P.E., Rasmussen,K., Riggs,B.L., and Spelsberg,T.C. (1992). Glucocorticoid regulation of alkaline phosphatase, osteocalcin, and proto-oncogenes in normal human osteoblast-like cells. J. Cell Biochem. *50*, 411-424.

Suda,T., Takahashi,N., Udagawa,N., Jimi,E., Gillespie,M.T., and Martin,T.J. (1999). Modulation of osteoclast differentiation and function by the new members of the tumor necrosis factor receptor and ligand families. Endocr. Rev. *20*, 345-357.

Sun,H., Charles,C.H., Lau,L.F., and Tonks,N.K. (1993). MKP-1 (3CH134), an immediate early gene product, is a dual specificity phosphatase that dephosphorylates MAP kinase in vivo. Cell *75*, 487-493.

Sun,Y.Q., McLeod,K.J., and Rubin,C.T. (1995). Mechanically induced periosteal bone formation is paralleled by the upregulation of collagen type one mRNA in osteocytes as measured by in situ reverse transcript-polymerase chain reaction. Calcif. Tissue Int. *57*, 456-462.

Suva,L.J., Seedor,J.G., Endo,N., Quartuccio,H.A., Thompson,D.D., Bab,I., and Rodan,G.A. (1993). Pattern of gene expression following rat tibial marrow ablation. J Bone Miner Res *8*, 379-388.

Suzuki,A., Guicheux,J., Palmer,G., Miura,Y., Oiso,Y., Bonjour,J.P., and Caverzasio,J. (2002). Evidence for a role of p38 MAP kinase in expression of alkaline phosphatase during osteoblastic cell differentiation. Bone *30*, 91-98.

Suzuki,A., Palmer,G., Bonjour,J.P., and Caverzasio,J. (1999). Regulation of alkaline phosphatase activity by p38 MAP kinase in response to activation of Gi protein-coupled receptors by epinephrine in osteoblast-like cells. Endocrinology *140*, 3177-3182.

Takahashi,N., Udagawa,N., Tanaka,S., Murakami,H., Owan,I., Tamura,T., and Suda,T. (1994). Postmitotic osteoclast precursors are mononuclear cells which express macrophage-associated phenotypes. Dev. Biol. *163*, 212-221.

Takano,Y., Ozawa,H., and Crenshaw,M.A. (1986). Ca-ATPase and ALPase activities at the initial calcification sites of dentin and enamel in the rat incisor. Cell Tissue Res. *243*, 91-99.

Takuma,A., Kaneda,T., Sato,T., Ninomiya,S., Kumegawa,M., and Hakeda,Y. (2003). Dexamethasone enhances osteoclast formation synergistically with transforming growth factor-beta by stimulating the priming of osteoclast progenitors for differentiation into osteoclasts. J. Biol. Chem. *278*, 44667-44674.

Talarmin,H., Rescan,C., Cariou,S., Glaise,D., Zanninelli,G., Bilodeau,M., Loyer,P., Guguen-Guillouzo,C., and Baffet,G. (1999). The mitogen-activated protein kinase kinase/extracellular signal-regulated kinase cascade activation is a key signalling pathway involved in the regulation of G(1) phase progression in proliferating hepatocytes. Mol. Cell Biol. *19*, 6003-6011.

Tamama,K., Fan,V.H., Griffith,L.G., Blair,H.C., and Wells,A. (2006). Epidermal growth factor as a candidate for ex vivo expansion of bone marrow-derived mesenchymal stem cells. Stem Cells *24*, 686-695.

Tamemoto,H., Kadowaki,T., Tobe,K., Ueki,K., Izumi,T., Chatani,Y., Kohno,M., Kasuga,M., Yazaki,Y., and Akanuma,Y. (1992). Biphasic activation of two mitogen-activated protein kinases during the cell cycle in mammalian cells. J. Biol. Chem. *267*, 20293-20297.

Tamura,Y., Okinaga,H., and Takami,H. (2004). Glucocorticoid-induced osteoporosis. Biomed. Pharmacother. *58*, 500-504.

Tan,K.B., Harrop,J., Reddy,M., Young,P., Terrett,J., Emery,J., Moore,G., and Truneh,A. (1997). Characterization of a novel TNF-like ligand and recently described TNF ligand and TNF receptor superfamily genes and their constitutive and inducible expression in hematopoietic and non-hematopoietic cells. Gene *204*, 35-46.

Tanaka,S., Takahashi,N., Udagawa,N., Tamura,T., Akatsu,T., Stanley,E.R., Kurokawa,T., and Suda,T. (1993). Macrophage colony-stimulating factor is indispensable for both proliferation and differentiation of osteoclast progenitors. J. Clin. Invest *91*, 257-263.

Tang,D.G., Tokumoto,Y.M., Apperly,J.A., Lloyd,A.C., and Raff,M.C. (2001). Lack of replicative senescence in cultured rat oligodendrocyte precursor cells. Science *291*, 868-871.

Tannin,G.M., Agarwal,A.K., Monder,C., New,M.I., and White,P.C. (1991). The human gene for 11 beta-hydroxysteroid dehydrogenase. Structure, tissue distribution, and chromosomal localization. J. Biol. Chem. *266*, 16653-16658.

Teitelbaum,S.L. (2000). Bone Resorption by Osteoclasts. Science *289*, 1504-1508.

Teitelbaum,S.L., Tondravi,M.M., and Ross,F.P. (1997). Osteoclasts, macrophages, and the molecular mechanisms of bone resorption. J. Leukoc. Biol. *61*, 381-388.

Tenenbaum,H.C. and Heersche,J.N. (1986). Differentiation of osteoid-producing cells in vitro: possible evidence for the requirement of a microenvironment. Calcif. Tissue Int. *38*, 262-267.

Thomas,D.M., Hards,D.K., Rogers,S.D., Ng,K.W., and Best,J.D. (1996). Insulin receptor expression in bone. J. Bone Miner. Res. *11*, 1312-1320.

Thomas,D.M., Hards,D.K., Rogers,S.D., Ng,K.W., and Best,J.D. (1996a). Insulin receptor expression in bone. J. Bone Miner. Res. *11*, 1312-1320.

Thomas,D.M., Rogers,S.D., Ng,K.W., and Best,J.D. (1996b). Dexamethasone modulates insulin receptor expression and subcellular distribution of the glucose transporter GLUT 1 in UMR 106-01, a clonal osteogenic sarcoma cell line. J. Mol. Endocrinol. *17*, 7-17.

Thrailkill,K., Quattrin,T., Baker,L., Litton,J., Dwigun,K., Rearson,M., Poppenheimer,M., Kotlovker,D., Giltinan,D., Gesundheit,N., and Martha,P., Jr. (1997). Dual hormonal replacement therapy with insulin and recombinant human insulin-like growth factor (IGF)-I in insulin-dependent

diabetes mellitus: effects on the growth hormone/IGF/IGF-binding protein system. J. Clin. Endocrinol. Metab *82*, 1181-1187.

Tondravi,M.M., McKercher,S.R., Anderson,K., Erdmann,J.M., Quiroz,M., Maki,R., and Teitelbaum,S.L. (1997). Osteopetrosis in mice lacking haematopoietic transcription factor PU.1. Nature *386*, 81-84.

Tournier,C., Thomas,G., Pierre,J., Jacquemin,C., Pierre,M., and Saunier,B. (1997). Mediation by arachidonic acid metabolites of the H2O2-induced stimulation of mitogen-activated protein kinases (extracellular-signal-regulated kinase and c-Jun NH2-terminal kinase). Eur. J Biochem. *244*, 587-595.

Tran,V.P., Vignery,A., and Baron,R. (1982). An electron-microscopic study of the bone-remodeling sequence in the rat. Cell Tissue Res *225*, 283-292.

Tsuda,E., Goto,M., Mochizuki,S.i., Yano,K., Kobayashi,F., Morinaga,T., and Higashio,K. (1997). Isolation of a Novel Cytokine from Human Fibroblasts That Specifically Inhibits Osteoclastogenesis. Biochemical and Biophysical Research Communications *234*, 137-142.

Tuveson,D.A., Shaw,A.T., Willis,N.A., Silver,D.P., Jackson,E.L., Chang,S., Mercer,K.L., Grochow,R., Hock,H., Crowley,D., Hingorani,S.R., Zaks,T., King,C., Jacobetz,M.A., Wang,L., Bronson,R.T., Orkin,S.H., DePinho,R.A., and Jacks,T. (2004). Endogenous oncogenic K-ras(G12D) stimulates proliferation and widespread neoplastic and developmental defects. Cancer Cell *5*, 375-387.

Udagawa,N., Takahashi,N., Akatsu,T., Tanaka,H., Sasaki,T., Nishihara,T., Koga,T., Martin,T.J., and Suda,T. (1990). Origin of osteoclasts: mature monocytes and macrophages are capable of differentiating into osteoclasts under a suitable microenvironment prepared by bone marrow-derived stromal cells. Proc. Natl. Acad. Sci. U. S. A *87*, 7260-7264.

Urist,M.R., Huo,Y.K., Brownell,A.G., Hohl,W.M., Buyske,J., Lietze,A., Tempst,P., Hunkapiller,M., and DeLange,R.J. (1984). Purification of bovine bone morphogenetic protein by hydroxyapatite chromatography. Proc. Natl. Acad. Sci. U. S. A *81*, 371-375.

Urist,M.R., Mizutani,H., Conover,M.A., Lietze,A., and Finerman,G.A. (1982). Dentin, bone, and osteosarcoma tissue bone morphogenetic proteins. Prog. Clin. Biol. Res *101*, 61-81.

Vaananen,H.K., Zhao,H., Mulari,M., and Halleen,J.M. (2000). The cell biology of osteoclast function. J. Cell Sci. *113 (Pt 3)*, 377-381.

Vaananen,K. and Zhao,H. (2002). Osteoclast function: biology and mechanisms. In Principles of bone biology, J.P.Bilezikian, L.G.Raisz, and G.A.Rodan, eds. (New York: Academic Press), pp. 127-139.

van Bezooijen,R.L., Ten,D.P., Papapoulos,S.E., and Lowik,C.W. (2005). SOST/sclerostin, an osteocyte-derived negative regulator of bone formation. Cytokine Growth Factor Rev. *16*, 319-327.

van der Geer,P., Hunter,T., and Lindberg,R.A. (1994). Receptor protein-tyrosine kinases and their signal transduction pathways. Annu. Rev. Cell Biol. *10*, 251-337.

van Staa,T.P., Laan,R.F., Barton,I.P., Cohen,S., Reid,D.M., and Cooper,C. (2003). Bone density threshold and other predictors of vertebral fracture in patients receiving oral glucocorticoid therapy. Arthritis Rheum. *48*, 3224-3229.

van Staa,T.P., Leufkens,H.G., Abenhaim,L., Zhang,B., and Cooper,C. (2000a). Oral corticosteroids and fracture risk: relationship to daily and cumulative doses. Rheumatology. (Oxford) *39*, 1383-1389.

van Staa,T.P., Leufkens,H.G., Abenhaim,L., Zhang,B., and Cooper,C. (2000b). Use of oral corticosteroids and risk of fractures. J. Bone Miner. Res. *15*, 993-1000.

van Staa,T.P., Leufkens,H.G., and Cooper,C. (2002). The epidemiology of corticosteroid-induced osteoporosis: a meta-analysis. Osteoporos. Int. *13*, 777-787.

van,B.T., Luttrell,L.M., Hawes,B.E., and Lefkowitz,R.J. (1996). Mitogenic signaling via G protein-coupled receptors. Endocr. Rev. *17*, 698-714.

Vayssiere,B.M., Dupont,S., Choquart,A., Petit,F., Garcia,T., Marchandeau,C., Gronemeyer,H., and Resche-Rigon,M. (1997). Synthetic Glucocorticoids That Dissociate Transactivation and AP-1 Transrepression Exhibit Antiinflammatory Activity in Vivo. Mol Endocrinol *11*, 1245-1255.

Verhaeghe,J. and Bouillon,R. (2002). Effects of diabetes and insulin on bone physiology. In Principles of Bone Biology., J.P.Bilezikian, L.G.Raisz, and G.A.Rodan, eds. (San Diego: Academic Press), pp. 741-755.

Verhaeghe,J., van Bree,R., van Herck,E., Thomas,H., Skottner,A., Dequeker,J., Mosekilde,L.I., Einhorn,T.A., and Bouillon,R. (1996). Effects of recombinant human growth hormone and insulin-like growth factor-I, with or without 17+¦-estradiol, on bone and mineral homeostasis of aged ovariectomized rats. J Bone Miner Res *11*, 1723-1735.

Vincent,A.M. and Feldman,E.L. (2002). Control of cell survival by IGF signaling pathways. Growth Horm. IGF. Res *12*, 193-197.

Vindelov,L.L., Christensen,I.J., and Nissen,N.I. (1983). A detergent-trypsin method for the preparation of nuclei for flow cytometric DNA analysis. Cytometry *3*, 323-327.

Vojtek,A.B., Hollenberg,S.M., and Cooper,J.A. (1993). Mammalian Ras interacts directly with the serine/threonine kinase Raf. Cell *74*, 205-214.

Vouret-Craviari,V., Van Obberghen-Schilling,E., Scimeca,J.C., Van,O.E., and Pouyssegur,J. (1993). Differential activation of p44mapk (ERK1) by alpha-thrombin and thrombin-receptor peptide agonist. Biochem. J *289 (Pt 1)*, 209-214.

Wang,P.Y., Liu,P., Weng,J., Sontag,E., and Anderson,R.G. (2003). A cholesterol-regulated PP2A/HePTP complex with dual specificity ERK1/2 phosphatase activity. EMBO J. *22*, 2658-2667.

Wang,Z., Cao,N., Nantajit,D., Fan,M., Liu,Y., and Li,J.J. (2008). Mitogen-activated protein kinase phosphatase-1 represses c-Jun NH2-terminal kinase-mediated apoptosis via NF-kappaB regulation. J. Biol. Chem. *283*, 21011-21023.

Wang,Z.Q., Hemken,P., Menton,D., and Gluck,S. (1992a). Expression of vacuolar H(+)-ATPase in mouse osteoclasts during in vitro differentiation. Am. J. Physiol *263*, F277-F283.

Wang,Z.Q., Ovitt,C., Grigoriadis,A.E., Mohle-Steinlein,U., Ruther,U., and Wagner,E.F. (1992b). Bone and haematopoietic defects in mice lacking c-fos. Nature *360*, 741-745.

Waters,S.B., Holt,K.H., Ross,S.E., Syu,L.J., Guan,K.L., Saltiel,A.R., Koretzky,G.A., and Pessin,J.E. (1995). Desensitization of Ras Activation by a Feedback Disassociation of the SOS-Grb2 Complex. Journal of Biological Chemistry *270*, 20883-20886.

Wei,S., Kitaura,H., Zhou,P., Ross,F.P., and Teitelbaum,S.L. (2005). IL-1 mediates TNF-induced osteoclastogenesis. J. Clin. Invest *115*, 282-290.

Weinstein,R.S. (2001). Glucocorticoid-induced osteoporosis. Rev. Endocr. Metab Disord. *2*, 65-73.

Weiss,A. and Schlessinger,J. (1998). Switching signals on or off by receptor dimerization. Cell *94*, 277-280.

Wheeler,M.A., Townsend,M.K., Yunker,L.A., and Mauro,L.J. (2002). Transcriptional activation of the tyrosine phosphatase gene, OST-PTP, during osteoblast differentiation. J. Cell Biochem. *87*, 363-376.

Whyte ,M.P.(2008). Hypophosphatasia: Nature's window on alikaline phosphatase function in humans. In Principles of bone biology, J.P.Bilezikian, L.G.Raisz, and T.J.Martin, eds. (San Diego: Academic Press), pp. 1573-1598.

Whyte,M.P. (1994). Hypophosphatasia and the role of alkaline phosphatase in skeletal mineralization. Endocr. Rev. *15*, 439-461.

Wilkie,A.O., Tang,Z., Elanko,N., Walsh,S., Twigg,S.R., Hurst,J.A., Wall,S.A., Chrzanowska,K.H., and Maxson,R.E., Jr. (2000). Functional haploinsufficiency of the human homeobox gene MSX2 causes defects in skull ossification. Nat. Genet. *24*, 387-390.

Wong,B.R., Rho,J., Arron,J., Robinson,E., Orlinick,J., Chao,M., Kalachikov,S., Cayani,E., Bartlett,F.S., III, Frankel,W.N., Lee,S.Y., and Choi,Y. (1997). TRANCE is a novel ligand of the tumor necrosis factor receptor family that activates c-Jun N-terminal kinase in T cells. J. Biol. Chem. *272*, 25190-25194.

Wong,C.W., McNally,C., Nickbarg,E., Komm,B.S., and Cheskis,B.J. (2002). Estrogen receptor-interacting protein that modulates its nongenomic activity-crosstalk with Src/Erk phosphorylation cascade. Proc. Natl. Acad. Sci. U. S. A *99*, 14783-14788.

Wong,M.M., Rao,L.G., Ly,H., Hamilton,L., Tong,J., Sturtridge,W., McBroom,R., Aubin,J.E., and Murray,T.M. (1990). Long-term effects of physiologic concentrations of dexamethasone on human bone-derived cells. J. Bone Miner. Res. *5*, 803-813.

Woo,K.M., Kim,H.M., and Ko,J.S. (2002). Macrophage colony-stimulating factor promotes the survival of osteoclast precursors by up-regulating Bcl-X(L). Exp. Mol. Med. *34*, 340-346.

Woods,D., Parry,D., Cherwinski,H., Bosch,E., Lees,E., and McMahon,M. (1997). Raf-induced proliferation or cell cycle arrest is determined by the level of Raf activity with arrest mediated by p21Cip1. Mol. Cell Biol. *17*, 5598-5611.

Wuthier,R.E. (1975). Lipid composition of isolated epiphyseal cartilage cells, membranes and matrix vesicles. Biochim. Biophys. Acta *409*, 128-143.

Wuthier,R.E. (1989). Mechanism of de novo mineral formation by matrix vesicles. Connect. Tissue Res. *22*, 27-33.

Xiao,G., Gopalakrishnan,R., Jiang,D., Reith,E., Benson,M.D., and Franceschi,R.T. (2002). Bone morphogenetic proteins, extracellular matrix, and mitogen-activated protein kinase signaling pathways are required for osteoblast-specific gene expression and differentiation in MC3T3-E1 cells. J Bone Miner Res *17*, 101-110.

Xiao,Z., Camalier,C.E., Nagashima,K., Chan,K.C., Lucas,D.A., de la Cruz,M.J., Gignac,M., Lockett,S., Issaq,H.J., Veenstra,T.D., Conrads,T.P., and Beck,G.R., Jr. (2007). Analysis of the extracellular matrix vesicle proteome in mineralizing osteoblasts. J. Cell Physiol *210*, 325-335.

Xu,Q., Konta,T., Nakayama,K., Furusu,A., Moreno-Manzano,V., Lucio-Cazana,J., Ishikawa,Y., Fine,L.G., Yao,J., and Kitamura,M. (2004). Cellular defense against H2O2-induced apoptosis via MAP kinase-MKP-1 pathway. Free Radic. Biol. Med. *36*, 985-993.

Yang,B.S., Hauser,C.A., Henkel,G., Colman,M.S., Van,B.C., Stacey,K.J., Hume,D.A., Maki,R.A., and Ostrowski,M.C. (1996). Ras-mediated phosphorylation of a conserved threonine residue enhances the transactivation activities of c-Ets1 and c-Ets2. Mol Cell Biol. *16*, 538-547.

Yang,J., Zhang,X., Wang,W., and Liu,J. (2010). Insulin stimulates osteoblast proliferation and differentiation through ERK and PI3K in MG-63 cells. Cell Biochem. Funct. *28*, 334-341.

Yang,S., Wei,D., Wang,D., Phimphilai,M., Krebsbach,P.H., and Franceschi,R.T. (2003). In vitro and in vivo synergistic interactions between the Runx2/Cbfa1 transcription factor and bone morphogenetic protein-2 in stimulating osteoblast differentiation. J. Bone Miner. Res. *18*, 705-715.

Yao,Z. and Seger,R. (2009). The ERK signaling cascade--views from different subcellular compartments. Biofactors *35*, 407-416.

Yasuda,H., Shima,N., Nakagawa,N., Mochizuki,S.I., Yano,K., Fujise,N., Sato,Y., Goto,M., Yamaguchi,K., Kuriyama,M., Kanno,T., Murakami,A., Tsuda,E., Morinaga,T., and Higashio,K. (1998). Identity of osteoclastogenesis inhibitory factor (OCIF) and osteoprotegerin (OPG): a mechanism by which OPG/OCIF inhibits osteoclastogenesis in vitro. Endocrinology *139*, 1329-1337.

Yu,G., Floyd,Z.E., Wu,X., Halvorsen,Y.D., and Gimble,J.M. (2011). Isolation of human adipose-derived stem cells from lipoaspirates. Methods Mol. Biol. *702*, 17-27.

Yu,G., Wu,X., Dietrich,M.A., Polk,P., Scott,L.K., Ptitsyn,A.A., and Gimble,J.M. (2010). Yield and characterization of subcutaneous human adipose-derived stem cells by flow cytometric and adipogenic mRNA analyzes. Cytotherapy. *12*, 538-546.

Yuan,F.L., Li,X., Lu,W.G., Li,C.W., Li,J.P., and Wang,Y. (2010). The vacuolar ATPase in bone cells: a potential therapeutic target in osteoporosis. Mol Biol. Rep. *37*, 3561-3566.

Zhang,P., Wong,C., Liu,D., Finegold,M., Harper,J.W., and Elledge,S.J. (1999). p21(CIP1) and p57(KIP2) control muscle differentiation at the myogenin step. Genes Dev. *13*, 213-224.

Zhang,S.Q., Yang,W., Kontaridis,M.I., Bivona,T.G., Wen,G., Araki,T., Luo,J., Thompson,J.A., Schraven,B.L., Philips,M.R., and Neel,B.G. (2004). Shp2 regulates SRC family kinase activity and Ras/Erk activation by controlling Csk recruitment. Mol. Cell *13*, 341-355.

Zhang,W. and Liu,H.T. (2002). MAPK signal pathways in the regulation of cell proliferation in mammalian cells. Cell Res. *12*, 9-18.

Zhang,W., Dziak,R.M., and Aletta,J.M. (1995). EGF-mediated phosphorylation of extracellular signal-regulated kinases in osteoblastic cells. J Cell Physiol *162*, 348-358.

Zhao,C., Irie,N., Takada,Y., Shimoda,K., Miyamoto,T., Nishiwaki,T., Suda,T., and Matsuo,K. (2006). Bidirectional ephrinB2-EphB4 signaling controls bone homeostasis. Cell Metab *4*, 111-121.

Zhao,Q., Jia,Y., and Xiao,Y. (2009). Cathepsin K: A therapeutic target for bone diseases. Biochemical and Biophysical Research Communications *380*, 721-723.

Zhao,S., Zhang,Y.K., Harris,S., Ahuja,S.S., and Bonewald,L.F. (2002). MLO-Y4 osteocyte-like cells support osteoclast formation and activation. J. Bone Miner. Res. *17*, 2068-2079.
Zheng,C.F. and Guan,K.L. (1993). Dephosphorylation and inactivation of the mitogen-activated protein kinase by a mitogen-induced Thr/Tyr protein phosphatase. J. Biol. Chem. *268*, 16116-16119.

Zheng,C.F. and Guan,K.L. (1994). Activation of MEK family kinases requires phosphorylation of two conserved Ser/Thr residues. EMBO J. *13*, 1123-1131.

Zhu,Q.Y., Liu,Q., Chen,J.X., Lan,K., and Ge,B.X. (2010). MicroRNA-101 targets MAPK phosphatase-1 to regulate the activation of MAPKs in macrophages. J Immunol. *185*, 7435-7442.

Zoorob,R.J. and Cender,D. (1998). A different look at corticosteroids. Am. Fam. Physician
Zuk,P.A., Zhu,M., Ashjian,P., De Ugarte,D.A., Huang,J.I., Mizuno,H., Alfonso,Z.C., Fraser,J.K., Benhaim,P., and Hedrick,M.H. (2002). Human adipose tissue is a source of multipotent stem cells. Mol. Biol. Cell *13*, 4279-4295.

Zuniga,A., Torres,J., Ubeda,J., and Pulido,R. (1999). Interaction of mitogen-activated protein kinases with the kinase interaction motif of the tyrosine phosphatase PTP-SL provides substrate specificity and retains ERK2 in the cytoplasm. J. Biol. Chem. *274*, 21900-21907.

Supplement

Addendum A

This section contains all the media, buffers and mixtures used for cell culture.

A1. Media, buffers and mixes used to isolate rMSCs

A1.1. Holding media

DMEM (pH 7.5) supplemented with 10 µg/ml penicillin and 10 µg/ml streptomycin containing no added FBS.

A1.2. Expansion media

DMEM (pH 7.5) supplemented with 10 µg/ml penicillin and 10 µg/ml streptomycin containing 20% FBS (v/v) FBS.

A1.3. Collagenase I enzyme mixture

0.75 mg/ ml Collagenase type I
(stock solution is 7.5 mg/ ml (w/v) in Hank's basic salt solution (HBSS)
1.5% (v/v) BSA
(stock solution is 10% (w/v) in 1 x PBS)
The mixture is made up to volume with HBSS.

A1.4. PBS (phosphate buffered saline)

134 mM NaCl
2.7 mM KCl
10 mM Na_2PO_4
1.8 mM KH_2PO_4
Before autoclaving, the pH was adjusted to 7.4.

A2. Complete growth medium

DMEM (pH 7.5) supplemented with 10 µg/ml penicillin and 10 µg/ml streptomycin containing 10% (v/v) FBS.

A.3. Media, buffers and mixes used for cell treatments

A3.1. Basal growth medium

DMEM (pH 7.5) supplemented with 10 µg/ml penicillin and 10 µg/ml streptomycin containing 1% (v/v) FBS was utilised as basal growth medium.

A3.2. Mitogenic induction using FBS

DMEM (pH 7.5) supplemented with 10 µg/ml penicillin and 10 µg/ml streptomycin containing either 5% (v/v) FBS, 10% (v/v) FBS or 20% (v/v) FBS was used to induce mitogenesis. These media is designated as DMEM/5% FBS, DMEM/10% FBS and DMEM/20% FBS, respectively.

A3.3. Osteogenic differentiation medium (Ost)

10% (v/v) FBS
10 mM glycerol-2-phosphate
50 µM ascorbic acid
10 nM Dex
Differentiation medium is made to volume with DMEM (pH 7.5).

A4. Chemicals used for tissue culture treatments

A4.1. Phorbol 12-myristate 13- acetate (PMA)

A stock solution of 2 mg/ml PMA in DMSO was prepared and aliquots were stored at -20 ^{o}C. All dilutions were made in DMSO. The DMSO vehicle concentration did not exceed 0.1% (v/v) in all experiments.

A4.2. Dexamethasone (Dex)

Dexamethasone was prepared at a stock concentration of 10 mM in absolute ethanol and stored at – 20 ^{o}C. All dilutions were carried out in absolute ethanol and the final vehicle concentration did not exceed 0.1% (v/v) in all experiments, unless otherwise indicated.

A4.3. Sodium orthovanadate (VO_4)

VO_4 was prepared at a stock concentration of 100 mM, boiled for 5 min after which the pH was adjusted to 10. Aliquots were stored at -20 ^{o}C. Prior to use, all aliquots were diluted with sterile Millipore water at pH 10 and boiled just before commencement of cell treatments.

A4.4. Phenylarsine oxide (PAO)

A stock solution of 20 mM PAO was prepared in DMSO with heating at 37 ^{o}C for 5 min. PAO aliquots were stored at – 20 ^{o}C. All dilutions were in DMSO, the concentration of which did not exceed 0.1% (v/v) for all PAO treatments.

A4.5. Wortmannin (WM)

WM was prepared at a stock concentration of 5 mM in DMSO and aliquots were stored at – 20 ^{o}C. DMSO was used for all WM. The DMSO vehicle concentration did not exceed 0.1% (v/v) for all WM treatments.

A4.6. Sanguinarine chloride (SC)

A 5 mM stock solution of SC was prepared in absolute ethanol and stored at – 20 ^{o}C. All SC dilutions were made in absolute ethanol, the final concentration of which did not exceed 0.1% (v/v) in all SC, unless otherwise indicated.

Addendum B

Buffers and solutions utilised in all assays are included in this section.

B1. Solutions used for the cell proliferation assay using [^{3}H] thymidine incorporation

B1. Lysis solution

0.1% (w/v) SDS
0.1% (w/v) NaOH

B2. Buffers and solutions employed in the cell cycle analysis using propidium iodide (PI)

B2.1. Citrate buffer

250 mM sucrose,
40 mM trisodium citrate
0.05% (v/v) DMSO
The buffer is used at pH 7.6.

B2.2. Stock Solution

3.4 mM trisodium citrate
0.1% (v/v) nonidet P40
1.5 mM spermine tetrahydrochloride
0.5 mM Tris (pH 7.6)
Note: Solutions A, B and C are all prepared in stock solution.

B2.3. Solution A

30 µg/ml Trypsin was dissolved in stock solution and the pH adjusted to 7.6. This solution was stored at -20 ^{0}C for subsequent use.

B2.4. Solution B

500 µg/ml Trypsin inhibitor
100 µg/ml Ribonuclease A
These components were dissolved in stock solution and the pH adjusted to 7.6. This solution was stored at 4 ^{0}C for subsequent use.

B2.5. Solution C

416 µg/ml PI
1.16 mg/ml Spermine tetrahydrochloride
These chemicals were dissolved in stock solution and the pH adjusted to 7.6. The storage tubes were wrapped in foil due to the light sensitivity of Propidium iodide. This solution was stored at -20 ^{0}C for subsequent use.

B3. Buffers and solutions employed in the cell cycle analysis using 5-Bromo-2'-deoxyuridine

B3.1. Fixative Solution

1% Paraformaldehyde
0.05% Nonidet P40/ Igepal
These components were made up with PBS (A1.4.).

B3.2. DNAse I digestion solution

20 µl Anti-BrdU- FITC antibody (BD 347583)
1 mg/ml DNAse I
0.005 M $CaCl_2$
0.01 M $MgCl_2$
These components were dissolved in PBS (A1.4.).

B3.3. Anti-BrdU-FITC Incubation Solution

Anti-BrdU-FITC
0.1% BSA
0.05% Nonidet/Igepal
These components were mixed in PBS. The component indicated in italics was added to the solution just before use. A volume of 20 µl anti-BrdU-FITC antibody was added to 20 µl of incubation solution.

B4. Buffers and solution used for alkaline phosphatase (ALP) extraction and enzyme activity measurement

B4.1. ALP extraction solution

10 mM Tris, pH 7.2
1% Triton X-100
2 mM PMSF

B4.2. Glycine assay buffer

1.11 M Glycine
11.1 mM $ZnCl_2$
11.5 mM $MgCl_2$
The pH of the glycine assay buffer is adjusted to 10.4 at 37 ^{o}C.

B4.3. Pnpp substrate solution for ALP assay

60 mM Pnpp in 1.5 mM $MgCl_2$
Note: The Pnpp substrate solution was wrapped in foil due to light sensitivity and kept on ice to prevent spontaneous loss of the terminal phosphate.

B5. Buffers and solutions used in the Pnpp hydrolysis assay for phosphatase activity

B5.1. Total protein extraction buffer for Pnpp hydrolysis assay for phosphatase activity

50 mM Tris-HCl; pH 7.5
1 mM EDTA
0.1% (v/v) Triton X-100
1 mM PMSF
10 µg/ml leupeptin
10 µg/ml pepstatin
2 µg/ml aprotinin
Prior to addition of leupeptin, pepstatin and aprotinin, the pH of the protein extraction buffer was adjusted to 7.5. The components indicated in italics were all added to the extraction buffer just before use.

B5.2. Bradford colour reagent

10% (w/v) Coomassie Brilliant Blue G-250
10% (v/v) 85% Phosphoric acid
5% (v/v) 95% Ethanol
This solution was filtered twice using Whatman filter paper before storage and kept in an airtight container wrapped in foil.

B5.3. Pnpp assay buffer

50 mM Tris-HCl, pH 7.5
1 mM EDTA
10 mM DTT
1 mM PMSF
5 mM Levamisole

B5.4. Pnpp substrate

60 mM pNPP
50 mM Tris-HCl (pH7.5)
1 mM EDTA
10 mM DTT
1 mM PMSF
5 mM Levamisole

B6. Solution used for the Senescence-associated β-galactosidase (SA-β-Gal) staining

B6.1. Fixative solution

2% (v/v) formaldehyde
0.2% (v/v) gluteraldehyde
The fixative solution was prepared in 1 x PBS (see above).

B6.2. SA-β-Gal staining solution

40 mM Sodium phosphate/ citrate buffer; pH 6
5 mM Potassium ferrocyanide
5 mM Potassium ferricyanide
150 mM NaCl
2 mM $MgCl_2$

B7. MTT mitochondrial activity assay stock solution

A 5 mg/ml MTT stock solution was prepared in 1 x PBS (see above), filter sterilised and stored at 4 ^{o}C. To prevent degradation of light-sensitive MTT, stock solution tubes were wrapped in tin foil prior to storage.

Addendum C

This segment includes all buffers and solutions used for total protein extraction, SDS PAGE and immunoblotting.

C1. Protein lysis buffer (pH 7.5)

0.1% (v/v) Triton X-100
50 mM Tris (pH 7.5)
120 mM NaCl
5 mM EDTA
1 mM EGTA
5 mM NaF
20 µM β-glycerophosphate
2 mM Na_3VO_4
1 mM PMSF
10 µg/ml leupeptin
10 µg/ml aprotinin
10 µg/ml pepstatin

The pH of the protein extraction buffer was adjusted to 7.5 prior to addition of leupeptin, pepstatin and aprotinin. The components indicated in italics were all added to the extraction buffer just before use.

C2. Protein gel electrophoresis

C2.1. 4% Stacking12% separating SDS-PAGE gel

Stacking gel	**Volume added**
distilled water	3.375 ml
Bisacrylamide (30: 0.8% w/v)	975 µl
1M Tris (pH 6.8)	625 µl
20% SDS	25 µl
10% (w/v) Ammonium persulphate	25 µl
TEMED	10 µl

Seperating gel	**Volume added**
distilled water	3.350 ml
Bisacrylamide (30: 0.8% w/v)	4.0 ml
1M Tris (pH 8.8)	2.5 ml
20% SDS	50 µl
10% (w/v) Ammonium persulphate	50 µl
TEMED	10 µl

C2.2. 5x SDS PAGE Sample application buffer

225 mM Tris-Cl (pH 6.8)
50% (v/v) Glycerol
5% (w/v) SDS
0.05% (w/v) bromophenol blue
250 mM dithiothretol (DTT)

C2.3. SDS PAGE running buffer

30 mM Tris base

384 mM Glycine
0.1% (v/v) SDS

C3. Protein transfer and immunoblotting

C3.1. Protein transfer buffer
30 mM Tris base
384 mM Glycine
10% (v/v) Methanol

C3.2. Ponceau S Stain
0.2% (w/v) Ponceau S in 5% (v/v) glacial acetic acid.

C3.3. TBS-T
10 mM Tris
150 mM NaCl
Prior to autoclaving, the pH was adjusted to 7.5.
0.1% (v/v) Tween-20

C3.4. Blocking Buffer
5% (w/v) fat-free milk powder in TBS-T

Addendum D

This section includes all buffers and solutions used for nucleic acid analysis.

D1. 10x MOPS buffer
200 mM MOPS
0.05 M sodium acetate
0.001 M EDTA
The pH was adjusted to 7.5 before autoclaving.

D2. RNA gel electrophoresis

D2.1. 1% Agarose / Formaldehyde gel
1.5 % (w/v) Agarose
5% (v/v) Formaldehyde
1 x MOPS

D.2.2. RNA sample application buffer
33.75% (v/v) Formaldehyde
0.25% (w/v) bromophenol blue
10% (v/v) glycerol
40 mM MOPS
10 mM sodium acetate
200 nM EDTA
Note: RNA sample application buffer is added in equal quantities to sample volumes.

D2.3. MOPS running buffer
20 mM MOPS
5 mM sodium acetate
0.1 mM EDTA

D2.4. TBE
127 mM Tris
42.37 mM Boric acid
1.2 mM EDTA

Addendum E

All primers used for QRT-PCR are listed below.

Primers for QRT-PCR

E.1. Reference gene employed for normalisation

Gene name:	ARBP (acidic ribosomal phosphoproteins)
Forward primer:	5' – AAA GGG TCC TGG CTT TGT CT – 3'
Reverse primer:	5' – GCA AAT GCA GAT GGA TCG – 3'
Annealing temperature:	52 ^{o}C
Amplicon size:	149
Reference:	van Wijngaarden *et al.*, 2007

E.2. Bone markers studied

Gene name:	cbfa I (Core-binding factor α-1)/ or Runx2 (Runt-related transcription factor 2)
Forward primer:	5'- GAT GAC ACT GCC ACC TCT GA -3'
Reverse primer:	5'- ATG AAA TGC TTG GGA ACT GC -3'
Annealing temperature:	53 ^{o}C
Amplicon size:	118
Reference:	Liu *et al.*, 2004

Gene name:	Msx 2
Forward primer:	5'- TCA CCA CGT CCC AGC TTC TAG -3'
Reverse primer:	5'- AGC TTT TCC AGT TCC GCC TCC -3'
Annealing temperature:	58 ^{o}C
Amplicon size:	202 bp
Reference:	Kuroda *et al.*, 2005

Gene name:	osterix
Forward primer:	5'- AGC GAC CAC TTG AGC AAA CAT -3'
Reverse primer:	5'- GCG GCT GAT TGG CTT CTT CT -3'
Annealing temperature:	53 ^{o}C
Amplicon size:	121 bp
Reference:	Matsubara *et al.*, 2008

E.3. Protein tyrosine phosphatase studied

Gene name:	MKP-1 (mitogen-activated protein kinase phosphatase 1)
Forward primer:	5'- CTG CTT TGA TCA ACG TCT CG -3'
Reverse primer:	5'- AAG CTG AAG TTG GGG GAG AT -3'
Annealing temperature:	50 ^{o}C
Amplicon size:	301
Reference:	Price *et al.*, 2004

Addendum F

This part is comprised of the FL-2 Area DNA histograms used to analyse the cell cycle phase distributions of the two nuclei populations identified in Experiments A and –B. Data was analysed using the software program, Modfit®. The relevant statistical parameters are given in colour coded tables where the colour code keys are indicated below the respective tables. The relevant density plots were used to demarcate the population of interest before the respective FL-2 Area DNA histograms were generated for cell cycle analysis.

F.1. **1% FBS Experiment A**
Population 1

Quality of Histogram and Fit

%CV	3.51	%Aneuploid	N/A
Cell #	3868	%B.A.D.	7.20
Avg Cell #	82	RCS	2.90

Key: Good Fair Poor

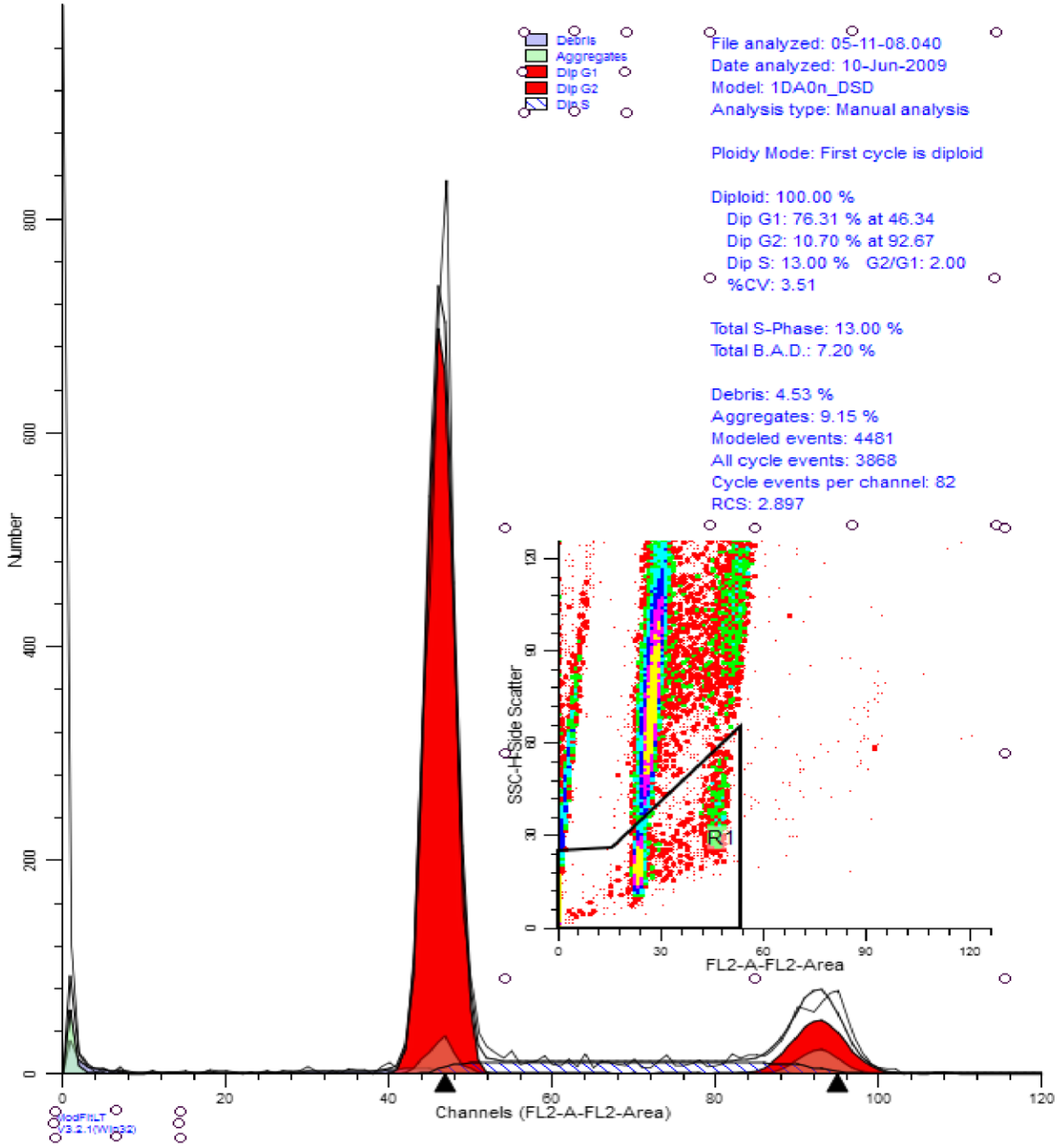

F.2. **1% FBS Experiment A**
Population 2

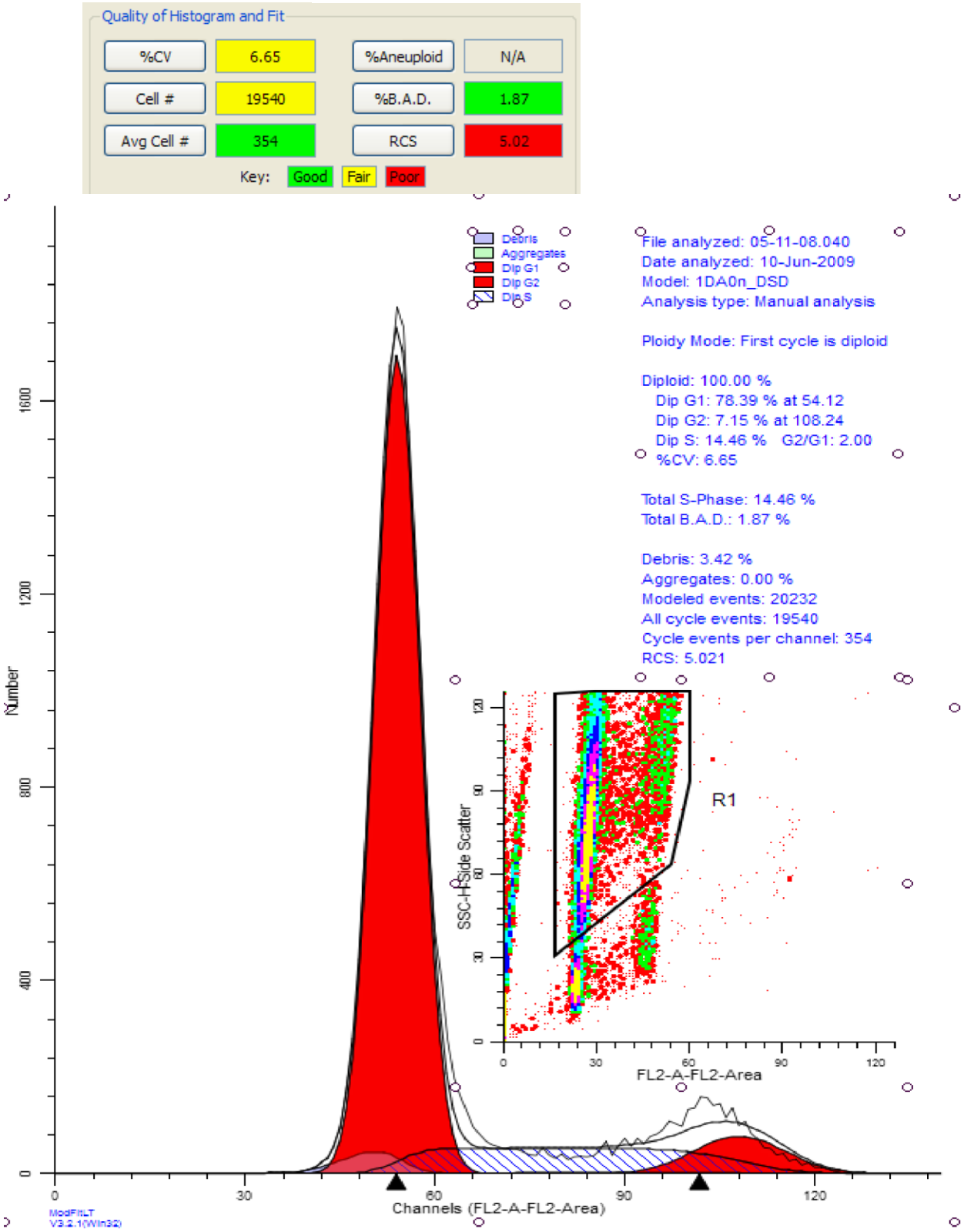

F.3. **5% FBS Experiment A**
Population 1

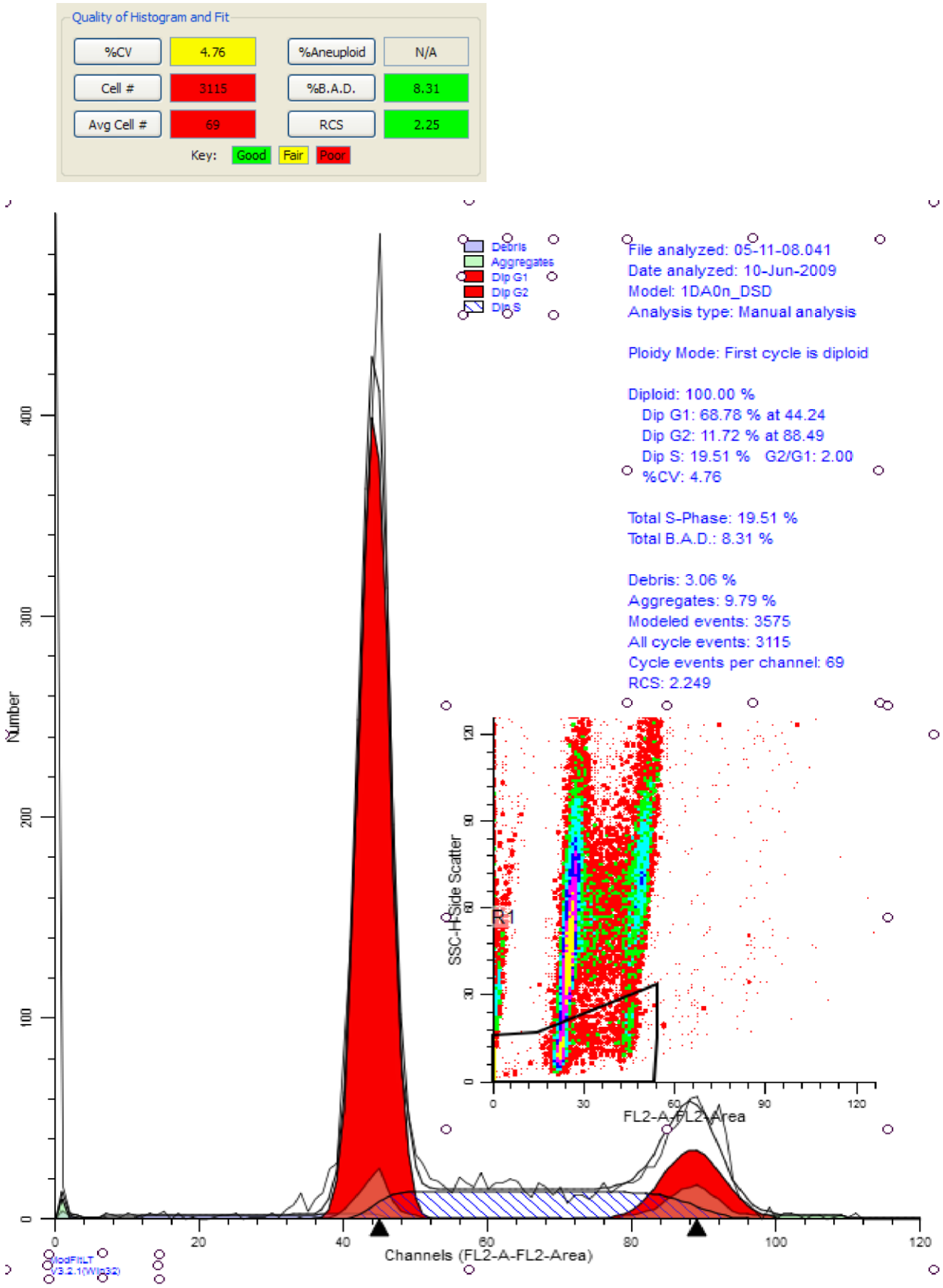

F.4. **5% FBS Experiment A**
Population 2

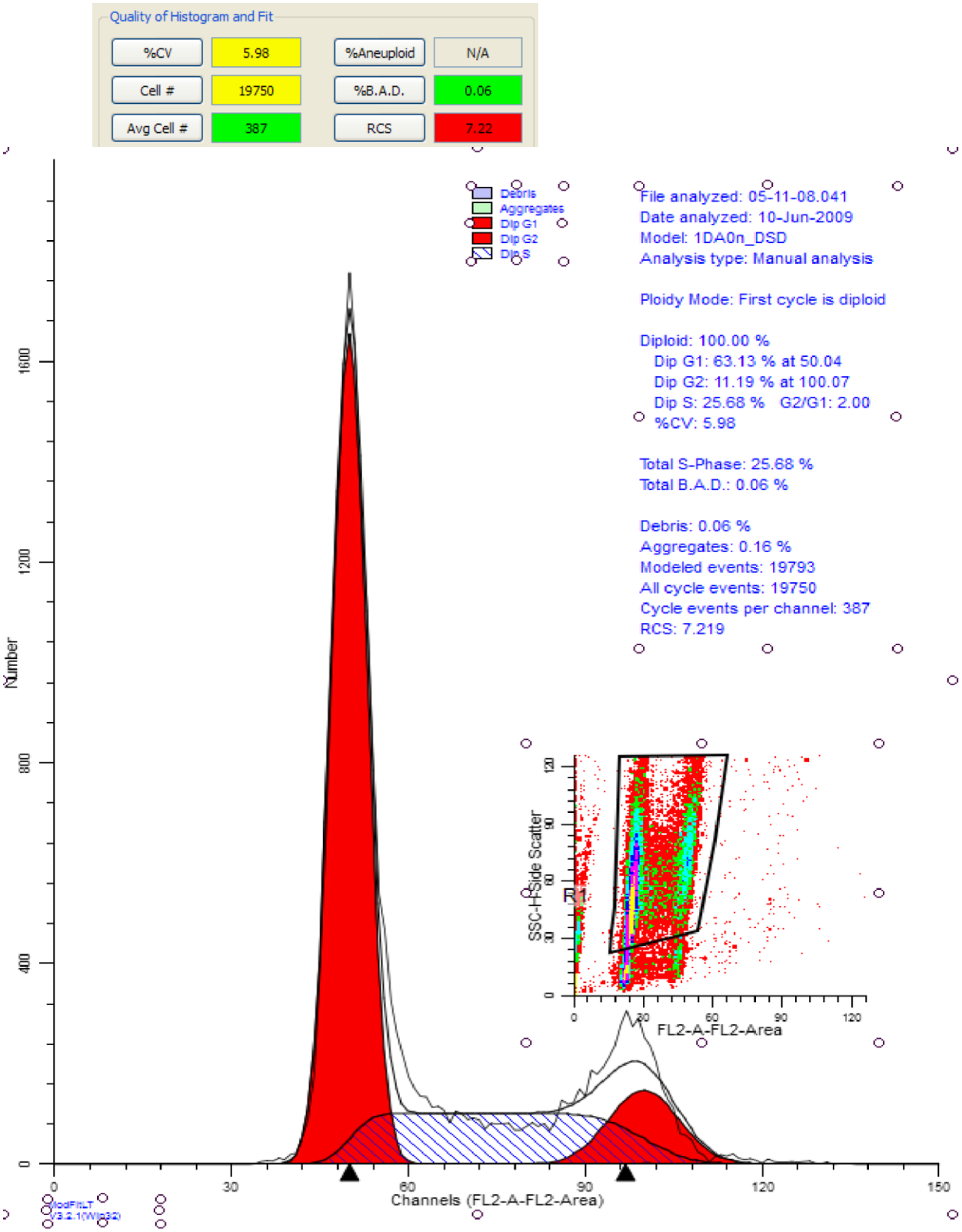

F.5. **10% FBS Experiment A**
Population 1

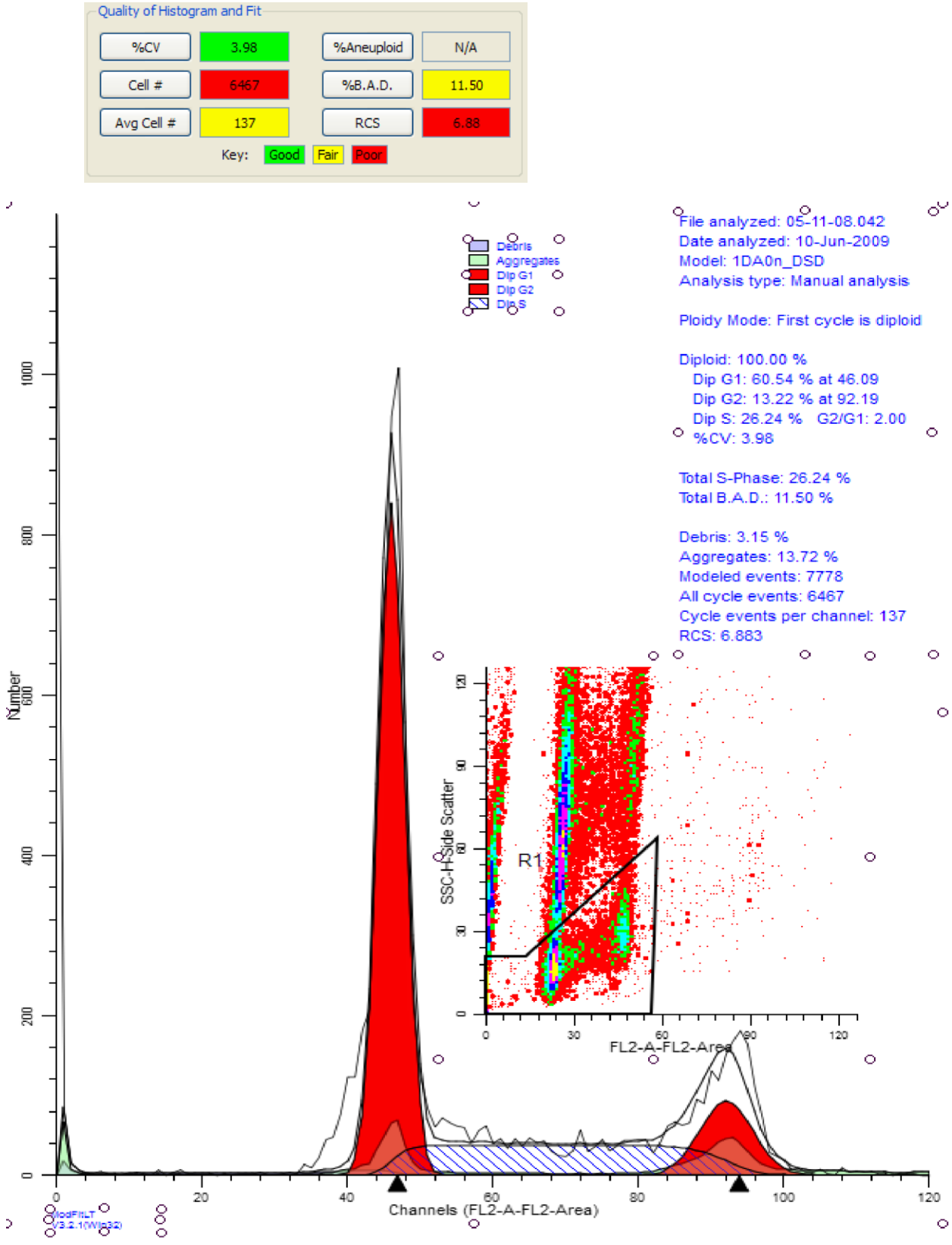

F.6. **10% FBS Experiment A**
Population 2

Quality of Histogram and Fit

%CV	5.60	%Aneuploid	N/A
Cell #	16037	%B.A.D.	0.12
Avg Cell #	304	RCS	5.33

Key: Good Fair Poor

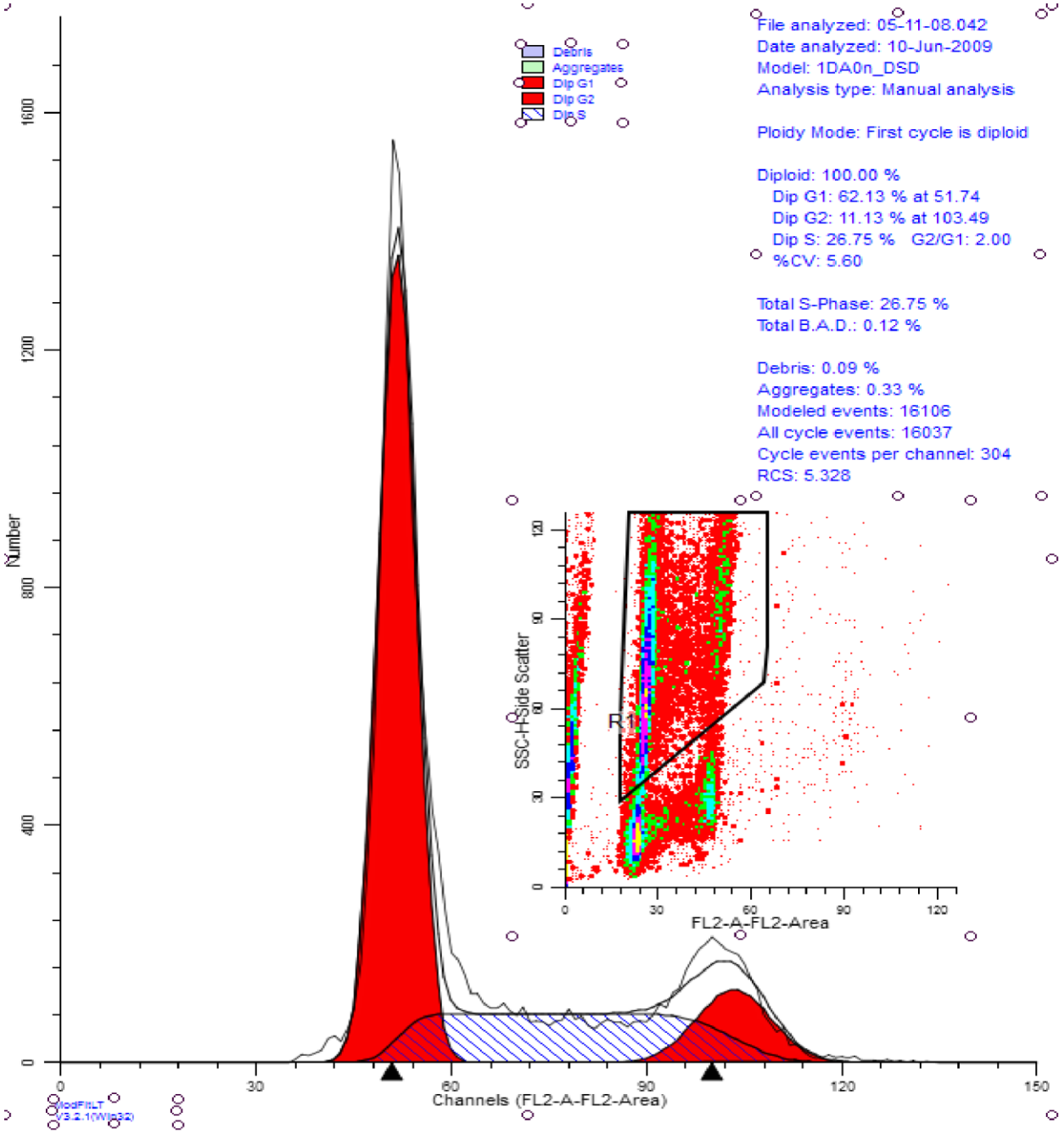

F.7. **20% FBS Experiment A**
Population 1

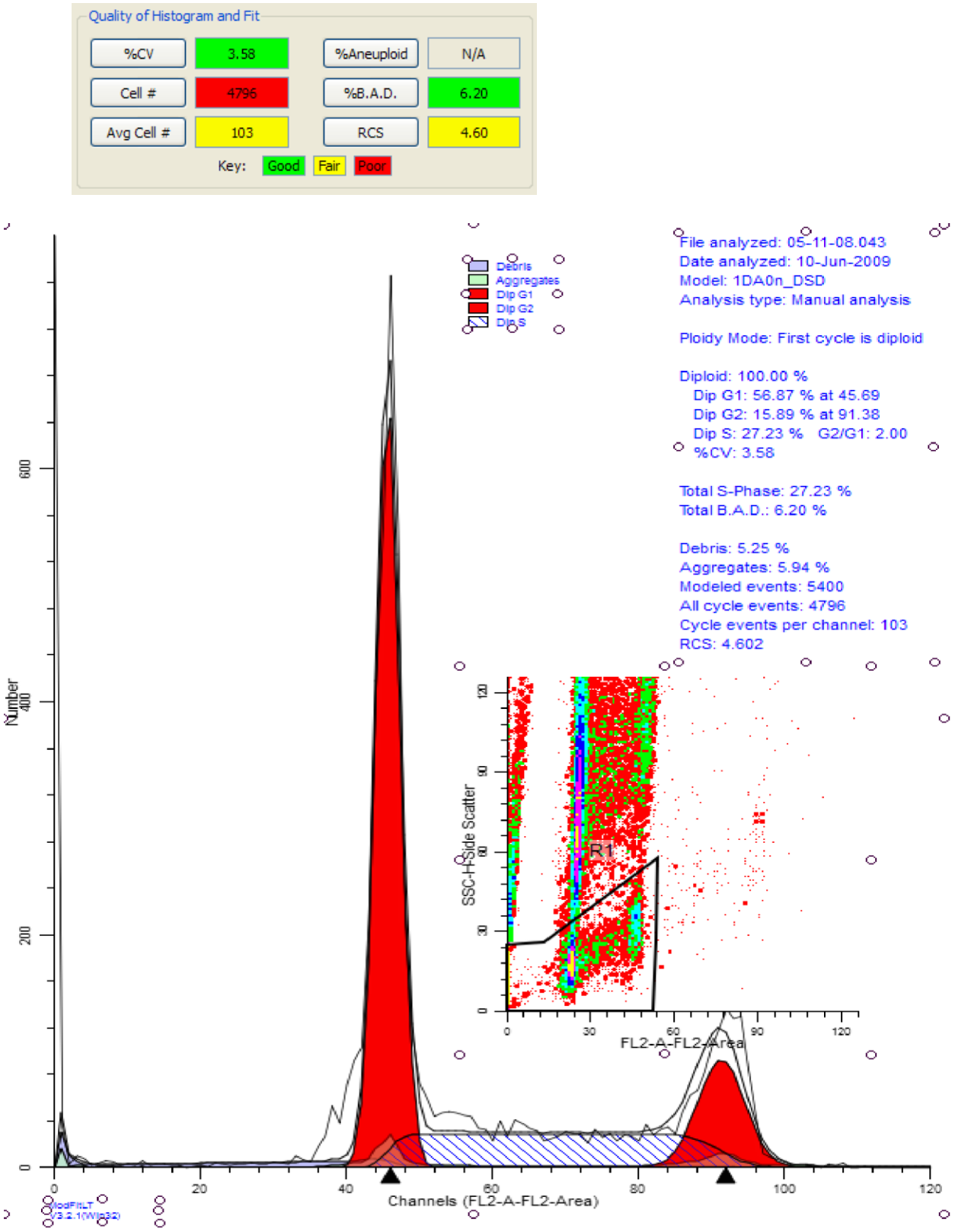

F.8. **20% FBS Experiment A**
Population 2

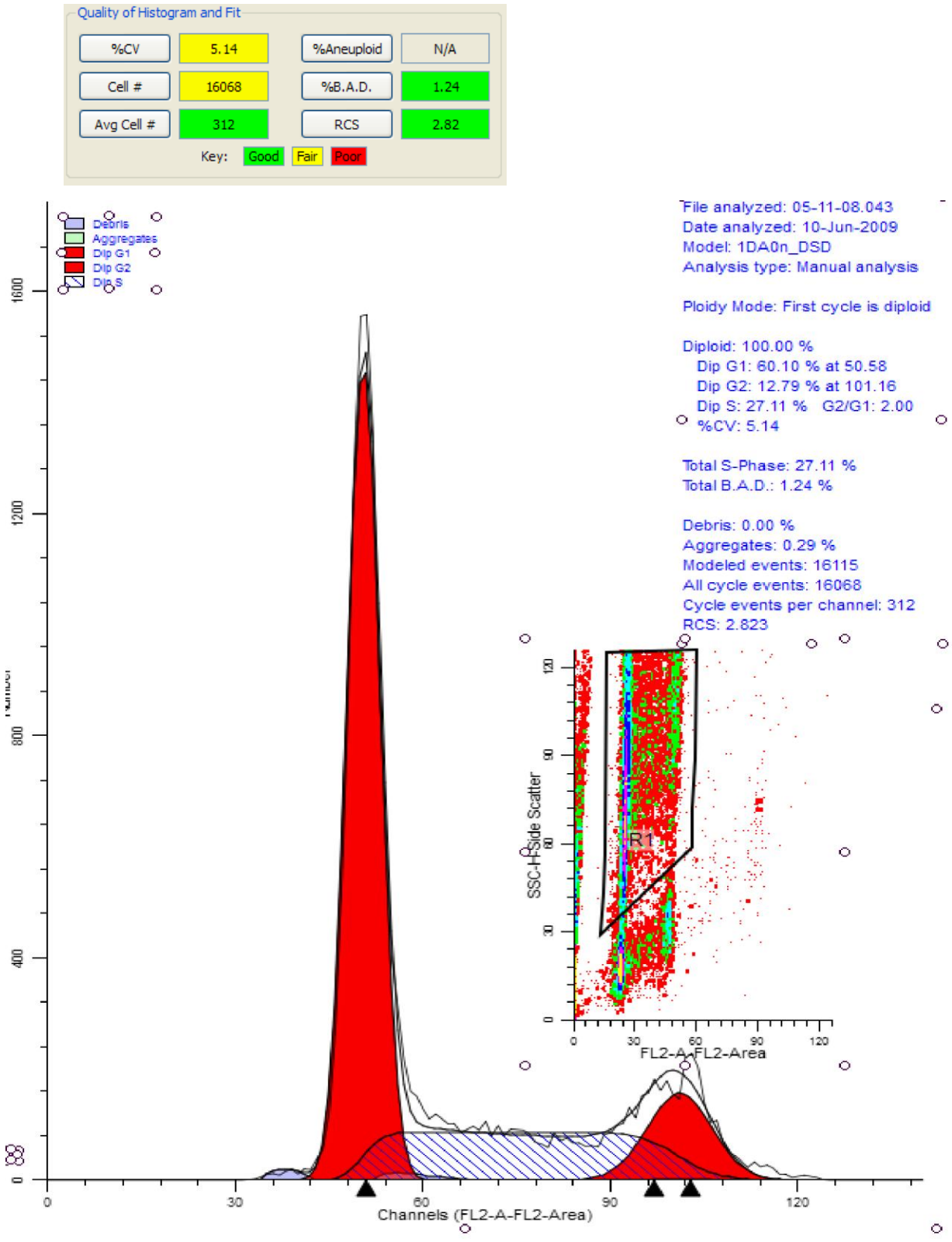

F.9. **PMA Experiment A**
Population 1

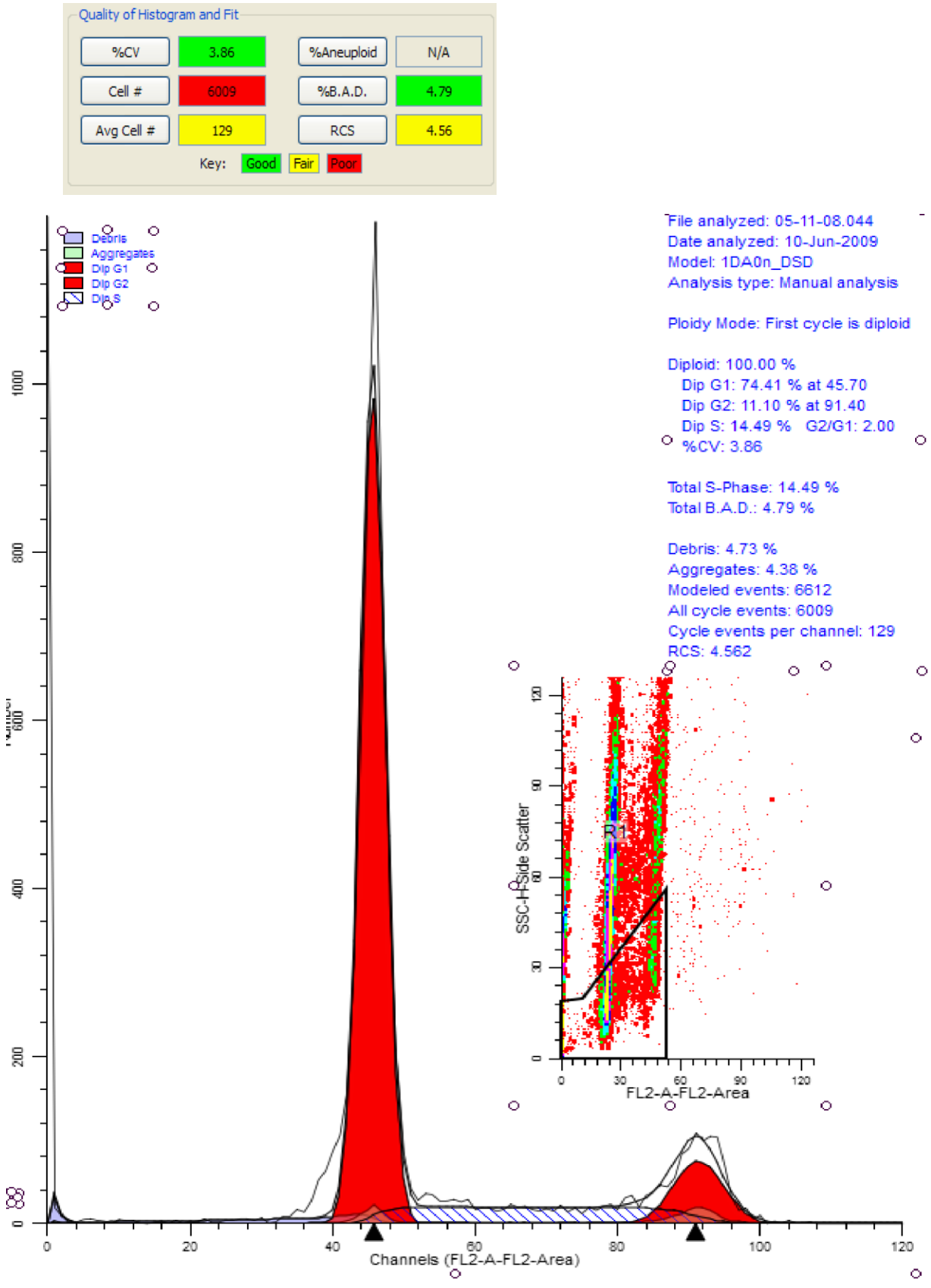

F.10. **PMA Experiment A**
Population 2

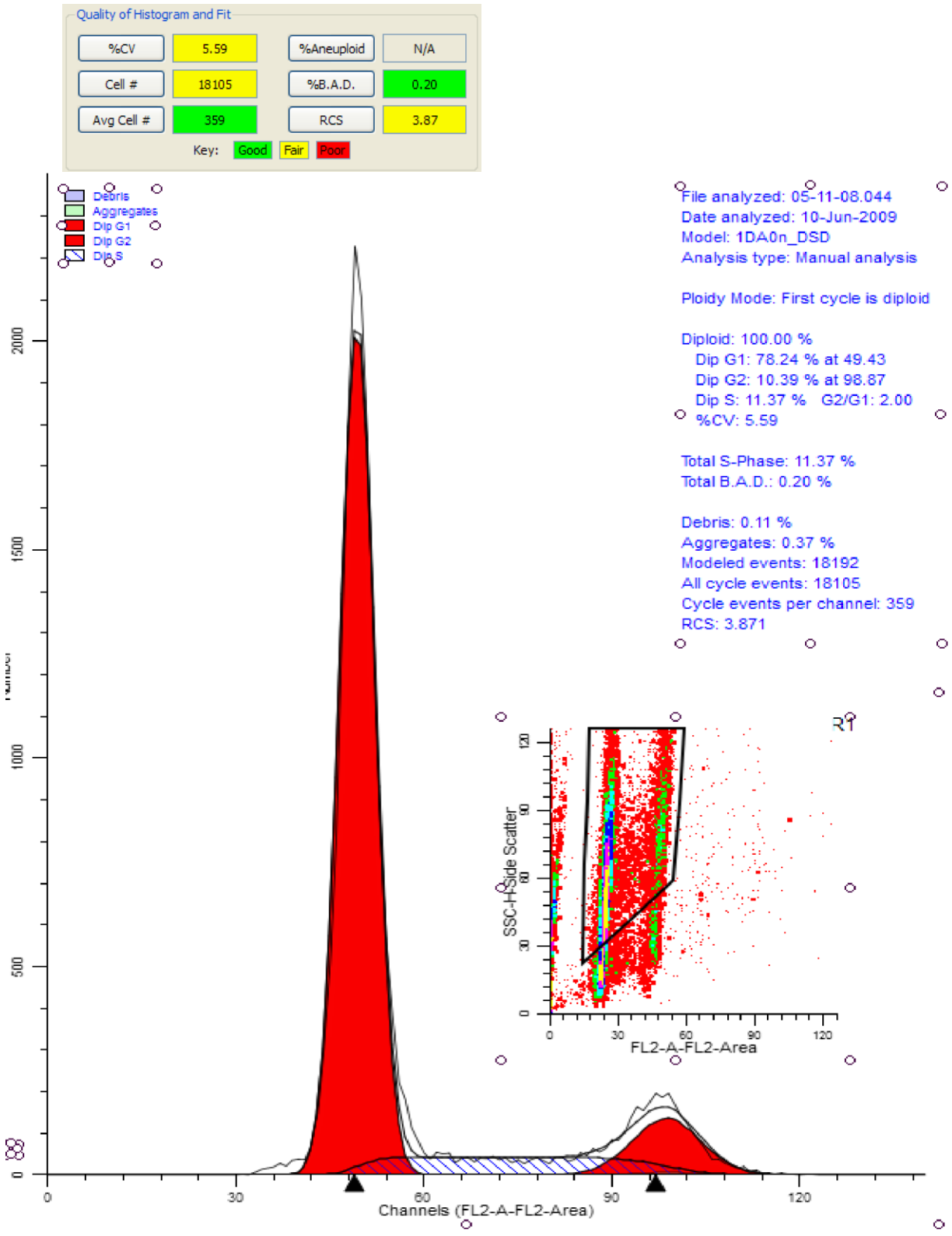

F.11. **1% FBS Experiment B**
Population 1

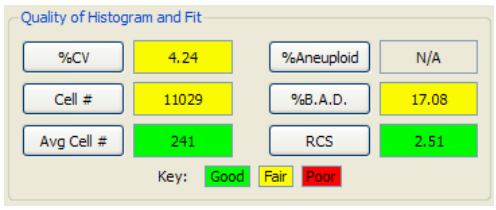

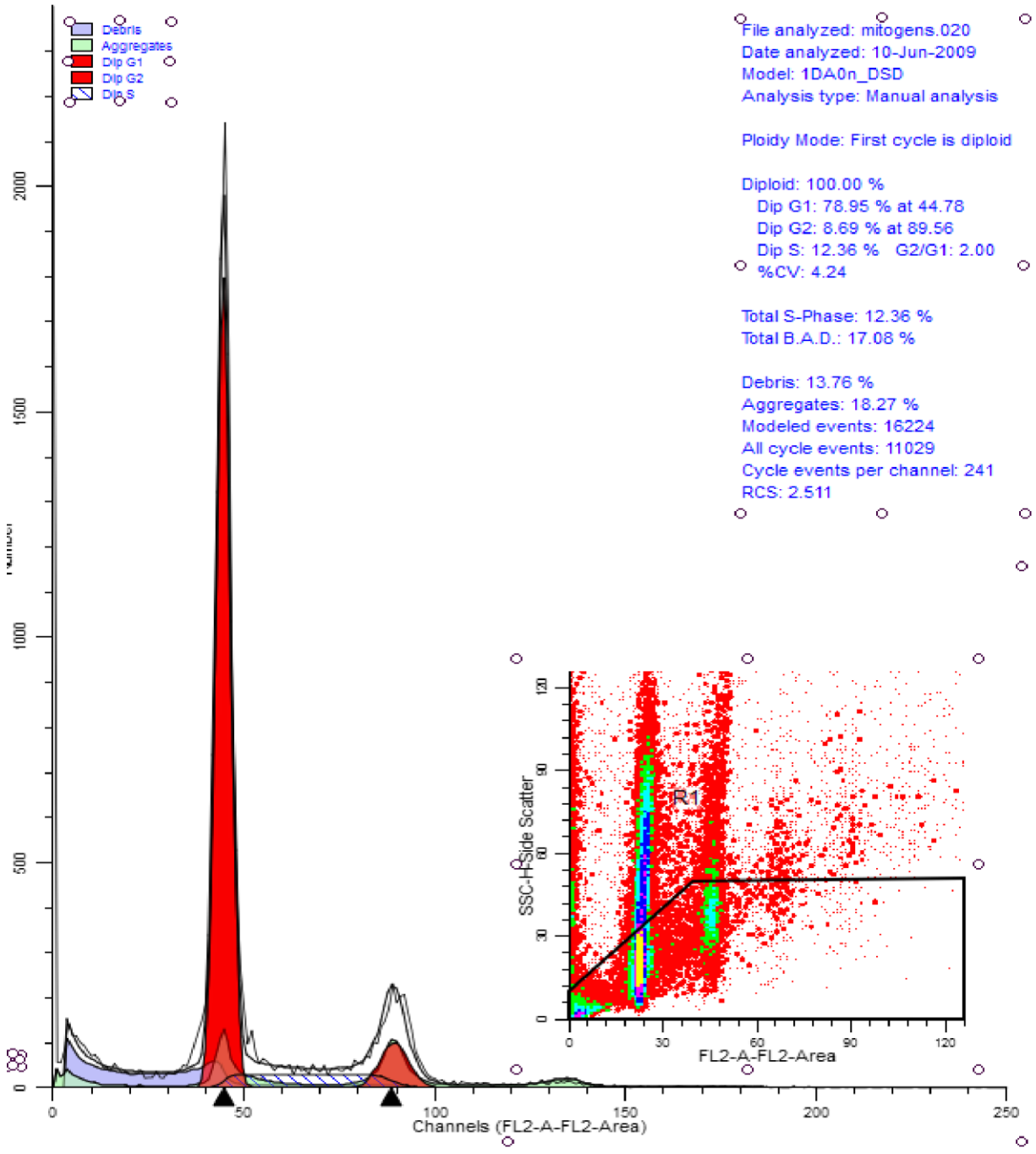

F.12. **1% FBS Experiment B**
Population 2

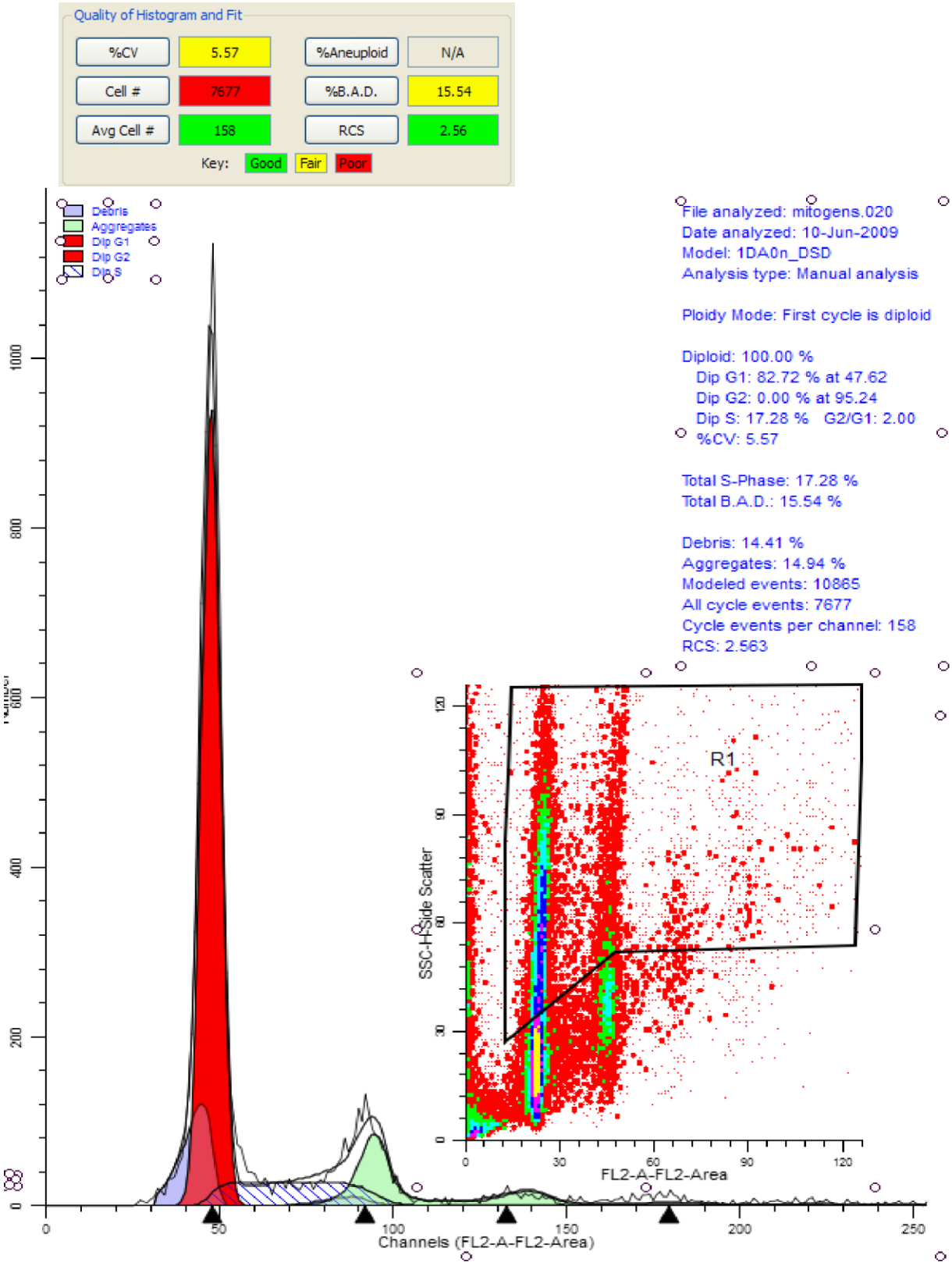

F.13. **5% FBS Experiment B**
Population 1

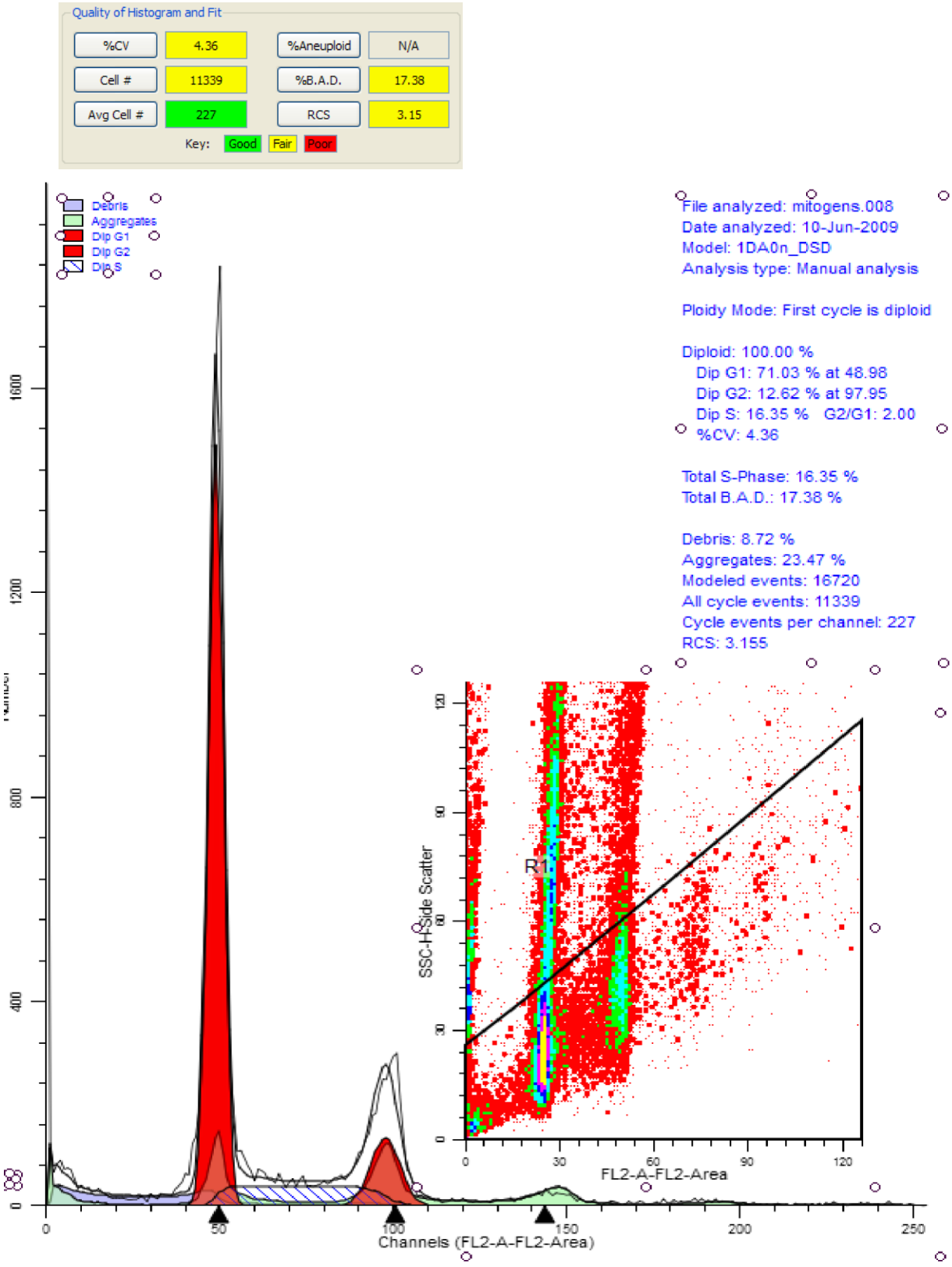

F.14. **5% FBS Experiment B Population 2**

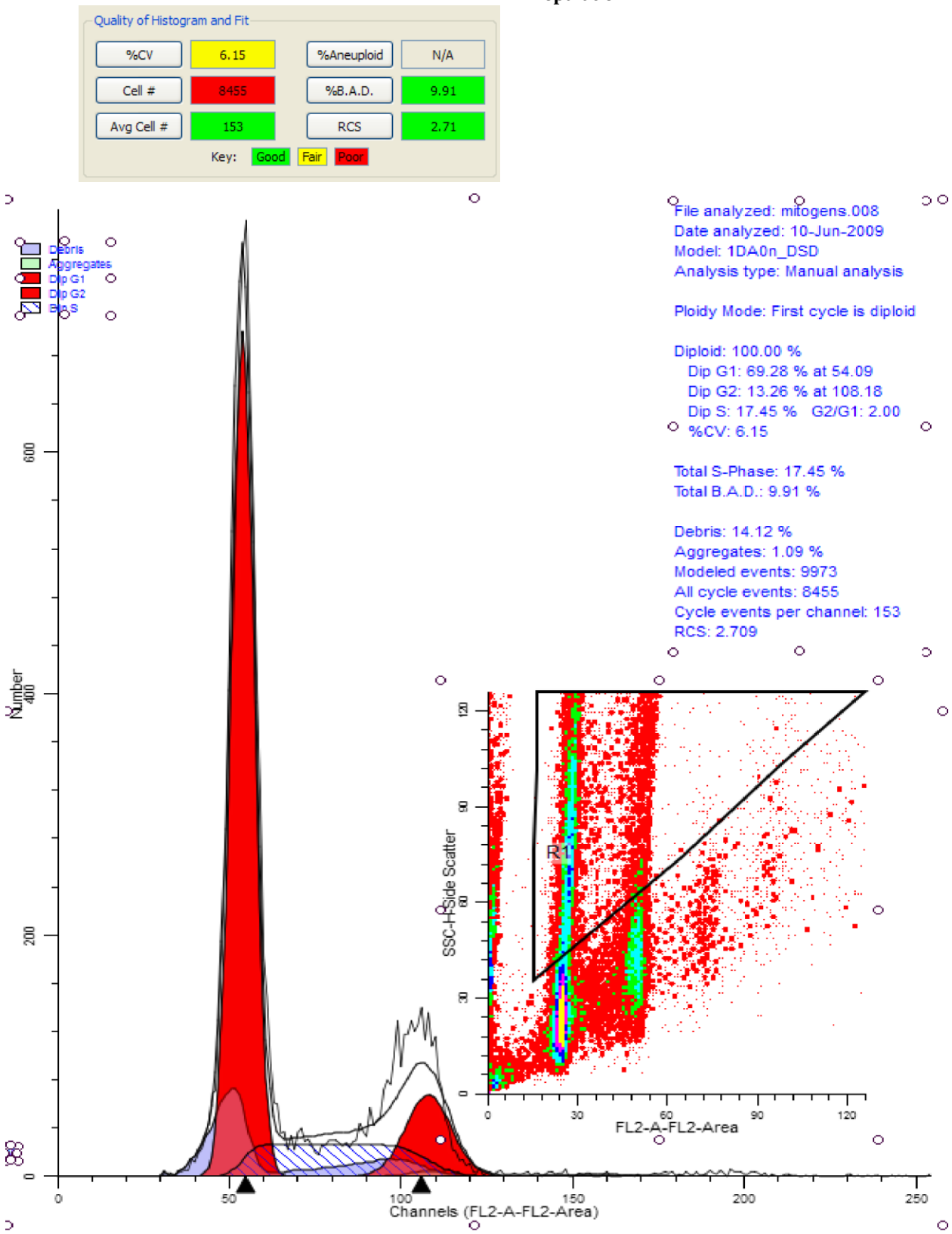

F.15. **10% FBS Experiment B**
Population 1

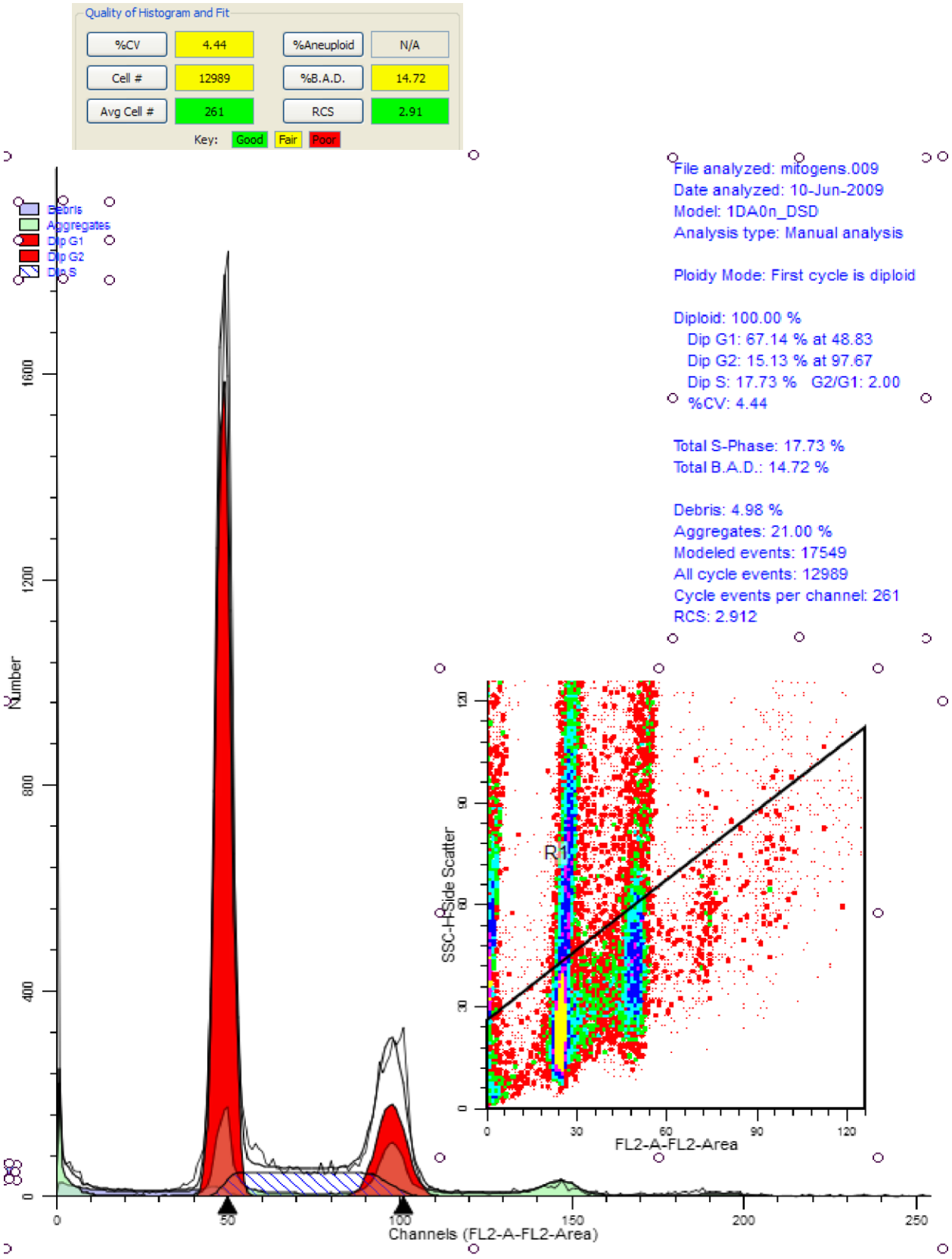

F.16. **10% FBS Experiment B**
Population 2

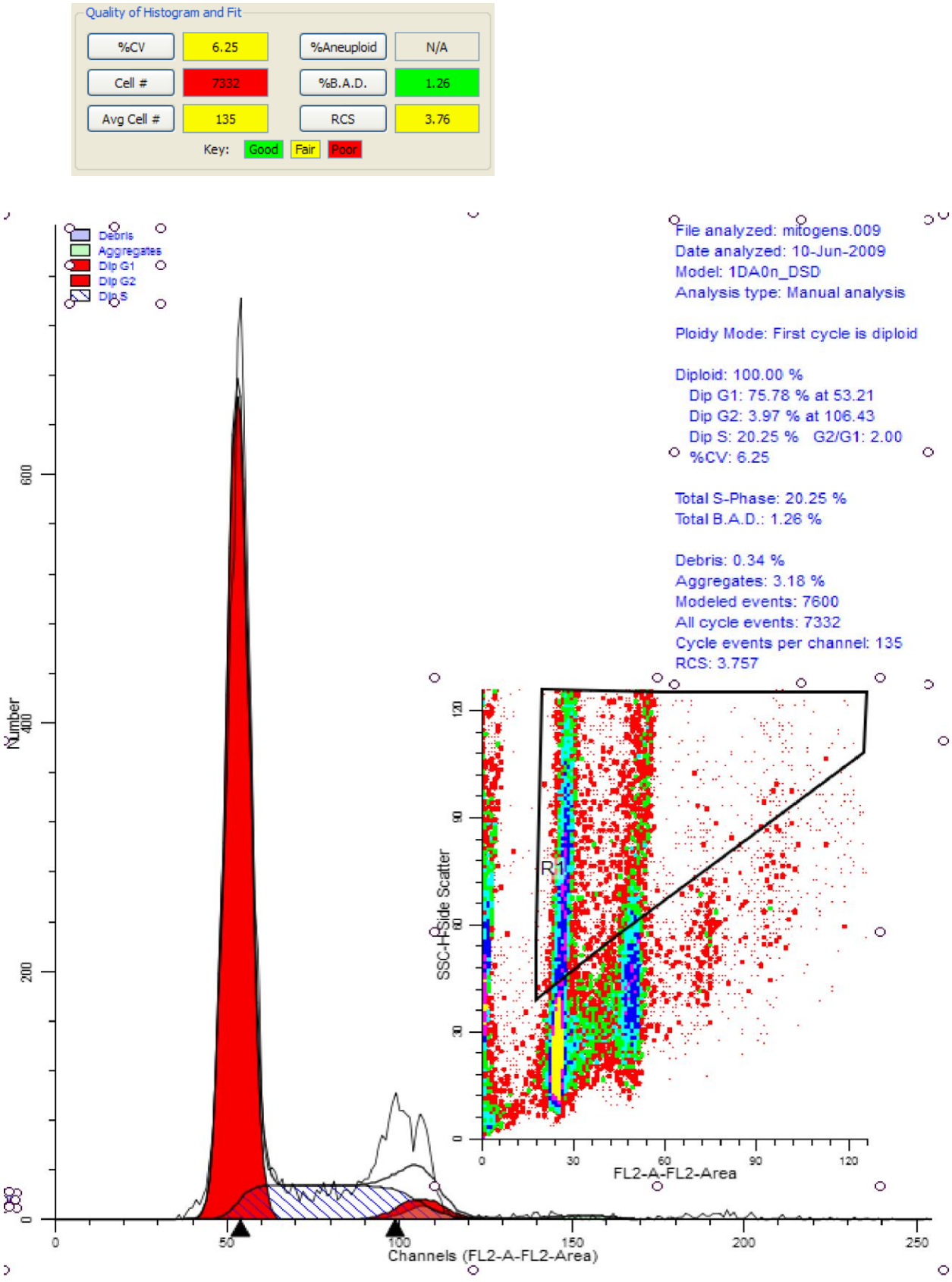

F.17. **20% FBS Experiment B**
Population 1

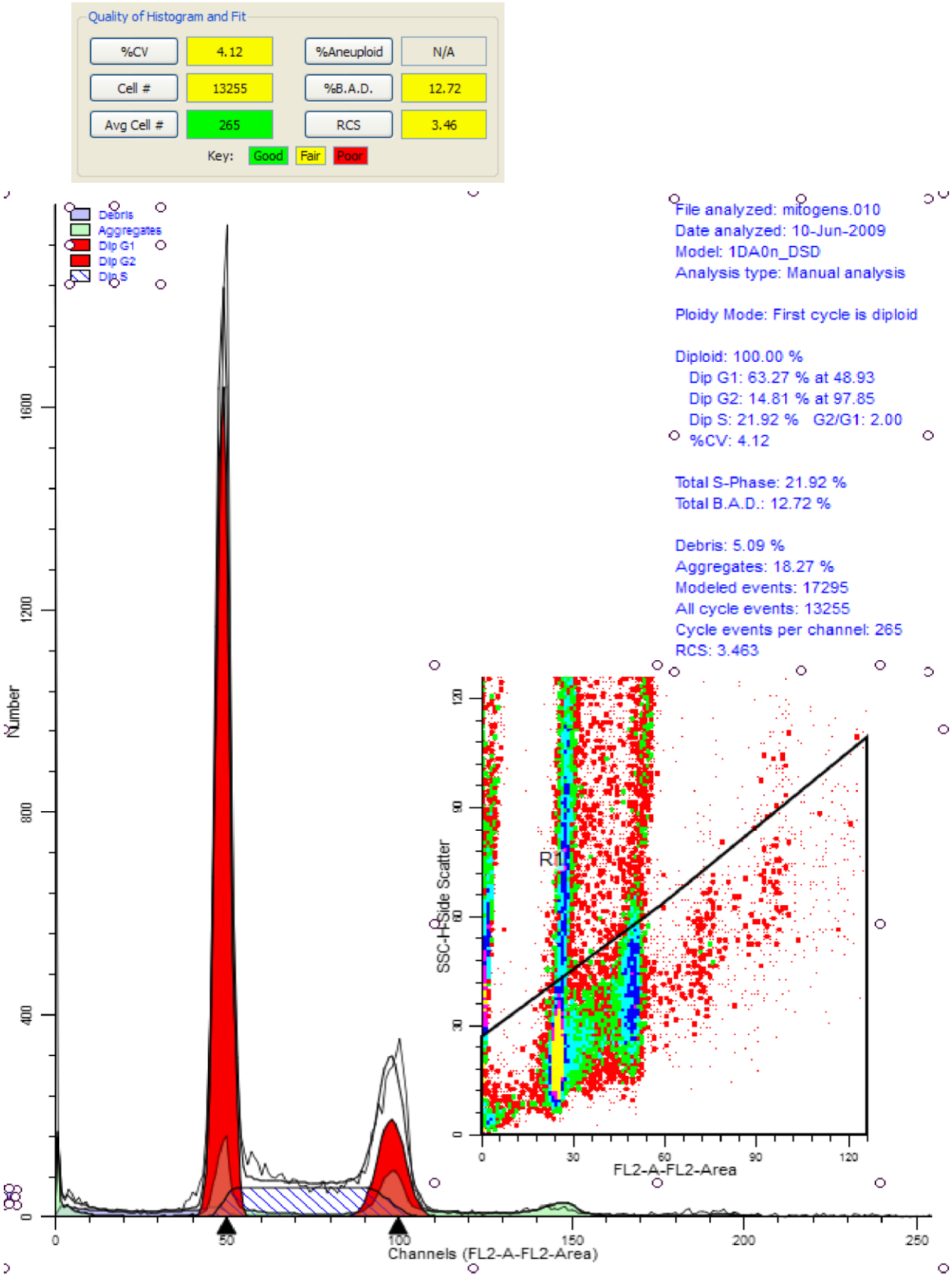

F.18. **20% FBS Experiment B**
Population 2

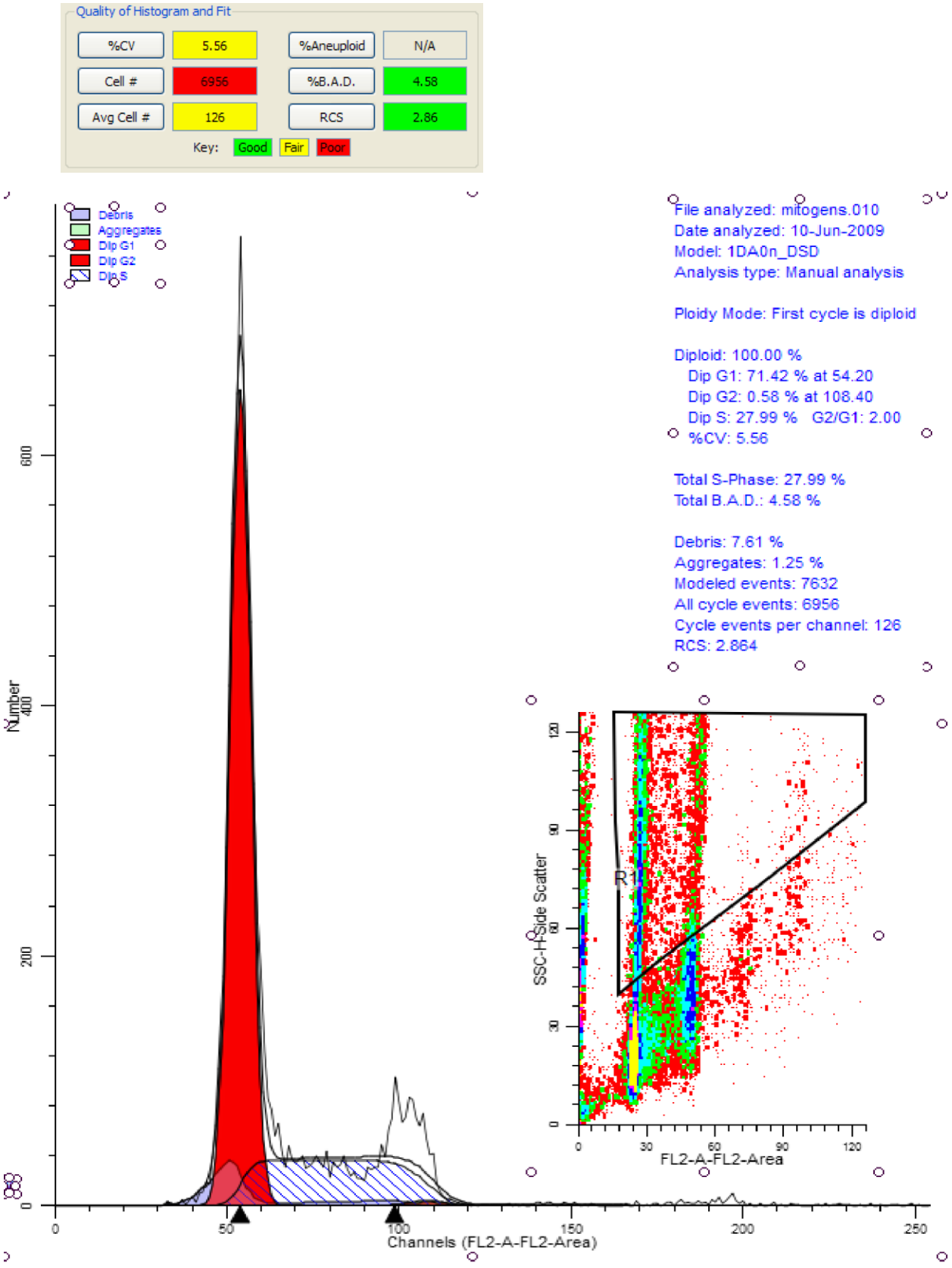

F.19. **PMA Experiment B**
Population 1

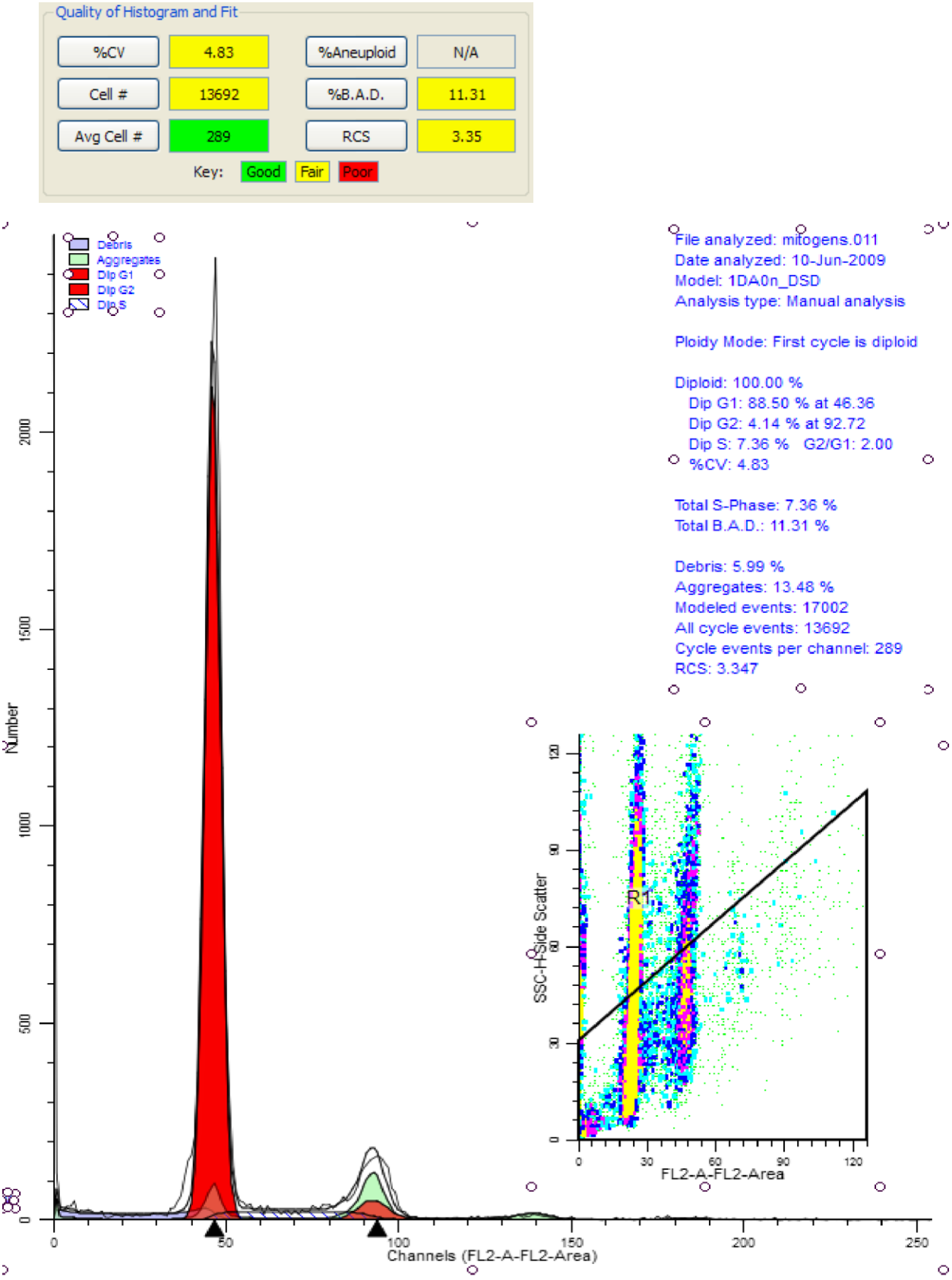

F.20. **PMA Experiment B**
Population 2